LBL-37551
UC-1501

Lawrence Berkeley Laboratory

UNIVERSITY OF CALIFORNIA

ENERGY & ENVIRONMENT DIVISION

Mathematical Modeling of the Nickel/Metal Hydride Battery System

B.K. Paxton
(M.S. Thesis)

September 1995

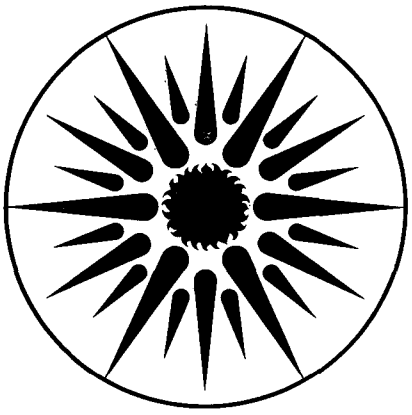

ENERGY AND ENVIRONMENT DIVISION

Prepared for the U.S. Department of Energy under Contract Number DE-AC03-76SF00098

DISCLAIMER

LBL-37551

Mathematical Modeling of the Nickel/Metal Hydride Battery System

Blaine Kermit Paxton
M.S. Thesis

Department of Chemical Engineering
University of California, Berkeley

and

Energy and Environment Division
Ernest Orlando Lawrence Berkeley National Laboratory
University of California
Berkeley, CA 94720

September 1995

This work was supported by the Assistant Secretary for Energy Efficiency and Renewable Energy, Office of Transportation Technologies, Electric and Hybrid Propulsion Division, of the U.S. Department of Energy under Contract No. DE-AC03-76SF00098.

LBL-37551

Mathematical Modeling of the Nickel/Metal Hydride Battery System

by

Blaine Kermit Paxton

B.S.E. (Tulane University) 1993

A thesis submitted in partial satisfaction of the

requirements for the degree of

Master of Science

in

Chemical Engineering

in the

GRADUATE DIVISION

of the

UNIVERSITY OF CALIFORNIA, BERKELEY

Committee in charge:

Professor John S. Newman, Chair
Professor Scott Lynn
Professor Gene I. Rochlin

1995

Abstract

A group of compounds referred to as "metal hydrides," when used as electrode materials, is a less toxic alternative to the cadmium hydroxide electrode found in nickel/cadmium secondary battery systems. For this and other reasons, the nickel/metal hydride battery system is becoming a popular rechargeable battery for electric vehicle and consumer electronics applications.

A model of this battery system is presented. Specifically the metal hydride material, $LaNi_5H_6$, is chosen for investigation due to the wealth of information available in the literature on this compound. The model results are compared to experiments found in the literature. Fundamental analyses as well as engineering optimizations are performed from the results of the battery model.

In order to examine diffusion limitations in the nickel oxide electrode, a "pseudo 2-D" model is developed. This model allows for the theoretical examination of the effects of a diffusion coefficient that is a function of the state of charge of the active material. It is found using present data from the literature that diffusion in the solid phase is usually not an important limitation in the nickel oxide electrode. This finding is contrary to the conclusions reached by other authors.

Although diffusion in the nickel oxide active material is treated rigorously with the pseudo 2-D model, a general methodology is presented for determining the best constant diffusion coefficient to use in a standard one-dimensional battery model. The diffusion coefficients determined by this method are shown to be able to partially capture the behavior that results from a diffusion coefficient that varies with the state of charge of the active material.

Preface

This thesis consists of two parts. The first part is a theoretical engineering study of a battery system. The second part is a study of some of the forces which influenced regulations which, in part, created the need for the battery study. The inclusion of the second part of this thesis is unnecessary; the engineering study on its own is sufficient to meet the requirements of a master's degree. This ancillary study is, for me, an opportunity to cross disciplinary boundaries, to look at a nontechnical issue which has greatly influenced my technical work.

At a deeper level, the combination of these two disparate studies is symbolic of the shift in my attitude towards science that has occurred since my matriculation as a graduate student. At the start of my studies, I thought science was the study of physical systems by the iterative process of proposing and testing conceptual and mathematical models that approximate and explain "real" behavior. I also believed that the "objective" nature of science made it a purer way of seeing the world. As I come to the end of my two-year tenure, I see science not as pure and theoretical, but as a profoundly social process, one that is filled with friendships, rivalries, individual personalities, and socialization rituals. Ironically, I also see science in a profound state of denial of its obvious social nature. It is surprising that even decades after the work of Kuhn[1] and Maslow[2], their ideas are so rarely discussed among the practitioners of science.

The view of science as a social process is not antithetical to the scientific method, but it does challenge those who believe that objectivity is lost when we express feelings about our work. These are the people who forget that objectivity is a human construction, and science, therefore, is just one more way of knowing the universe. The people who believe that science, because of its "objectivity", is somehow a purer form of knowledge, are themselves playing God by passing judgment on what is ultimately true and what is

not. I insist that science is not a sacred form of knowledge and that its practitioners should strive to embrace other disciplines and respect other ways of knowing. It is in this spirit that Chapter 6 is included in this thesis.

The previous words are not meant to be an indictment of any single person or the Department of Chemical Engineering. They are just observations of general attitudes that I have experienced throughout my life, but which, until now, have gone unnoticed or unappreciated. In fact, I owe a great debt to the many individuals, including my adviser, in the Department who have treated me exceptionally fairly and kindly while I have been conducting research in both the technical and non technical realms.

(1) T. S. Kuhn, *The Structure of Scientific Revolutions*, University of Chicago Press, Chigago (1962).

(2) A. H. Maslow, *The Psychology of Science: A Reconnaissance*, Harper & Row, Publishers, New York (1966).

Table of Contents

Acknowledgments

This work was supported by the Assistant Secretary for Energy Efficiency and Renewable Energy, Office of Transportation Technologies, Electric and Hybrid Propulsion Division of the U. S. Department of Energy under Contract No. DE-AC03-76SF0098.

Chapter 1: Introduction

1.1 Motivation

Nickel/metal hydride batteries offer a solution to many of the problems associated with the production, use, and disposal of nickel-cadmium batteries, while at the same time offering similar levels of performance. The formal potentials of the two materials are almost identical, and the specific charge of cadmium hydroxide is 366.1 mAh/g, which is comparable to a specific charge of 366.8 mAh/g for $LaNi_5H_6$, a common metal hydride compound.

One primary advantage of metal hydride compounds is their low toxicity compared to that of cadmium. In its ionic form, cadmium is toxic at concentrations in the part per billion range. Metal hydride compounds, on the other hand, are composed of less toxic materials such as nickel, titanium, zinc, and vanadium. This is an advantage at both the production and disposal stages of the battery's life cycle. Another advantage of metal hydride compounds over cadmium is that metal hydride electrodes do not display the "memory effect" which can limit the discharge of batteries using the cadmium electrode.

Because of their advantages, it appears that metal hydride batteries will be the first non-lead acid batteries to see large-scale use in electrical vehicles. On March 9, 1994, General Motors announced that it signed a partnership agreement with Ovonic Battery Company to develop nickel/metal hydride batteries for its next generation of electric vehicles.[1] Ovonic Battery Company, a subsidiary of Energy Conversion Devices, has been developing nickel/metal hydride batteries for several years and appears to have a corner on this market in the United States.[2,3]

Mathematical models of single cells can aid in the design and scale-up of entire battery systems. Since a computer simulation of a discharge can run in just a few minutes, a single parameter such as the thickness of an electrode can be changed many times in order to

optimize a cell's operation in terms of utilization, average voltage, specific energy, or specific power. Additionally, extensions of a single-cell model can be used to aid in scale-up of battery systems; heat generation and heat removal from a stack of individual cells can be modeled in order to determine maximum limits on the dimensions of a battery module, for example.[51]

With a mathematical model, a researcher can also determine operating parameters which, in real-life battery systems, are essentially unmeasurable. With a model, the concentrations of the electrolyte inside the pores of the electrode during operation can be observed, for example. Theoretical observations of this type can help elucidate fundamental operating mechanisms of a cell.

A significant part of this thesis is an examination of solid-state diffusion limitations in the nickel electrode. Some researchers have suggested that hydrogen diffusion in the solid phase is a primary limitation of the nickel electrode,[4,5,6,7,43] and recently a diffusion coefficient for hydrogen was measured as a function of state of charge of the nickel active material.[8] The theoretical consequences of these diffusion-coefficient data are examined for the first time in this thesis.

1.2 The nickel/metal hydride battery: a technical overview

For persons unfamiliar with the nickel/metal hydride battery system or with electrochemical cells, in general, this section provides a short "primer" for the rest of the thesis. The cell of interest contains what is informally referred to as the "nickel" positive electrode. In its fully charged state, the active material is not nickel metal, but is NiOOH (nickel oxyhydroxide), and in its fully discharged state the active material is $Ni(OH)_2$. (In this thesis, when a reference is made to this material, in general, the informal term "nickel" or the more formal terms "nickel oxide" or "nickel active material" will be used.) The negative electrode consists of a "metal hydride" compound. A metal hydride is simply a metal or an alloy into which hydrogen can diffuse. Since the hydrogen atom is very small, it can fit in the interstices or "holes" of the metallic lattice; in electrochemical parlance, this process is called "intercalation."

The reactions that occur at the positive and negative electrodes are written below (charging to the right).

Positive Electrode

$$\text{Desired: } Ni(OH)_2 + OH^- \leftrightarrow NiOOH + H_2O + e^-$$
$$\text{Overcharge: } 2OH^- \leftrightarrow H_2O + \tfrac{1}{2}O_2 + 2e^-$$

Negative Electrode

$$\text{Desired: } M + H_2O + e^- \leftrightarrow MH + OH^-$$
$$\text{Overcharge: } H_2O + e^- \leftrightarrow OH^- + \tfrac{1}{2}H_2$$

As can be seen from these reactions, the positive and negative reactions are stoichiometrically "opposite" of each other; while one electrode is consuming water and producing hydroxyl ions, the other electrode is consuming hydroxyl ions and producing water. The side reaction at the negative electrode usually accounts for an insignificant

fraction of the total charging current except at very high voltages, but the side reaction at the positive electrode is known to be severe at voltages regularly "seen" during charging of the cell. The interference of the side reaction at the nickel electrode makes the experimental and theoretical study of this electrode difficult.

A cut-away view of actual nickel/metal hydride batteries is shown below. The term "prismatic" simply refers to a rectangular cell, as can be seen in the figure. The battery consists of alternating layers of positive and negative electrodes with separator material in between them. Each of the positive electrode/separator/negative electrode combinations is termed a cell.

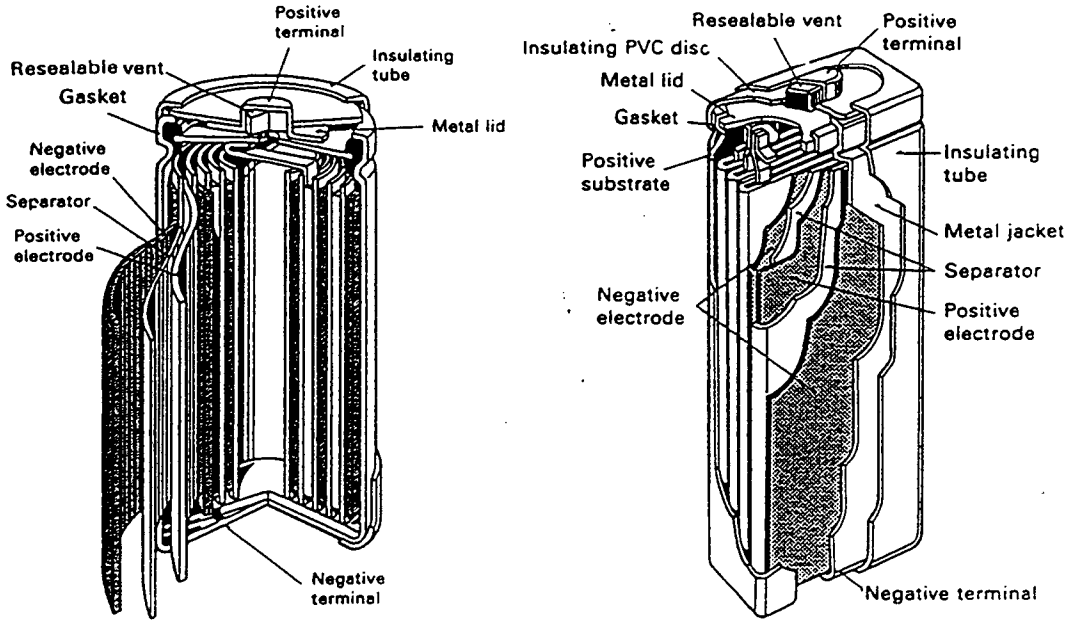

Figure 1-1: A cut-away diagram of typical nickel/metal hydride batteries (from Berndt[52])

In this model, we restrict ourselves to looking at a single cell. A diagram of a single idealized nickel/metal hydride cell is shown below.

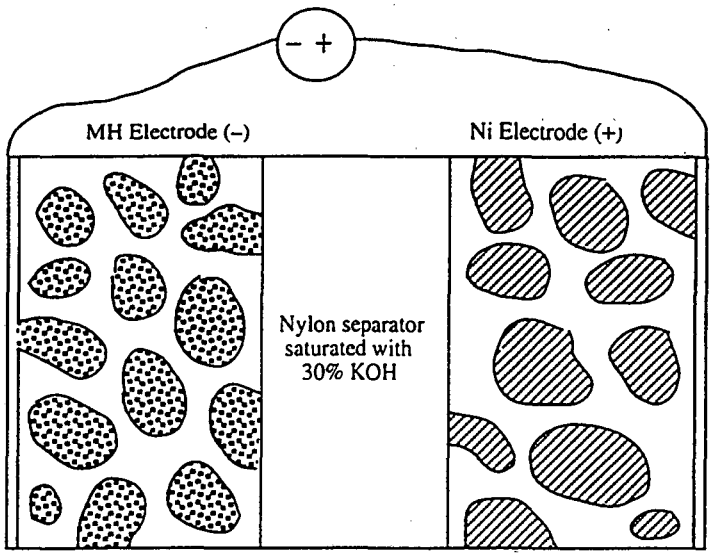

Figure 1-2: Diagram of the nickel/metal hydride cell

As implied by this diagram, both of the electrodes in this system are porous. The length scales of the channels (or spaces) between the solid active material particles are on the order of 1 to 10 μm.

The electrolyte used in this system is 30 weight percent aqueous KOH. This electrolyte is the one used in both commercial "alkaline" cells as well as rechargeable nickel/cadmium batteries.

1.3 Previous work

Many researchers have modeled the nickel electrode, the metal hydride electrode, or other systems containing one of these materials. Modeling the nickel electrode can be complicated due to the fact that the transport parameters of nickel oxide are strong functions of the electrode's state of charge. Specifically, the proton diffusivity and the electronic conductivity vary by up to three orders of magnitude over the range of oxidation states of the nickel active material.[8,20,22]

Fan and White examined the nickel oxide electrode in a model of the nickel-cadmium battery.[9,10] They applied porous electrode theory,[16] and assumed that σ, the electronic conductivity of the solid phase, was independent of the state of charge. They did not model the diffusion of protons in the solid phase; they assumed that the solid phase was a "solution" of NiOOH and $Ni(OH)_2$, the relative concentrations of which were proportional to the state of charge. They applied this solid-solution approximation to the kinetic expression when they assumed that the activities of NiOOH and $Ni(OH)_2$ were proportional to their mole fractions in the solid phase. Fan and White accounted for lattice expansion upon intercalation by letting the electrode porosities vary as a function of the state of charge of the cell.

Mao *et al.*[5] formulated a model of the nickel/hydrogen battery. The model of the nickel electrode was a pseudo 2-D model which examined the ohmic drop across a discharging film of nickel active material by including the electronic conductivity as a function of the state of charge. They used the conductivity function that is presented by Micka and Rousar[15] (see discussion on the electronic conductivity of nickel active material under section 1.4). Mao *et al.* accounted for diffusion in the solid active material and used a diffusion coefficient of 4.6×10^{-11} cm^2/s as measured by MacArthur.[4] Recently, De Vidts and White[7] applied this model of the nickel electrode to the nickel/cadmium system and performed a sensitivity analysis on some key parameters.

Sinha and Bennion[11,21] modeled the nickel electrode using a film-type model. In this model, the active material exists as a film on a metallic substrate. This model was specifically designed to represent an electrode manufactured by the sintered plaque technique. In this model they defined the surface overpotential as,

$$\eta = \Phi_1 - \Phi_2 - \frac{j\delta}{\sigma} - \frac{RT}{F}\ln\frac{c_P}{c_P^{\beta}} \qquad (1\text{-}1)$$

where j is the transfer current, δ is the thickness of the film, c_P is the concentration of protons, and σ is the conductivity of the film, which can vary widely with the concentration of protons in the solid phase. It is not clear how the authors let the electronic conductivity of the film vary, but they may have let it vary linearly with the concentration of protons, *i.e.*, a solid solution may have been assumed to exist in the film. Also, the film thickness, δ, was a constant in this model.

Bouet and Richard[12] developed a 2-dimensional model of the nickel electrode that attempts to capture proton diffusion limitations in the solid particles. They let the proton diffusion coefficient vary with the state of charge, but they did not present a key parameter used in the diffusion coefficient function. Nor did they examine the effects of the diffusion coefficient function on the discharge behavior of the nickel electrode.

Weidner and Timmerman[17] presented a one-dimensional model of a film of nickel oxide undergoing discharge. They accounted for kinetic resistances at the solid-solution interface, proton diffusion through the film, and ohmic drop across the film. They used a diffusion coefficient of 4.6×10^{-11} cm^2/s [4] and the electronic conductivity function presented by Micka and Rousar.[15] By performing a sensitivity analysis they concluded that "polarization losses due to diffusional limitations of protons is (sic) a critical factor in determining the characteristics of the discharge curve."

Lanzi and Landau[14] investigated the effect of "sinter fracture" on the performance of the nickel electrode. They hypothesized that, as the electrode is cycled, the porous nickel plaque, on which the active material is deposited, becomes cracked due to the stresses associated with the expansion and contraction of the active material. Then, they reasoned, some of the active material becomes "isolated" because to the loss of contact to the highly-conductive nickel substrate. They examined this effect by artificially isolating certain areas of the electrode in a one-dimensional model. They varied the electronic conductivity of the active material in these isolated zones to determine its effect on the potential drop across the electrode as well as on the reaction distribution across the electrode.

Micka and Rousar[15,18] also attempted to model the nickel electrode. They concentrated their analysis on the reaction rate distribution and the concentration polarization across the electrode during discharge.

Viitanen[13] developed a model of a cylindrical $LaNi_5$ metal hydride electrode. This author performed a sensitivity analysis by examining the effect of particle size, porosity, and electrolyte conductivity on the polarization of the electrode during discharge.

Yang *et al.*[19,19a] presented a simple model of the discharge of a metal hydride electrode for planar, cylindrical, and spherical particle geometries. They achieved good agreement with experimental data by assuming that one of the rate limitations of the dehydriding reaction is the transition of hydrogen from an absorbed state inside the bulk of the material to an adsorbed state on the active material surface. By a four-parameter curve fit they attempted to "back out" the kinetic parameters of this intermediate reaction step for several hydride materials.

1.4 Sources of experimental data

In order to model a battery system accurately, a wealth of data is needed. Not only are thermodynamic, kinetic, and transport data needed for the electrode materials, but physical parameters such as densities are needed as well. It is also necessary to know how the electrodes are constructed and used in common battery systems; information such as electrode thicknesses, active material loadings, and the amount of binding materials in the electrodes is necessary to formulate a model which will most correctly represent real battery systems.

One of the first steps in modeling a system is to determine if an adequate amount of experimental data exists in the literature. For this reason, a review of experimental data sources is presented in this section instead of later in the thesis. Experimental data are presented below for nickel active material, various metal hydride materials, and for the electrolyte.

Nickel Active Material

From an impedance study, Motupally[8,20] found the diffusion coefficient of hydrogen in a film consisting of 88% nickel oxide and 12% cobalt oxide as a function of the state of charge. He fit the results in the form.

$$D_s = D_1\left[\theta + \left(\frac{D_2}{D_1}\right)^{1/2}(1-\theta)\right]^2 \qquad (1\text{-}2)$$

In this equation, θ is the state of charge of the material; D_1 is the diffusion coefficient of pure NiOOH, which he finds to be 3.4×10^{-8} cm^2/s; and D_2 is the diffusion coefficient of pure $Ni(OH)_2$, which he finds to be 6.4×10^{-11} cm^2/s. Substituting these values in and neglecting swelling of the active material, we can get an equation in terms of the hydrogen concentration in the solid. (The assumed density of nickel oxide is in table 2-1.)

$$D_s = 3.4\times10^{-8}\left[1 - 0.95661\left(\frac{c_s}{c_{max}}\right)\right]^2 \qquad (1\text{-}3)$$

In their publication on a model of the nickel oxide electrode, Bouet and Richard[12] claim that they measured an exchange current density of 6.5×10^{-5} A/cm^2 at 50% state of charge, but give no details of their experimental procedure. Sinha[11,21] measured the exchange current density and apparent transfer coefficients with a film electrode. He found an average exchange current density of 6.1×10^{-5} A/cm^2, an average cathodic transfer coefficient of 0.10, and an average anodic transfer coefficient of 0.17. However, these data were determined only from the Tafel region of the electrode polarizations. The present author took Sinha's raw data for the three polarizations in 30 weight percent KOH and curve fit them to the general Butler-Volmer equation in order to include the points in the linear region. The average values of the kinetic parameters determined from these three curve fits are

$$i_o = 1.04\times10^{-4}\ \text{A/cm}^2 \quad ; \quad \alpha_a = 0.13 \quad ; \quad \alpha_c = 0.074 \qquad (1\text{-}4)$$

where i_o is the exchange current density, α_a is the anodic transfer coefficient, and α_c is the cathodic transfer coefficient.

At the present time there are no reliable data for the electronic conductivity of either pure nickel hydroxide or the nickel active material, in general, as a function of state of charge. In Micka and Rousar's nickel electrode model,[15] they use a conductivity function they say "was taken from the work of Antonenko and coworkers:"

$$\sigma = 0.1185\ \exp(-8.459 c_{norm}^4)\ \text{S/cm} \qquad (1\text{-}5)$$

Only one of the two papers referenced as the source of this function could be found by this author. In this article,[22] a conductivity function is presented, but no mention of its origin is proffered. In addition, the conductivity function appearing in this paper is far different in

form from the approximation used by Micka and Rousar. The conductivity function appearing in the reference was fit by the present author to the following function.

$$\sigma = 0.084396 \exp(-209.54 c_{norm}^{12.785}) + 0.032373 \exp(-3.4758 c_{norm}^{2.9716}) + 0.013333 \operatorname{sech}^{50}(c_{norm}-0.7) \text{ S/cm} \quad (1\text{-}6)$$

There are other articles in the literature which measure the conductivity of nickel hydroxide and/or nickel oxyhydroxide, but the reported values are not consistent with each other. Natan *et al.* [23] reported a conductivity of pure NiOOH of 0.033 S/cm and about 3.3×10^{-5} S/cm for pure $Ni(OH)_2$, values that are almost an order of magnitude lower than the ones found from reference 22. Lun'kov *et al.* [24] report conductivities on the order of 10^{-7} S/cm for $Ni(OH)_2$ and on the order of 10^{-5} S/cm for NiOOH, but the table in which they present their results is difficult to interpret.

The dependence of the open-circuit potential of nickel oxide on the state of charge of the electrode has been the subject of a couple of studies. It was first shown by Conway and Gileadi[25] that the potential of the nickel electrode is a "mixed potential" due to the interference of the oxygen reaction at higher states of charge. Below about 50% state of charge they measure the "reversible potential" of the nickel electrode "by extrapolating the anodic and cathodic e.m.f. decay lines, plotted logarithmically in time, to the potential of their intersection." Above 50% state of charge they say that they are only able to measure "stationary potentials," the potential achieved after about a week of relaxation. The potential function that they determine is presented in figure 1-3.

Two questions need to be raised concerning this study's results. The first question concerns the certainty with which the authors report the values of the state of charge. The authors duly note that the potential of the nickel electrode during most of its charging cycle is above that of the oxygen evolution reaction. What they do not address is the extent that this side reaction might be occurring when they are passing current in order to achieve a desired state of charge.

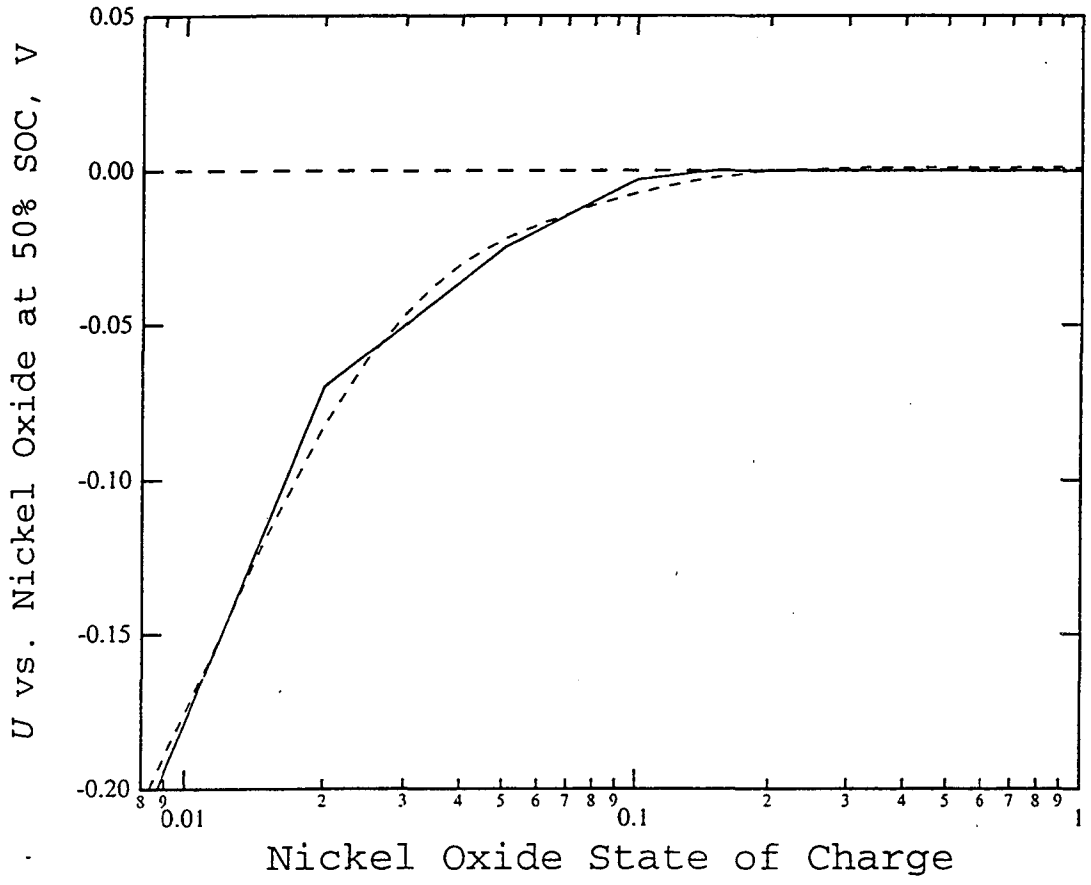

Figure 1-3: The open-circuit potential of nickel active material as a function of state of charge (adapted from Conway and Geleadi[25]). The dotted line is a curve fit of the experimental data.

The second question that is raised by this study is more serious and also concerns the oxygen side reaction. The authors calculate the "reversible potentials" by measuring potentials for up to a hundred hours of time and extrapolating the anodic and cathodic decay slopes to their point of intersection. It is not reported what self-discharge mechanisms might be occurring during this time. It is reasonable to suspect that since the potential of the nickel electrode at high states of charge is more positive than the oxygen reaction, the electrode could self-discharge by means of the oxygen evolution reaction, thereby invalidating the experiments at those potentials. (These comments are not meant to discredit these authors' work, but merely to point out, explicitly, the limitations of studying the nickel oxide electrode at high states of charge.)

Bernard *et al.* [26] measured "reversible potentials" as a function of the state of charge of both the α and β forms of nickel oxyhydroxide in what they call the "activated" and "de-activated" states. As well as suffering from the same uncertainties of Conway and Gileadi, the potentials they measure for these four different materials are quite divergent, and since they fail to state explicitly what they mean by "activated" and "de-activated" states, their work is not considered, by this author, to be reliable.

Hydride Materials

A hydride material is, in general, any element or alloy that has bonded with hydrogen. For electrochemical systems, the term "hydride" refers to a metallic hydride, one in which the hydrogen atoms form weak, reversible chemical bonds by insertion into the interstices or "holes" of the metallic lattice. Fuller and Newman[27] review the general classes of metallic hydrides commonly used as negative electrode materials in the nickel/metal hydride battery system.

While the number of extant metal hydrides is large, the number that have been seriously considered for electrochemical energy storage is few. Palladium was the first extensively studied metal hydride,[28] but palladium has unfavorable energetics and is both

too heavy and too expensive for electrochemical applications. The archetypal metal hydride considered for electrochemical energy storage is $LaNi_5$ and its substituted derivatives. Considered along with $LaNi_5$ is the compound $MmNi_5$, where Mm represents "Mischmetal," a mixture of several rare earth metals that behave similarly to lanthanum. Mischmetal offers the advantage of lower cost. $LaNi_5$ and its substituted derivatives can store 6 hydrogen atoms per formula unit (*i.e.*, $LaNi_5H_X$ $0 \leq x \leq 6$) at a potential around 0 V *vs.* the standard hydrogen electrode (SHE).

The information in this subsection is not meant to be a comprehensive review of all the data that exist on all compounds; rather it is a sample of data that illustrates the relative amounts of data available for different types of metal hydrides. Many of these data are not used in the model formulation, but the author hopes it might be of use to researchers in the future looking for data for specific compounds. Therefore, some readers may just want to skim over this section.

Kinetic Parameters

Matsouka *et al.* [29] report exchange current densities as a function of the state of charge for $Mm_xNi_{3.7}Mn_{0.5}Al_{0.4}$ where $0.885<x<1.0$ as well as the effect on the exchange current density of elemental composition for $MmNi_{3.6}Mn_{0.5}Al_{0.4}M_{0.1}$ where M=Cr, Fe, Co, or Cu. They report exchange current densities in the range of 1000 to 2000 mA/g, but the specific surface areas of the materials are not presented. Notten and Einerhand[30] also report some exchange current densities for several AB_5 compounds such as $La_{0.8}Nd_{0.2}Ni_{2.5}Co_{2.4}Si_{0.1}$. They report values in the range of 190 to 588 mA/g at 15% of the theoretical hydrogen capacity, but they also do not report the specific surface area of their samples. These latter authors present an interesting chart correlating i_o and metal-hydrogen bond strengths for several elemental metal hydrides. Van Rijswick[31] reports an exchange current density of 0.5 mA/cm^2 for $LaNi_4Cu$ in a 6 N KOH solution. Ratnakumar *et al.*[32] report exchange current densities for $LaNi_5$ (0.75 mA/cm^2 for oxidation and 0.82 mA/cm^2 for reduction) and for $LaNi_{4.8}Sn_{0.2}$ (2.25 mA/cm^2 for oxidation and 2.6 mA/cm^2

for reduction). Machida *et al.*[33] present exchange current densities for the hydrogen evolution reaction on $LaNi_5$ as well as some nickel-titanium compounds. From the data presented by Machida, the apparent transfer coefficients could also be determined.

Ratnakumar *et al.*[32] report anodic and cathodic apparent transfer coefficients for $LaNi_5$ and for $LaNi_{4.8}Sn_{0.2}$. Their values are α_a=0.25 and α_c=0.54 for $LaNi_5$, and α_a=0.46 and α_c=0.44 for $LaNi_{4.8}Sn_{0.2}$.

Diffusion Coefficients

Diffusion coefficients have been sought for metal hydrides by three different methods: quasi-elastic neutron scattering (QNS), proton nuclear magnetic resonance (NMR), and galvanostatic electrochemical procedures. The results of these three methods are summarized, but few details or relative advantages of the methods are discussed.

- Quasi-elastic Neutron Scattering

Neutron scattering studies are based on a "jump diffusion model" for the mobility of hydrogen in the lattice that presupposes a diffusion coefficient invariant with the hydrogen content of the metal. Fischer *et al.*[34] report a D_s of $(1.2 \pm 0.5) \times 10^{-6}$ cm^2/s for $LaNi_5$ at standard temperature and pressure. They report that this value is an order of magnitude larger than that obtained by NMR studies. Lebsanft *et al.*[35] report diffusion coefficients for Ti_2NiH_2, FeTiH, and $LaNi_5H_6$ by the neutron scattering technique, also. They found that the diffusion coefficients followed an Arrhenius dependence on temperature. For $LaNi_5H_6$ they report the following function:

$$D_s = 8.8 \cdot 10^{-5} \cdot \exp\left[-\frac{0.242\ eV}{kT}\right]\ cm^2/s \quad 248 \leq T \leq 318\ K \tag{1-7}$$

It is notable that at 298 K the above equation for $LaNi_5H_6$ gives a D_s of 7.1×10^{-9} cm^2/s, a value three orders of magnitude smaller than that reported by Fischer *et al.* Viitanen cites

these two studies and uses a value less than their average, 1×10^{-8} cm^2/s, in her model of a metal hydride electrode.[13]

- Electrochemical Procedures

Züchner and Boes[36] report D_s for several palladium and palladium/silver alloys as a function of electrochemical potential as well as temperature. Assuming one had the potential *vs.* composition curves for the compounds, the diffusion dependence on hydrogen concentration could be determined. Van Rijswick[31] reports a D_s of ~1×10^{-9} cm^2/s for $LaNi_4Cu$ measured with a porous electrode and compares this to a cited value of 2×10^{-8} cm^2/s for $LaNi_5$ from an NMR study.[37] The value he reports he calls a "lumped diffusion parameter" apparently because he did not attempt to subtract any ohmic effects in the solid or solution phases. Züchner and Rauf[38] present temperature-dependent D_s's for the 001 and 100 crystal orientations of $LaNi_5$ in the temperature range of $285\leq T\leq345$ K at low concentrations of hydrogen. They report D_s's of approximately 2×10^{-8} cm^2/s at 298 K.

- Proton NMR

As indicated earlier, Halstead *et al.*[37] present a D_s of 2×10^{-8} cm^2/s for $LaNi_5$. Willems and Buschow[39] cite several papers using proton NMR and QNS and find an average value of 3.6×10^{-8} cm^2/s.

Thermodynamic Data

H_2 pressure *vs.* composition isotherms are presented by Anani *et al.*[40] for $LaNi_5$. Ratnakumar *et al.*[32] also report H_2 pressure *vs.* composition isotherms for $LaNi_5$ as well as for $LaNi_{4.8}Sn_{0.2}$. Willems[41] presents the open-circuit potential as a function of the state of charge for $LaNi_5$. The employees of Ovonic Battery Company have published a few very general papers describing the Ti-Zr-V-Ni-Cr hydrides that they are investigating, but

because most of their information in proprietary, they do not publish much data. They have, however, published H_2 pressure *vs.* composition isotherms for a few materials.[2,3]

Additional Data on $LaNi_5$

As can be seen from the information just presented, $LaNi_5$ is the only compound for which a complete set of kinetic, thermodynamic, and transport data exists. For this reason, $LaNi_5$ is the material that is used in the model described by this thesis. Some more data are presented below on the phase transitions that occur as $LaNi_5$ is cycled in a battery system.

For temperatures below approximately 350 K, $LaNi_5H_X$ consists of two distinct phases: a pure α phase for a hydrogen content less than the stoichiometry $LaNi_5H_{0.3}$ and a pure β phase for a hydrogen content greater than $LaNi_5H_{6.5}$.[44] As expected, the open-circuit potential data for the material show that a plateau exists inside the two-phase region from approximately $LaNi_5H_{0.5}$ to approximately $LaNi_5H_6$ (see figure 2-10). Above 350 K, two plateaus in the open-circuit potential are observed due to the formation of a γ phase with the approximate composition $LaNi_5H_{3.5}$.[45] The open-circuit potential at room temperature for stoichiometries greater than about $LaNi_5H_6$ does not appear to be within the useful range for electrochemical energy storage.[41]

Since a phase transition is known to occur during the operation of a $LaNi_5$ electrode, it is natural to wonder whether the kinetics of the phase-transition might be a limitation in this system. No data could be found on the kinetics of this phase transition specifically, but van Vucht *et al.*[46] measured the rate of dehydriding conditioned $LaNi_5H_{6.7}$ by lowering the surrounding H_2 pressure from 30 atm to 1 atm at various temperatures and recording the subsequent rate of H_2 evolution. They found that at 20 °C, this material discharged over 90% of the hydrogen it contained in twenty-five minutes, and when 10% of the lanthanum was substituted with zirconium, over 95% of the hydrogen was discharged in less than

eight minutes. This study did not consider which mechanisms might limit the hydriding/dehydriding process.

Solution Properties

Potassium hydroxide in water is a well characterized system. The following are the data sources that were consulted for use in the model. The density of KOH was taken from *Perry's Chemical Engineers Handbook.*[47] Yushkevich *et al.*[48] measured the conductivity of a KOH solution at 25 °C. The mean molal activity coefficient for KOH and the osmotic coefficient of water at 20 °C were obtained from Robinson and Stokes.[49] Lengyel *et al.*[50] found that the transference number of the K^+ ion in KOH is essentially constant over a wide range of solution concentrations. Bhatia *et al.*[42] measured the differential diffusion coefficient of concentrated KOH at 25 °C, 45 °C, and 65 °C.

1.5 Content of thesis

From the motivations presented and the review of past modeling work and available experimental data, the formulation of a model of the nickel/metal hydride battery system appears feasible as well as desirable to battery researchers working on this system. This thesis consists of six chapters; the first chapter is the introduction to the battery study, and the fifth chapter contains a summary and caveats of the work.

The second chapter gives a detailed description of the formulation of the fundamental model equations and boundary conditions as well as the numerical procedure used to solve the equations. The second chapter contains a preliminary analysis of the model results including discharge curves, concentration profiles during operation, and reaction rate distributions inside the electrodes; as well as optimizations of the electrode thickness and porosity.

The third chapter concentrates on a pseudo two-dimensional model of the nickel electrode that incorporates concentration-dependent solid-state diffusion limitations. In this chapter an attempt is made to illustrate when diffusion effects may limit the electrode's performance.

The fourth chapter details a method by which a material with complex diffusion characteristics, such as nickel oxide, can be treated with a one-dimensional model (which requires a constant diffusion coefficient). This methodology is explained and applied to the nickel oxide system.

The sixth chapter consists of a political and organizational analysis of the California Air Resources Board in the late 1980's prior to its promulgation of what is called the Zero-Emission Vehicle (ZEV) Rule, a regulation that has dramatically influenced rechargeable battery research in the United States.

References

(1) M. Wald, "G.M. Signs Electric Car Battery Deal," *New York Times* 10 March 1994.

(2) S. Ovshinsky, M. Fetcenko, and J. Ross, "A Nickel Metal Hydride Battery for Electric Vehicles," *Science*, **260**, 176 (1993).

(3) M. Fetcenko, S. Venkatesan, and S. Ovshinsky, "Selection of Metal Hydride Alloys for Electrochemical Applications," *Electrochemical Society Proceedings*, Vol. 92-5, 141 (1992).

(4) D. MacArthur, "The Proton Diffusion Coefficient for the Nickel Hydroxide Electrode," *J. Electrochem. Soc.*, **117**, 729 (1970).

(5) Z. Mao, P. De Vidts, R. White, and J. Newman, "Theoretical Analysis of the Discharge Performance of a NiOOH/H_2 Cell," *Journal of the Electrochemical Society*, **141**, 54 (1994).

(6) G. Briggs and P. Snodin, "Aging and the Diffusion Process at the Nickel Hydroxide Electrode," *Electrochimica Acta*, **27**, 565 (1982).

(7) P. De Vidts and R. White, "Mathematical Modeling of a Nickel-Cadmium Cell: Proton Diffusion in the Nickel Electrode," *J. Electrochem. Soc.*, **142**, 1509 (1995).

(8) S. Motupally, C. Streinz, and J. Weidner, "Proton Diffusion in Nickel Hydroxide Films," *J. Electrochem. Soc.*, **142**, 1401 (1995).

(9) D. Fan and R. White, "A Mathematical Model of a Sealed Nickel-Cadmium Battery," *J. Electrochem. Soc.*, **138**, 17 (1991).

(10) D. Fan and R. White, "Mathematical Modeling of a Nickel-Cadmium Battery -- Effects of Intercalation and Oxygen Reactions," *J. Electrochem. Soc.*, **138**, 2952 (1991).

(11) M. Sinha and D. Bennion, "A Mathematical Model for the Porous Nickel Hydroxide Electrode," *J. Electrochem. Soc.*, short abstract #22, **128**, 326C (1981).

(12) J. Bouet and F. Richard, "A Discharge Model for the Ni Hydroxide Positive Electrode," *J. Electrochem. Soc.*, short abstract #31, **137**, 373C (1989).

(13) M. Viitanen, "A Mathematical Model for Metal Hydride Electrodes." *J. Electrochem. Soc.*, **140**, 936 (1993).

(14) O. Lanzi and U. Landau, "Effect of Sinter Fracture and Ohmic Resistance on Capacity Retention in the Nickel Oxide Electrode," *J. Electrochem. Soc.*, **138**, 2527 (1991).

(15) K. Micka and I. Rousar, "Theory of Porous Electrodes - XVI. The Nickel Hydroxide Electrode," *Electrochimica Acta*, **25**, 1085 (1980).

(16) J. Newman and W. Tiedemann, "Porous Electrode Theory with Battery Applications," *AIChE Journal*, **21**, 25 (1975).

(17) J. Weidner and P. Timmerman, "Effect of Proton Diffusion, Electron Conductivity, and Charge-Transfer Resistance on Nickel Hydroxide Discharge Curves," *J. Electrochem. Soc.*, **141**, 346 (1994).

(18) K. Micka and I. Rousar, "Theory of Porous Electrodes - XVI. Correction for Anodic and Cathodic Reaction Rates for Nickel Hydroxide Electrode," *Electrochimica Acta*, **27**, 765 (1982).

(19) Q. Yang, M. Ciureanu, D. Ryan, and J. Ström-Olsen, "Hydrogen Surface Concentration and Overpotential for Galvanostatic Discharge of Hydride Electrodes I. Development of the Model," *J. Electrochem. Soc.*, **141**, 2108 (1994).

(19a) Q. Yang, M. Ciureanu, D. Ryan, and J. Ström-Olsen, "Hydrogen Surface Concentration and Overpotential for Galvanostatic Discharge of Hydride Electrodes II. Quantitative Numerical Calculations," *J. Electrochem. Soc.*, **141**, 2113 (1994).

(20) Sathya Motupally, *Measurement of the Diffusion Coefficient of Protons in Nickel Hydroxide Films as a Function of State of Charge*, master's thesis, University of South Carolina, 1992.

(21) Manojit Sinha, *A Mathematical Model for the Porous Nickel Hydroxide Electrode*, dissertation, University of California, Los Angeles, 1982.

(22) V. Barsukov and L. Sagoyan, "Calculation of the Charge-storage Capacity of Metal-ceramic Electrodes of Chemical Current Sources II. Calculation of Steady-state Potential," *Soviet Electrochemistry*, **9**, 1392 (1973).

(23) M. Natan, D. Bélanger, M. Carpenter, and M. Wrighton; "pH-Sensitive $Ni(OH)_2$-Based Microelectrochemical Transistors," *J. Phys. Chem.*, **91**, 1834 (1987).

(24) A. Lun'kov, S. Milovkanov, and D. Oleinikova; "High Frequency Impedance Study of Conductivity and Dielectric Permitivity of Active Mass of Nickel Oxide Electrodes," *Soviet Electrochemistry*, **24**, 1365 (1988).

(25) B. Conway and E. Gileadi, "Electrochemistry of the Nickel Oxide Electrode - Part IV. Electrochemical Kinetic Studies of Reversible Potentials as a Function of Degree of Oxidation," *Canadian Journal of Chemistry,* **40**, 1933 (1962).

(26) R. Barnard, C. Randell, and F. Tye, "Studies Concerning Charged Nickel Hydroxide Electrodes. I. Measurement of Reversible Potentials," *Journal of Applied Electrochemistry*, **10**, 109 (1980).

(27) T. Fuller and J. Newman, "Metal Hydride Electrodes" (review). From *Modern Aspects of Electrochemistry V.27*, R. White, J. Bockris, and B. Conway, editors. Plenum Press, New York (1995).

(28) F. Lewis, *The Palladium Hydrogen System*, Academic Press, London (1967).

(29) M. Matsouka, M. Terashima, and C. Iwakura, "Effect of Alloy Composition on Charge and Discharge Characteristics of the Negative Electrode for Nickel-Hydrogen Batteries," *Electrochimica Acta*, **38**, 1087 (1993).

(30) P. Notten and R. Einerhand, "Electrocatalytic Hydride-Forming Compounds for Rechargeable Batteries," *Advanced Materials*, 3, 343 (1991).

(31) M. van Rijswick, "Metal Hydride Electrodes for Electrochemical Energy Storage," From *Hydrides for Energy Storage*, A. Anderson and A. Maeland, editors, Permagon Press (1978).

(32) B. Ratnakumar, C. Witham, B. Fultz, and G. Halpert, "Electrochemical Evaluation of La-Ni-Sn Metal Hydride Alloys," *J. Electrochem. Soc.*, **141**, L89 (1994).

(33) K. Machida, M. Enyo, G. Adachi, and J. Shiokawa, "The Hydrogen Electrode Reaction Characteristics of Thin Film Electrodes of Ni-Based Hydrogen Storage Alloys," *Electrochimica Acta*, **29**, 807 (1984).

(34) P. Fischer, A. Furrer, G. Busch, and L. Schlapbach, "Neutron Scattering Investigations of the $LaNi_5$ Hydrogen Storage System," *Helvetica Physica Acta*, **50**, 421 (1977).

(35) E. Lebsanft, D. Richter, and J. Töpler, "Study of the Diffusion of Hydrogen in Potential Hydrogen Storage Materials," *Zeitscrift für Physikalische Chemie, Neue Folge*, **116**, 707 (1979).

(36) H. Züchner and N. Boes, "Electrochemical Methods for Diffusion Measurements," *Berichte der Bunsen-Gesellschaft*, **76**, 783 (1972).

(37) T. Halstead, N. Abood, and K. Buschow, "Study of the Diffusion of Hydrogen in $LaNi_{5+x}H_6$ compounds by ^1H NMR Relaxation," *Solid State Communications*, **19**, 425 (1976).

(38) H. Züchner and T. Rauf, "Electrochemical Measurements of Hydrogen Diffusion in the Intermetallic Compound $LaNi_5$," *Journal of the Less-common Metals*, **172-174**, 611 (1991).

(39) J. Willems and K. Buschow, "From Permanent Magnets to Rechargeable Hydride Electrodes," *Journal of the Less-common Metals*, **129**, 13 (1987).

(40) A. Anani, A. Visintin, K. Petrov, S. Srinivasan, J. Reilly, J. Johnson, R. Schwarz, and P. Desch, "Alloys for H_2 Storage in Ni/H_2 and NiMH Batteries," *Journal of Power Sources*, 261 (1994).

(41) J. Willems, "Metal Hydride Electrodes Stability of $LaNi_5$-Related Compounds," *Philips Journal of Research*, **39**, 1, (1984).

(42) R. Bhatia, K. Gubbins, and R. Walker, "Mutual Diffusion in Concentrated Aqueous Potassium Hydroxide Solutions," *Transactions of the Faraday Society*, **64**, 2091 (1968).

(43) C. Zhang and S. Park, "The Anodic Oxidation of Nickel in Alkaline Media Studied by Spectroelectrochemical Techniques," *J. Electrochem. Soc.*, **134**, 2966 (1987).

(44) M. Post and J. Murray, "Calorimetric Identification of a Eutectoid Phase Separation in the $LaNi_5$-H_2 System at T≈350 K," *Journal of Solid State Chemistry*, **86**, 160-163 (1990).

(45) P. Selvan and K. Yvon, "Investigation of the Intermediate Hydride Phase β-$LaNi_5H_{3.5}$ by High Pressure and High Temperature Gravimetry," *Journal of the Less-Common Metals*, **171**, L17–L21 (1991).

(46) J. van Vucht, F. Kuijpers, and H. Bruning, "Reversible Room-temperature Absorption of Large Quantities of Hydrogen by Intermetallic Compounds," *Philips Research Reports*, **25**, 133-140 (1970).

(47) *Perry's Chemical Engineers' Handbook*, 5th edition, Robert H. Perry, editor. McGraw-Hill, Tokyo (1973).

(48) V. Yushkevich, I. Maksimova, and V. Bullan, "Electric Conductivity of KOH Solutions at High Temperatures," *Soviet Electrochemistry*, **3**, 1342 (1967).

(49) R. Robinson and R. Stokes, *Electrolyte Solutions*, 2nd ed. (rev). Butterworth & Co., London (1959).

(50) S. Lengyel, J. Giber, Gy. Beke, and A. Vértes, "Determination of the Transference Numbers in Concentrated Aqueous Solutions of Sodium and Potassium Hydroxide," *Acta Chim. Hung. Tomus*, **39**, 357 (1963).

(51) J. Newman and W. Tiedemann, "Temperature Rise in a Battery Module with Constant Heat Generation," *J. Electrochem. Soc.*, **142**, 1054 (1995).

(52) D. Berndt, *Maintenance-free Batteries*. Research Studies Press. Somerset, England (1993).

Chapter 2: One-dimensional Nickel/Metal Hydride Cell Model

2.1 Formulation of the model

The nickel/metal hydride battery system consists of a metal hydride negative electrode and a nickel oxide positive electrode. The separator is usually made of felt or a porous nylon material, and the electrolyte is 30 weight percent KOH in water. Both of the electrodes are porous electrodes, as implied in the diagram below.

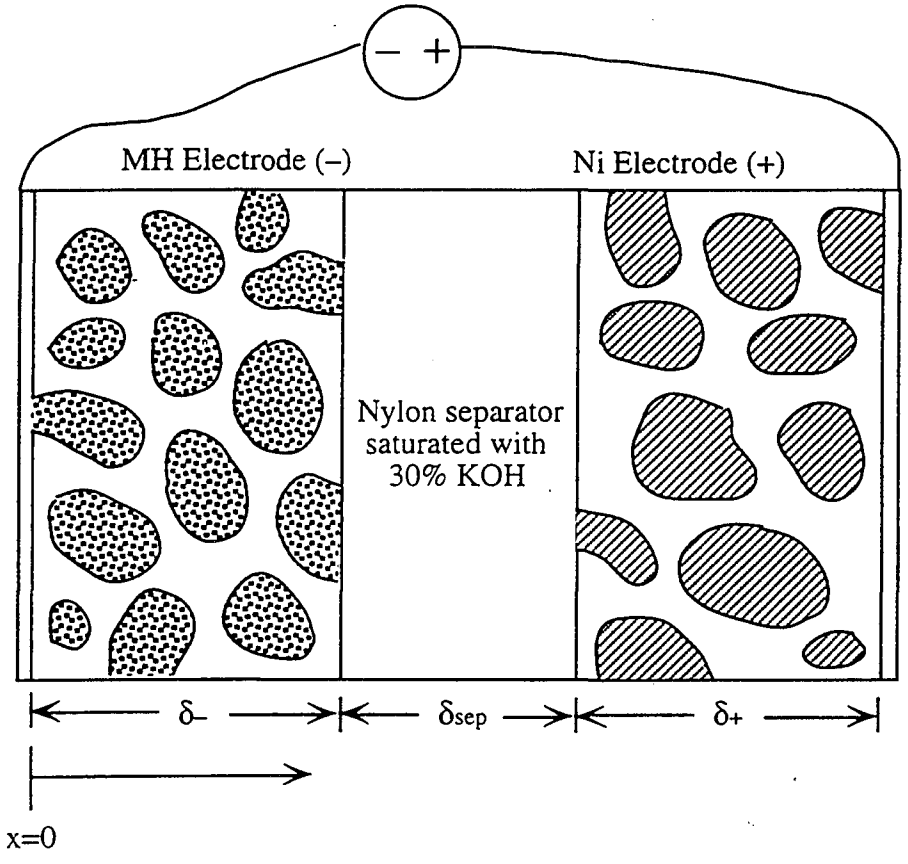

Figure 2-1: Diagram of an idealized nickel/metal hydride cell.

Both electrodes are modeled using the porous electrode theory reviewed by Newman and Tiedemann.[1] In this theory "the electrode is treated as the superposition of two continua, one representing the solution and the other representing the matrix [solid phase]."

These two phases are in intimate contact at an interface which has a specific surface area, a. A detailed characterization of the electrode's internal geometry is unnecessary, as the control volume is larger than the microstructure of the electrode but small in relation to its overall dimensions.

Transport in the solution phase is modeled using concentrated solution theory.[2] Since we assume that all the electrode materials are sparingly soluble in the alkaline solution, there are only three mobile species: $K^+_{(aq)}$, $OH^-_{(aq)}$, and H_2O. For 1:1 electrolytes, electroneutrality stipulates that

$$c = c_+ = c_- \tag{2-1}$$

where c is the concentration of the electrolyte, and c_+ and c_- are the concentrations of the cations and anions of the electrolyte salt.

The basis of concentrated solution theory is that the gradient in the electrochemical potential is the driving force for mass transfer. This can be expressed in terms of the individual ionic velocities.

$$c_i \nabla \mu_i = \sum_j K_{ij}(\upsilon_j - \upsilon_i) \tag{2-2}$$

where the υ's are the ionic velocities and the K_{ij}'s can be considered to be friction coefficients. We can write one of these equations for each of the species and subsequently invert them to obtain the more familiar flux equations composed of diffusion, migration, and convection terms. Choosing H_2O and OH^- as the two independent species, we obtain the two equations for the superficial fluxes,[12]

$$N_- = -\varepsilon D \nabla c - \frac{t_-^0}{F} i_2 + c v^{\blacksquare} \tag{2-3}$$

$$N_0 = -\varepsilon D \nabla c_0 + c_0 v^{\blacksquare} \tag{2-4}$$

where ε is the porosity of the electrode, D is the salt diffusion coefficient, t_-^0 is the transference number of the anion, i_2 is the current carried by the solution phase, and $v^{\blacksquare}$ is the volume average velocity of the solution. Based on preliminary calculations and the findings of Sinha,[9] we do not include the flux contribution due to convection (i.e., the last term in equations (2-3) and (2-4) above). The validity of this assumption is confirmed by an analysis of the simulation results in section 2.3.

It has been shown that the volume changes accompanying intercalation for both $LaNi_5$ and NiOOH can be severe. Geugan *et al.*[4] measured a 25.7% volume change for $LaNi_5$, and Davolio *et al.*[5] estimated a 15.2% volume change for nickel oxide upon intercalation. Even so, it is assumed that the porosities of the composite electrodes do not change during cycling, and the porosity values are calculated using the average densities of the active materials (see table 2-1, section 2.3). For this case, the material balance in solution is

$$\varepsilon\frac{\partial c_i}{\partial t} = -\nabla\cdot N_i + a j_i \qquad (2\text{-}5)$$

where j_i is the pore wall flux of species i due to faradaic reaction at the solid/solution interface and a is the specific surface area of the electrode in cm^2/cm^3.

The stoichiometry of the nickel electrode reaction is probably complex,[8] but we assume an idealized reaction for the purposes of this model. Since both electrodes intercalate hydrogen during cycling, the metal hydride and nickel electrode reactions can be written in the general form

$$M + H_2O + e^- \leftrightarrow MH + OH^- \qquad (2\text{-}6)$$

where M could represent either $La_{1/6}Ni_{5/6}$ (or another metal hydride) or NiOOH. For the nickel electrode the discharging reaction proceeds to the right, and for the metal hydride electrode the discharging reaction proceeds to the left. For either electrode, the pore wall flux of hydroxide ions can be defined as

$$j_- = -\frac{\nabla \cdot i_2}{aF} \tag{2-7}$$

Substituting equation (2-7) and equations (2-3) and (2-4) (sans the convective terms) into equation (2-5), we obtain the concentration dependences on current flow.

$$\varepsilon \frac{\partial c}{\partial t} = \nabla \cdot (\varepsilon D \nabla c) - \frac{t_+^0 (\nabla \cdot i_2)}{F} \tag{2-8}$$

$$\varepsilon \frac{\partial c_0}{\partial t} = \nabla \cdot (\varepsilon D \nabla c_0) + \frac{\nabla \cdot i_2}{F} \tag{2-9}$$

In equations (2-8) and (2-9), the diffusion coefficient is actually a corrected diffusion coefficient to account for the tortuosity of the porous electrode. This correction is[30]

$$D = D_0 \varepsilon^{0.5} \tag{2-10}$$

where D_0 denotes the differential diffusion coefficient of the salt that would be measured outside of any porous structure. The material balance on the solvent, equation (2-9), does not need to be included in the model; this is in harmony with the neglect of the volume average velocity.[1] We solve for the concentration of water in the solvent by knowing that the solution density is equal to the density of the solute plus the density of the solvent; this equality leads to the equation

$$c_0 = \frac{\rho - c M_e}{M_0} \tag{2-11}$$

where ρ is the solution density and M_e and M_0 are the molar masses of the electrolyte and solvent respectively. At the outer boundaries of the cell we apply a zero-flux boundary condition to the electrolyte.

$$\nabla c = 0 \quad \text{at} \quad x = 0 \,,\, \delta_- + \delta_{sep} + \delta_+ \tag{2-12}$$

If we define the potential in the solution phase, Φ_2, to be a potential measured by a reference electrode, the current in solution is related to the potential in the solution phase by[6]

$$i_2 = -\kappa\nabla\Phi_2 - \frac{\kappa RT}{F}\left(t_+^0 + \frac{c}{c_0}\right)\nabla\ln(f_{\pm}c) \tag{2-13}$$

where $f_{\pm}$ is the mean molar activity coefficient of the salt and κ is the effective electric conductivity of the solution given by the equation[30]

$$\kappa = \kappa_0\varepsilon^{1.5} \tag{2-14}$$

where κ_0 denotes the electric conductivity of the solution that would be measured outside of any porous structure.

From Kirchhoff's current law, we know that the total current, I, is given by

$$I = i_1 + i_2 \tag{2-15}$$

where i_1, the current in the solid phase, is related to the potential in the solid phase by Ohm's law

$$i_1 = -\sigma\nabla\Phi_1 \tag{2-16}$$

For the current we apply the following boundary conditions:

$$i_2 = 0 \quad \text{at} \quad x=0\,,\ \delta_-+\delta_{sep}+\delta_+ \tag{2-17}$$

$$i_2 = I \quad \text{at} \quad x=\delta_-\,,\ \delta_-+\delta_{sep} \tag{2-18}$$

If the kinetics follow a simple one-step reaction mechanism and the solid phase is assumed to behave ideally, then the Butler-Volmer form of the kinetic equation can be written

$$\nabla \cdot i_2 = a i_0 \left[\exp\left(\frac{\alpha_a F}{RT}\eta_s\right) - \exp\left(\frac{-\alpha_c F}{RT}\eta_s\right) \right] \tag{2-19}$$

where i_0, the exchange current density, is the function given below.

$$i_0 = i_0'\left(\frac{a_{\pm}}{a_{\pm,\mathrm{ref}}}\right)^{\alpha_c}\left(\frac{c_s}{c_{s,\mathrm{ref}}}\right)^{\alpha_c}\left(\frac{a_0}{a_{0,\mathrm{ref}}}\right)^{\alpha_a}\left(\frac{c_t - c_s}{c_t - c_{s,\mathrm{ref}}}\right)^{\alpha_a} \tag{2-20}$$

In this equation, i_0' is the reference exchange current density and is a constant, $a_{\pm}$ is the mean molar activity of the electrolyte, a_0 is the activity of water, c_s is the concentration of intercalated hydrogen in the solid phase, and c_t is the maximum concentration of hydrogen in the solid phase. The reference activities and concentrations in the equation are the ones at which the experimental measurement of i_0' was made. Since the overall reaction is similar for nickel oxide and for $LaNi_5$ as shown in equation (2-6), equations (2-19) and (2-20) are applicable to both electrodes.

The open-circuit potential is taken to be

$$U = U^{\theta} + \mathrm{f}(c_s) \tag{2-21}$$

where U^{θ} is the open-circuit potential of the electrode at 50% state of charge and $\mathrm{f}(c_s)$ is an experimentally measured function of the solid-phase hydrogen concentration.

The potential in the solution phase is the potential measured with a reference electrode. For computational convenience, the reference in each electrode is chosen as an electrode of the same composition at 50% state of charge. The surface overpotential, η_s, is then defined by

$$\eta_s = \Phi_1 - \Phi_2 - U^{\theta} + U^{\theta}_{\mathrm{ref}} - \mathrm{f}(c_s) \tag{2-22}$$

where $U^{\theta}_{\mathrm{ref}}$ is the standard open-circuit potential of the reference electrode. Since U^{θ} and $U^{\theta}_{\mathrm{ref}}$ are defined to be the same quantity, eq. (2-22) becomes just

$$\eta_s = \Phi_1 - \Phi_2 - f(c_s) \tag{2-23}$$

Since we use this definition for η_s in each electrode, we must account for the difference in the formal potentials of the two reference electrode materials. This difference in potentials is added to obtain the cell voltage at the positive electrode/separator interface. In other words, we define our reference electrode to be a $LaNi_5$ electrode over the range $0 < x < \delta_- + \delta_{sep}$ and a nickel oxide reference electrode over the range $\delta_- + \delta_{sep} < x < \delta_- + \delta_{sep} + \delta_+$. Taking the gradient of equation (2-23) and subsequently substituting in equations (2-13) and (2-16) gives the following equation for the surface overpotential in terms of the current in the solution phase of the electrode.

$$\nabla\eta_s = \frac{-(I - i_2)}{\sigma} + \frac{i_2}{\kappa} + \frac{RT}{F}\left(t_+^0 + \frac{c}{c_0}\right)\nabla\ln(f_{\pm}c) - \nabla f(c_s) \tag{2-24}$$

Finally, the concentration of hydrogen in the solid phase is allowed to vary within an individual particle. The particles in this model are assumed to be spherical particles with a radius, R. For both electrodes, a constant diffusion coefficient is assumed. Therefore, the diffusion into the solid particles is governed by the simple time-dependent diffusion equation in spherical coordinates.

$$\frac{\partial c_s}{\partial t} = D_s\left[\frac{1}{r^2}\frac{\partial}{\partial r}\left(r^2\frac{\partial c_s}{\partial r}\right)\right] \tag{2-25}$$

The boundary conditions are

$$j_H = -D_s\frac{\partial c_s}{\partial r}\bigg|_{r=R} \tag{2-26}$$

and

$$\frac{\partial c_s}{\partial r}\bigg|_{r=0} = 0 \tag{2-27}$$

where j_H is the pore wall flux of hydrogen at the surface of a particle.

For the diffusion equation inside a single particle we use a solution based on the superposition integral. This method of solution has been used previously for this type of application.[26,31] What follows is a brief summary of the method; the interested reader can consult some of the more in-depth analyses for further details.[32,33]

The superposition integral allows for the determination of the flux into the particle knowing the history of the concentration at the particle's surface. In other words, we do not need to keep track of the concentration distribution inside the particle during the simulation. The equation below is the result of the application of this method to diffusion in a spherical particle.

$$-\frac{1}{D_s a F}\nabla\cdot i_2 = \sum_{k=1}^{n-1}\left(\frac{c_s(k)-c_s(k\text{-}1)}{\Delta t}\right)\left[a_i((n\text{-}k+1)\Delta t)-a_i((n\text{-}k+1)\Delta t)\right] + \left(\frac{c_s(n)-c_s(n\text{-}1)}{\Delta t}\right)a_i(\Delta t) \tag{2-28}$$

In the equation above, the a_i's are defined as the integral of the gradient of the dimensionless concentration as a function of time for a step change in concentration at the surface of a particle, and the surface concentration, c_s, is a function of time. The summation takes place over time and proceeds from k=1, the first time step, to n, the present time step.

To apply this solution, we substitute equation (2-19) into equation (2-28) and get

$$\sum_{k=1}^{n-1}\left(\frac{c_s(k)-c_s(k\text{-}1)}{\Delta t}\right)\left[a_i((n\text{-}k+1)\Delta t)-a_i((n\text{-}k+1)\Delta t)\right] + \left(\frac{c_s(n)-c_s(n\text{-}1)}{\Delta t}\right)a_i(\Delta t) = -\left(\frac{1}{D_s F}\right) i_0\left[\exp\left(\frac{\alpha_a F}{RT}\eta_s\right)-\exp\left(\frac{-\alpha_c F}{RT}\eta_s\right)\right] \tag{2-29}$$

where i_0 is defined by equation (2-20).

2.2 Numerical Solution Procedure

A detailed discussion of the general process of linearizing and solving a set of differential equations is given by Newman.[6] What follows are some particular details of the solution method used in this model. These procedures have been used before for solving models of this type, but they have never been documented.

The four equations-- (2-8), (2-19), (2-24), and (2-29) -- which are reprinted below, comprise the model. These four equations are linearized and solved using the BAND[6] matrix-solving subroutine. The following is a description of how each of the equations was discretized and linearized.

$$\textbf{(A)}\quad \varepsilon\frac{\partial c}{\partial t} = \nabla\cdot(\varepsilon D\nabla c) - \frac{t_+^0\,(\nabla\cdot i_2)}{F}$$

$$\textbf{(B)}\quad \nabla\eta_s = \frac{-(I - i_2)}{\sigma} + \frac{i_2}{\kappa} + \frac{RT}{F}\left(t_+^0 + \frac{c}{c_0}\right)\nabla\ln(f_{\pm}c) - \nabla f(c_s)$$

$$\textbf{(C)}\quad \nabla\cdot i_2 = a i_0\left[\exp\left(\frac{\alpha_a F}{RT}\eta_s\right) - \exp\left(\frac{-\alpha_c F}{RT}\eta_s\right)\right]$$

$$\textbf{(D)}\quad \sum_{k=1}^{n-1}\left(\frac{c_s(k) - c_s(k\text{-}1)}{\Delta t}\right)\left[a_i((n\text{-}k+1)\Delta t) - a_i((n\text{-}k+1)\Delta t)\right] + \left(\frac{c_s(n) - c_s(n\text{-}1)}{\Delta t}\right)a_i(\Delta t)$$

$$= -\left(\frac{1}{D_s F}\right) i_0\left[\exp\left(\frac{\alpha_a F}{RT}\eta_s\right) - \exp\left(\frac{-\alpha_c F}{RT}\eta_s\right)\right]$$

Equation A was put in finite difference form by performing a general material balance on the K^+ cations at each mesh point. For each mesh point, j=1 to j=NJ-1, the material balance was performed for a control volume from j=n-1/2 to j=n+1/2. It was assumed during the derivation that the porosity to the left of j=n was not necessarily the same as the porosity to the right of j=n. This allowed the derived equation to be applied at points j=N1 and j=N2, the two electrode separator interfaces, where the porosities are, in fact, not equal to one another. (Additionally, it could be assumed that the mesh spacing on each side of a

mesh point was not necessarily the same. This would allow for different mesh spacing in different regions of the cell. This procedure is not used in this model, though.)

By discretizing the equation in this fashion, the need to calculate explicitly the second derivative of the concentration was eliminated. In addition, this process obviated the need to calculate second derivatives of the electrolyte diffusion coefficient.

Equations B and C form a couple since they are both primarily functions of the variables η_s and i_2. In each electrode, there are two boundary conditions on this set of equations-- namely i_2=0 at the outside edge of each electrode and i_2=I at each electrode/separator interface. The discussion that follows concentrates on the negative electrode, but the same discretization procedure is followed, albeit in the reverse, for the positive electrode.

At point j=1 the boundary condition, i_2=0, is entered into the second equation "space" in BAND. From points j=2 to j=N1, equation B is entered into the second equation "space" as a two point, order h^2, backward difference approximation. In other words the equation is applied over the region from points j=n−1 to j=n, and the values are entered into BAND at the point j=n. Therefore, the derivatives of η_s, c_s, and c are all calculated using just the points j=n and j=n-1, and the order h^2 approximation is achieved by taking the average of the coefficients of these derivatives at both points j=n and j=n−1. In summary, equation B is essentially solved across the electrode from point j=1, where the boundary condition exists, to j=N1.

The opposite is true of equation C. The boundary condition at the electrode/separator interface, i_2=I, is entered into the third equation "space" in BAND at j=N1. For the points j=1 to j=N1-1, equation C is entered as a two point, order h^2, forward difference approximation. In other words, the equation is applied over the region from j=n to j=n+1, and the resulting values are entered at point j=n. The derivative of i_2 is calculated across

points j=n and j=n+1, similar to the way the derivatives in the second equation are calculated.

In the separator region, points j=N1+1 to j=N2–1, i_2 is set equal to I, and η_s is set equal to zero. In the positive electrode region the boundary condition i_2=I is entered into the third equation "space" in BAND at j=N2, and the boundary condition i_2=0 is entered into the second equation "space" in BAND at j=NJ. The above procedure is then "reversed" for entering the equations so that the second equation is applied over points j=n to j=n+1 and entered at j=n, and the third equation is applied over points j=n–1 to j=n and entered at j=n. A graphic representation of the way equations two and three are set up is shown below.

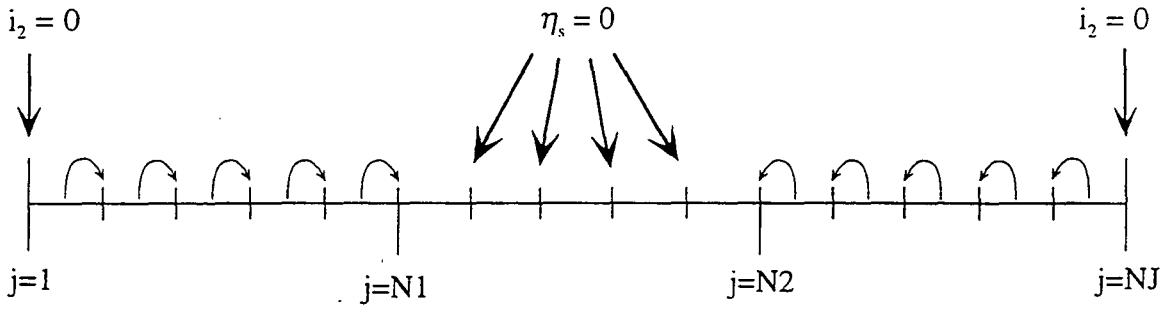

Figure 2-2: Graphic representation of the discretization of equation B.

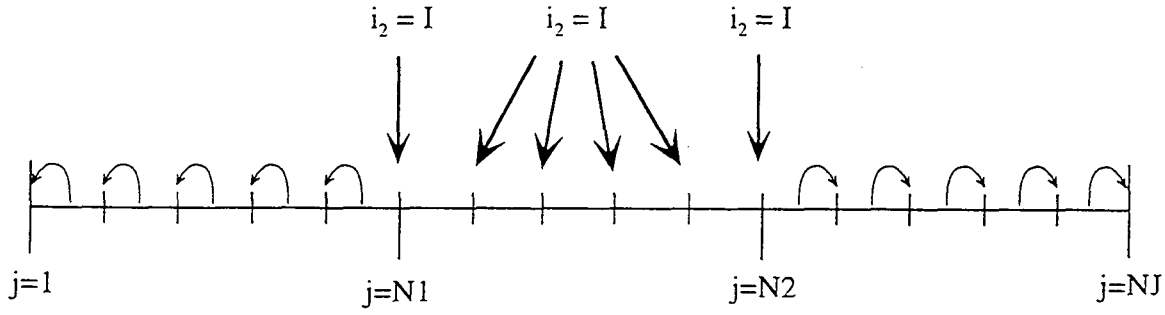

Figure 2-3: Graphic representation of the discretization of equation C.

Equation D contains no derivatives, and so does not involve any other points besides j=n. In a sense it "responds" to the current, concentration, and overpotential values that are solved for by the other equations. It uses these values to determine the solid-phase surface concentration in the particles. The fourth equation is applied at points j=1 to j=N1 and at j=N2 to j=NJ; from j=N1+1 to j=N2-1, c_s is set equal to zero.

The linearization of the Butler-Volmer part of equations C and D is best approached by breaking the expression up into separate functions f(c), f(c_s), and f(η_s). Then the equation can be linearized by taking its first order Taylor series expansion as shown below.

$$\begin{aligned} f(c)f(c_s)f(\eta_s) \approx\ & f(c^\circ)f(c_s^\circ)f(\eta_s^\circ) + f(c^\circ)f(c_s^\circ)\left(\frac{\partial f(\eta_s)}{\partial \eta_s}\right)\Delta\eta_s + \\ & f(c^\circ)f(\eta_s^\circ)\left(\frac{\partial f(c_s)}{\partial c_s}\right)\Delta c_s + f(c_s^\circ)f(\eta_s^\circ)\left(\frac{\partial f(c)}{\partial c}\right)\Delta c + \text{higher order terms} \end{aligned} \tag{2-30}$$

In this equation, $\Delta\eta_s = \eta_s - \eta_s^\circ$, $\Delta c_s = c_s - c_s^\circ$, $\Delta c = c - c^\circ$, and the derivatives are calculated at c°, c_s°, and η_s°. The superscript, o, represents the "old" guess for a variable during the iterative process of converging on a solution.

2.3 Fundamental analysis of the nickel oxide/$LaNi_5$ cell undergoing discharge

The analysis of some fundamental results from simulations using the model are contained in this section. All the simulations, unless otherwise noted, were obtained by using the parameters in tables 2-1 and 2-2.

Table 2-1: System-specific parameters.

Parameter	Nickel Oxide	$LaNi_5$
D_s (cm^2/s)	1×10^{-8}	2×10^{-8} [10,21]
σ (Ω^{-1} cm^{-1})	28 +	1000 +
i_0' (mA/cm^2)	0.104 *	0.785 [11]
α_a	0.13 *	0.25 [11]
α_c	0.074 *	0.54 [11]
ρ_{ave} (g/cm^3)	3.55 [18,19]	7.49 [4,7]
c_t (mol/cm^3)	0.0383 ɜ	0.1025 ɜ

+ assumed ; * see Section 1.3 ; ɜ calculated

Table 2-2: Adjustable parameters.

Parameter	Nickel Oxide	$LaNi_5$
δ (μm)	843	350
ε	0.387	0.396
ε_{act}	0.507	0.481
ε_f	0.106	0.123
R (μm)	2.5	1.5

The diffusion coefficient of hydrogen in nickel oxide is set large enough so that no diffusion limitations will occur. This follows from the analysis in Chapter 3. The initial state of charge of the nickel electrode was set to 99.5% of its theoretical maximum, and the initial state of charge of the $LaNi_5$ electrode was set to 97% of its theoretical maximum. These figures were chosen from the fact that manufacturers of nickel/metal hydride batteries normally leave more unreacted capacity in the metal hydride electrode to avoid hydrogen production at this electrode on overcharge.[20] For these analyses, the discharge rates are expressed in terms of the fraction of the total capacity that theoretically would be discharged in one hour. Therefore, the "0.5 C rate" corresponds to a theoretical discharge time of 2 hours. Since the capacity of the cell corresponding to the adjustable parameters given in table 2-2 is 43.4 mAh/cm^2, the 0.25 C discharge rate, for example, would correspond to a superficial current density across the cell of 10.9 mA/cm^2.

Sample voltage *vs.* capacity discharge curves are presented in figure 2-4. As expected, the general form of the discharge curves is dominated by the near-Nernstian behavior of the nickel oxide electrode's thermodynamics (see section 2.5 for discussion). It is also notable that diffusion limitations in the solid phase of the negative electrode, at first glance, appear to be slight, as evidenced by the high utilization at low discharge rates.

Bennett *et al.*[34] and Brigder *et al.*[35] were some of the first researchers to examine the nickel oxide/$LaNi_5$ cell. From these two closely related studies, several voltage *vs.* capacity discharge curves were selected and compared to a theoretical discharge curve predicted by this model. This comparison is presented in figure 2-5. It can be seen from the graph that the qualitative shape of the theoretical discharge curve corresponds to the shape of, at least, parts of the three experimental curves. Each of the three experimental discharge curves was from a different cell running under different performance conditions. In addition, each of these cells was poorly characterized in terms of the physical parameters necessary to exactly duplicate the runs with the model; most numerical values for the active

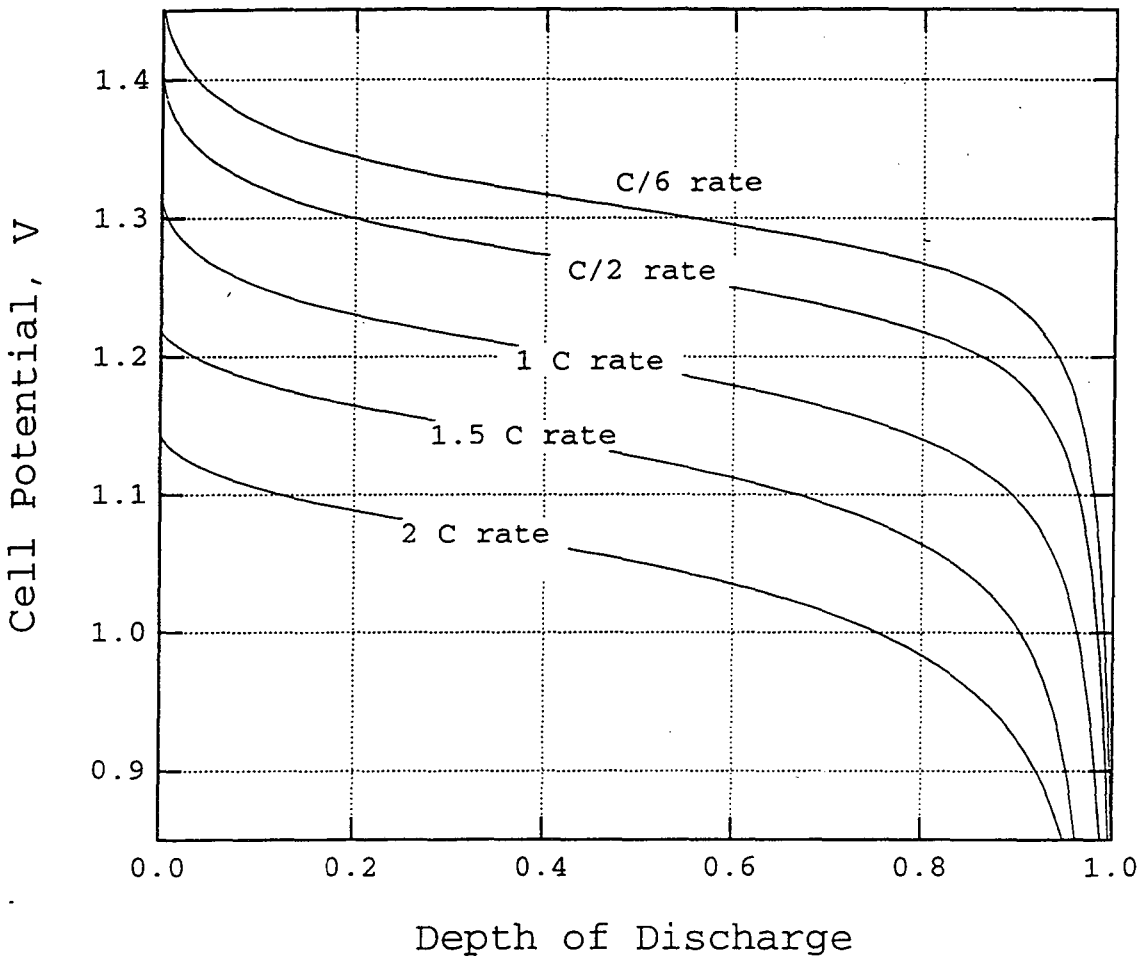

Figure 2-4: Sample discharge curves for the nickel oxide/$LaNi_5$ battery system. Parameters for these simulations are contained in tables 2-1 and 2-2. The Nernstian behavior of the nickel oxide electrode dominates the form of these curves.

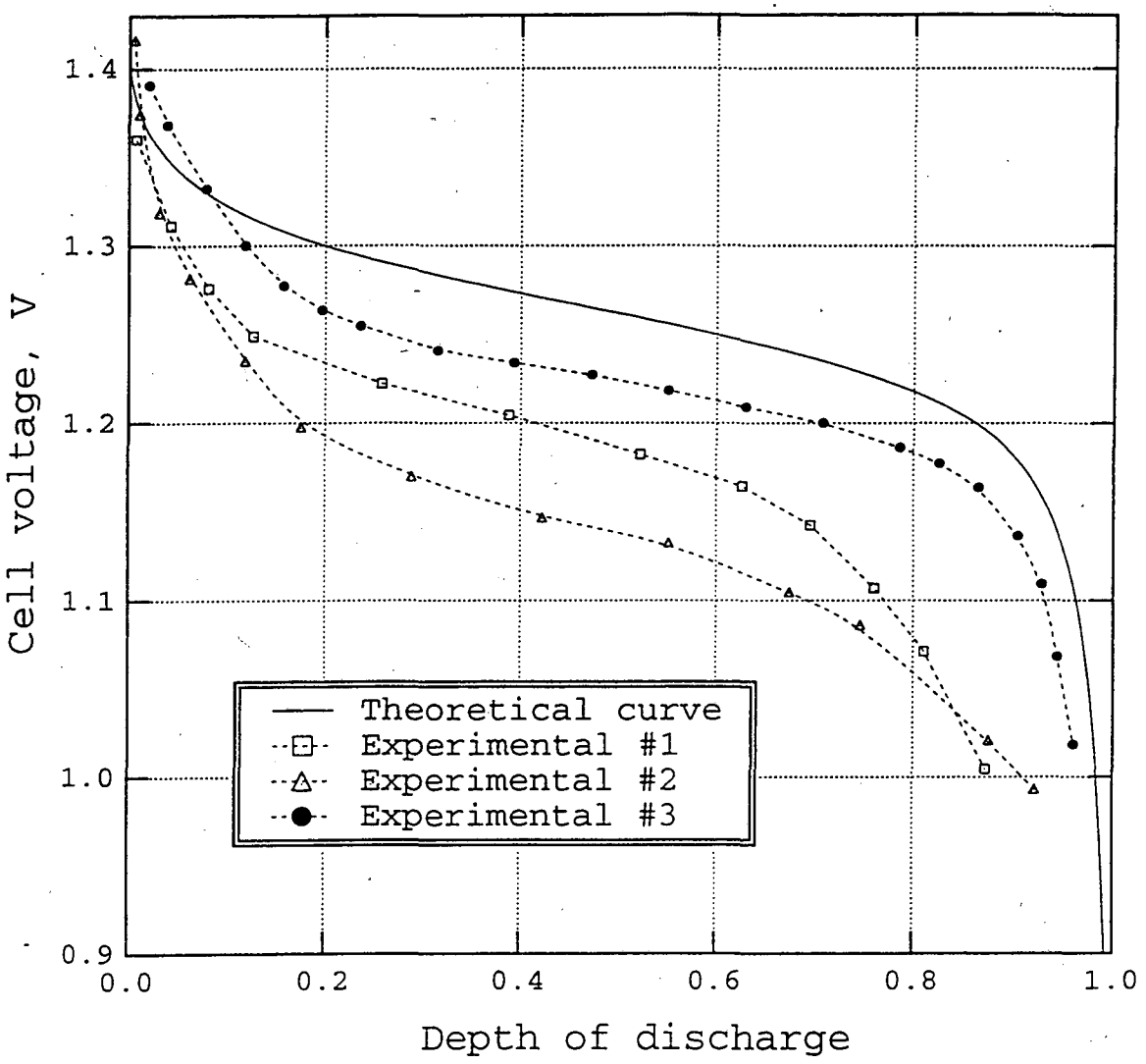

Figure 2-5: A theoretical discharge curve at the 0.5 C rate is compared to three discharge curves at the same rate from references 34 and 35. Since the cells used in the experimental determinations were not well characterized, a detailed analysis of differences between the experimental and theoretical curves is not possible.

material loadings, porosities, electrode and separator thicknesses, and filler concentrations were unavailable for these experiments. Therefore, a detailed analysis of the differences between the theoretical and experiment curves is not possible.

The nickel oxide electrode is known to be activation limited. To explore the degree of this limitation, a potential map was constructed for the one hour discharge rate. Figure 2-6 presents the three major contributions to the potential drop across the cell: the potential loss across the solid/solution interface of the negative electrode, the potential drop across the separator, and the potential loss across the solid/solution interface at the positive electrode. The curves in this figure show the cumulative effect of these potential drops across the cell. Because of the definitions of Φ_1 and Φ_2, the potential losses at the solid/solution interfaces are a combination of the activation potential and the open-circuit potential of each electrode material. The approximate value of the activation potential at each electrode can be determined by evaluating $\Phi_1-\Phi_2$ at 50% depth of discharge. The simulation for this figure was performed at the 1 C discharge rate.

As this figure demonstrates, the activation potential at the nickel oxide electrode is the largest potential limitation of this system. As mentioned previously (Section 1.3), only one source of data could be found for all the kinetic parameters of the nickel oxide electrode, a Ph.D. thesis by Sinha.[9] Since this is the major limitation of the system, a closer look at this data source is in order.

Manojit Sinha's thesis consists of a model of the nickel oxide electrode and results from several experiments designed to measure the kinetic parameters of the nickel electrode. To prepare the nickel active material for the kinetic experiments, he deposited a hydroxide film from a solution of 1.8 molar nickel nitrate and 0.2 molar cobalt nitrate onto the end of a 3.175 mm diameter nickel rod. To measure the film thickness, he spread a layer of epoxy over the film surface and then cut the epoxy-coated nickel rod in half in

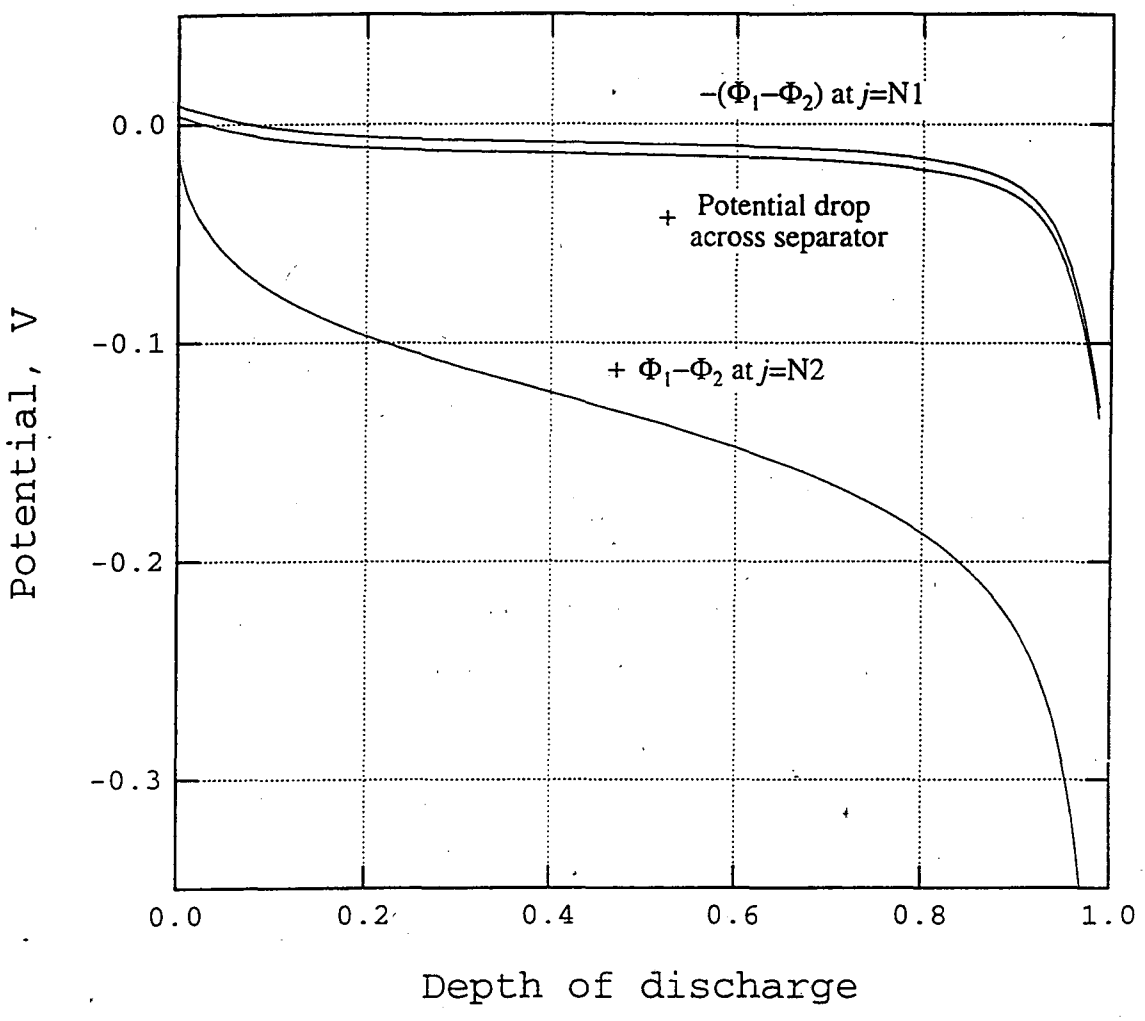

Figure 2-6: The three main sources of potential loss in the discharging cell are shown above for a 1 C discharge rate. The largest loss is due to the activation potential at the nickel oxide electrode. Positive "potential losses" for the negative electrode near full charge are due to the selection of the reference electrode.

order to obtain a side-on view of the deposited hydroxide. From the SEM images he presents, it can be seen that the film is very rough and, in some places, cracked. Sinha does not discuss the complications that arise due to a rough or cracked film and never explicitly states what surface area he used to calculate the exchange current density. It is assumed by this author that he used the cross-sectional area of the rod as the surface area for his calculations. The obvious conclusion from this assumption is that the actual exchange current density could be significantly lower than the one he presents and therefore lower than the one used in this model.

Since the activation potential at the nickel electrode is large and since few data exist for these kinetic parameters, the effect of this parameter on cell performance is of great importance in the design of battery systems containing the nickel oxide electrode. Figure 2-7 presents discharge curves of the cell for various values of the exchange current density of the nickel electrode. Doubling the exchange current density (from its value of 1.04×10^{-4} A/cm^2) has the effect of enhancing the cell voltage by about 30 mV, and halving this parameter has the effect of depressing the cell voltage by about 60 mV. The cell potential decreases severely for exchange current densities below about 5×10^{-5} A/cm^2. These results lead us to conclude that the actual exchange current density of nickel oxide cannot be much lower than the one that is presented by Sinha since the nickel electrode does not exhibit such severe polarizations as those shown by some of the discharge curves in figure 2-7.

There has been considerable speculation about the role of the variable electronic conductivity of nickel oxide as a limitation during discharge. Although it has apparently been known for some time that fully discharged nickel oxide is a very poor electronic conductor,[17] experimental data for this system are scant. The few papers that exist on the subject[22,23,24] do not agree with each other even within an order of magnitude (see discussion in section 1.3). This is one of the reasons that the electronic conductivity of nickel oxide is not included in this study as a function of the state of charge. The other

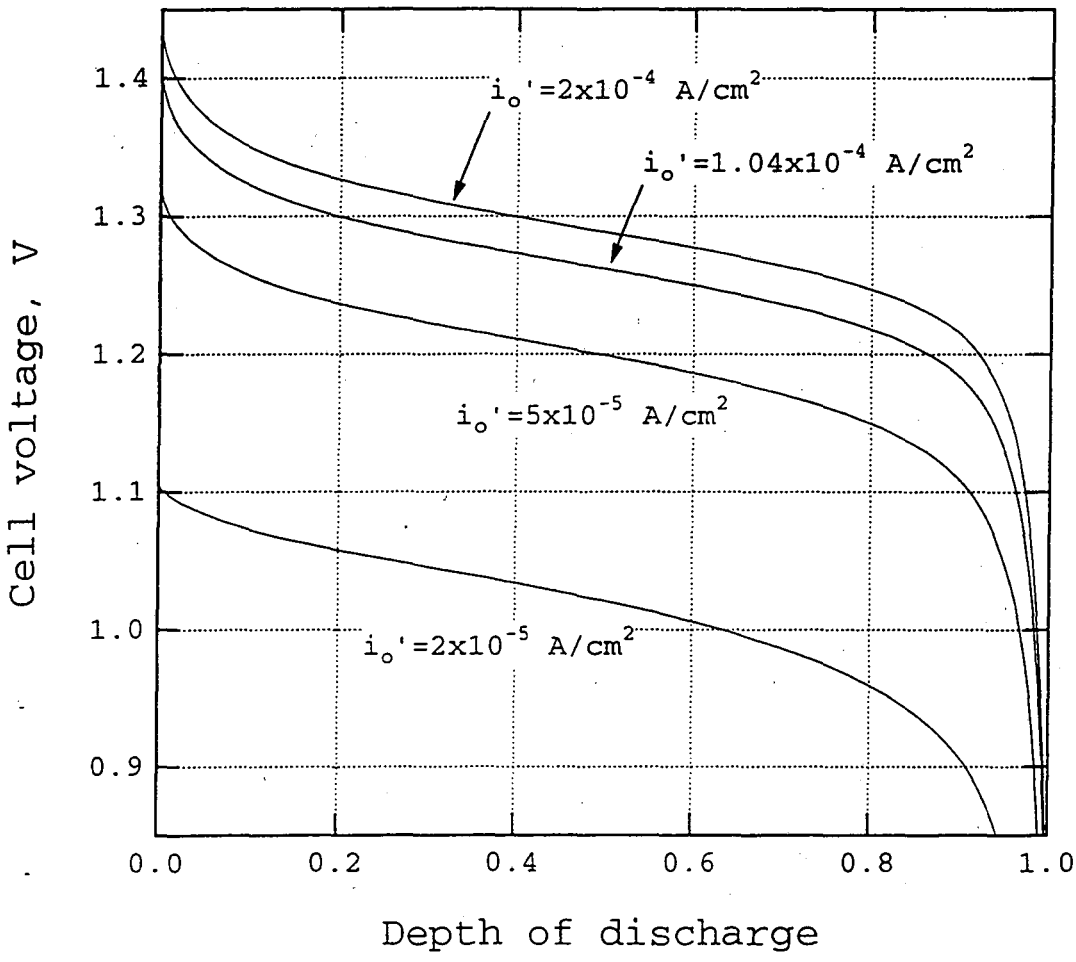

Figure 2-7: Effect of the exchange current density of the nickel oxide electrode on simulated discharge curves. The cell potential drops sharply below a value of $i_o'=5x10^{-5}$ A/cm^2.

main reason is that additives are currently used by battery manufacturers to enhance the electronic conductivity of nickel active material. These additives can be carbon, nickel metal flakes or powder, or most importantly, cobalt hydroxide.[20,25]

The mechanism of passivation that has been proposed is that as a single particle (or film) of nickel oxide discharges, the state of charge of the exterior portion of the film reduces before that of the interior. This leads to the conductivity of the exterior portion decreasing rapidly, effectively limiting the transport of electrons from the film's interior to the solid/solution interface. (This mechanism occurs concurrently with a reduction in the diffusivity of hydrogen at the edge of the film, which reduces the ability of hydrogen to diffuse through the film, also.) A one-dimensional model, such as this one, is of very limited use in looking at a phenomenon so complex, because the model implicitly assumes that the solid-phase transport properties are constant. Even so, we can determine a constant value of the electronic conductivity that will cause transport of electrons to become an important limitation in the electrode. It was found that a bulk electronic conductivity of 0.1 S/cm was necessary to cause a potential drop of approximately 10 mV across the solid phase of the nickel electrode during discharge.

Figure 2-8 presents some electrolyte concentration profiles across the cell during a one hour discharge. As shown in this figure, the concentration profile develops quickly, essentially becoming fully developed in about six minutes. The concentration polarization in this cell is shown not to be severe; the total concentration difference across the cell at this discharge rate is less than 0.9 molar.

Per the findings of Sinha,[9] the convective component of the solution-phase transport was not incorporated into this model. Based on the results shown in figure 2-8, we can test to see whether this was a good assumption. Since the flux of the electrolyte is given by the equation

$$N_{-} = -\varepsilon D \nabla c - \frac{t_{-}^{0}}{F} i_2 + c v^{\blacksquare} \qquad (2\text{-}3)$$

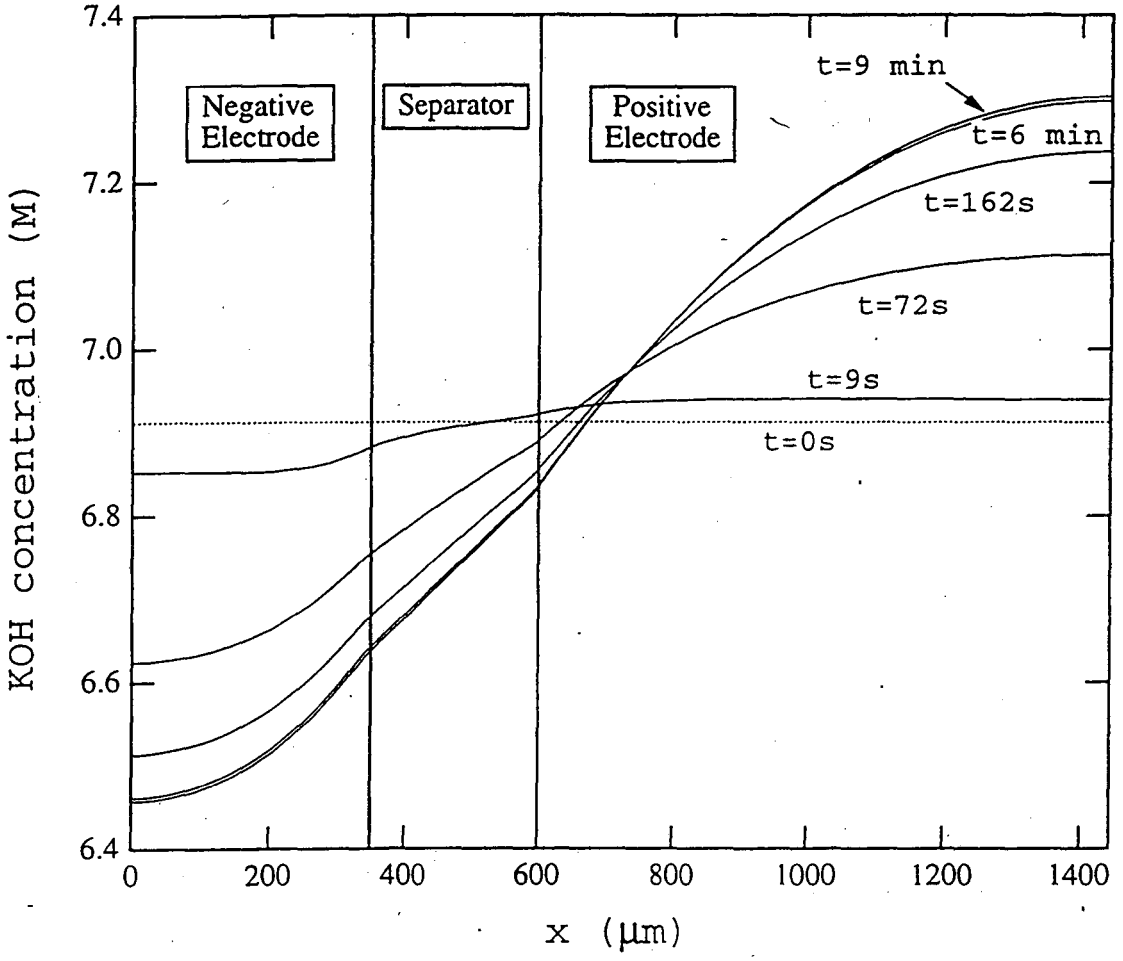

Figure 2-8: Concentration profiles developing in a cell at the 1 C discharge rate. The profile is essentially fully developed after one-tenth of the total discharge time. The original concentration in the cell is 6.91 M (30 wt%).

we can evaluate each of these terms and compare their magnitudes. The first two terms were calculated assuming that ε=0.39, Δc = 0.9 M, and i_2=I, with the Δc term coming from the simulation results. The last term was calculated by evaluating the partial molar volumes of the solvent and electrolyte,[6] $\overline{V}_0$ and $\overline{V}_e$, at c=6.91 M, setting i_2=I, and using the equation[1]

$$v^{\blacksquare} = i_2 \left[\frac{\overline{V}_0}{F} - \frac{\overline{V}_e}{F}(1-t_-^0) \right] \tag{2-31}$$

This last term, therefore, does not depend on the simulation results, but is an average value one would expect for this system.

Table 2-3: Estimates of the magnitude of the individual contributions to the solution-phase transport of KOH.

Component of the Flux	Magnitude (mol/cm^2 s)
Diffusion $(-\varepsilon D \nabla c)$	-1.0×10^{-7}
Migration $\left(-\frac{t_-^0}{F} i_2\right)$	-4.0×10^{-7}
Convection $(+cv^{\blacksquare})$	$+4.7\times10^{-8}$

We can see from this table that the convective term is a factor of two less than that of the diffusion term and an order of magnitude less than the migration term. A convective flux which is 10% of the total flux might change the concentration variations by, at most, 10%, thus having an even smaller percentage change in the total concentration. The influence of this on the cell potential , through the reaction kinetics, should be even smaller. Similarly, Pollard found that changing the convective velocity, in another battery simulation, had no discernable effect on the results.[36]

Figure 2-9 presents the reaction rate distribution in the negative electrode at selected times during a two hour discharge. As with other electrode materials which do not have open-circuit potentials that are strong functions of composition,[26] this electrode shows interesting reaction distributions as the discharge proceeds. The open-circuit potential of $LaNi_5$ as a function of the hydrogen concentration in the lattice is shown in figure 2-10.

As can be seen in figure 2-9, during the first half of the discharge, the reaction distribution remains qualitatively unchanged. The reaction proceeds preferentially at the front of the electrode due to the accessibility to the reactant species diffusing across the separator from the positive electrode. After the first half of discharge, as the active material at the front of the electrode becomes depleted, the peak of the reaction distribution moves to the rear of the electrode in a wave-like fashion. This can be seen in the sequential reaction distribution curves at 72, 84, and 96 minutes. Towards the end of discharge, the reaction rate begins to "level out" again as can be seen in the last curve at 112 minutes. This leveling out is due to the fact that the open-circuit potential of this material begins to slope strongly when the active material reaches about 10% state of charge (as can be seen in figure 2-10).

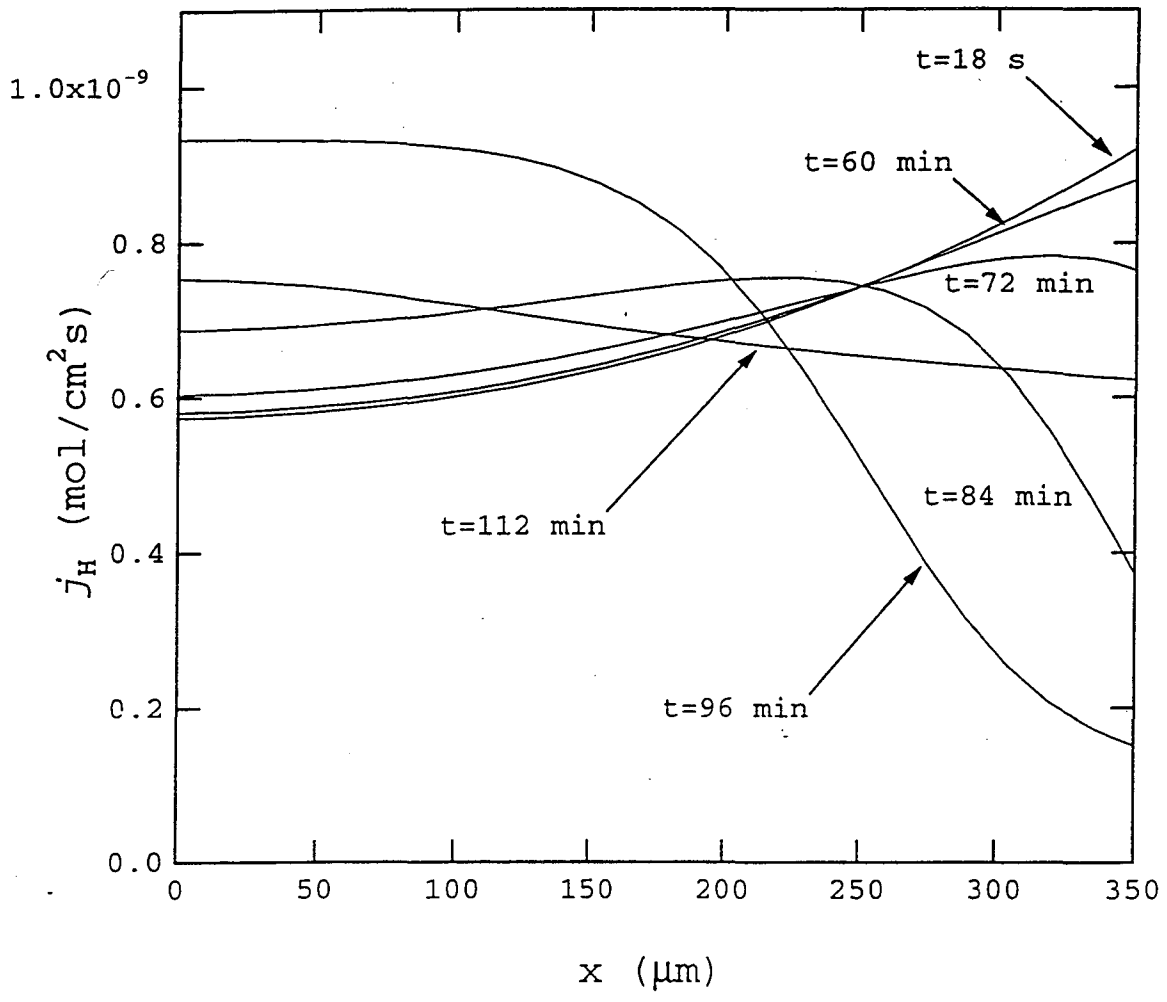

Figure 2-9: The absolute value of the pore wall flux of hydrogen in the negative electrode at selected times during discharge. The pore wall flux is proportional to the reaction rate. This discharge is at the C/2 rate.

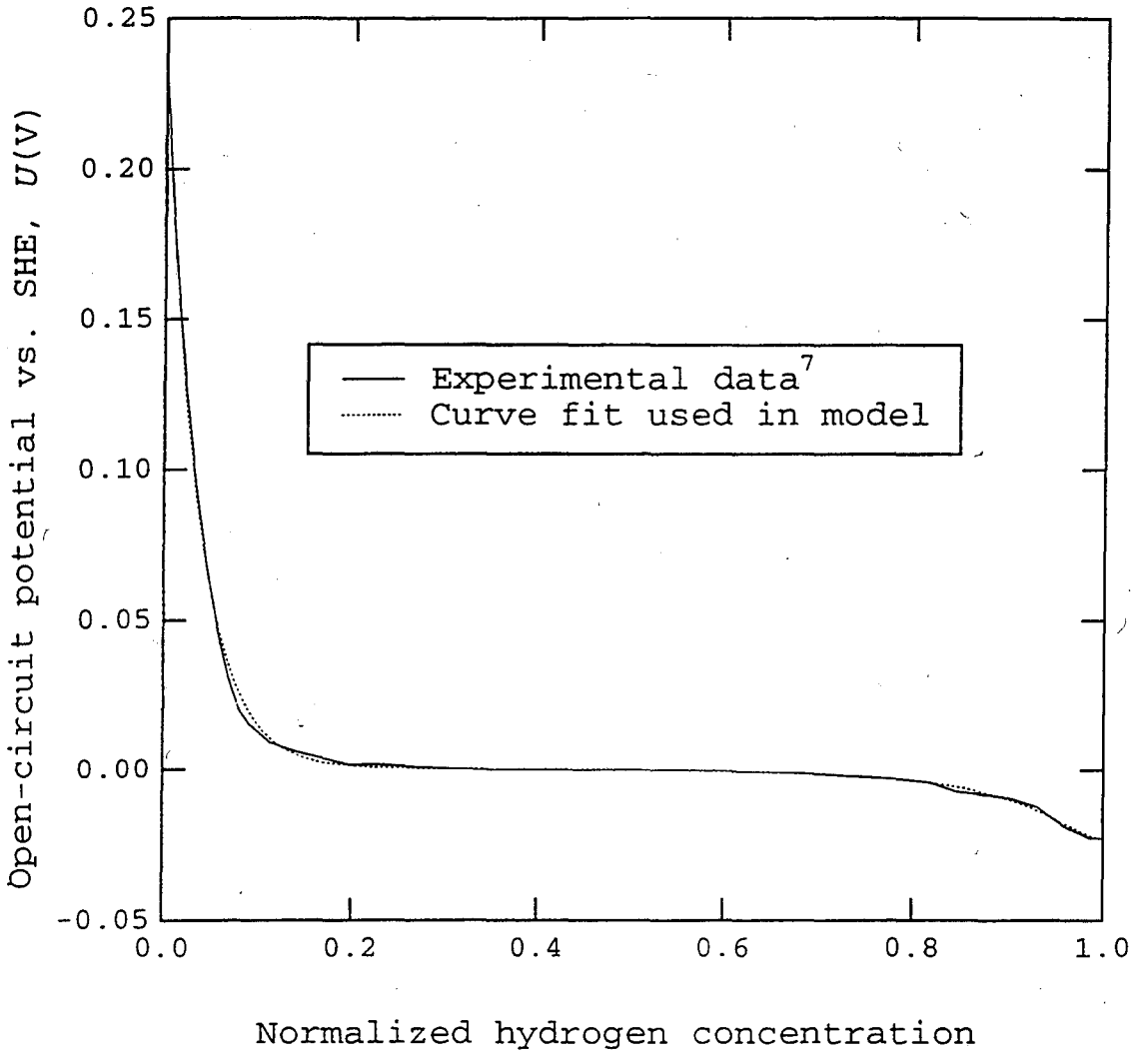

Figure 2-10: The open-circuit potential of $LaNi_5$ as measured by Willems.[7] The curve fit used in the model is also shown.

2.4 Optimization of the nickel oxide/$LaNi_5$ cell undergoing discharge

By varying the parameters of the nickel oxide/$LaNi_5$ cell, we can optimize this system's performance. For the following analyses, the electrode thicknesses and the electrode porosities of the cell are optimized in terms of specific energy and average specific power. For these simulations, all the electrode properties are those that appear in tables 2-1 and 2-2, except for the properties that are being varied. Since these optimizations are performed in terms of the specific energy and the average specific power of the cell, they are a measure of performance on a "per mass" basis. The mass by which the actual energy and power are divided is the combined mass of the composite electrode materials, the separator, and the electrolyte occupying the pores of these regions.

The first optimization is performed by varying the thickness of the electrodes. Several Ragone plots are presented in figure 2-11. The curves are presented in terms of the negative electrode thickness, but during these simulations, the ratio of the thicknesses of the electrodes was kept constant so that the relative capacities of the electrodes would not change. The thickness of the separator was kept constant at 250 μm. It can be seen from these plots that in the "knee" region of the curves, where a tradeoff between specific energy and specific power exists, the performance of the system increases as the negative electrode thickness is decreased from 700 μm to about 350 μm. This is due to a reduction in the ohmic drop across the cell, which is approximately proportional to the thickness of the electrodes. For electrodes thinner than about 350 μm, the performance of the cell begins to decrease, since the weight of the separator begins to be a significant fraction of the total weight of the cell.

The discharge times in the "knee" region of the graph are less than 30 minutes. For the longer discharge times associated with the operation of consumer electronics and electric vehicles, it is more difficult, on this graph, to determine where the maximum

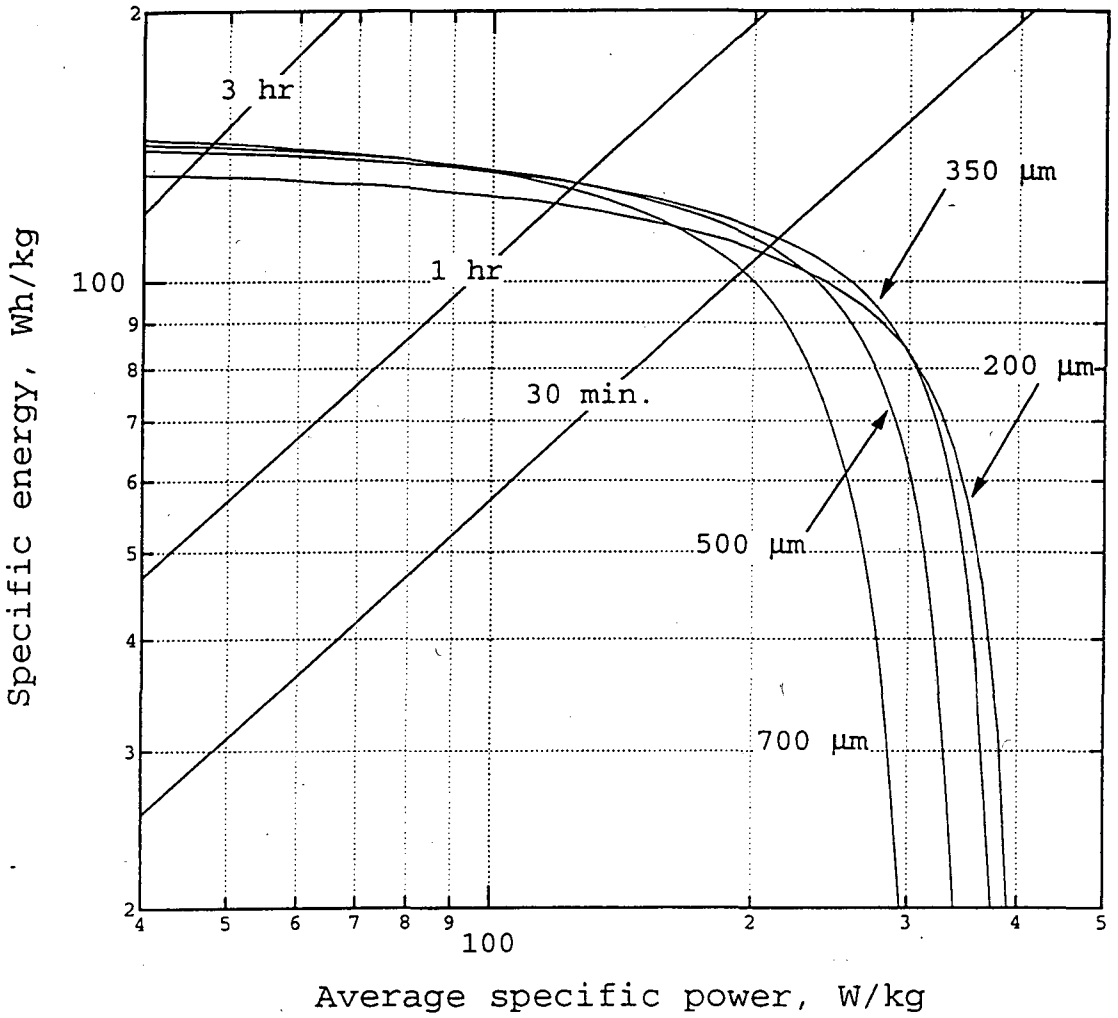

Figure 2-11: Ragone plots obtained by varying the thickness of the negative electrode. The ratio of the electrode thicknesses was kept constant, and the thickness of the separator was kept constant at 250 micrometers.

energy and power exist for a given discharge rate. In figure 2-12, the specific energy of the cell is graphed as a function of the negative electrode thickness for a three-hour and a one-hour discharge time. Since the actual discharge time (as opposed to theoretical maximum discharge time) was kept constant for the simulations used to construct each of these curves, the average specific power is directly proportional to the specific energy released by the cell. For the one-hour discharge time, the maximum energy occurs at a negative electrode thickness of about 500 μm. For the three-hour discharge time, the maximum energy occurs at about 700 μm. A relatively large "plateau" exists around the maximum for the three-hour discharge; from a negative electrode thickness of 550 μm to about 1000 μm the specific energy is within 1% of its maximum value. This suggests that there may be some design flexibility available if other considerations dictate thinner or thicker electrodes than the value at which the maximum specific energy occurs. (Note: the small fluctuations in these, otherwise continuous, curves appear to be just numerical artifacts that result from a rounding off of the electrode thicknesses in order to ensure that the electrode/separator interfaces lie exactly at a mesh point.)

The effect of the electrode porosity on the specific energy and power was examined also. For these simulations, as the porosity of an electrode was decreased, the corresponding volume fraction of the active material/filler mixture was increased. In addition, since we assume that the electrode is composed of idealized spherical particles, the specific surface area of the electrode follows the simple geometric relationship

$$a = \frac{3\varepsilon_{act}}{R} \tag{2-32}$$

For an electrode consisting of same-sized particles, this relationship rigorously holds only for porosities greater than ≈0.26. For these simulations, though, it is assumed that this

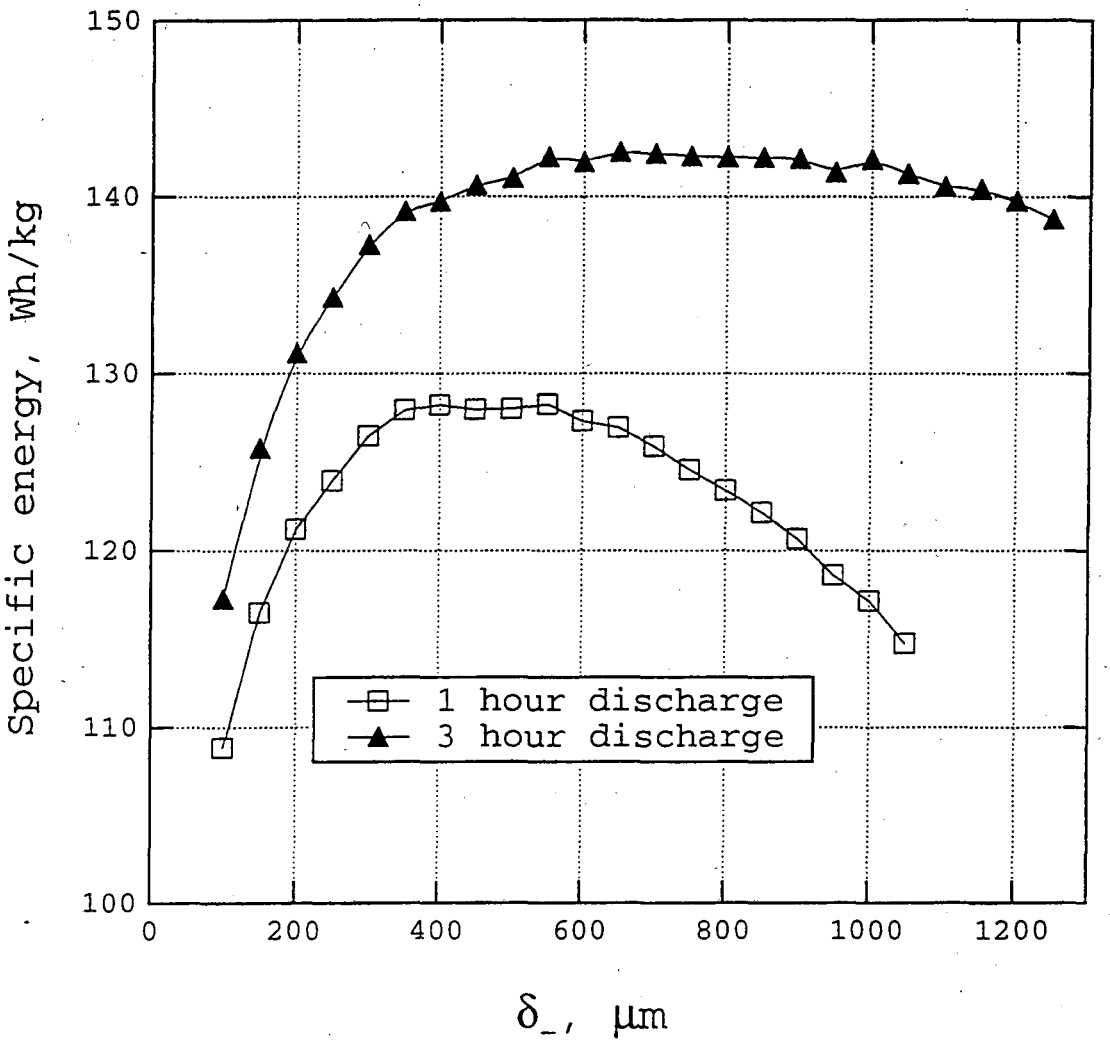

Figure 2-12: The specific energy as a function of the negative electrode thickness for two discharge times. The ratio of the positive and negative electrode thicknesses was kept constant for these simulations.

relationship holds for porosities less than this value. This could be possible if there were a distribution of particle sizes in the electrode.

With these assumptions made, when the porosity is decreased, diffusion limitations will increase while kinetic limitations will decrease and the active material loadings will increase. The other specifications incorporated into this analysis are that (1) the ratio of the active material volume fraction to the volume fraction of the filler in each electrode is 7:1, (2) the porosities of the electrodes are set equal to each other, and (3) the ratio of positive to negative electrode capacity is kept constant.

Figure 2-13 shows Ragone plots for porosities of 0.2 to 0.6. In the "knee" region it can be seen that the performance of the cell increases as the porosity is decreased from 0.6 to a value of about 0.3. Below this value, diffusion limitations start to dominate the system behavior. Figure 2-14 shows the theoretical optimum porosity for discharge times of one and three hours. The theoretically ideal porosity for a one-hour discharge is 0.22, and that for a three-hour discharge is 0.14. Since this theoretical analysis assumes that the electrode material is completely wetted by the electrolyte and that the surface area increases for decreasing porosity, even at very low porosities, this analysis should be considered only to set the lowest bounds for the porosity at which the true maximum in specific energy might occur.

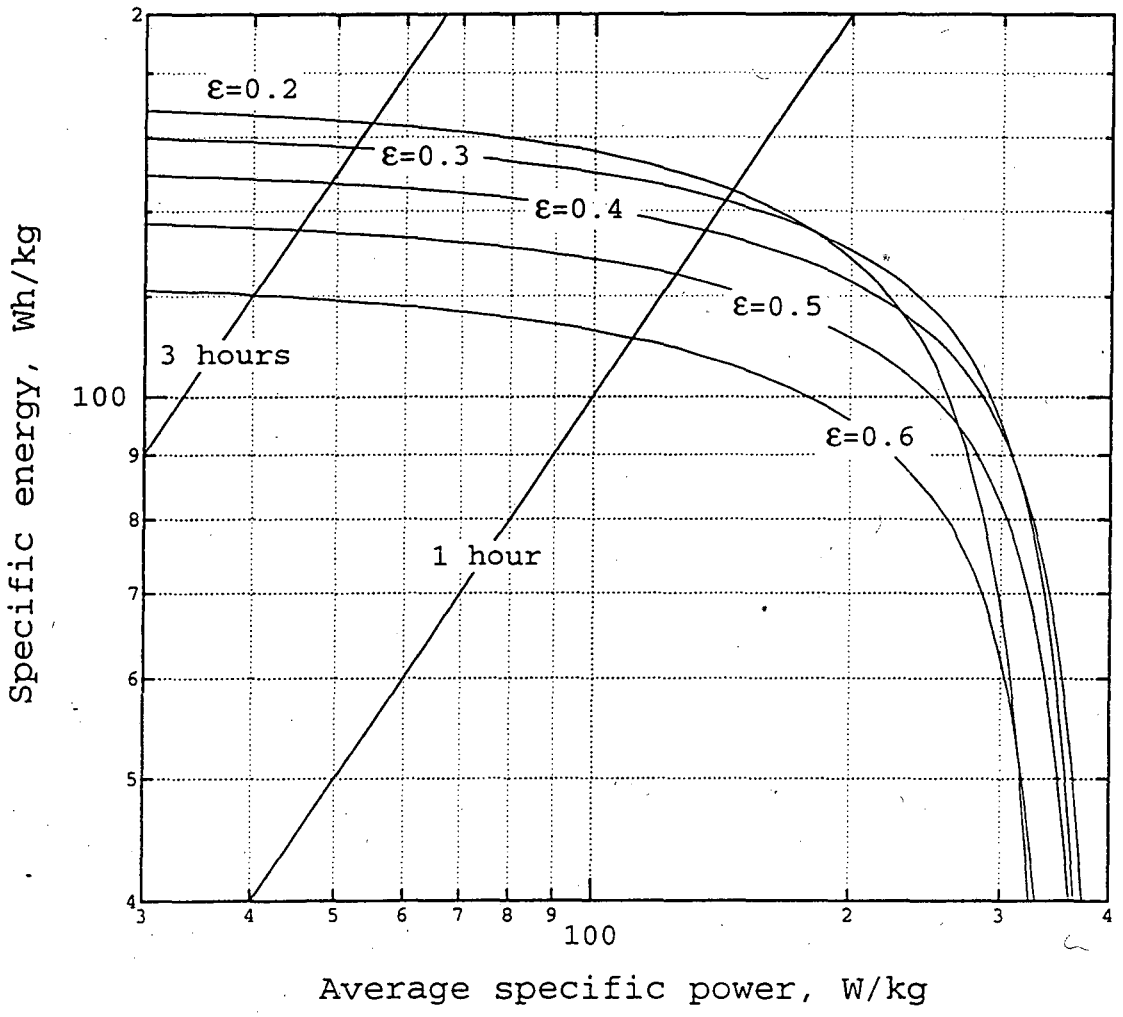

Figure 2-13: Ragone plots obtained by varying the porosity of both electrodes. Diffusion limitations are not significant until the porosity drops below a value of about 0.3.

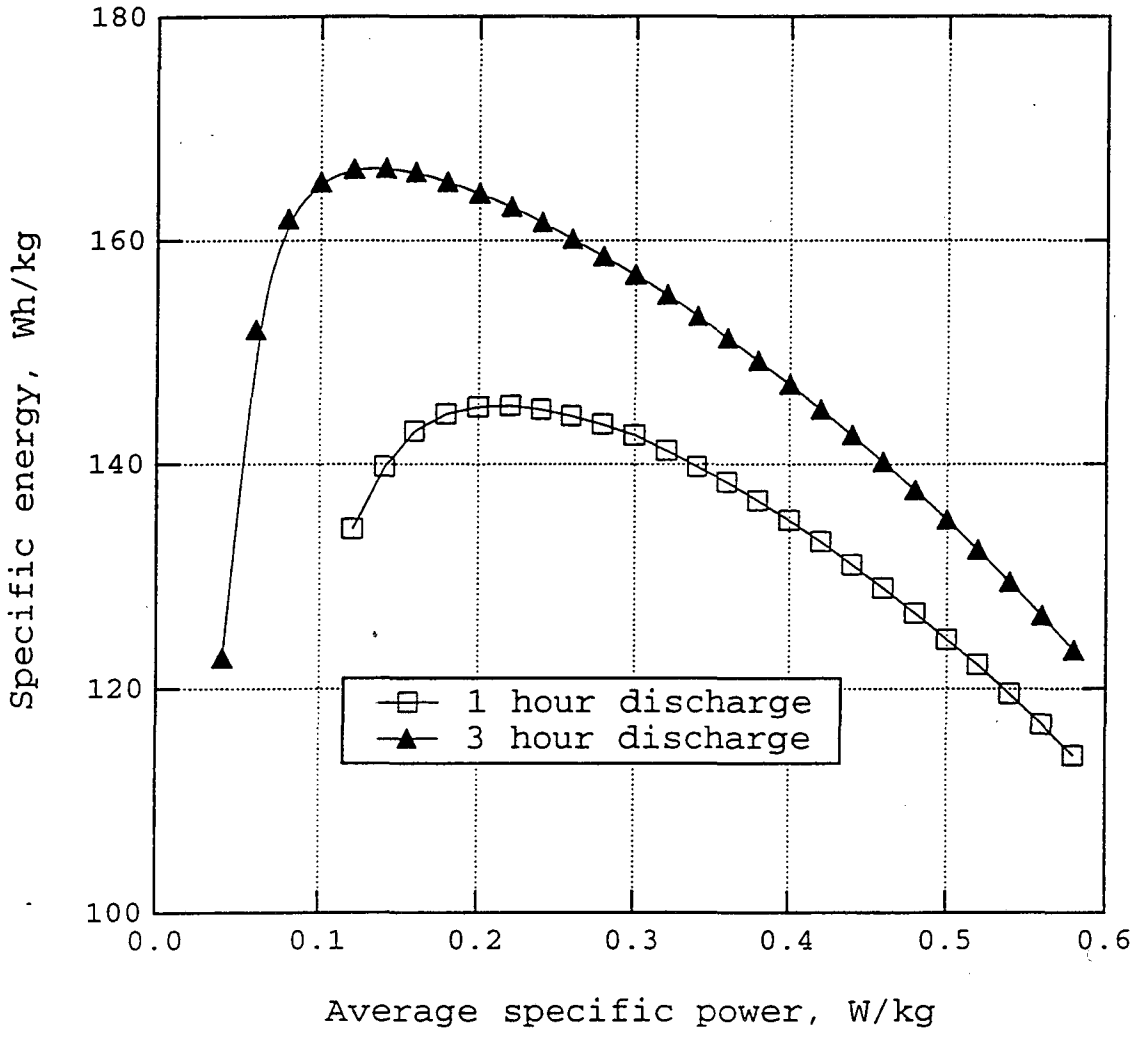

Figure 2-14: The specific energy as a function of electrode porosity for two rates of discharge. The specific surface area of the electrodes was allowed to vary with the porosity.

2.5 Explanation of some sources of data for the model

Nickel oxide

Because of the interference with the oxygen evolution reaction, the "true" open-circuit potential of the intercalation reaction in nickel oxide is virtually impossible to obtain.[13] Therefore we are forced to make an educated guess of the nature of the open-circuit potential function by experimentally observing the potential of the electrode at slow discharge rates. Several authors have published experimental discharge curves for nickel oxide.[14,15,16,17] Two main features of these discharge curves can be noted: (a) during most of the discharge, the curves appear approximately Nernstian, and (b) at low states of charge the potential slope is steeper than the that predicted by Nernstian thermodynamics.

This second feature of the experimental discharge curves is confirmed by the data of Conway and Geliadi[13] when they measure "reversible potentials" of nickel oxide at low states of charge where the rate of the oxygen side reaction is negligible. The equation used in the model appears below in terms of c_n, the normalized electrochemically active hydrogen concentration in the lattice, where $c_n=c_s/c_t$. The second part of the function in the equation is a curve fit of the data of Conway and Geleadi at very low states of charge. The overall function of equation (2-33) was made continuous by finding the point where the first derivatives of the two functions matched.

$$f(c_s) = \begin{cases} \frac{RT}{F}\ln\frac{(1-c_n)}{c_n} & c_n \le 0.9455 \\ -0.052335 - 0.054284\exp(-18.652(1-c_n)) - 0.37142\exp(-104.15(1-c_n)) & 0.9455 \le c_n \le 1 \end{cases} \quad (2\text{-}33)$$

$LaNi_5$

The open-circuit potential of $LaNi_5$[7] was fit to the function

$$U \text{ (vs. SHE)} = 9.712\times 10^{-4} + 0.23724 \exp(-28.057 c_n) - \frac{2.7302\times 10^{-4}}{((c_n - 1.01989)^2 + 0.010768)} \quad (2\text{-}34)$$

where c_n is the normalized concentration of hydrogen in the active material (see figure 2-10).

KOH Solution

All of the following data were fit to functions of c, the electrolyte concentration, with the units of moles/cm^3. Some of the data have theoretical dependences on concentration that differ from the functional form of the curve fits below. This is because the data needed to be fit only at higher solute concentrations where these functions provided more accuracy. All the curve fits below apply, at least, to the range of 1 M < c < 14 M except for the activity coefficient of water in KOH solution which is only strictly applicable up to 6M; values beyond this concentration must be extrapolated from the function given below. The density of KOH[27] was fit to the following function.

$$\rho \text{ (g/cm}^3) = 1.001 + 47.52c - 776.22c^2 \quad (2\text{-}35)$$

The mean molar activity coefficient[29] was fit to the function

$$f_{\pm} = 0.7002 + 28.992c + 19438c^2 ; \quad (2\text{-}36)$$

the activity coefficient of water in KOH was determined from the above data using the Gibbs-Duhem equation and fit to the function

$$f_{H_2O} = 1.0002 + 2.1251c - 2016.8c^2 + 40378c^3 \; ; \qquad (2\text{-}37)$$

the differential diffusion coefficient[30] was fit to the function

$$D\ (\mathrm{cm^2/s}) = 2.8509\times 10^{-5} - 2.9659\times 10^{-4}c^{1/2} + 0.013768c - 0.14199c^{3/2} + 0.42661c^2 \; ; \qquad (2\text{-}38)$$

and the conductivity[28] was fit to the function

$$\kappa\ (\mathrm{S/cm}) = 0.02325 + 210.95c - 22077c^2 + 6.2907\mathrm{x}10^5c^3 \; . \qquad (2\text{-}39)$$

Note: The functions presented above for the mean molar activity coefficient of KOH and the activity coefficient for the solvent, which were used in the model, are incorrect. The correct functions are

$$f_{\pm} = 1.004 - 36.23c^{1/2} + 1374.3c - 17850.7c^{3/2} + 55406c^2 + 7.16856\times 10^5c^{5/2} \qquad (2\text{-}40)$$

$$f_{H_2O} = 1.0002 - 21.238c - 4131.2c^2 \qquad (2\text{-}41)$$

Upon realizing this error, the correct functions were inserted into the model. In no cases was the new output of the model more than 0.5% different from the previous output.

List of symbols

(The following list of symbols applies to all chapters of the text.)

a	specific interfacial area, cm^2/cm^3
$a_{\pm}$, a_0	mean molar activity of the electrolyte and activity of water in the solution, mol/cm^3
c, c_0	concentration of the salt and water in the electrolytic solution, mol/cm^3
c_H	concentration of hydrogen inside a particle, mol/cm^3
c_s	concentration of hydrogen at the surface of a particle, mol/cm^3
c_t	maximum concentration of hydrogen in a particle, mol/cm^3
D, D_s	diffusion coefficient of the electrolytic solution and of hydrogen in the solid phase, cm^2/s
$f_{\pm}$	mean molar activity coefficient of KOH
F	Faraday's constant, 96487 C/eq.
i	current density, A/cm^2
i_0, i_0'	exchange current density and the reference exchange current density, A/cm^2
I	superficial current density, A/cm^2
j_n	pore wall flux of species n across the solid/solution interface, mol/cm^2 s
N_i	flux of species i in the solvent, mol/cm^2 s
r	radial distance from the center of a particle of active material, cm
R	universal gas constant, 8.314 J/mol K
R_s	radius of a particle of active material, cm
t	time, s
t_i^0	transference number of species i
T	temperature, K
U, U^{θ}	open-circuit potential and open-circuit potential at 50% state of charge of an electrode, V
$v^{\blacksquare}$	volume average velocity of the solution, cm/s
x	distance from the current collector of the negative electrode, cm

α_a, α_c	anodic and cathodic apparent transfer coefficients
δ_-, δ_+, δ_s	thickness of the negative electrode, positive electrode, and separator; cm
ε	porosity
η_s	overpotential at the electrode/electrolyte interface, V
κ	conductivity of the electrolyte, S/cm
ρ, ρ_s	density of the solution and solid phases, g/cm^3
σ	conductivity of the solid phase, S/cm
Φ	electrical potential or the potential measured with respect to a reference (as defined in text), V

Subscripts

f	filler
s	solid phase or separator
0	water in the electrolytic solution or a transport property measured outside of any porous structure
1	solid phase
2	solution phase
+	positive electrode or cation
–	negative electrode or anion

Superscripts

o	the "old" value of a variable during the numerical solution procedure

References

(1) J. Newman and W. Tiedemann, "Porous-Electrode Theory with Battery Applications," *AIChE Journal*, **21**, 25 (1975).

(2) J. Newman, D. Bennion, and C. Tobias, "Mass Transfer in Concentrated Binary Electrolytes," *Berichte der Bunsengesellschaft*, **69**, 608 (1965).

(3) S. Lengyel, J. Giber, Gy. Beke, and A. Vertes, "Determination of the Transference Numbers in Concentrated Aqueous Solutions of Sodium and Potassium Hydroxide," *Acta Chim. Hung. Tomus*, **39**, 357 (1963).

(4) A. Guegan, M. Latroche, J. Achard, Y. Chabre, and J. Bouet, "Correlations Between the Structural and Thermodynamic Properties of $LaNi_5$ Type Hydrides and Their Electrodes' Performances," Abstract No. 53, Electrochemical Society Meeting in Miami, 1994.

(5) G. Davolio, A. Da Pieve, and E. Soragni; "On the Mechanical Properties of Nickel Oxide Electrodes," p. 197, *Nickel Hydroxide Electrodes* Vol. 90-4, D. Corrigan, editor. Electrochemical Society, Inc., Pennington, NJ, 1990.

(6) J. Newman, *Electrochemical Systems*, 2nd ed., Prentice Hall, Inc., 1991.

(7) J. Willems, "Metal Hydride Electrodes Stability of $LaNi_5$-Related Compounds," *Phillips Journal of Research*, **39**, 1 (1984).

(8) P. Bourgault and B. Conway, "The Electrochemical Behavior of the Nickel Oxide Electrode - Part II. Quasi-Equilibrium Behavior," *Canadian Journal of Chemistry*, **38**, 1557 (1960).

(9) Manojit Sinha, *A Mathematical Model for the Porous Nickel Hydroxide Electrode*, dissertation, University of California at Los Angeles, 1982.

(10) T. Halstead, N. Abood, and K. Buschow, "Study of the Diffusion of Hydrogen in $LaNi_{5+x}H_6$ compounds by ^1H NMR Relaxation," *Solid State Communications*, **19**, 425 (1976).

(11) B. Ratnakumar, C. Witham, B. Fultz, and G. Halpert, "Electrochemical Evaluation of La-Ni-Sn Metal Hydride Alloys," *J. Electrochem. Soc.*, **141**, L89 (1994).

(12) J. Newman and T. Chapman, "Restricted Diffusion in Binary Solution," *AIChE Journal*, **19**, 343 (1973).

(13) B. Conway and E. Gileadi, "Electrochemistry of the Nickel Oxide Electrode - Part IV. Electrochemical Kinetic Studies of Reversible Potentials as a Function of Degree of Oxidation," *Canadian Journal of Chemistry*, **40**, 1933 (1962).

(14) A. Zimmerman and P. Effa, "Efficiency and Utilization in Nickel Electrodes," Proceedings of the 18th Intersociety Energy Conversion Engineering Conference, Orlando, p. 1508. American Institute of Chemical Engineers, New York (1983).

(15) J. Weidner and P. Timmerman, "Effect of Proton Diffusion, Electron Conductivity, and Charge-Transfer Resistance on Nickel Hydroxide Discharge Curves," *J. Electrochem. Soc.*, **141**, 346 (1994).

(16) J. Bouet and F. Richard, "A Discharge Model for the Ni Hydroxide Positive Electrode," *176th Meeting of the Electrochemical Society*, (1989).

(17) P. Milner and U. Thomas, "The Nickel-Cadmium Cell" (review). From *Advances in Electrochemistry and Electrochemical Engineering - Volume 5.* P. Delahay and C. Tobias, editors. John Wiley and Sons, New York (1967).

(18) G. Davolio, A. Da Pieve, and E. Soragni, "On the Mechanical Stability of Nickel Oxide Electrodes," From *Nickel Hydroxide Electrodes*, D. Corrigan, editor. p. 281, The Electrochemical Society (1990).

(19) A. Zimmerman and P. Effa, "Nickel Hydroxide Active Material Densities," Report SD-TR-88-02, The Aerospace Corporation, Los Angeles (1988).

(20) D. Berndt, *Maintenance-free Batteries*. Research Studies Press. Somerset, England (1993).

(21) H. Züchner and T. Rauf, "Electrochemical Measurements of Hydrogen Diffusion in the Intermetallic Compound $LaNi_5$," *Journal of the Less-Common Metals*, **172-174**, 611 (1991).

(22) V. Z. Barsukov and L. Sagoyan, "Calculation of the Charge-storage Capacity of Metal-ceramic Electrodes of Chemical Current Sources II. Calculation of Steady-state Potential," *Soviet Electrochemistry*, **9**, 1392 (1973).

(23) M. Natan, D. Bélanger, M. Carpenter, and M. Wrighton, "pH-Sensitive $Ni(OH)_2$-Based Microelectrochemical Transistors," *J. Phys. Chem.*, **91**, 1834 (1987).

(24) A. Lun'kov, S. Milovkanov, and D. Oleinikova, "High Frequency Impedance Study of Conductivity and Dielectric Permitivity of Active Mass of Nickel Oxide Electrodes," *Soviet Electrochemistry*, **24**, 1365 (1988).

(25) V. Barsukov, L. Sagoyan, N. Meshcheryakova, and A. Gerasimov, "Mechanism of the Effect of Cobalt Addition on the Properties of the Nickel Oxide Electrode," *Soviet Electrochemistry*, **21**, 17 (1985).

(26) T. Fuller, M. Doyle, and J. Newman, "Simulation and Optimization of the Dual Lithium Ion Insertion Cell," *J. Electrochem. Soc.*, **141**, 1 (1994).

(27) *Perry's Chemical Engineers' Handbook*, 5th edition, Robert H. Perry editor. Mc Graw-Hill, Tokyo (1973).

(28) V. Yushkevich, I. Maksimova, and V. Bullan, "Electric Conductivity of KOH Solutions at High Temperatures," *Soviet Electrochemistry*, **3**, 1342 (1967).

(29) R. Robinson and R. Stokes, *Electrolyte Solutions*, 2nd ed. (rev). Butterworth & Co., London (1959).

(30) R. Bhatia, K. Gubbins, and R. Walker, "Mutual Diffusion in Concentrated Aqueous Potassium Hydroxide Solutions," *Transactions of the Faraday Society*, **64**, 2091 (1968).

(31) M. Matlosz, *Experimental Methods and Software Tools for the Analysis of Electrochemical Systems*, a dissertation, University of California, Berkeley (1985).

(32) C. Wagner, "On the Numerical Solutions of Voltera Integral Equations," *J. Mathematics and Physics*, **34**, 28 (1954).

(33) A. Acrivos and P. Chambré, "Laminar Boundary Layer Flows with Surface Reactions," *Ind. Eng. Chem.*, **49**, 1025 (1957).

(34) R. Bennett, N. Bridger, R. Dell, and T. Markin, "Improved Nickel-Hydrogen Cells," Harwell Laboratory Report #G 1204, Didcot, Oxon. United Kingdom (1978).

(35) N. Bridger, R. Dell, and T. Markin, "Chemical Storage of Hydrogen in Nickel-hydrogen Batteries," Harwell Laboratory Report #R 8644, Didcot, Oxon. United Kingdom (1977).

(36) R. Pollard, *Mathematical Modeling of the Lithium-Aluminum Iron Sulfide Battery.* a dissertation, University of California, Berkeley (1979).

Chapter 3: A Pseudo Two-dimensional Model of the Nickel Oxide Electrode

3.1 Introduction

As stated in Chapter 1, many researchers have suggested that diffusion in the solid phase of nickel oxide is a limitation of the discharging process. As with other intercalation compounds, it is known that nickel oxide has transport characteristics that vary with the oxidation state of the material. Specifically, the proton diffusivity and the electronic conductivity both vary by several orders of magnitude over the range of states of charge seen by the nickel oxide electrode.

This model does not take into account the changes in the electronic conductivity as a function of state of charge. This decision was made for two reasons. First, experimental measurements of the electronic conductivity of nickel oxide that appear in the literature are not consistent with each other (see section 1.3). Second, additives are currently used by battery manufacturers to boost this material's electronic conductivity,[1] so the "problem" of poor electronic conductivity appears, at least partially, to be solved.

It is desirable to look more closely at the diffusion process in order to understand the ways in which it might limit the performance of the nickel electrode. In 1970, MacArthur[2] measured diffusion coefficients for the charging and discharging processes in the nickel oxide electrode, although he did not measure them as a function of the state of charge of the material. He determined a diffusion coefficient of 3.1×10^{-10} cm^2/s for charging and 4.6×10^{-11} cm^2/s for discharging. Subsequently, these values were incorporated into several models of the nickel electrode which showed that solid-state diffusion could be a major limitation.[3,4,5] We can determine a length scale at which diffusion would become important by setting the dimensionless diffusion parameter to unity

$$\frac{D_s t}{L^2} = 1 \qquad (3\text{-}1)$$

Assuming a discharge time of one hour and MacArthur's diffusion coefficient of 4.6×10^{-11} cm^2/s leads to a length of 4.1 μm. Since particle radii in pasted nickel oxide electrodes are about 1 to 5 μm and film thicknesses in sintered nickel plaque electrodes are on the order of 1 μm,[1] we can easily see, without the aid of a complex model, that modest diffusion limitations can be expected.

Recently, Motupally used electrochemical impedance spectroscopy (EIS) to determine the diffusion coefficient of nickel oxide as a function of the state of charge of the active material. The function he measured is shown in figure 3-1. The diffusion coefficients at high states of charge are relatively large and remain that way for most of the discharge. Below approximately 30% state of charge, though, the diffusion coefficient drops sharply to its minimum value of 6.4×10^{-11} cm^2/s. (Note that this minimum value measured by Motupally is still 40% larger than the diffusion coefficient MacArthur measured for the discharging process.)

Until now, no one has closely examined the implications and predictions of incorporating this diffusion coefficient function into a mathematical model of an electrode. That is the goal of this chapter.

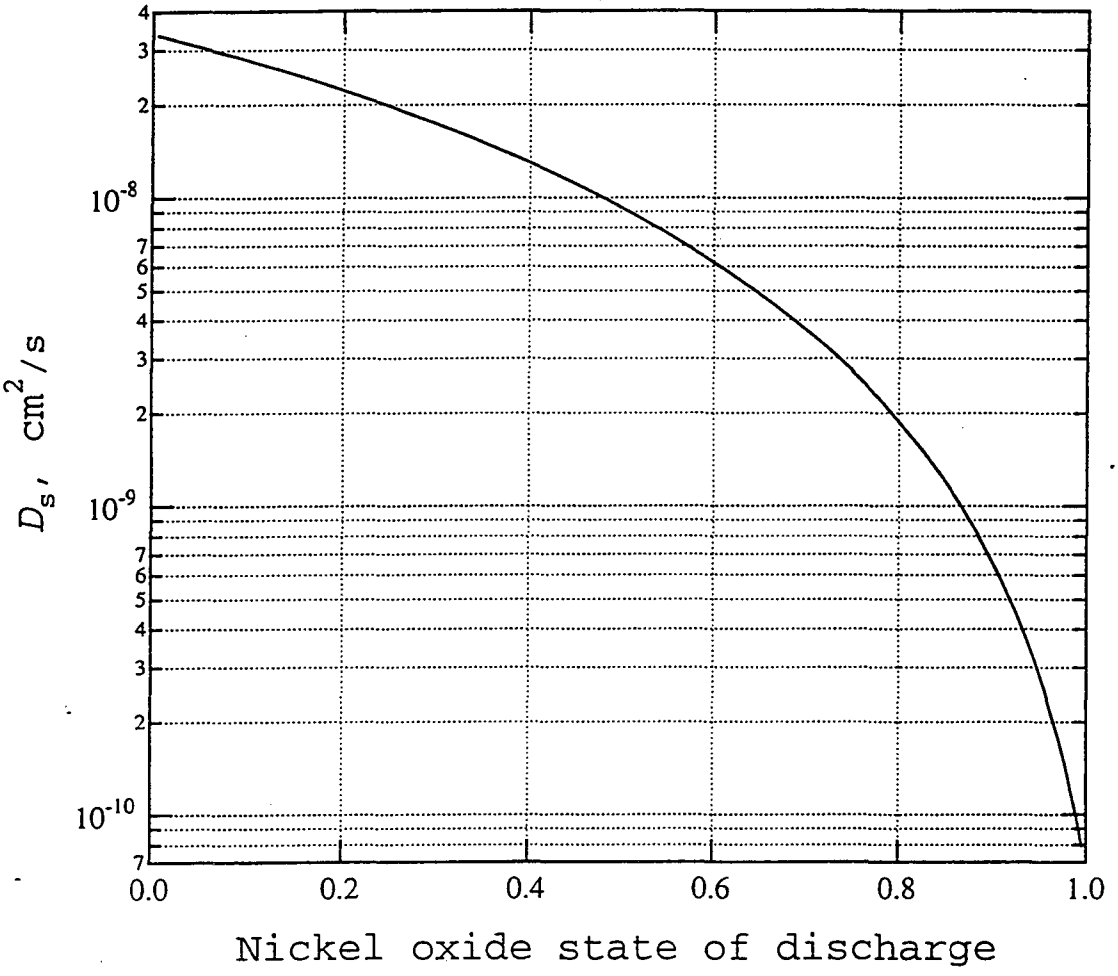

Figure 3-1: The diffusion coefficient of hydrogen in nickel oxide presented as a function of the state of discharge of the active material as measured by Motupally.[6,7]

3.2 Formulation of the 2-D model extensions

In the 1-D model, the surface concentration of hydrogen in each electrode is determined using the superposition integral (see discussion in section 2.1). The superposition integral, however, can be used to model diffusion only when the diffusion coefficient is a constant value. In order to examine the effects of a variable diffusion coefficient, a "pseudo 2-D" model must be used.

What is meant by a "pseudo 2-D" model is this. In the 1-D model, we solve the four main equations across the cell in the x-direction as shown in figure 2-1. In the "pseudo 2-D" model, we treat diffusion into a single particle as a separate problem to be solved at each mesh point in the positive electrode. We assume that since the radius of a single particle is small compared to the thickness of the electrode, diffusion occurs only perpendicular to the x-direction. (We did not need to worry about defining a coordinate system perpendicular to the x-direction in the 1-D model, because the solution method incorporating the superposition integral requires that we know only the "history" of the concentration of hydrogen at the surface of the particle during the discharge.)

In the positive electrode, we assume a spherical particle and treat the diffusion equation in spherical coordinates

$$\frac{\partial c_H}{\partial t} = \frac{1}{r^2}\frac{\partial}{\partial r}\left(D_s r^2 \frac{\partial c_H}{\partial r}\right) \tag{3-2}$$

where the diffusion coefficient, D_s, is an arbitrary function of the hydrogen concentration in the solid, c_H. Since we know that the flux of hydrogen into a particle is proportional to the reaction rate at the surface of the particle by the equation

$$D_s \frac{\partial c_H}{\partial r}\Big|_{r=R} = -\frac{\nabla \cdot i_2}{aF} \tag{3-3}$$

we can combine equation (2-19) with equation (3-3) to get

$$i_0\left[\exp\left(\frac{\alpha_a F}{RT}\eta_s\right) - \exp\left(\frac{-\alpha_c F}{RT}\eta_s\right)\right] = -D_s\frac{\partial c_H}{\partial r}\Big|_{r=R} \tag{3-4}$$

where i_0, the exchange current density, is the function given by equation (2-20). This is the boundary condition at the surface of the particle. The other boundary condition is the no-flux boundary condition at the center of the particle

$$\frac{\partial c_H}{\partial r}\Big|_{r=0} = 0 \tag{3-5}$$

The boundary condition represented by equation (3-4) is complex due to the fact that the exchange current density, i_0, is a function of the hydrogen concentration at the surface of the particle. Therefore, the solution for the diffusion equation in the particle must satisfy both the right and left sides of equation (3-4). To satisfy this boundary condition, we solve the diffusion equation by an iterative method described below.

At each mesh point we use the new guesses for c, c_s, and η_s to find a guess for the pore wall flux of hydrogen by evaluating the left side of equation (3-4). Using this guess for the hydrogen flux as the boundary condition, we solve for the concentration distribution across the particle. The surface concentration is then read from this new concentration distribution, and the left side of equation (3-4) is reevaluated to determine a new guess for the pore wall flux of hydrogen. A new concentration profile across the particle is determined using the new value for the flux, and this iterative process is repeated until the solution is converged.

The next step is entering this new value of the surface concentration into the BAND matrix solver. At each mesh point, the new surface concentration that was determined by the iterative process described above is entered as the new guess for the surface concentration at the current time step with the simple equation

$$c_s = c_s^0 + \Delta c_s \tag{3-6}$$

These new values are combined with the results from the first three equations (equations A, B, and C in section 2.2) and sent to BAND. The solution process for the four main variables is an iterative process itself; therefore, the solution procedure consists of an iteration for c_s at each mesh point within an iteration for the four main variables at each time step.

3.3 Analysis of model results

For the simulations contained in this chapter, all the model parameters are the same as the ones in tables 2-1 and 2-2 unless otherwise noted. The diffusion coefficient we use in the model comes from the work of Motupally.[6,7] If we assume a constant density for nickel oxide, we can obtain an equation for the diffusion coefficient of hydrogen as a function of the active hydrogen concentration in the solid phase.

$$D_s = 3.4\times 10^{-8}\left[1 - 0.95661\left(\frac{c_s}{c_{max}}\right)\right]^2 \qquad (3\text{-}7)$$

Since this diffusion coefficient function is crucial to the following analysis, the experimental work used to obtain this function should be closely examined. Motupally used the technique of electrochemical impedance spectroscopy (EIS) to investigate the diffusion process in thin films of nickel active material. To prepare the films, he cathodically deposited an oxide layer from an aqueous mixture of 1.8 molar $Ni(NO_3)_2$, 0.175 molar $Co(NO_3)_2$, and 0.075 molar $NaNO_3$ onto a gold-sputtered quartz wafer. To determine the thickness of the films, he used an electrochemical quartz crystal nanobalance (EQCN) to measure the change in mass of the wafer as the material was deposited. He reports that these measurements correspond well with the thicknesses predicted by measuring the current passed during the deposition and assuming a density of nickel oxide of 3.5 g/cm^3.

After the films were prepared, he conditioned them by cycling them 20 times in a 3 weight percent KOH solution. For each diffusion coefficient determination, he discharged the film from the fully charged state to the desired state of charge (SOC). Then "after data were collected at a particular SOC, the electrode was charged again, cycled twice at 5 mVs^{-1} and discharged to the next SOC." By doing this, he minimized the uncertainty about the SOC at which each measurement was made. At the conclusion of his experiments, an

elemental analysis of the active material determined that his films contained 88% nickel oxide and 12% cobalt oxide.

There are two main potential sources of error in this work. One concerns assumptions implicit in the model used by Motupally to obtain his results, and the other arises from the method of deposition of the film. In the model, he must assume that the active material is a much better conductor of electrons than of protons when a potential gradient is applied. Otherwise the material would be a "mixed conductor" of both protons and electrons. In his publication,[6] Motupally states that, "There may be an SOC between 15 and 0% where the diffusion coefficient extracted may be a mixed one which could be overpredicted by a factor of four."

The other uncertainty concerns his method of depositing the oxide film. He makes the assumption that the film he prepares is flat and uniform across the deposition surface, and he does not confirm this assumption with scanning electron microscopy (SEM) images. In practice, cathodically-deposited films can be cracked and highly non-uniform.[8,9] A severely cracked film would effectively change the geometry and "length scale" of the diffusion process inside the solid active material and would, therefore, invalidate the impedance model Motupally presents based on a uniform film thickness. In future works, researchers should consider preparing films by sputtering or a sol-gel technique. These methods have been useful for other authors' investigations of nickel oxide films.[10,11,12] In all cases, assumptions about the uniformity or "smoothness" of a film should be verified by SEM images.

For these two reasons, we desire not only to look at the diffusion coefficient function that Motupally presents but also at values that are fractions of this function. This will allow us to make an analysis of some "worst case" scenarios for the values of the diffusion coefficient.

Initial simulations of the model of the nickel oxide electrode were performed in a cell with the same characteristics as those described in Chapter 2; essentially the new nickel

oxide electrode model was substituted for the old one in this cell. Figure 3-2 presents simulations of the cell at three different discharge rates. For each discharge rate a simulation using the diffusion coefficient function in equation (3-7) is compared to a simulation where the diffusion coefficient in the positive electrode has been set to a large constant value where no diffusion limitations should occur. Two observations can be made from these simulations. One is that diffusion limitations under the conditions of these simulations appear to be slight. (It should be noted that the particle radius in the positive electrode for these runs was set to 4 μm, up from 2.5 μm in the initial runs of Chapter 2; diffusion limitations at the smaller particle size were, of course, even smaller.) The second observation is that the diffusion limitations that do exist appear to be greatest at the intermediate discharge rate. This feature of the discharge curve comparison may be better examined in figure 3-3. This figure is an enlargement of the bottom right corner of figure 3-2, near the end of discharge, where the diffusion limitations become apparent. Intuitively, it may be expected that the separation between the two discharge curves should always increase as the discharge rate increases. That does not occur in this system because at higher discharge rates the kinetic limitations at the nickel electrode push the cell to the cutoff voltage before the concentrations in the particles can reach the levels where diffusion will be severely inhibited.

It was desired to determine at what particle sizes and discharge rates diffusion limitations predicted by Motupally's function would inhibit the discharge of the nickel oxide electrode. In order to determine this, the "pseudo 2-D" model and the 1-D model without diffusion limitations were both discharged at various discharge rates and for various particle sizes. During these runs, the nickel electrode was galvanostatically discharged until it reached a polarization of 400 mV. From these runs, the utilization of the electrode material was recorded for both models. From these two values of the utilization, a "percentage of utilization loss due to diffusion limitations" was calculated according to the formula

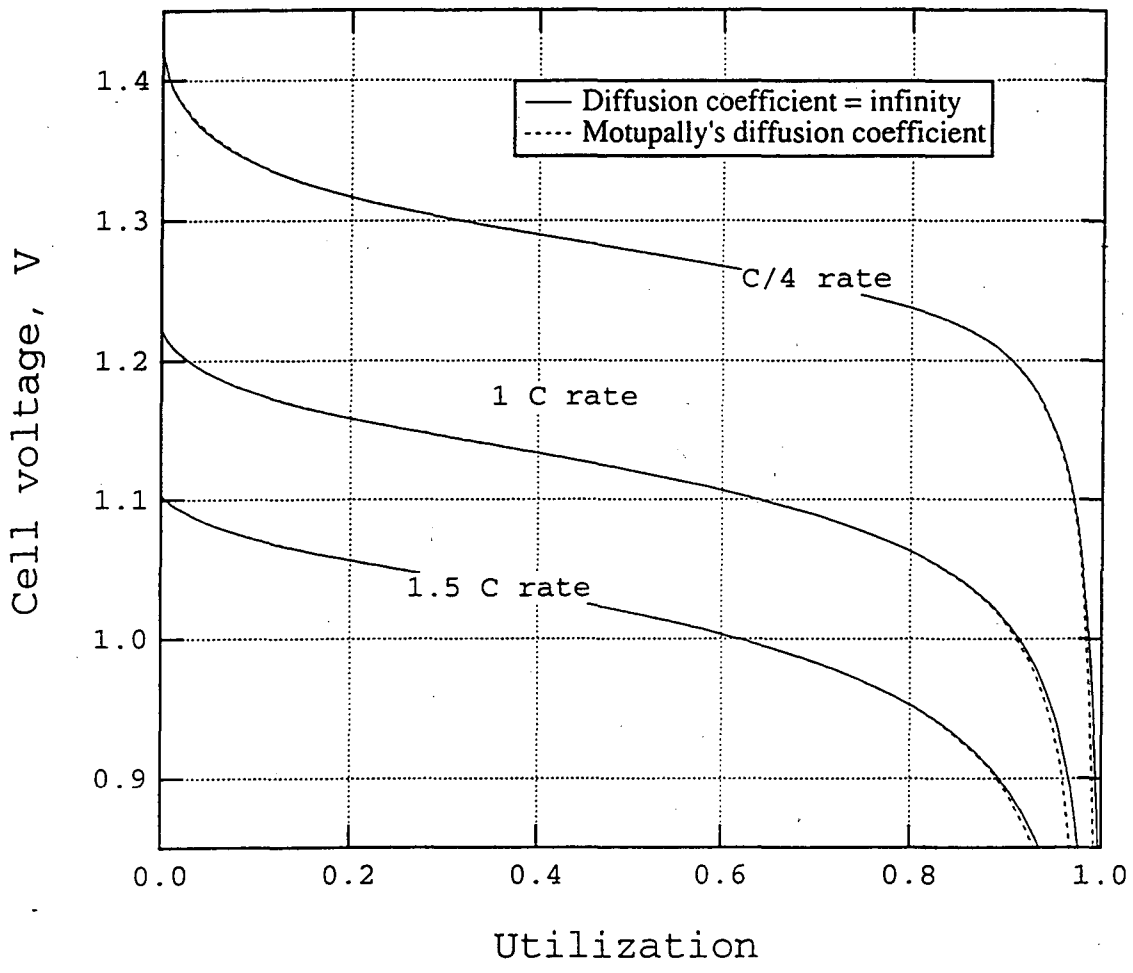

Figure 3-2: Discharge curves for a nickel oxide/ $LaNi_5$ cell. Simulations run with the diffusion coefficient from Motupally[6,7] are compared to simulations with no diffusion limitations in the solid phase of the positive electrode. Radii of the nickel oxide particles are 4 μm.

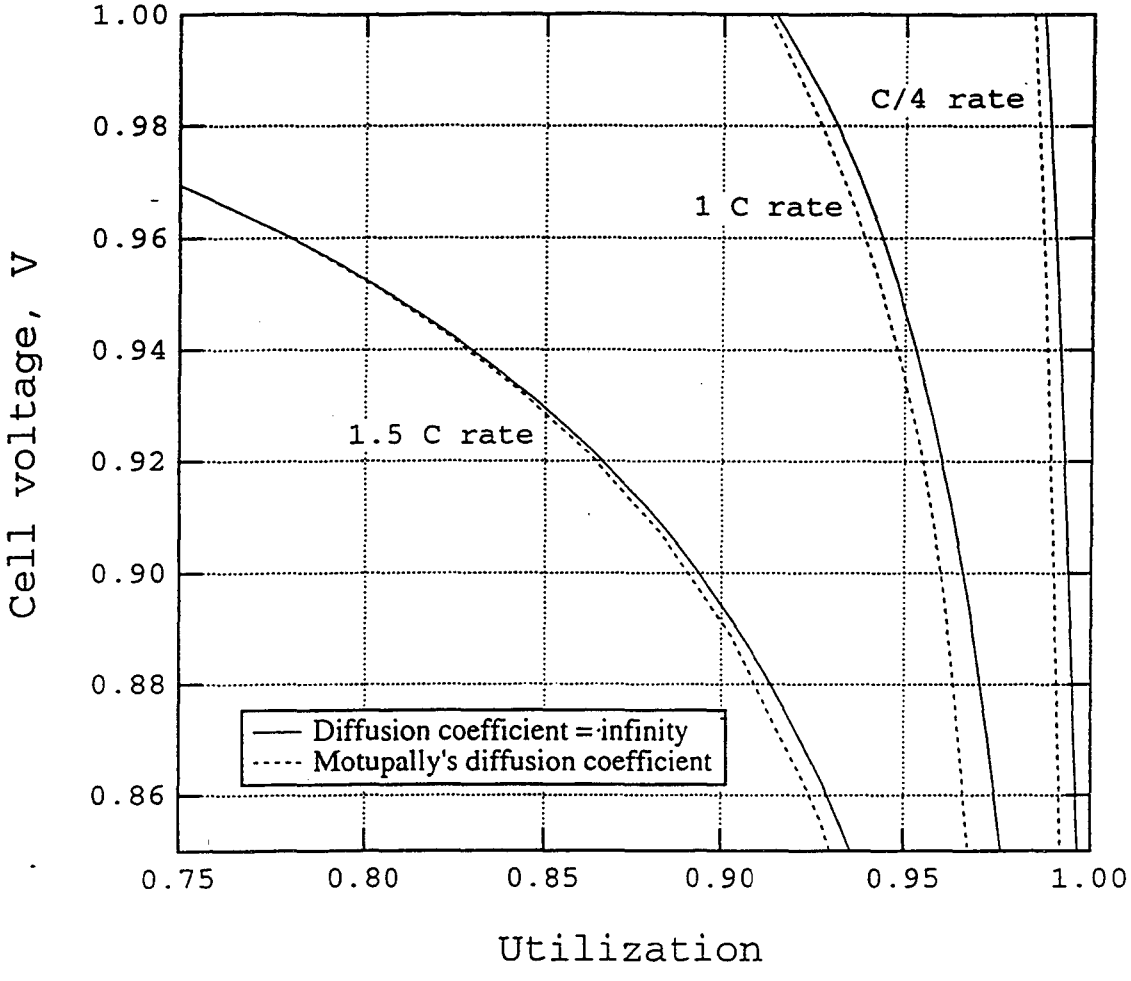

Figure 3-3: An enlargement of figure 3-2, showing the end of the discharge curves. The simulation using Motupally's diffusion coefficient function at the 1 C rate shows the greatest capacity loss as compared to the simulation with no diffusion limitations.

$$\% \text{ Loss} = \frac{U_{1\text{-}D} - U_{2\text{-}D}}{U_{1\text{-}D}} \times 100 \qquad (3\text{-}8)$$

where $U_{1\text{-}D}$ is the utilization from the 1-D simulation and $U_{2\text{-}D}$ is the utilization from the pseudo 2-D simulation. It was found that the percentage of utilization lost due to diffusion limitations never exceeded 3% for any value of the discharge rate or particle size. Figure 3-4 is a graph of the particle size *vs.* discharge rate at which a 2% utilization loss due to diffusion is expected to occur. Since utilization losses are lower than 2% below the line in this figure, an alternative way of interpreting this graph is that it is "the maximum particle size allowable at a given discharge rate to avoid a utilization loss in excess of 2%." The simulations used to prepare this graph assumed an electrode thickness of 843 μm, but the predictions in this plot should be approximately correct for different electrode thicknesses about this value as the potential drops in both the solid and solution phases of the electrode are small compared to the activation potential.

Figure 3-4 confirms that the diffusion limitations predicted by Motupally's function are small. As stated in section 3-1, particle radii in pasted nickel oxide electrodes are about 1 to 5 μm, and film thicknesses in sintered nickel plaque electrodes are on the order of 1 μm.[1] The "length scales" at which serious diffusion limitations are predicted to exist are greater than those in nickel oxide electrodes that are currently being manufactured.

These last two analyses were repeated assuming that the diffusion coefficient that Motupally found was overestimated by a factor of four. In figure 3-5, the same general voltage *vs.* time behavior for a nickel oxide/$LaNi_5$ cell can be seen for this diffusion coefficient function. Of course, the "utilization losses" are more severe, but again the greatest utilization losses appear to be at the intermediate discharge rates.

Figure 3-6 is analogous to figure 3-4, but the simulations incorporate a diffusion coefficient function one-fourth of the earlier one. In this graph we can see that the

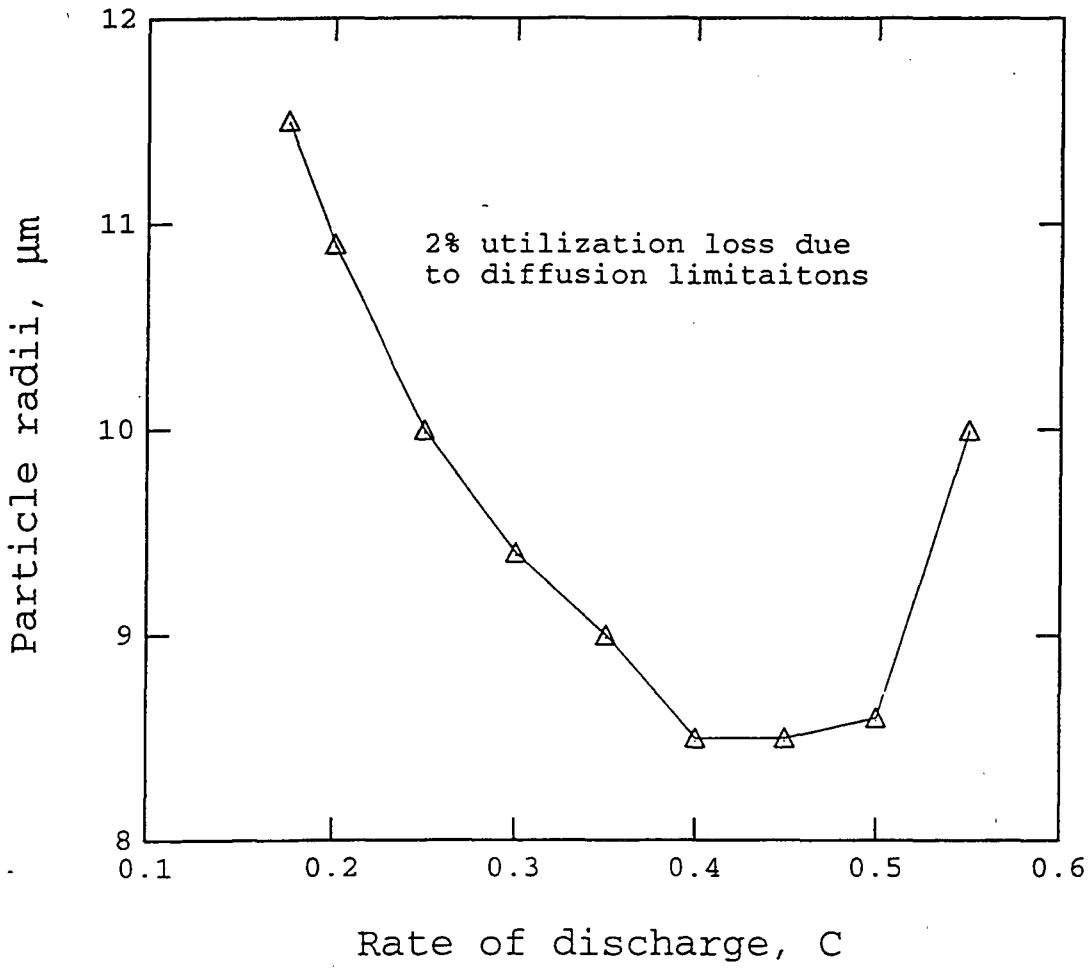

Figure 3-4: A graph showing the maximum particle size allowable to still avoid diffusion limitations in the nickel electrode at a given discharge rate. Parameters for the nickel electrode are given in table 2-2. The greatest diffusion limitations are seen around the 0.5 C rate.

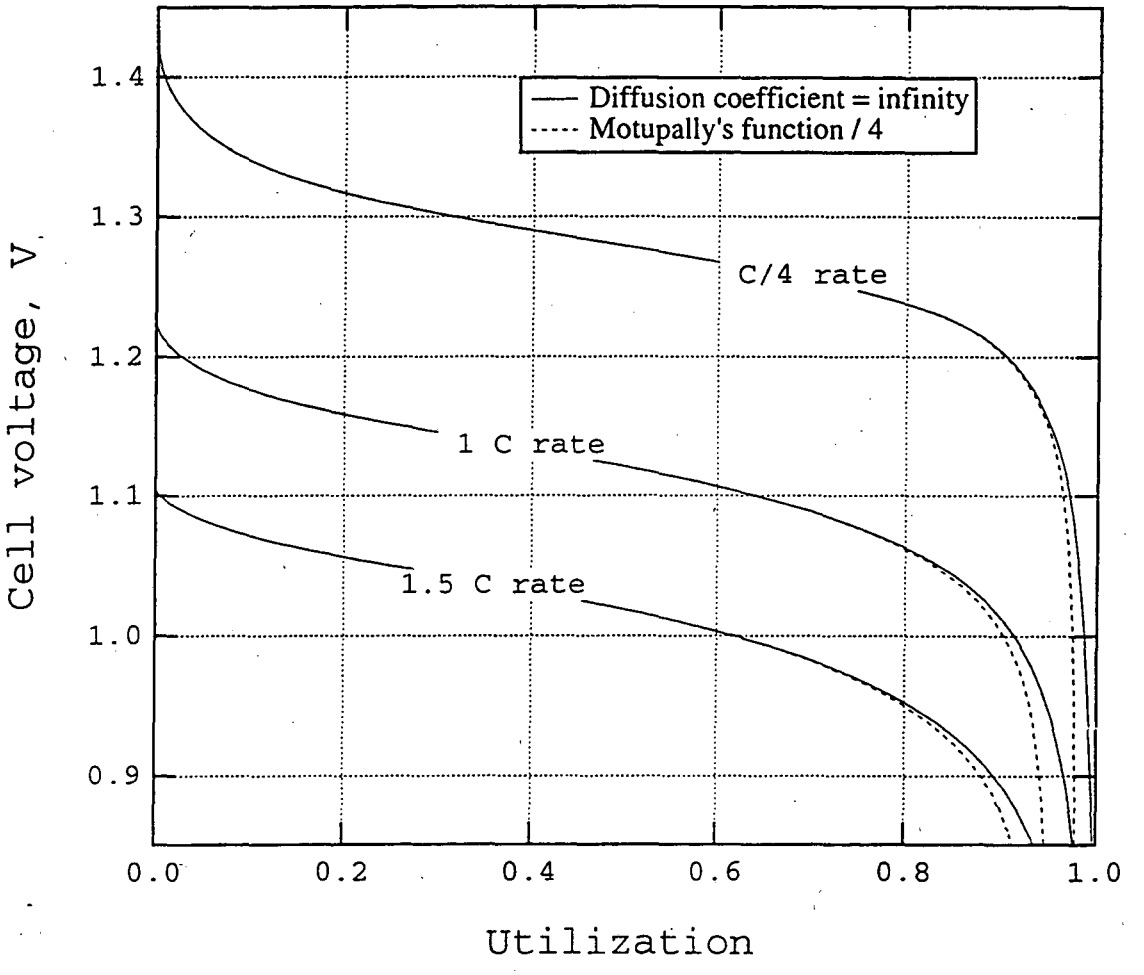

Figure 3-5: Simulations run with the diffusion coefficient from Motupally[6,7] divided by four are compared to simulations with no diffusion limitations in the solid phase of the positive electrode. Radii of the nickel oxide particles are 4 μm.

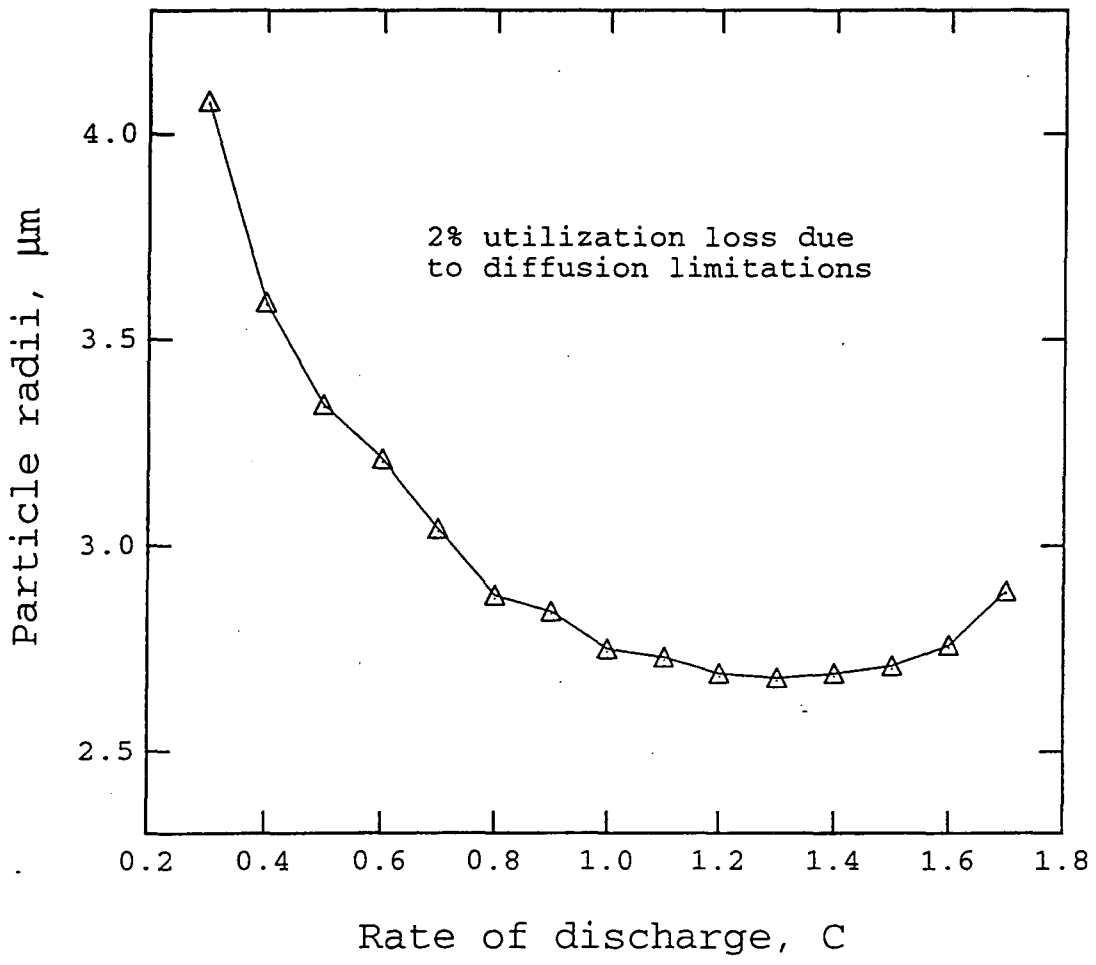

Figure 3-6: A graph showing the maximum particle size allowable to still avoid diffusion limitations in the nickel electrode at a given discharge rate assuming Motupally's diffusion coefficient function divided by four. The greatest diffusion limitations are seen around the 1.3 C rate.

"maximum particle sizes allowable to avoid diffusion limitations" are much smaller than those shown in figure 3-4. The greatest diffusion limitations are predicted about the 1.3 C discharge rate, and the minimum in this plot is a radius of about 2.7 μm.

More simulations were performed assuming that the actual diffusion coefficient function for nickel oxide was lower than that measured by Motupally. Figure 3-7 shows the potential drop across just the nickel oxide electrode as a function of utilization assuming several different diffusion coefficient functions. The discharge process was cut off when the potential drop across the nickel electrode reached 400 mV. For these simulations, Motupally's diffusion coefficient was divided by an integer, n, and n was varied to obtain the results. This figure shows that, even for a diffusion coefficient function one-tenth the value of the one assumed for the pseudo 2-D model, the utilization at the 1 C rate is still 92.0%. This is compared to a utilization of 96.7% for the original diffusion coefficient function given by equation (3-7).

To examine the diffusion process more closely, the concentration distribution inside a single particle was examined. Figure 3-8 shows concentration distributions inside a particle of nickel oxide at the end of discharge. As in figure 3-7, runs were performed for diffusion coefficient functions that were fractions of Motupally's function, and all of the simulations were performed at the 1 C rate and for particle radii of 4 μm. The particle selected for these simulations was in the center of the nickel oxide electrode.

This figure shows that the surface concentration at the end of discharge for all the values of n are very similar. The lowest normalized surface concentration was 0.973 for n=1, and the highest normalized surface concentration was 0.982 for n=10. This small range of surface concentrations arises due to the interaction between the diffusion process and the thermodynamics of the electrode. As the electrode nears its fully discharged state, the diffusion coefficient drops sharply and leads, therefore, to an accumulation of hydrogen near the particle's surface. Since the energetics of the surface reaction are dependent only

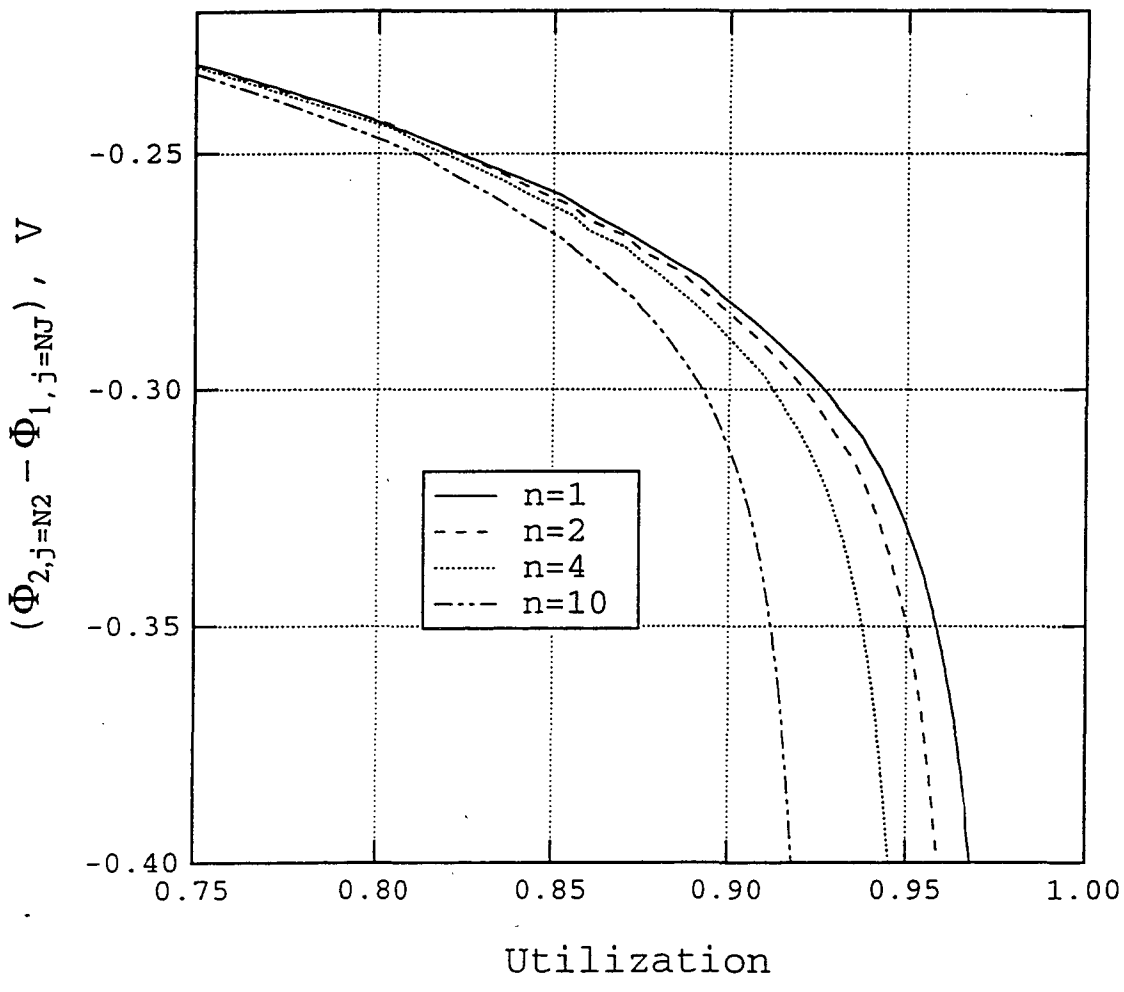

Figure 3-7: The potential drop across the nickel oxide electrode as a function of utilization at the 1 C discharge rate. Simulations were performed using the diffusion coefficient of Motupally divided by a number, n. Radii of the nickel oxide particles are 4 μm.

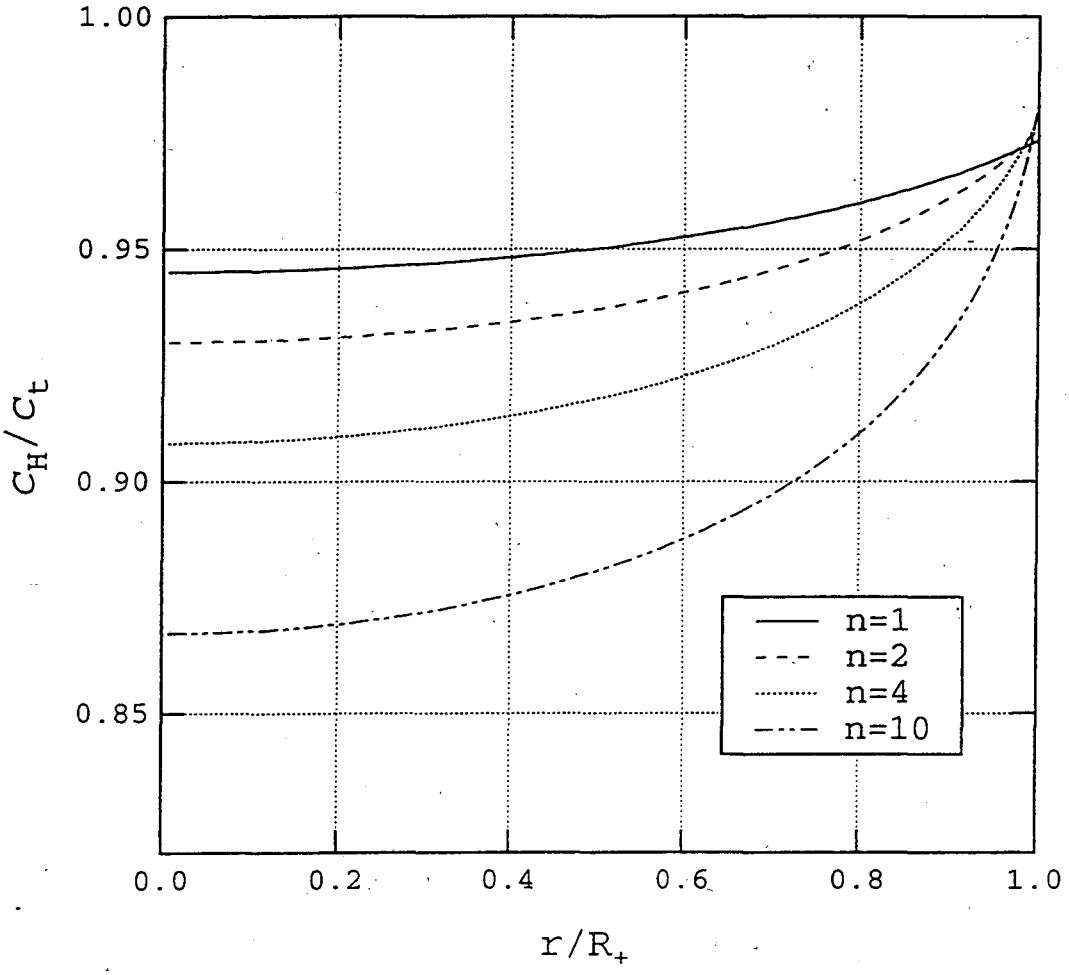

Figure 3-8: The normalized hydrogen concentration inside a single particle of nickel oxide at the end of discharge at the 1 C rate. Simulations were performed using the diffusion coefficient of Motupally divided by a number, n. R_+ = 4.0 μm.

on the surface concentration, the open-circuit potential function of the material drives the electrode quickly to the cutoff voltage. Note that the difference in the open-circuit potential function given by equation (2-33) between 98 and 99% utilization is 93 mV.

3.4 Conclusions

From the preceding analysis we can conclude that, if the diffusion characteristics of the nickel oxide active material are described by the function of Motupally, then diffusion limitations in modern nickel oxide electrodes should be slight. If the diffusion coefficient function is up to 4 times smaller than this function, as Motupally said might be possible, then diffusion limitations could be significant for length scales greater than approximately 3 μm.

Since the particle radii assumed for the positive electrode in the 1-D model are 2.5 μm, in radius, it is therefore possible to neglect diffusion limitations in the solid phase of this electrode for the analyses in Chapter 2.

Additional experiments are needed to complement the work of Motupally. It is suggested that the process of depositing the nickel oxide film could be improved in order to achieve a more uniform film. Some other methods could include sputtering and sol-gel methods.

References

(1) D. Berndt, *Maintenance-free Batteries*. Research Studies Press, Somerset, England (1993).

(2) D. MacArthur, "The Proton Diffusion Coefficient for the Nickel Hydroxide Electrode," *J. Electrochem. Soc.*, **117**, 729 (1970).

(3) J. W. Weidner and P. Timmerman, "Effect of Proton Diffusion, Electron Conductivity, and Charge-Transfer Resistance on Nickel Hydroxide Discharge Curves," *J. Electrochem. Soc.*, **141**, 346 (1994).

(4) Z. Mao, P. De Vidts, R. White, and J. Newman, "Theoretical Analysis of the Discharge Performance of a NiOOH/H_2 Cell," *J. Electrochem. Soc.*, **141**, 54 (1994).

(5) P. De Vidts and R. White, "Mathematical Modeling of a Nickel-Cadmium Cell: Proton Diffusion in the Nickel Electrode," *J. Electrochem. Soc.*, **142**, 1509 (1995).

(6) S. Motupally, C. Streinz, and J. Weidner, "Proton Diffusion in Nickel Hydroxide Films," *J. Electrochem. Soc.*, **142**, 1401 (1995).

(7) Sathya Motupally, *Measurement of the Diffusion Coefficient of Protons in Nickel Hydroxide Films as a Function of State of Charge*, master's thesis, University of South Carolina, 1992.

(8) R. Armstrong and E. Charles, "Some Aspects of the A.C. Impedance Behaviour of Nickel Hydroxide and Nickel/Cobalt Hydroxide Electrodes in Alkaline Solutions," *Journal of Power Sources*, **27**, 15 (1989).

(9) Manojit Sinha, *A Mathematical Model for the Porous Nickel Hydroxide Electrode*, dissertation, University of California, Los Angeles, 1982.

(10) S. Yamada, T. Yoshioka, M. Miyashita, K. Urabe, and M. Kitao, "Electrochromic Properties of Sputtered Nickel-oxide Films," *Journal of Applied Physics*, **63**, 2116 (1988).

(11) W. Estrada, A. Anderson, and C. Granqvist, "Electrochromic Nickel-oxide-based Coatings Made by Reactive DC Magnetron Sputtering: Preparation and Optical Properties," *Journal of Applied Physics*, **64**, 3678 (1988).

(12) A. Agrawal, J. Cronin, and R. Zhang, "Review of Solid State Electrochromic Coatings Produced Using Sol-gel Techniques," *Solar Energy Materials and Solar Cells*, **31**, 9 (1993).

Chapter 4: Variable Diffusivity in Intercalation Materials - A Study of Nickel Oxide

4.1 Introduction

Like nickel oxide, there are other materials that have a diffusion coefficient that varies with the amount of intercalated material in the crystal lattice.[1,2] If the diffusion coefficient function of these materials is known, along with the other relevant parameters, the model described in Chapter 3 can be applied to examine diffusion limitations in those systems also.

There are drawbacks to the rigorous approach, presented in Chapter 3, of formulating and running a "pseudo 2-D" model, though. First, many researchers do not have the time either to formulate a full 2-D model themselves or to modify an existing model to incorporate the data from a different material. Furthermore, the two-dimensional model takes about five to ten times as long to run each simulation as compared to a more traditional one-dimensional model based on porous electrode theory. Since these one-dimensional models are in more common use in industry and academia, it would be useful to be able to modify these models to capture some of the effects of a variable diffusion coefficient function. An approach whereby the "best" constant diffusion coefficient is selected and used to capture variable-diffusion effects is presented in this chapter.

This method examines the diffusion behavior in an idealized spherical particle of an intercalation material when a constant flux rate into the particle is specified. From the surface concentration *vs.* time behavior of the diffusion process that occurs when a variable diffusion coefficient is specified, a constant diffusion coefficient can be selected that best matches the variable-diffusion-coefficient behavior. This process is repeated at different flux rates so that a "best" constant diffusion coefficient can be determined for a given flux rate. The next section describes this process in greater detail.

4.2 Theory

A simple model of diffusion occurring in a single spherical particle is derived. To do this, the diffusion equation in spherical coordinates is used with the assumption that the diffusion coefficient, D_s, can be a general function of the diffusing species's concentration in the lattice. Since we are considering hydrogen diffusion in nickel oxide, we choose the variable, c_H, to represent the concentration of hydrogen in the solid phase. This methodology, though, is applicable to other intercalating materials in other systems.

$$\frac{\partial c_H}{\partial t} = \frac{1}{r^2}\frac{\partial}{\partial r}\left(D_s r^2 \frac{\partial c_H}{\partial r}\right) \tag{4-1}$$

A constant-flux boundary condition is specified at the surface of the particle,

$$j_H = -D_s \frac{\partial c_H}{\partial r}\Big|_{r=R} \tag{4-2}$$

and a zero flux boundary condition is specified at the center of the particle.

$$\frac{\partial c_H}{\partial r}\Big|_{r=0} = 0 \tag{4-3}$$

In this simplified model, it is assumed that the particle does not undergo expansion and contraction as the intercalating material diffuses in and out of the lattice; therefore, the radius of the particle, R, is a constant.

Next, we can define a dimensionless flux rate, Φ,

$$\Phi = \frac{j_H R}{D_o c_t} \tag{4–4}$$

where j_H is the pore wall flux of hydrogen, R is the radius of the particle, and D_o is the largest single value of the diffusion coefficient over the range of state of charge of the

material (in this case, $D_o = 3.4\times 10^{-8}$ cm^2/s; see section 1.4). For a given material, the denominator of this dimensionless group will be a constant.

Once the diffusion equation is discretized, we run the model of diffusion in a single spherical particle for several different values of Φ. From these simulations we record the surface concentration of hydrogen as a function of the total utilization of active material in the particle. We are interested only in the surface concentration of the particle because, in an electrode, the surface concentration is the only concentration on which the electrode behavior depends. In figure 4-1, several of these curves are graphed for the diffusion coefficient function given by equation (3-7).

For each of these curves, our goal is to determine a constant diffusion coefficient that will best approximate the surface concentration *vs.* utilization behavior. The process of finding this "best" diffusion coefficient is quite tricky. This can be seen from figure 4-2 in which several surface concentration curves predicted from using a constant diffusion coefficient are compared to a surface concentration curve for $\Phi = 5.43\times 10^{-2}$. From this graph, we can see that none of the constant diffusion curves describes the "true" behavior of the diffusion process at all degrees of utilization. Even so, it is our task to try to pick the single diffusion coefficient that best describes this complex behavior.

There are several ways that we could define the "best" diffusion coefficient, but the two most straightforward methods are (1) to find the diffusion coefficient that produces the best least-squares curve fit of the variable-diffusion-coefficient surface-concentration behavior and (2) to find the diffusion coefficient that produces a curve that terminates at the same utilization of active material as the curve-fit of the variable diffusion coefficient. We can call the first method finding "the best curve fit" and the second method "matching the transition time" of the two diffusion processes. In some cases, the diffusion coefficients predicted by these two methods will be very different. Figure 4-3 shows the variable diffusion curve for $\Phi = 5.43\times 10^{-2}$ along with the constant diffusion curves corresponding

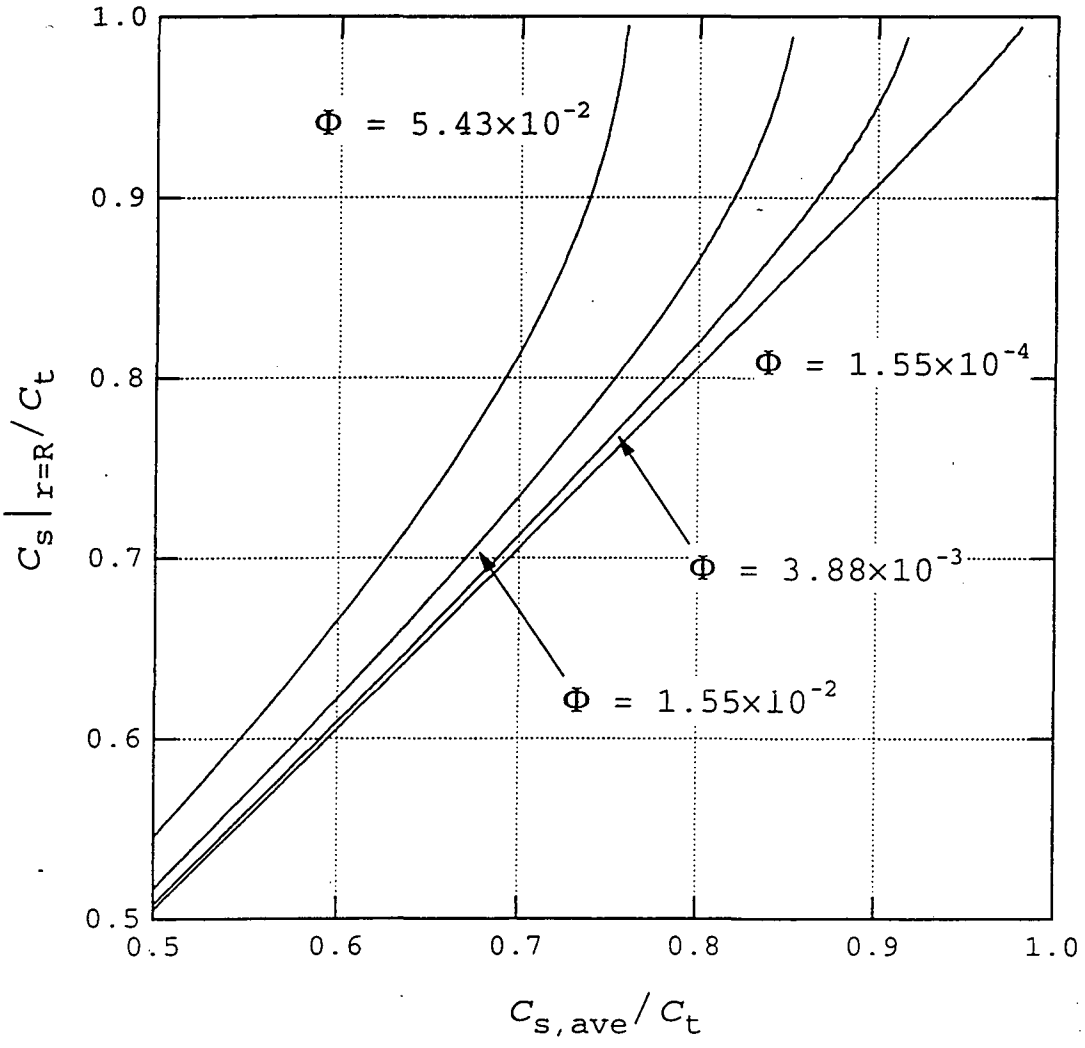

Figure 4-1: The surface-concentration behavior of a particle of nickel oxide undergoing discharge when using Motupally's diffusion-coefficient function.

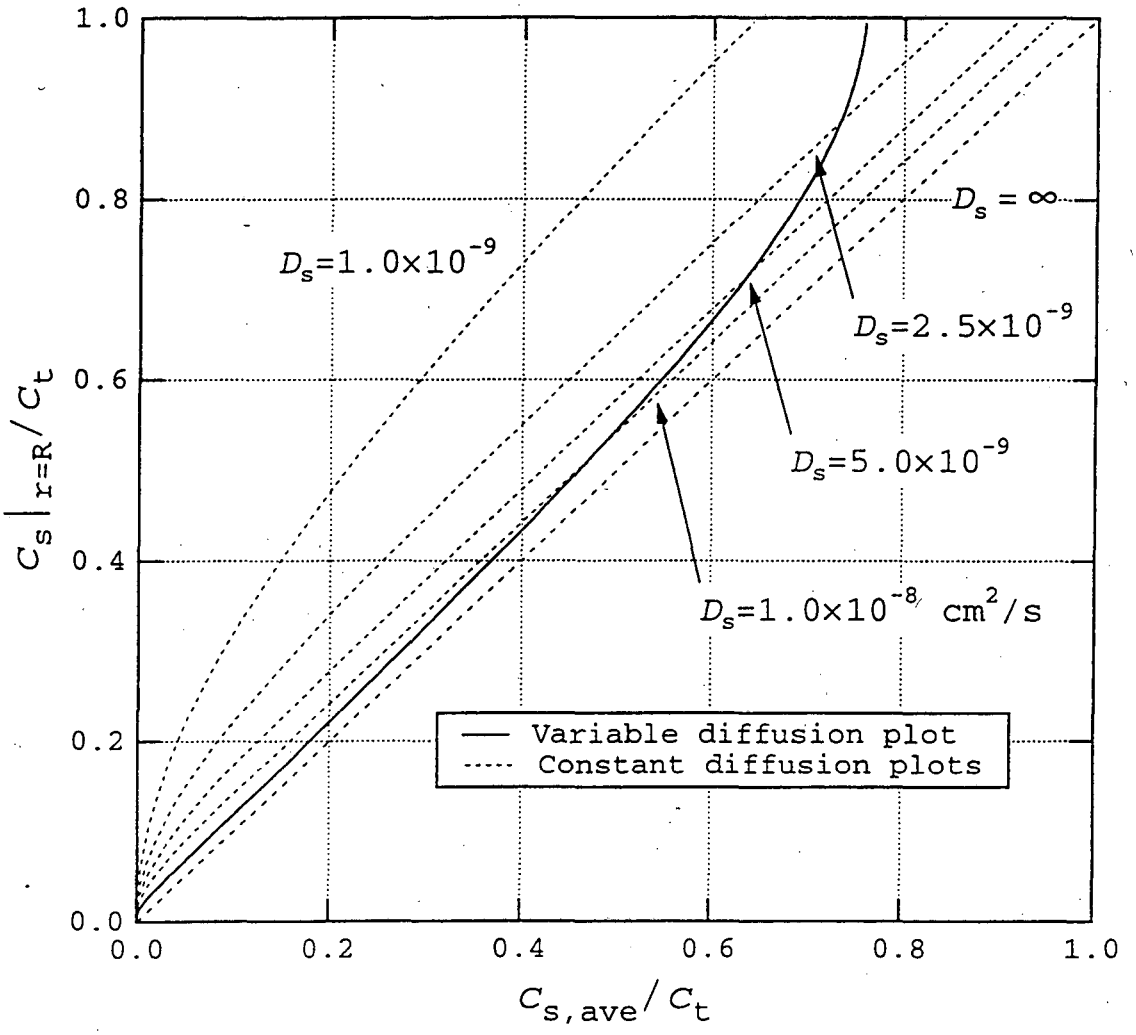

Figure 4-2: A graph comparing the surface-concentration behavior for the variable diffusion case ($\Phi=5.43\times10^{-2}$) with plots of the surface-concentration behavior using a constant diffusion coefficient.

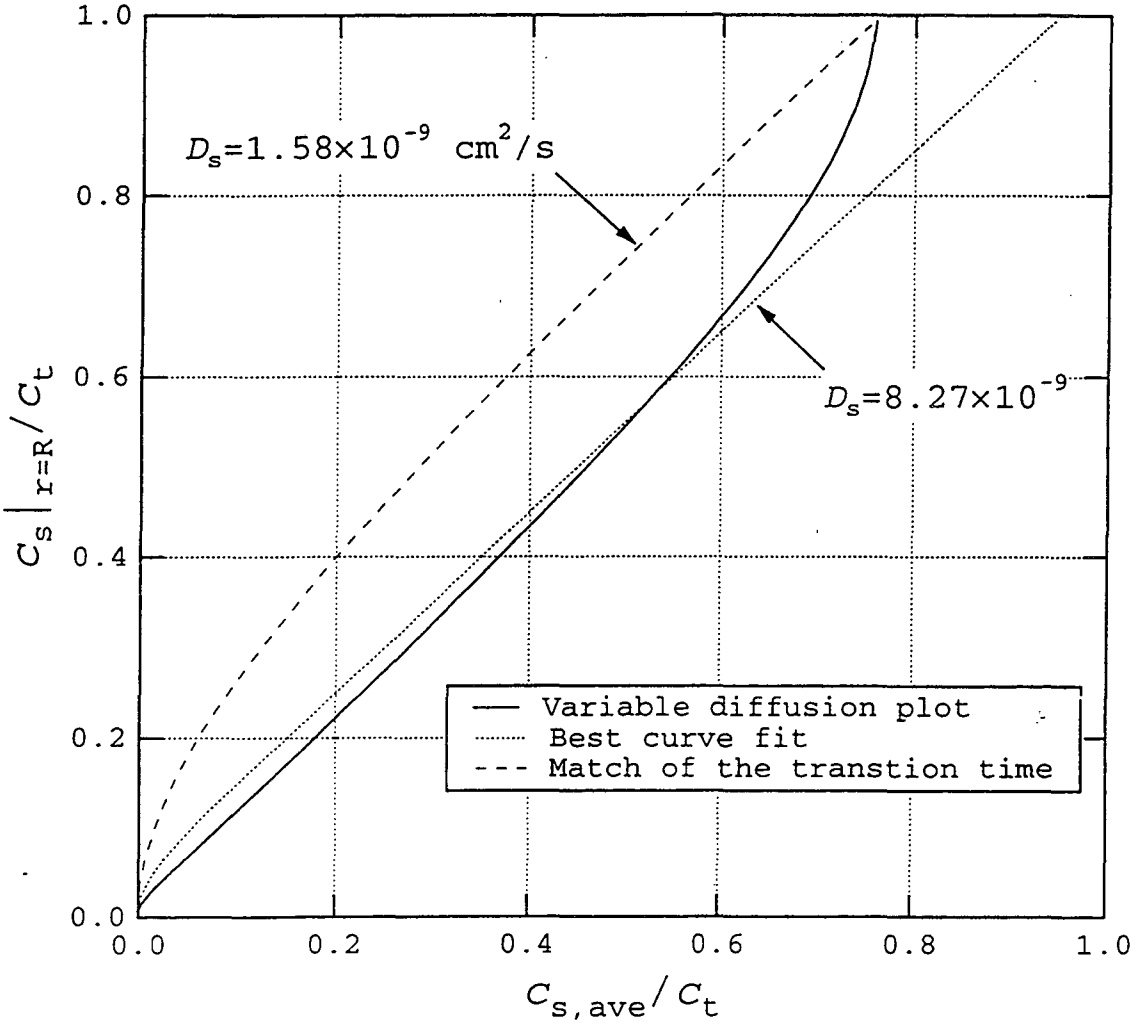

Figure 4-3: Graph of surface concentration *vs.* average concentration for variable diffusion ($\Phi=5.43\times10^{-2}$). Plots of the constant-diffusion solutions for the best curve fit and for the matching transition time are also shown.

to the best curve fit and the one that matches the transition time of the variable curve. In this case, the diffusion coefficients corresponding to the best curve fit is over five times greater than the one for the match of the transition times. (Note that the best curve fit was, necessarily, only performed for the range of utilizations seen by the variable diffusion coefficient's surface concentration curve.) The "variable" surface concentration curve in this figure was produced for a fast discharge rate; the pore wall flux corresponded to a total maximum discharge time of 3 minutes.

Once a constant diffusion coefficient has been determined for each value of the dimensionless flux, a curve can be generated that relates these two quantities. Figure 4-4 shows how the normalized diffusion coefficient depends on the dimensionless flux for the matching of the transition times, and figure 4-5 shows the corresponding plot for a best least-squares curve fit of the two surface-concentration curves. A polynomial approximation of the results is represented in both graphical (dashed line) and equation form in each of these figures.

Although this procedure has been applied only to the discharging process, the charging process could also be examined in this manner. We would expect that, for the nickel oxide system, the diffusion coefficients predicted would be close to the maximum value, D_o, for the diffusion coefficient function in figure 3-1. In figure 4-6, three surface concentration curves are plotted for diffusion associated with the charging process. For these simulations, the particle was assumed to have an initial uniform concentration of hydrogen equal to 99.5% of its theoretical maximum, and a constant flux boundary condition was specified, this time for hydrogen leaving the particle. It can be seen from this figure that, for higher dimensionless flux rates, the concentration at the surface drops quickly but then approaches the limit of an infinitesimal flux rate. Therefore, for a wide range of flux rates, the "transition-time" procedure used to examine the discharging process would predict a large diffusion coefficient. In figure 4-7, the surface-concentration curve for $\Phi=5.43\times 10^{-2}$ is compared to the surface-concentration curves predicted assuming

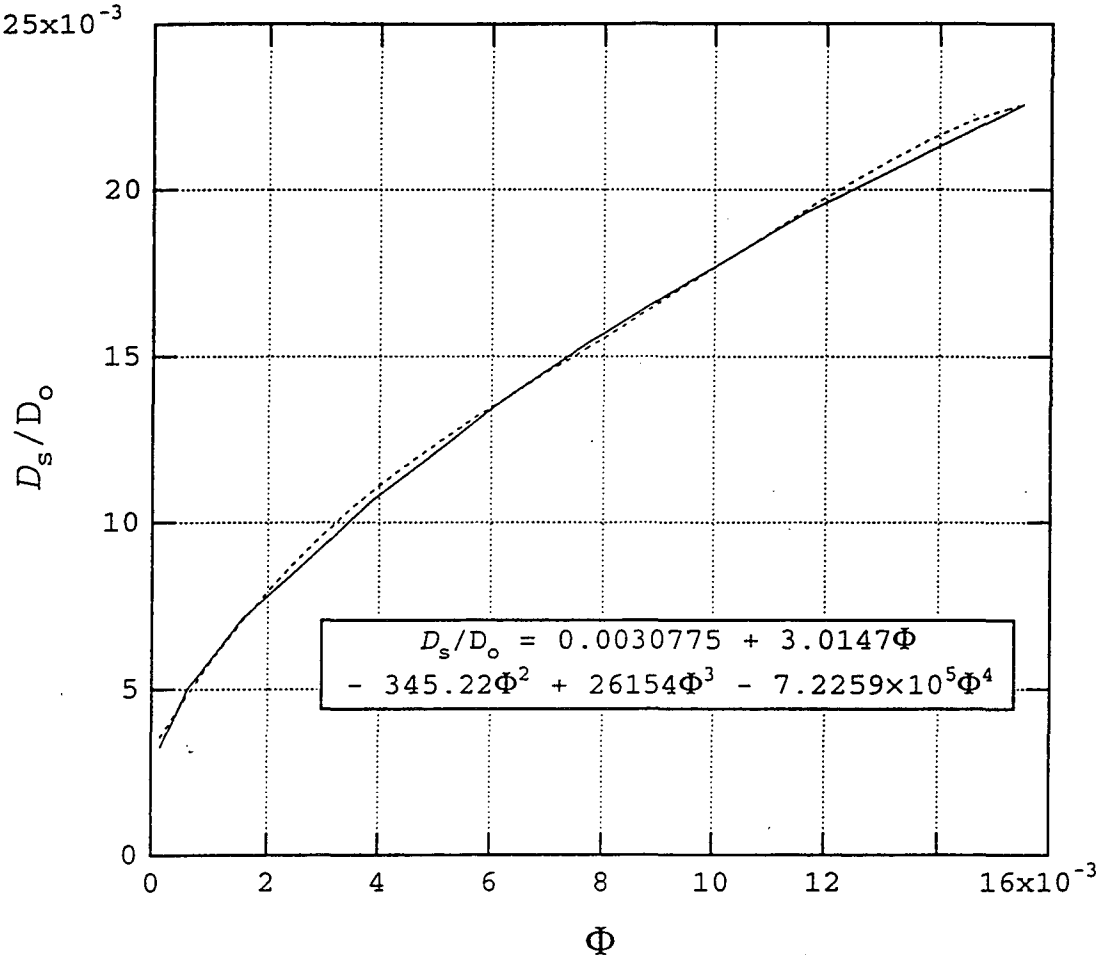

Figure 4-4: A graph showing the relationship between the normalized diffusion coefficient and the dimensionless flux based on matching the transition times of the surface concentration curves for constant and variable diffusion coefficient functions in a spherical particle of nickel oxide. The dashed line is a polynomial approximation.

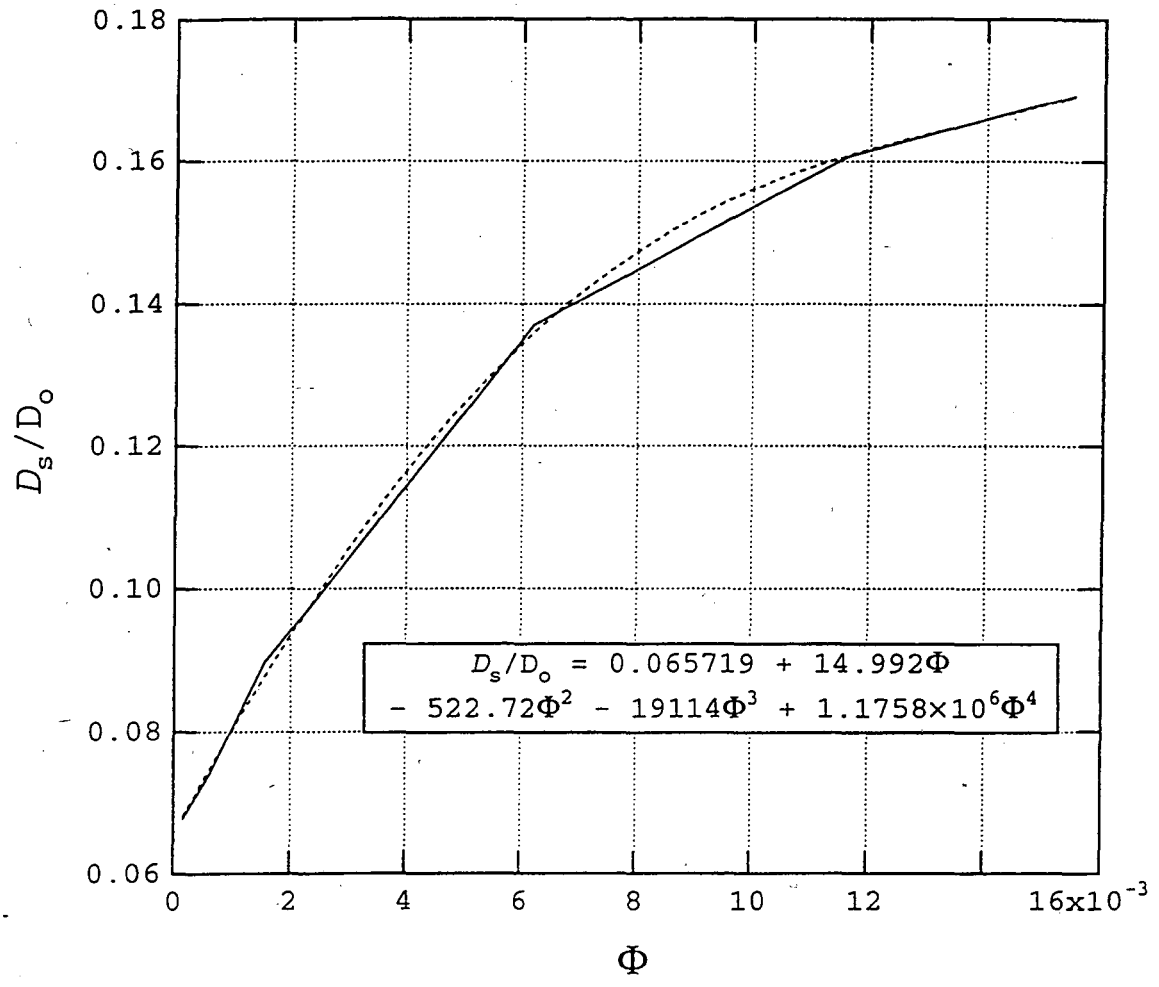

Figure 4-5: A graph showing the relationship between the normalized diffusion coefficient and the dimensionless flux based on finding the best least-squares curve fit of the surface concentration curves for constant and variable diffusion coefficient functions in a spherical particle of nickel oxide. The dashed line is a polynomial approximation.

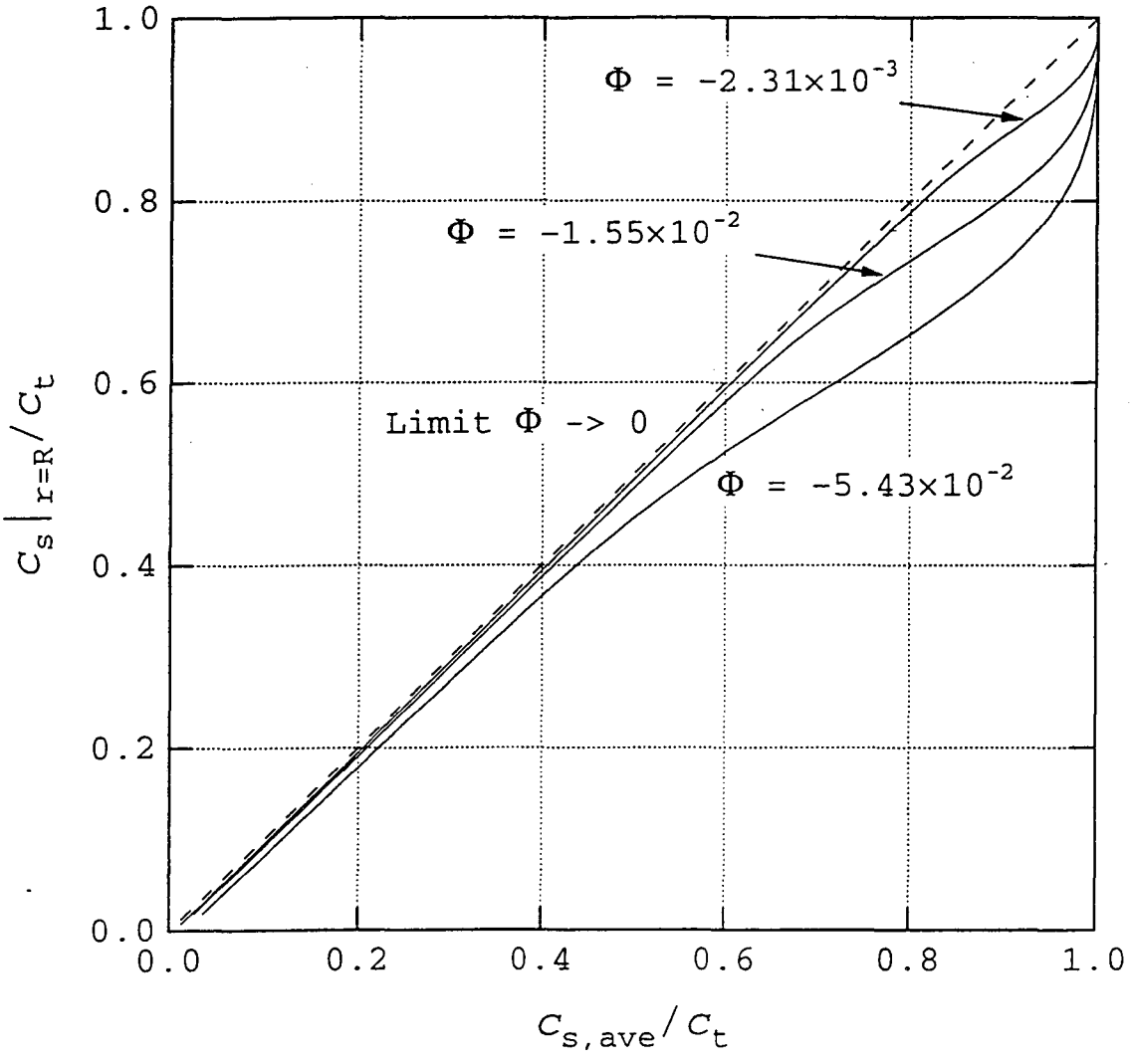

Figure 4-6: The normalized concentration of hydrogen in a particle of nickel oxide during charge. The curves at different values of Φ all converge towards the curve for the limit as $\Phi \rightarrow 0$ at the end of the charging process.

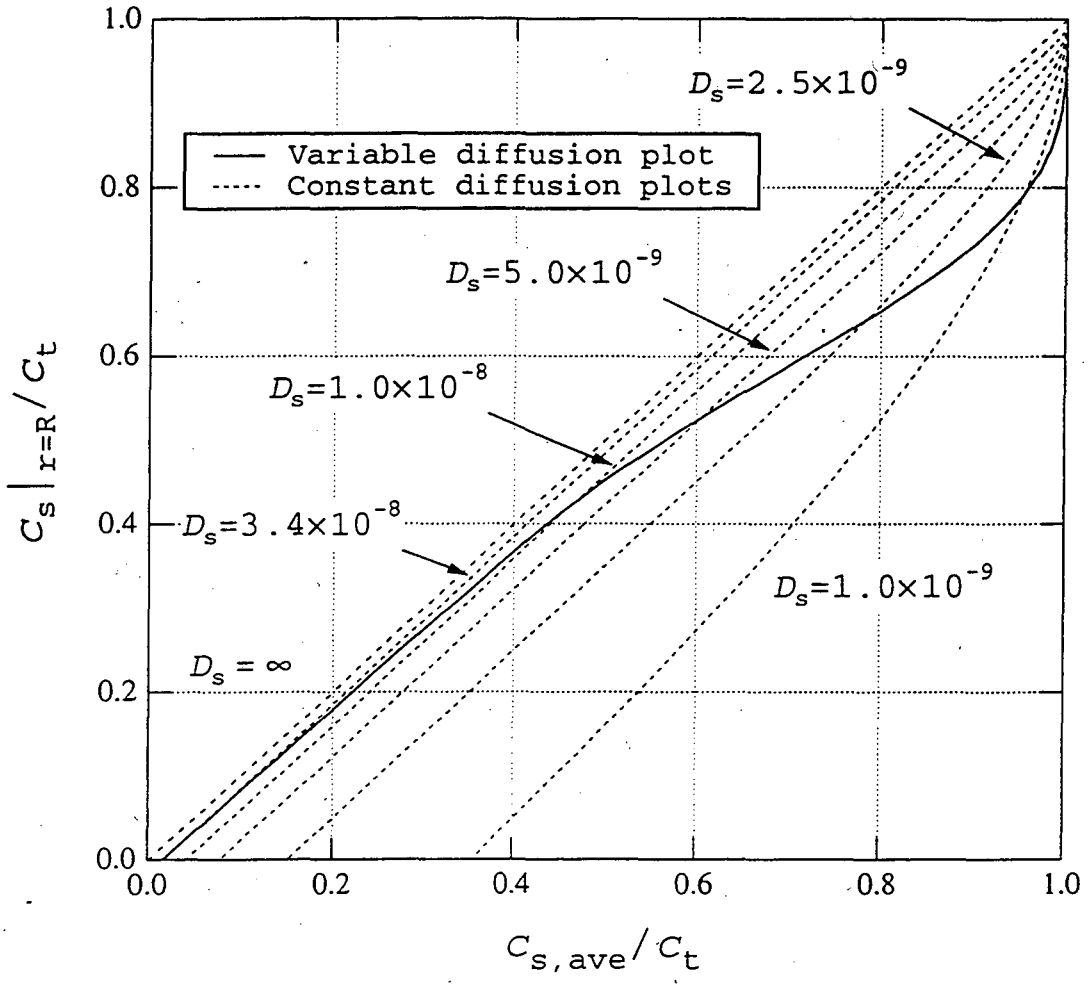

Figure 4-7: A graph comparing the surface-concentration behavior on charge for the variable diffusion case (Φ=5.43×10^{-2}) with plots of the surface-concentration behavior using a constant diffusion coefficient.

various constant diffusion coefficients. It is shown explicitly in this figure that even for a large flux rate (equivalent to a 3 minute charging time), the surface concentration curve terminates at an average concentration close to that predicted using a diffusion coefficient the value of D_o (in this case 3.4×10^{-8} cm^2/s). A comparison of figures 4-2 and 4-7 shows the dramatic asymmetry between the solid-state diffusion behavior during the charging and discharging processes, even though the same diffusion coefficient function is used for both simulations; it appears that diffusion of hydrogen out of nickel oxide is easier than diffusion in. Since, from figures 4-6 and 4-7, it appears that diffusion limits the charging process much less than the discharging process, the charging process is not examined further in this chapter.

The next step is determining how to use these relationships in a full model of an electrode. To do this we assume that the reaction distribution across an electrode is uniform, in other words that all the particles in the electrode discharge at the same rate. This assumption is good for materials like nickel that have a sloping open-circuit potential as a function of the state of charge of the active material.[3] It holds true less for materials that have "flat" open-circuit potential functions. Knowing the active-material volume fraction, ε_{act}, and the radius of the spherical particles, R, we can get a specific surface area from the geometric relationship

$$a = \frac{3\varepsilon_{act}}{R} \tag{4-5}$$

When we know the specific surface area, it is easy to determine an average pore wall flux of hydrogen at the surface of the particles from the relationship

$$j_{H,ave} = \frac{I}{a\delta nF} \tag{4-6}$$

where I is the superficial current density and δ is the thickness of the electrode.

Substituting equation 4-6 into equation 4-4 and assuming a constant radius of the particles in the electrode, we can get a value of the average dimensionless pore wall flux.

$$\Phi_{ave} = \frac{j_{H,ave} R}{D_o c_t} = \frac{IR^2}{3D_o c_t \delta n F \varepsilon_{act}} \qquad (4\text{-}7)$$

Then, using the relationships between the diffusion coefficient and the dimensionless pore wall flux (figures 4-4 and 4-5), we can estimate a constant diffusion coefficient that best suits the current at which we want to discharge an electrode. The model can then be run with this estimated value of D_s.

4.3 Application to a nickel oxide electrode

These relationships were tested to see how well they predicted the "true" diffusion behavior in the nickel electrode as predicted by the pseudo 2-D model described in Chapter 3. The idealized reaction of the nickel active material (written with charging to the right) is

$$Ni(OH)_2 + OH^- \leftrightarrow NiOOH + H_2O + e^- \quad (4\text{-}8)$$

As the electrode discharges, hydrogen diffuses from the surface into the center of the particles. As stated earlier, this diffusion process has been reported by several authors to be a possible limitation of the discharging process of the nickel oxide electrode. All the parameters used for these simulations are those from tables 2-1 and 2-2 except for the particle radius which is set to 4 μm.

Simulations incorporating the diffusion coefficients predicted by the functions given in figure 4-4 and 4-5 were compared to the results from the full 2-D model in order to test their accuracy. In figure 4-8, discharge curves at three different rates are presented. The curves show the polarization across the nickel electrode assuming the reference electrode in solution is a nickel oxide electrode at 50% state of charge. $\Phi_{1,\,j=NJ}$ represents the electric potential in the solid phase at the current collector, and $\Phi_{2,\,j=N2}$ represents the potential in the solution phase with respect to a reference electrode at the electrode-separator interface of the electrode.

From this figure, it can be seen that the "matching-transition-time" correlation predicts the low-discharge-rate behavior well, but underpredicts the potential at the 1 C and 1.5 C discharge rates. The "best curve-fit" correlation appears to predict the discharge behavior well for all rates down to about 90% utilization. On subsequent simulations, though, it was found that the diffusion coefficients that were predicted using this

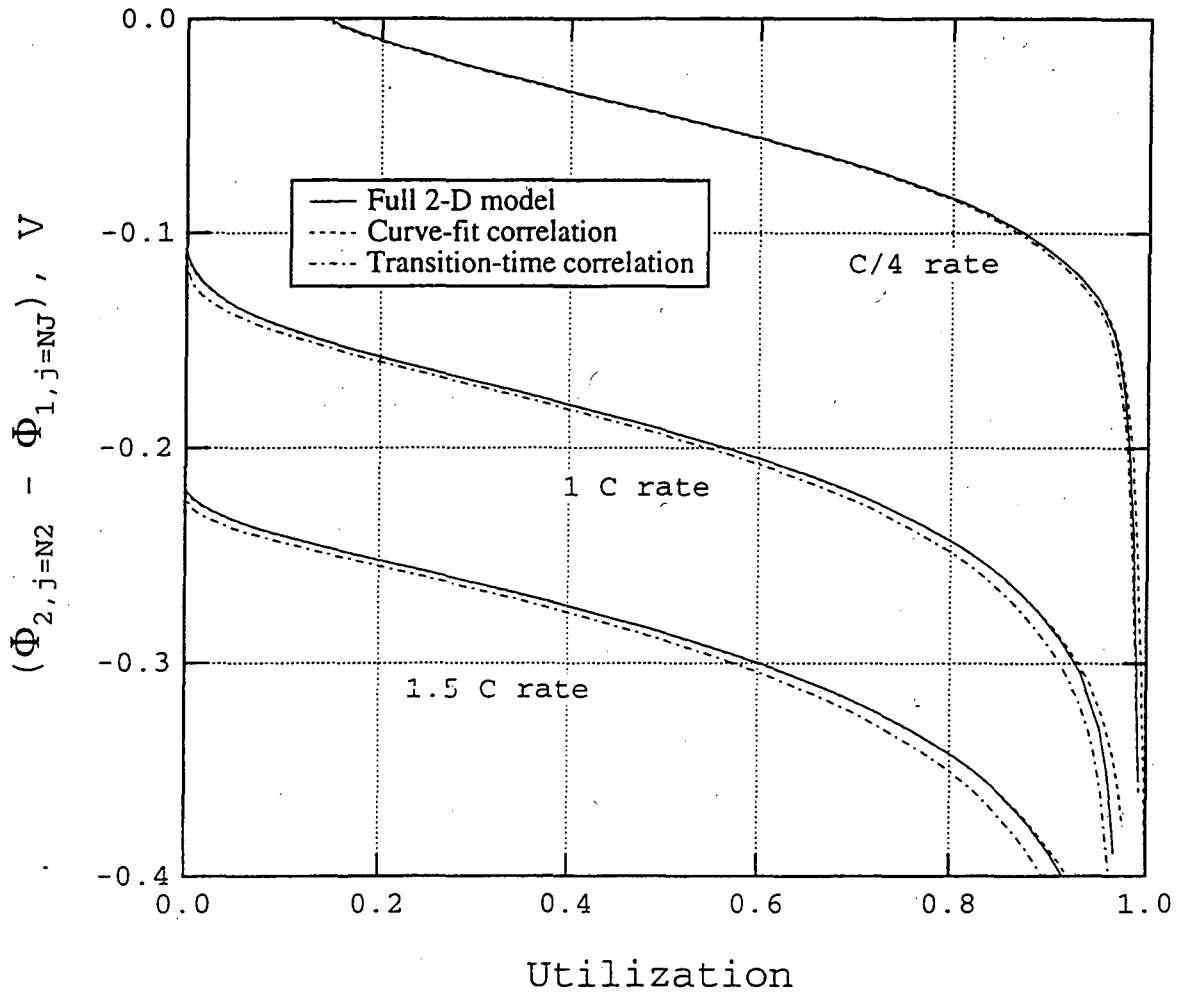

Figure 4-8: Polarization of the nickel electrode for discharges at three different rates. Polarizations incorporating Motupally's diffusion coefficient function are compared to polarizations produced using the "constant" diffusion coefficient functions from figures 4-4 and 4-5.

correlation were not limiting the diffusion process in the electrode at all. In other words, the discharge curves predicted using the "best-curve-fit" correlation would have been the same as if a diffusion coefficient of infinity were selected. Therefore it was found that the electrode examined above was not diffusion limited until about 90% utilization. The high-utilization discharge behavior of this electrode can be seen more clearly in figure 4-9, an enlargement of the lower right portion of the graph in figure 4-8.

With the kinetic parameters that are used in this model (table 2-1), rates higher than about 2 C are severely polarized, and the discharge potential is driven below the cutoff potential before significant concentration gradients can develop in the solid active material. In the limit of a case where facile kinetics exist and the reaction-rate distribution across the electrode is uniform, we can reason that the "transition-time" correlation would underpredict the electrode's polarization for most of the discharge, but at the end of discharge, the polarization curve predicted by this correlation would "rejoin" the actual discharge curves since it corresponds to the time at which the surface concentration reaches its limit. This predicted behavior can be seen in figure 4-9 for the C/4 rate and to a lesser degree for the 1 C rate.

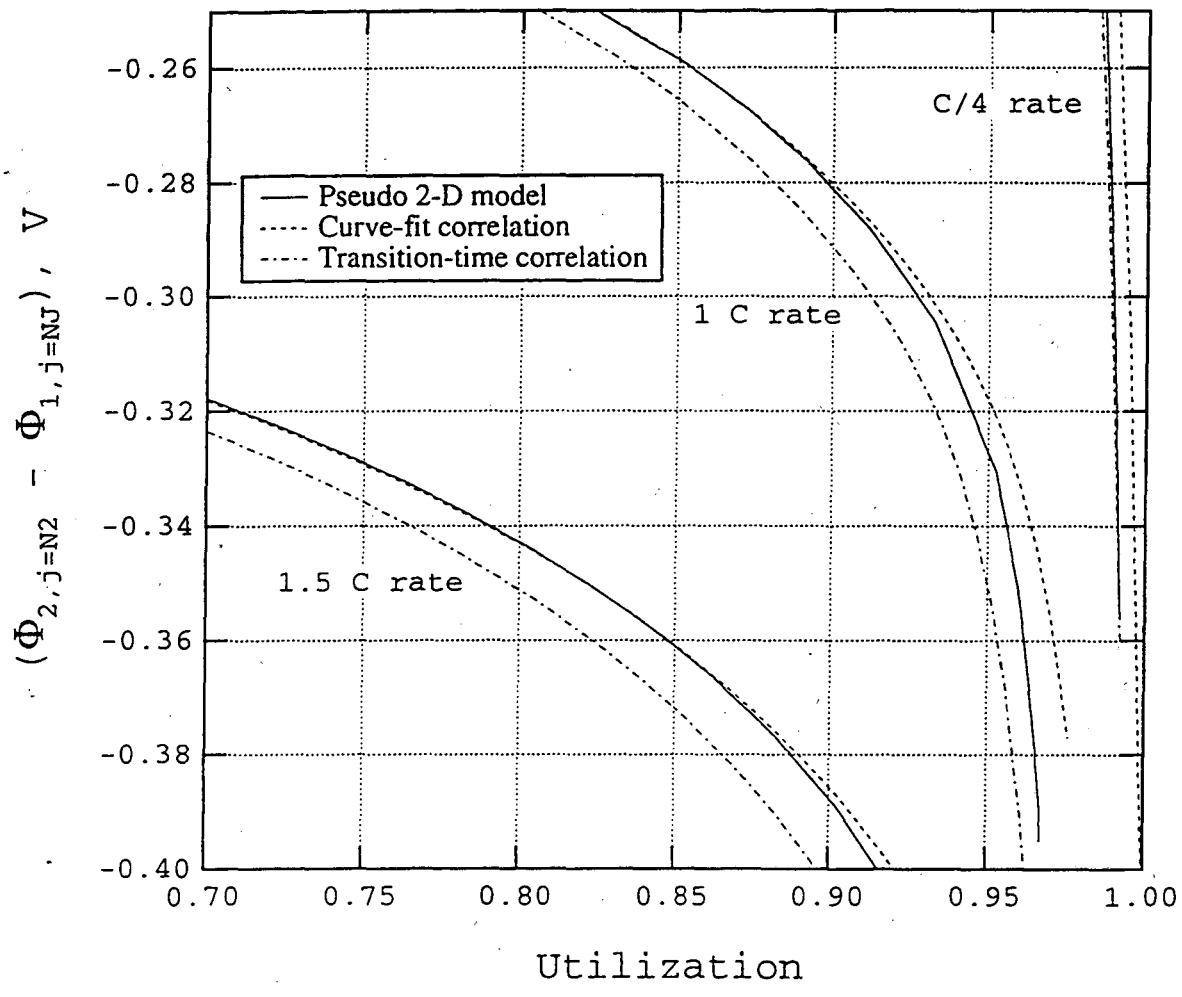

Figure 4-9: An enlargement of figure 4-8 at the end of discharge. The transition-time approximation for the C/4 and 1 C rates start to "rejoin" the curves of the true 2-D behavior.

4.4 Conclusions

A methodology has been presented that may be useful for the theoretical study of intercalation materials that exhibit a diffusion coefficient that varies as a function of the state of charge of the material. For researchers using models based on the assumption of a constant diffusion coefficient, this method may be useful in selecting the "best" constant-diffusion coefficient to use in a simulation.

Diffusion limitations in nickel oxide were examined to determine if this methodology might be useful for this system. It was found that the "best curve-fit" correlation essentially corresponded to the case where diffusion would not restrict the discharge of the system. The "transition-time" correlation underpredicted the potential of the nickel electrode at higher rates of discharge, but may be the better one to use for this system as it predicts that diffusion will always be a greater limitation of the electrode than predicted by the "true" variable diffusivity behavior. The "transition-time" correlation also predicts the correct utilization of the electrode in the limiting case of facile kinetics and uniform reaction-rate distribution.

References

(1) D. Guyomard and J. Tarascon, "Li Metal-Free Rechargeable $LiMn_2O_4$/Carbon Cells: Their Understanding and Optimization," *J. Electrochem. Soc.*, **139**, 937 (1992).

(2) P. Fiordiponti, M. Pasquali, G. Pistoia, and F. Rodante, "$(Mo_{0.3}V_{0.7})_2O_5$ as a Solid Solution Cathode for Li Cells. Part I. Electrochemical Behaviour of Primary Cells," *Journal of Power Sources*, 7, 133 (1981/1982).

(3) T. Fuller, M. Doyle, and J. Newman, "Simulation and Optimization of the Dual Lithium Ion Insertion Cell," *J. Electrochem. Soc.*, **141**, 1 (1994).

Chapter 5: Summary and Caveats of the Battery Study

This thesis presents a mathematical model of what is called the "metal hydride" battery system. Specifically, a model is presented of the nickel oxide/KOH/$LaNi_5$ cell. In Chapter 2, a fundamental study was undertaken to explore some of the operating characteristics of this cell, and an optimization of the electrode thickness and the porosity was performed in terms of the specific energy and power of the cell. It was found that a large "plateau" exits for the optimum value of the electrode thickness, indicating that some design flexibility may be available in this area. The analysis of this system was restricted to the discharge performance of the cell due to the lack of the inclusion of the oxygen side reaction in the nickel oxide electrode, which has been shown to be important during charging and overcharging of systems containing this electrode material.

A central theme of this thesis has been the effects of solid state diffusion limitations in the nickel oxide electrode. Using data on the diffusion coefficient of hydrogen in the solid phase as a function of the state of charge of the electrode, it is shown in Chapter 3 that diffusion limitations are usually not the main limiting factor during the discharge of this battery system. In Chapter 4, a general approach to modeling an electrode material with a diffusion coefficient that is a strong function of its state of charge is presented. An analysis of the nickel oxide electrode is presented using this methodology.

Both of the models presented in this thesis only examine the performance of a single cell. From these models, many, but not all, of the operating characteristics of a battery system can be examined. One of the primary concerns of battery designers is the number of cells that can safely and effectively be placed in a cell stack. It is desirable to place large numbers of cells together in a battery, as this decreases the ratio of the mass of the battery casing to the mass of the entire battery. The primary drawback to placing large numbers of cells in a stack is the ability of the stack to conduct away excess heat generated on charge and discharge of the system. Since this model consists of a single cell, it cannot

be used to optimize a battery system in this manner. This model, however, could be used as part of a multiple-cell battery model in order to address these concerns.[1]

As indicated in section 1.4, the metal hydride compound, $LaNi_5$, undergoes a phase change as hydrogen is inserted and removed from the metal lattice. This type of behavior can be rigorously modeled using what is known as a "shrinking-core model.[2]" This approach was not pursued in this thesis for three reasons. First, although it is known that two distinct phases of the hydrided metal exist, the exact range of stoichiometries of each phase is still a subject of investigation; this composition information is essential to the formulation of this type of model. Second, the model presented in this thesis was designed to be general, and by modeling the phase behavior of $LaNi_5$, I would be restricting the usefulness of the model to only this material. Third, it appears that diffusion in $LaNi_5$ and some of its substituted derivatives is not the main limitation of the nickel/metal hydride battery system; evidence is presented in section 1.4 to this effect.

References

(1) C. Pals, *Thermal Modeling of the Lithium/Polymer Battery*, master's thesis, University of California, Berkeley (1994).

(2) R. Pollard, *Mathematical Modeling of the Lithium-Aluminum Iron Sulfide Battery*. a dissertation, University of California, Berkeley (1979).

Chapter 6: Study of the Organizational and Political Forces which Contributed to the California Air Resources Board's "Zero-Emission Vehicle Rule."

"Facts are easy. It is the atmospheres that made them possible that are elusive" **- Doris Lessing**[27]

6.1 Summary

Since the 1960s, California has had the strictest emissions standards for motor vehicles. This history of strict regulation by the California Air Resources Board (CARB) deeply affects this organization's policies. Specifically, the recent "Zero-Emission Vehicle" Rule, passed in September of 1990 and mandating the sale of electric vehicles in California, is examined. This paper attempts to describe some of the organizational and political forces which motivated the enactment of this regulation.

6.2 Introduction

The following is a story of two "atmospheres." The first is the urban atmosphere of the State of California -- one that at the present time is contaminated with ozone, carbon monoxide, and other chemical components of smog. The other atmosphere is the regulatory -- the one that blankets California, the one populated by politicians, technocrats, and rule makers.

This story is coevolutionary; it is a tale of how these atmospheres influence each other, how severe urban air pollution in cities like Los Angeles create political and organizational pressures which influence rule making by the United States EPA as well as the California Air Resources Board. In turn, the state and federal fiats promulgated by

these organizations, directly affect the quality of the physical atmosphere above California's metropolitan areas.

The period of time which is examined is the late 1980's leading up to the enactment of what is known as the "Zero-Emission Vehicle (ZEV) Rule"-- a rule which, starting in 1998, will mandate that electric vehicles be sold in the State of California. The question we concern ourselves with is, "What were the causes for the enactment of this regulation?" This paper attempts to demonstrate (1) that the ZEV rule functioned to relieve certain political and organizational tensions that were faced by CARB at the turn of this decade and (2) that the impacts of the ZEV Rule were not critically examined by CARB prior to its enactment. But as this is a coevolutionary tale, the answers that are proffered are non deterministic. Indeed, there are no simple or deterministic responses to this sort of question. What are proposed are partial truths, sideways glimpses at the "real" reason the ZEV rule was enacted. This is a story belonging to recent political history, but the controversy surrounding the ZEV rule has not subsided; on May 1, 1995, the governors from four midwestern states sent a letter with heavy political overtones to California Governor Pete Wilson, urging him to abandon the ZEV Rule.[22]

Before I begin the story, I should delineate what this story is not. This article is not a structural analysis of the Air Resources Board. I do not claim to know the intricacies of internal operations at CARB-- how information travels, how accountability is maintained, or which key personalities are involved in the decision-making process. Neither is this a study of classical politics. I cite no campaign contribution totals, tell no stories of nepotistic favors, and detail no strategic procedural maneuvers on the part of members of the Board. The perspective I present is one of an outsider. I only present the public artifacts from the internal decision-making process at CARB and look for patterns that will suggest the motivating factors for the enactment of the ZEV Rule. Fortunately, for the task at hand, there are many artifacts, and the puzzle pieces tell a convincing story when they are assembled.

Since the facts are necessary to understand the aforementioned "atmospheres," this is where we must begin. On September 27, 1990 the California Air Resources Board passed a body of regulations referred to as the "Low-Emission Vehicle" (LEV) regulations. These regulations created four levels of emissions standards that passenger vehicles must meet starting in 1998. The vehicles meeting each of these four, increasingly stringent levels were labeled (1) Transitional Low-emission Vehicles (TLEVs), (2) Low-Emission Vehicles (LEVs), (3) Ultra Low-Emission Vehicles (ULEVs), and (4) Zero-Emission Vehicles (ZEVs). Car makers were given overall fleet-average limits for certain pollutants and were allowed to meet these limits with any combination of LEVs, TLEVs, and ULEVs. The regulation concerning Zero-Emission Vehicles was quite a bit different, though. This "ZEV Rule" required that from 2 to 10% of all the vehicles sold in California starting in 1998 had to emit no pollution (the specific timetable is given below). Since only electric vehicles do not emit pollution while being driven, these were essentially the types of vehicles stipulated by this rule.

Table 6-1: Timetable of mandatory production of electric vehicles

Year	Percentage Production
1998	2%
2001	5%
2003	10%

By passing this regulation, CARB captured the imagination of two generations of Americans. Since the 1950's, electric cars have been touted in news articles as the vehicles of the future. Since they run silently on the "invisible" fuel of electricity, they seem to be magical. Gone is the hissing, sputtering, and belching of the internal combustion engine.

Electric vehicles have no oil filters to change, no valves to adjust, no fuel tank to fill. They have no radiator, no fuel pump, no water pump, no spark plugs, almost none of the parts that we associate with "traditional" automobiles. And most importantly, they have no exhaust pipe.

Until CARB passed its ruling in 1990, electric vehicles were a dream that was always just a few years away. In 1966 Ford said that it would have a salable electric vehicle in five years.[23] In 1973 it was estimated that thirty companies including Ford, General Motors, Westinghouse, and General Electric had electric vehicles in the prototype or limited-production stage.[26] And in 1990, GM released details (and photos!) of its slick, sporty new electric vehicle, the Impact. Just by looking at the titles of some articles that have appeared in magazines over the past forty years, we can understand that America has always expected the imminent appearance of electric vehicles on America's roads.

Table 6-2: Titles of selected articles about electric vehicles from the past forty years

Publication	Date	Title
Science Digest	August 1955	"Predict Electric Auto's Return"
Saturday Evening Post	March 12, 1960	"Are Electric Cars Coming Back?"
U.S. News and World Report	September 26, 1966	"New Talk of an Electric Car"
Reader's Digest	May 1973	"Is the Electric Car Coming Back?"
Science News	October 2, 1976	"Return of the Electric Auto"
Motor Trend	November 1990	"The Shape of Things to Come?"

To a special subset of Americans, whom I will blithely refer to as "environmentalists," electric vehicles meant even more than the magic of silent operation or the promise of a vehicle without fluids to change and spill. To them electric vehicles symbolized clean transportation that could be powered by the sun. From the much-publicized solar-electric car races in the California desert to the odd concept car on display at auto shows, the idea of an electric car as the clean vehicle of the future has been embedded in the psyche of the United States. Electric vehicles also symbolize independence from a hierarchical system of energy distribution. Because they have the potential to be charged by means of photovoltaic cells, electric vehicles promised a potential severing of the umbilical cord linking individuals to the petrochemical industry as well as to large electric utilities.

When the Air Resources Board acted in dramatic fashion by passing the ZEV Rule on September 27, 1990; it released forty years of American anticipation of this silent, futuristic, mysterious form of transportation. To those who had seen the electric vehicle referred to as the eventual future of transportation in the United States, the decision made by CARB in the fall of 1990 was, undeniably, the "right" thing to do.

By passing this regulation, CARB raised the ire of some of the most powerful political and financial interests in this country. Immediately after the passage of the ZEV regulation, the auto industry and the petroleum industry joined forces in an attempt to repeal the rule.[15] For them this rule represented a threat to their virtual monopoly on ground transportation in the United States. Their vociferous arguments concerning excessive costs, the undeveloped state of battery technology, and non existent infrastructure needed to support electric vehicles have moved a few legislators to try to defeat the rule, but on the whole the opponents of the Rule have only persuaded themselves of their righteousness.

The Zero-Emission Vehicle Rule promises much; CARB states that the rule offers no less than the hope of the eventual elimination of urban air pollution. With their claims of electric vehicles' lower operating costs, noise-free operation, and a longer and more

dependable life span, CARB sees itself as paving the way to a whole new era of transportation possibilities.

But could a measure such as the ZEV Rule, which was promulgated by a scientific/technical organization and that currently has the support of both the people and the state legislature,[3,24,25] have been enacted for reasons other than solely to reduce urban air pollution? By taking a look at the history of the California Air Resources Board and the technical documents supporting the ZEV Rule, I hope to draw some strong inferences that the Rule served other purposes besides reducing urban air pollution. I hope to demonstrate that at the time of this rule's enactment, CARB was in a political and organizational crisis that threatened both its historical leadership position in the regulation of mobile source emissions as well as its jurisdictional authority over the regulation of pollution in the Los Angeles basin. Furthermore, it is shown that these crises created needs which would be at least partially satisfied by the highly symbolic concept of electric vehicles as well as the closely related idea of a "zero-emission vehicle".

6.3 A Short History of CARB

To understand some of the symbolic motivations for the ZEV Rule we must first take a look at the rich history of the California Air Resources Board. CARB began its life as the Motor Vehicle Pollution Control Board (MVPCB), which was created by the legislature in 1960. It is at this time that scientific consensus on the origins of urban air pollution had crystallized, and city dwellers started looking towards government for help in alleviating the now severe air pollution problems plaguing California's metropolitan areas.

The first action of the MVPCB was the required installation of positive crankcase ventilation (PCV) valves on both new and used automobiles starting in 1963. These devices captured unburned hydrocarbons that built up in the engine's crankcase and routed them back to the combustion chamber. Previous studies by the MVPCB indicated that 25%

of automobile emissions could be eliminated by the installation of these devices, and at a few dollars apiece these devices were a cost-efficient emissions-reduction measure.[1]

To say that these devices were a success is a broad understatement -- they were reliable, they did not decrease engine performance, and they were cheap. A natural consequence of the early success of this "experimental" effort was that the state of California was immediately labeled by the rest of the country as the leader of mobile source emissions regulations. During the period following the PCV valve rule, the plaudits poured in from across the country in the form of editorials, media attention, and a steady stream of supplicants seeking information about the MVPCB and its regulations.[1]

Another broad understatement would be to say that California, and specifically the MVPCB, enjoyed its position as the innovator of automobile pollution control. From some of the very first public documents published by The Board we start to see a very self-congratulatory and self-aggrandizing tone emerging from the organization. Emblematic of this attitude was the cover of the MVPCB's 1967 Biennial Report which featured a picture of Hubert Humphrey and an accompanying quote lauding California's regulatory efforts.

"The whole Nation is indebted to you Californians for your long and productive campaign to achieve meaningful control of air pollution from new motor vehicles. We have all learned from your experience. By the fall of 1967 citizens in every part of the land will begin to derive benefits like those you in California are deriving this fall from the control of air pollution from new cars. I wish the rest of the Nation were no further behind you than this in controlling the other major sources of air pollution."

—Vice-President Humphrey,
Los Angeles, Nov. 4, 1965

Figure 6-1: From the cover of the MVPCB's 1967 Biennial Report[1]

It is exactly this sort of smug, self-righteous tone that characterizes the MVPCB's (and later CARB's) documents from the 1960s until the present. Take for another example a sentence from the same document that reads,

> " [The Board] has always had the complete cooperation of all segments of public and private life, as indicated by various advisory committees... [and] the Board has established a worldwide reputation for its pioneer accomplishments in pollution reduction."

As evidenced from these examples, what we witness in the first few years of the existence of the MVPCB is (to use a colloquial expression) the copping of an attitude. This is not to say that the actions that the MVPCB took in the early 1960's were unimportant or were not desperately needed. Nor is this to say that a certain amount of pride shouldn't be considered a just reward for legislators and government executives who had the courage to set unprecedented regulations. It is, though, a warning that this pride can easily be transformed into a type of organizational hubris that can lead to both wasteful political posturing and irrational rule making.

This aforementioned attitude was not just a characteristic of the original MVPCB; it is still one of the defining features of the current Air Resources Board. Compare, for example the previous quotes with a statement that appears as the introduction of an article about the LEV regulations in the February 1991 edition of CARB's monthly newsletter, "Air Review."[20]

> "The ARB's 20 year tradition of setting the world's toughest standards was continued when it adopted new emission limits for 'ultra-clean' models which will include the required production of non-polluting electric cars."

Indeed, if we scan a few of the made-for-the-public documents published by CARB, we see repeated references to CARB as a "leader" or "bold innovator" in the fight against pollution as well as references to CARB's "tradition of leadership" or the "worldwide

recognition" CARB has received due to its stringent pollution limits. Reflecting these comments in a recent personal interview, the public relations director for CARB, Jerry Martin, referred to CARB as the "big dog" of the regulatory arena when this author hazarded a comparison of CARB and the EPA.[16] It is also worth mentioning that this attitude is not just carried by the regulatory agency, but by the people of California themselves as evidenced from recent editorials in newspapers such as the Los Angeles Times.[6,7]

What is suggested by these quotes is that due to a series of successful pollution control actions taken by CARB, there is now an organizational "pressure" to maintain a perceived leadership position vis-à-vis the federal government in the regulation of mobile source emissions. A quote from CARB's communications director, Bill Sessa, in 1992 confirms that this hypothesis is more than just speculation.[21]

> "Through the Air Resources Board, California administers the world's strictest emission standards for motor vehicles of all types. Other agencies, including the federal Environmental Protection Agency and similar organizations in other countries, often use the Board standards as a precedent when setting standards of their own."

From the evidence presented, I suggest that CARB is reluctant to see itself displaced from its current position of leadership. Since CARB has been in a leadership position for close to three decades now, it even may be that it is organizationally unacceptable for CARB to fall behind the federal government's pollution control standards. In the following section I attempt to demonstrate that such a "pressure" existed at the time of the implementation of the LEV body of regulations.

6.4 Motivations for The LEV Rules in General

In the case of the 1990 LEV rules there are definite indications that the national Clean Air Act of 1990 prodded CARB to promulgate new, stricter emissions regulations. The mobile source emissions regulations contained in the 1990 Clean Air Act were essentially copies of emissions regulations that were already in effect in California. Specifically the rules enacted by the 1990 Clean Air Act were (1) that by 1998 pollution control equipment on new cars must be warrantied for 100,000 miles and (2) that by 1996 stricter emissions limits on hydrocarbons and nitrogen oxides must be met by all new cars.[2] Since these two regulations were already in effect in California, it was imperative that CARB act if it intended to stay ahead in the emissions limit "game."

One indication we have when trying to determine if the Clean Air Act of 1990 forced CARB to pass new regulations is the timing of the two actions; the LEV rules were passed on September 27, 1990; and the Clean Air Act of 1990 was signed into law less than two months later on November 15, 1990. This coincidence alone does not prove that CARB was acting to maintain its leadership position, but it does suggest such a motivation, especially since CARB, at this time, had not passed any significant body of regulations since 1981.[9]

Another factor motivating the LEV Rules was that, in 1986, the EPA began making efforts to usurp CARB's regulatory authority over pollution control efforts in the Los Angeles basin. In the early 1980's EPA defined several areas of the country that had especially severe urban pollution problems. These "non-attainment areas" were given until 1987 to meet ambient air quality standards for ozone and other chemical components of smog.[11] In late 1986 it was apparent that the four-county area comprising a district known as the South Coast Air Quality Management District (SCAQMD), which includes the Los Angeles basin, would not meet these standards by the 1987 deadline. In September of 1986, the EPA launched a rigorous review of the SCAQMD's pollution-abatement plans,[10]

and in 1987 it announced sanctions banning the construction of any new large point sources of pollution (such as refineries and electric plants) within the district.[11] While largely symbolic (because no one had any plans to build facilities such as these), this action broke the tradition of CARB having regulatory oversight over the SCAQMD. In response to this action, the obviously concerned CARB chairperson, Jananne Sharpless, stated that the sanctions "are not going to get us clean air" but that they could "erode the credibility" of the Air Resources Board and California as leaders in the fight against air pollution.[11]

To combat these aggressive actions by the EPA, the SCAQMD formulated a 20 year plan for attaining the established pollution limits. This plan, released in the summer of 1989, called for 125 new regulations ranging from new zoning rules to new fuel formulations specifically tailored to the basin's climate and existing smog problem. By the SCAQMD's own calculations, though, these rules were not enough to bring the basin's pollution levels down to compliant levels. The plan, therefore had to lean heavily on new rules that CARB had yet to formulate -- specifically the LEV rules that CARB would pass in 1990.[8] Therefore it became essential that CARB's new regulations had to be stringent enough, or appear stringent enough, not only actually to reduce pollution levels, but also to cause the EPA to retreat from its hostile stance towards pollution control efforts and allow CARB and the SCAQMD to regain their autonomy with respect to controlling urban air pollution in the Los Angeles basin. In this situation, like with the Clean Air Act of 1990, CARB's credibility as a "tough on pollution" agency was being threatened.

The preceding evidence gives reason to believe that the LEV rules in general were formulated to (1) maintain a perceived leadership position of the California Air Resources Board vis-à-vis the federal government in the regulation of mobile source emissions and (2) to win the turf battle with the EPA over the authority to regulate pollution in the Los Angeles Basin. But what about the Zero-Emission Vehicle Rule specifically? What purpose did it serve CARB?

I don't pretend to answer that question completely, but I do suggest some possibilities. For one, the ZEV rule guaranteed that CARB would always be the leader in pollution control -- after all, how can any vehicle emit less than zero emissions? Another possibility is that it was a decisive break with the old incremental mobile source emissions policies of the past, and that this type of bold new symbol was what CARB needed to keep the EPA from usurping its authority over the SCAQMD. Admittedly, these suggestions are overly deterministic, but they do raise some interesting questions. In the following section I attempt to provide some more circumstantial evidence supporting the assertion that the ZEV itself served a symbolic function for CARB by (1) demonstrating that the rule will not necessarily be effective in reducing emissions, (2) that it may not be the most cost effective approach to reducing pollution, and that because of these uncertainties (3) CARB deliberately ignored the efficacy or the cost-effectiveness of "zero-emission vehicles" when enacting this rule.

6.5 The ZEV Rule

The 1988 California Clean Air Act

To serve as a backdrop for the following discussion of the enactment of the ZEV Rule, it is appropriate to examine the legislation that gave CARB the authority to pass the LEV and ZEV Rules. In 1988, the legislature passed the California Clean Air Act (CCAA) to give CARB broader authority to require more than just 'end-of-the-pipe' pollution control measures for automobiles. Among other provisions, the CCAA enacted Heath and Safety Code sections 43013 and 43018 which, in tandem, give CARB the authority to set "in use performance standards and motor vehicle fuel specifications" for the control of air emissions. In light of the assertions I intend to make, HSC 43013 subsection (a) is particularly interesting, and the text of this rule is reprinted below.

43013. (a) The state board may adopt and implement motor vehicle emissions standards, in use performance standards, and motor vehicle fuel specifications for the control of air contaminants and sources of air pollution which the state board has found to be necessary, cost-effective, and technologically feasible to carry out the purposes of this division. (p.C-4)[12]

In addition subsection (c) of section 43018 states,

"...the state board shall adopt standards and regulations which shall result in the most cost-effective combination of control measures on all classes of motor vehicles and motor vehicle fuel, including, but not limited to, all of the following:

(1) Reductions in motor vehicles exhaust and evaporative emissions.

(2) Reductions in emissions from in-use emissions from motor vehicles through improvement in emission system durability and performance.

(3) Requiring the purchase of low-emission vehicles by state fleet operators.

(4) Specification of vehicular fuel composition." (p. C-5)[12]

What these sections of the CCAA clearly demonstrate is that CARB was required to justify all of its actions on the bases of efficacy, economics, and technological feasibility. Therefore if CARB did not justify the ZEV component of the LEV rules by these criteria, it not only ignored standard evaluative procedures, but it also evaded the law. The following sections attempt to demonstrate that this is exactly what CARB did in passing the Zero-Emission Vehicle Rule.

The Technical Support Document

A month before it passed the final package of Low-Emission Vehicle rules on September 27, 1990, CARB released a supporting document justifying its actions. This document, entitled the "Technical Support Document for the Proposed Regulations for Low Emission Vehicles and Clean Fuels (Release Date: August 13, 1990)", contained all of the economic as well as technical justifications for the entire body of LEV rules. This hefty 400+ page tome chronicles in tedious detail the "reactivity adjustment factors" for air contaminants, reformulated gasoline specifications, and methodologies that will be used to test vehicles under this new program. What is missing in this extensive analysis, though, is any technical or economic justification for the ZEV rule. In fact, it seems that the whole structure of the document is designed to downplay this part of the regulations. Examining each of the aforementioned evaluative criteria in turn will allow us to see just how shallow the official justification for the ZEV rule was.

- Efficacy of the ZEV Rule

First of all, there was no attempt to demonstrate that the ZEV Rule would reduce air emissions, and in fact, there was no attempt even to quantify the emissions that would be caused by "Zero-Emission Vehicles." Despite their deceiving sobriquet, electric vehicles do create quantifiable emissions. These emissions are not produced by the vehicles themselves, but are instead created by the facilities that produce the electricity needed to charge the vehicles' batteries. In addition, emissions are produced by the manufacture of batteries (which must be periodically replaced). In the Technical Support Document these emissions not only went unquantified, they were not even acknowledged by the persons who prepared the report.

Additionally, there is a logical argument that the required production of a certain number of electric vehicles would produce an offsetting increase in air pollution due to

older, more polluting vehicles remaining on the road for a longer period of time. This logic goes something like the following:

(1) Since electric vehicles have a lower utility than conventional vehicles, only a few people will buy them at a price which is profitable to the manufacturer. Therefore electric vehicles must be sold at an unprofitable price; thus -
(2) Since the manufacturer will want to maintain its desired profit margin, the price of conventional vehicles will have to be raised, effectively subsidizing the sales of electric vehicles; thus
(3) On average due to the higher cost, consumers will buy fewer new, less polluting conventional vehicles, resulting in older, more polluting vehicles remaining on the road longer.

Admittedly this argument incorporates assumptions about the elasticity of the automobile market, consumer preferences, and the amount of pollution created by older vehicles; but it is not altogether unrealistic. Using economic data and some reasonable assumptions, one can calculate that an offsetting emissions increase could be 20 to 30% of the emissions reduction created by electric vehicles (see section 6.7 for assumptions and calculations). As with the quantifiable emissions from power plants, CARB failed to explore or even acknowledge the possibility of this type of offsetting emissions increase. The possibility of this sort of offsetting emissions increase is also closely tied into assumptions about the capital costs of electric vehicles, which CARB neglected to discuss as well.

- Economic Efficiency

The analysis found in the Technical Support Document concerning capital costs of electric vehicles leaves much to be desired. To emphasize the brevity of this analysis the entire section on electric vehicle economics is reprinted below.

Zero-Emission Vehicles (ZEVs)

> The staff consulted with electric vehicle experts on the projected cost differential of a commercial, moderate volume electric vehicle compared to a conventional vehicle. They estimated that by year 2000, electric vehicles would be comparable in cost to conventional vehicles except for the additional cost of the batteries. In the year 2000, advanced production batteries were estimated to cost an additional $1350 for light-duty vehicles and $2700 for medium duty vehicles (to accommodate the larger size and load capacities). (p.IX-7)

Obviously the greater part of this paper could be spent discussing the deficiencies in this analysis, but for the sake of brevity I will hold myself to a few paragraphs. The first and most obvious warning sign in the above passage is the term "electric vehicle experts." The entire document neglects to include footnotes, so we are not allowed to know who these "experts" are. And a prima facie scan of the thirty-four references given at the end of the report does not reveal any sources for this sort of knowledge. Also, this statement does not acknowledge the lower utility of electric vehicles with respect to conventional vehicles. An alternative economic picture comes from one Chrysler executive who estimated that their electric minivan would cost up to $20,000 more than their standard minivan and only go 100 miles between charges.[14] The point is that, at this time, the costs of mass producing an electric vehicle are uncertain.

Equally as suspicious is that the one bit of quantitative information supplied by this document, the estimated battery cost for a ZEV, is grossly underestimated. The document states that for a light duty vehicle the extra cost of the batteries would be $1350. Some simple calculations demonstrate that $1350 would not come close to paying for enough batteries to give even a highly efficient electric car a reasonable range. To demonstrate this I have taken data from several different sources and calculated both the cost and weight of a

battery pack needed to give an efficient electric car a 120 mile range (See section 6.7 for a sample calculation). These values are compared in the table below with the $1350 estimate proffered by the "electric vehicle experts" in the CARB report.

Table 6-3: Cost and weight comparisons of battery systems to CARB estimate

BATTERY SYSTEM	COST *	SOURCE	WEIGHT
• Not specified	$1350	CARB (1990)[12]	1360 lbs.+
• Lead / Acid	$2034	from CARB raw data (1994)[13]	1360 lbs.
• Metal Hydride	$6000	from Klein and Salkind, and Ovshinsky [4,5]	640 lbs.
• Not specified	$4125	U.S.A.B.C. † [13] mid-term goal	560 lbs.

* analysis above is normalized for a 120 mile range in a light duty vehicle (5.9 miles/kWh)
+ The only batteries that could conceivably be this inexpensive are lead/acid batteries
† The United States Advanced Battery Consortium is a government and industry alliance whose goal is to develop batteries for electric vehicles. The value given above is their cost goal for a battery system that meets several other performance criteria.

One thing to note from the above table is that CARB apparently based their cost estimates on the common lead/acid battery, which is proportionally much heavier than true "advanced production" batteries (such as metal hydride or lithium polymer batteries) as implied in the Technical Support Document. It is questionable as to whether a car with a 1360 pound battery pack could be as efficient as this analysis assumes.

Overall there are other relevant economic topics which CARB fails to address. These other omissions include: (1) no mention or estimate of the costs of the infrastructure which would have to be established to recharge a vehicle at a residence or business, and (2)

no macroeconomic analysis of how this rule might affect California's economy as a whole. From all of the above evidence, it is clear that CARB did not fulfill its mandate to demonstrate that electric vehicles are economically feasible.

- Technical Feasibility

As long as the California Air Resources Board has existed they have publicly endorsed the philosophy of "technology-forcing." This philosophy holds that rules can be developed before a technology has been completely proven in order to stimulate further development of the desired technology. As Bill Sessa explains,[21]

> "... the Board does not adopt emission standards based on current technology. Instead, its standards reflect the Board's judgment about the potential development of technology by the time the cars are built."

This philosophy has been applied during CARB's history to stimulate the production of PCV valves and more efficient catalytic converters, but the primary difference between those previous regulations and the ZEV regulation is the cost of the technology. When CARB mandated lower emissions limits to stimulate the development of PCV valves and catalytic converters they knew that the cost of these devices would be only a small percentage of the total cost of an automobile. In sharp contrast, the ZEV rule specifies a technology that will potentially cost thousands of dollars more than the average price of a new car.

Concerning the California Clean Air Act, it seems that by formulating their policy on electric vehicles under the philosophy of "technology forcing," CARB has not complied with their legal requirement of mandating only technologically feasible devices. What must be realized, though, when embarking upon a debate of the technical merits of a certain device is the fluidity of the term "technological feasibility." Since technologically feasible solutions do exist for almost all environmental problems at some cost (*e.g.* launching

hazardous wastes into the sun) and since electric vehicles have been available for over one hundred years, we must infer that the legal use of the term "technologically feasible" takes on meaning only by considering whether a given technology provides a certain utility at a reasonable price compared to other competing technologies. In light of electric vehicles' lower utility and potentially steeper price, it does not appear that electric vehicles are "technologically feasible" either.

A Simple Analysis Based on CARB Data

Recently in this country there has been a movement towards more flexible or market-based emissions regulations. The "bubble cap" limits for sulfur dioxide emissions from power plants in the East are a good example. For the most part, the LEV rules *are* flexible-- they don't require a particular technology nor do they mandate that *all* cars meet certain emissions limits. The LEV rules just set overall fleet-average limits with which auto makers must comply. As discussed earlier, the ZEV Rule was a traditional "command and control" type regulation, essentially mandating the production of one specific technology, and as such, it stands in sharp contrast to the rest of the LEV body of regulations.

Assuming that CARB was truly looking for the best way to reduce vehicular emissions through mandating the use of a specific technology, we can speculate that the use of an electrically preheated catalytic converter would be a viable alternative to electric vehicles. From other data that are offered in the Technical Support Document, a simple analysis was performed comparing the ZEV Rule as it stands to a hypothetical rule requiring the installation of electrically preheated catalysts in all new vehicles. In the table below, these two options are evaluated on the bases of cost, efficacy, and technology.

Table 6-4: Evaluation of the ZEV rule compared to the mandatory installation of electrically preheated catalysts

Evaluative Criterion	ZEV Rule	Electrically Preheated Catalytic Converter
• Cost to consumers	Uncertain, but up to several thousand $$ per vehicle. (also reduced utility)	$150 per vehicle (p. IX-4)
• Efficacy	Good, but only affects a small % of new vehicles.	Guaranteed 25% to 35% reduction in emissions.
• Technology	Uncertain	Proven and reliable.

With so many question marks in the electric-vehicle column, why would an ostensibly scientific/technical organization such as the Air Resources Board choose the regulatory course they did? When asked this very question, CARB has responded that because of California's growing population the Board needs to look "further into the future" for solutions to mobile-source emissions problems.

This assertion is interesting both with regard to the CCAA's mandates and with regard to standard methodological procedures established for the evaluation of pollution control measures. Does CARB reason that because electric vehicles *seem* to reduce pollution, that they do not have to quantify the emissions from power plants and compare them to conventional automobile emissions? Also, does this statement imply that because of California's severe air pollution problems the cost effectiveness of a particular technology becomes *less* important to the process of formulating sound policy. Clearly there is more afoot here than just sloppy procedure in an otherwise rational attempt to curb urban air pollution.

One Other Factor

There are other factors that have influenced the adoption of the ZEV rule that do not fit squarely with the political or organizational motives set forth in this chapter. One of the

most important of these factors that has not received much attention is the role of General Motors prototype electric car, the "Impact." Unlike many of the previous electric vehicles produced by American carmakers which were adapted to existing automobile forms, this vehicle was completely redesigned from the ground up. The result was a slick-looking, high-power sports car which could compete in look and feel with many internal combustion automobiles on the market. The troubles with the car were that it had a range of only about 80 miles[18] and that even in mass production it would be very expensive. (In October of 1994, a GM Impact was on display at UC Berkeley. When this author asked the sales representative if she had driven the car, she said that they had to truck it in because they were afraid that a full charge would not make the sixty mile round trip from San Francisco to Berkeley to San Rafel and back during heavy traffic.)

In the interview with Jerry Martin from CARB, he said that the members of the Air Resources Board had the opportunity to look at an Impact just prior the actual vote on the LEV package of regulations. He indicated that to the Board, the Impact was "proof" that electric vehicles could be marketed successfully to the public.[16] We also find that in CARB's "Final Statement of Reasons" for the adoption of the LEV rules, they make repeated references to the Impact, calling it "competitive in performance" to gasoline-powered vehicles.[17]

6.6 Conclusions

In this paper I have tried to show that the ZEV rule was adopted by CARB at least partially to satisfy certain organizational and political needs and not solely to reduce urban air pollution. But while all of the information compiled in this analysis is valid, the nature of the evidence is still largely circumstantial. From information cited in CARB made-for-the-public documents, public statements by CARB officials, and the political milieu in which CARB is embedded; it is apparent that CARB is motivated by factors other than pure

economic and technical rationality. Even so, this does not mean that these motivations necessarily *caused* the ZEV rule to be promulgated. Likewise a thorough inspection of the LEV rule Technical Support Document shows that the economic, technological, and effectiveness of the ZEV rule were not adequately examined prior to its enactment; but this, again, does not necessarily mean that there was a conspiracy to ignore data in order to enact self-serving policy.

In conclusion, I feel it is important to state explicitly the nature of this type of analysis and the limitations embodied in a critique of this sort. As Robert Bartlett writes in his essay, *Evaluating Environmental Policy Success or Failure*, "Clearly desirable are multiple evaluations, done with a keen appreciation of the strengths and limitations of each approach and a frank recognition of the advantages of others." (p.183)[14] To this end I must admit that I have not condemned the ZEV rule, but have merely postulated a thesis and supported it with details. Evaluating whether the adoption of mandatory production quotas of electric vehicles is overall beneficial to society embodies many other ethical and methodological assumptions about policy analysis and life in general. Likewise, while it is clear that from a cost-benefit standpoint, for example, the ZEV rule is folly, that does not mean that it does not have merit within other contexts and other evaluative criteria.

In Bartlett's essay he repeatedly draws upon the example of the programmatic failure of the Comprehensive Environmental Response, Compensation, and Liability Act (CERCLA), or "Superfund," legislation. He presents evidence that few sites have been cleaned up at an exorbitant price to taxpayers and that there are many more cost effective means of reducing environmental risks. In contrast to this "narrow" analysis, he also stresses that a broader, richer view of the legislation can be gleaned by examining the institutional and symbolic consequences of the legislation, stating that "waste reduction, hazardous waste disposal, landfills, and recycling all mean something different now throughout America society" due to the CERCLA legislation. In the same way, the ZEV rule passed by CARB will certainly result in dramatic changes in popular conceptions of

transportation, pollution, and the institutions surrounding these social concerns. It would be interesting to try to approach the ZEV rule from a broader, more context-based perspective. From this type of analysis, maybe we could overcome the desire to try to label the ZEV rule as a success or failure, but instead attempt to gain a richer appreciation of the forces motivating the adoption of the rule and the potential consequences it may have in the concepts, roles, and routines of our daily lives.

6.7 Appendices

Appendix A -- Calculation of the Offsetting Emissions Increase of Mandating the Production of Electric Vehicles

During the first years of production, many auto makers predict that electric vehicles will be more expensive that conventional vehicles. I assume the following:

- Cost of a new "conventional vehicle" - $15,000
- Cost of a new electric vehicle - $21,000
- Percentage production mandated - 5%

Assuming that the electric vehicle would sell only at the price of a conventional vehicle, an auto maker would have to discount the electric vehicle by $6000. Spreading that cost out to the remaining conventional vehicles raises their price an average of $300. We know that an increase in price of a commodity will decrease its demand, so what we need is an economic measure called a "price elasticity of demand." The price elasticity of demand, η^D, is defined as "the percentage change in demand divided by the percentage change in price" and is a number usually between 0 and about -2. One estimate (although determined in 1957) for the η^D for automobiles is -1.20.[19]

$$\eta^D = \frac{\%\text{ change in demand}}{\%\text{ change in price}} = \frac{\frac{\Delta D}{D}}{\frac{\Delta P}{P}}$$

$$\Rightarrow \quad \Delta D = D\eta^D\left(\frac{\Delta P}{P}\right)$$

If we set the original demand without the ZEV Rule to be equal to 1, then we find that $\Delta D = -0.024$. This implies that, for these estimates, sales of conventional vehicles would fall by 2.4%.

Let's assume that the pollution reduced by putting one electric vehicle on the road is the quantity, **x**. Since the production percentage assumed is 5%, for every 1 electric vehicle sold, 20 conventional vehicles are sold. Therefore, to determine the reduction in purchases of conventional vehicles for each electric vehicle put on the road, we must multiply ΔD by 20. This yields a value of 0.48 vehicles.

For last part of the calculation, it is necessary to assume how much pollution is reduced by putting a new vehicle on the road as compared to putting an electric vehicle on the road. We will assume that this amount is 0.5x. (What we are really doing here is saying that there is an average amount of pollution generated by "older cars" that we will call **x**. If an "older car" was replaced by an electric vehicle all of that pollution would be eliminated. If that "older car" was replaced with a new car, we are assuming that half of that pollution would be eliminated.) So for every electric vehicle put on the road, there will be a resulting emissions increase of (0.48 vehicles)•(0.5x per vehicle) = 0.24**x**, a 24% offsetting increase in emissions.

Appendix B -- Sample Calculation of Cost and Weight of a Battery Pack

For both of these calculations we must first establish a "mileage" for the proposed electric vehicle. In a 1994 CARB document a value of 5.9 miles per kWh is given for an efficient electric vehicle. Based on this figure, and specifying a desired range of 120 miles, we are ready to calculate the cost and weight of the battery pack.

- Cost

The information necessary to make a calculation of the cost of a battery pack is the cost of the battery divided by the amount of energy that it can store. This quantity is usually given in the units of dollars per kWh. The formula we would therefore use is given below.

$$\text{Cost} = \text{range} \times \frac{1}{\text{mileage}} \times \frac{\$}{\text{kWh}}$$

For example, for the lead/acid battery we know that the cost of the system is about $100 per kWh. Therefore the total cost is computed as shown below.

$$\text{Cost} = 120 \text{ miles} \times \frac{\text{kWh}}{5.9 \text{ miles}} \times \frac{\$100}{\text{kWh}} = \$2034$$

- Weight

The information necessary to make this calculation is called the "specific energy" of a battery system, and this quantity is usually expressed in units of watt•hours per kilogram. The formula we would use is given below.

$$\text{Weight} = \text{range} \times \frac{1}{\text{mileage}} \times \frac{1}{\text{specific energy}}$$

Therefore, for the lead/acid battery which has a specific energy of about 33 watt•hours per kilogram, the following computation will give us the weight.

$$\text{Weight} = 120 \text{ miles} \times \frac{\text{kWh}}{5.9 \text{ miles}} \times \frac{\text{kilogram}}{33 \text{ watt•hours}} \times \frac{1000 \text{ watts}}{1 \text{ kW}}$$

$$\text{Weight} = 616 \text{ kilograms} = 1360 \text{ pounds}$$

References

(1) California Motor Vehicle Pollution Control Board, SMOG, *The Silent Enemy* (1967 Biennial Report).

(2) Gary C. Bryner, *Blue Skies, Green Politics - The Clean Air Act of 1990.* Congressional Quarterly Press, Washington, (1993).

(3) M. McKesson, "Chrysler To Meet Clean Air Deadline," *The San Francisco Chronicle*. Section B, p. 1. V.98, May 6, 1994.

(4) M. Klein and A. Salkind, "Design and Cost Analysis for a Nickel-Metal Hydride Electric Vehicle Battery," Abstract No. 25, 183rd Meeting of the Electrochemical Society, Honolulu, HI (1993).

(5) S. Ovshinsky, M. Fetchenko, and J. Ross, "A Nickel Metal Hydride Battery for Electric Vehicles," *Science*, **260**, 176 (1993).

(6) "The Drive to Be as Clean as Possible" (editorial), *The Los Angeles Times*. Section B, p.6. V.109, September 28, 1990.

(7) "Taking a Stand Against Smog" (editorial), *The Los Angeles Times*. Section II, p.6. V. 108, August 15, 1989.

(8) M. Dolan, "State Board OKs Clean Air Plan," *The Los Angeles Times*. Section I, p.1. V. 108, August 16, 1989.

(9) Matthew L. Wald, "California's Pied Piper of Clean Air," *The New York Times*. Section 3, p.1. V. 141, September 13, 1992.

(10) Larry B. Stammer, "AQMD Under Most Rigorous Investigation in Its 10 Years," *The Los Angeles Times*. Section I, p.3. V.105, September 10, 1986.

(11) Larry B. Stammer, "EPA Takes a Harder Stand on Enforcing Clean Air Act," *The Los Angeles Times*. Section I, p.3. V.106, April 24, 1987.

(12) *Technical Support Document for the Proposed Regulations for Low-Emission Vehicles and Clean Fuels (Release Date: August 13, 1990).* California Air Resources Board.

(13) *Draft Technical document for the Low-Emission Vehicle and Zero-Emission Vehicle Workshop on March 25, 1994 -- Zero-Emission Vehicle Update.* California Air Resources Board.

(14) Robert V. Bartlett, "Evaluating Environmental Public Policy Success and Failure" in *Environmental Policy in the 1990s.* Norman J. Vig and Michael E. Kraft, editors. Congressional Quarterly Press, Washington (1994).

(15) J. Marshall, "Electric Cars Will Cost Jobs, Consultants Say," *The San Francisco Chronicle*, Section D, p.3. V.98, February 15, 1994.

(16) Personal Interview with Jerry Martin, date: March 11, 1994.

(17) *Proposed Regulations for Low-Emission Vehicles and Clean Fuels-- Final Statement of Reasons (Release Date: July 1991).* California Air Resources Board.

(18) GM's Impact Fact Sheet obtained from GM representative in October, 1994.

(19) Gregory C. Chow, *Demand for Automobiles in the United States.* Amsterdam: North Holland Publishing Co., 1957.

(20) California Air Resources Board, "Futuristic Standards Adopted for 'Ultra Clean' Cars Fuel," *Air Review*, V.3 No.1 (February, 1991).

(21) Letter on Public File to Michael Jarvie from Bill Sessa. October 7, 1992.

(22) R. B. Gunnison, "Electric Car Push Angers Governors," *The San Francisco Chronicle*, Section A, p.2, V.102. May 23, 1995.

(23) "Poised for a Comeback: Electric Autos," *U.S. News and World Report*, October 17, 1966.

(24) "State Mandate Essential to Electric Car's Future" (editorial), *The San Francisco Chronicle*, V. 101. May 12, 1994.

(25) R. B. Gunnison, "State's electric Car Mandate Withstands Lobbyists' Pressure," *The San Francisco Chronicle*, Section A, p.15, V.101. May 13, 1994.

(26) H. Manchester, "Is the Electric Car Coming Back?," p.229, *Reader's Digest*, May 1973.

(27) D. Lessing, *Under My Skin: Volume One of My Autobiography, to 1949.* HarperCollins, New York (1994).

Appendix A: Computer Program for the Model of the Nickel Oxide/$LaNi_5$ Cell

```
C     BLAINE PAXTON
C     DR. NEWMAN'S GROUP
C     METAL HYDRIDE BATTERY MODEL (CGS VERSION) (VARIABLE TIME STEPPING)
C     BEGAN: SEPTEMBER 28, 1994
C     WORKING: JANUARY 18, 1995


C     THIS IS A MODEL FOR THE GALVANOSTATIC DISCHARGE OF A METAL HYDRIDE
C     BATTERY.  SEVERAL DESIGN PARAMETERS ARE INPUT FROM A DATA FILE NAMED
C     "MHDATA".  THESE PARAMETERS ARE THEN USED TO CALCULATE THE TIME-
C     DEPENDENT OUTPUT PARAMETERS SUCH AS THE CELL VOLTAGE, THE SOLUTION AND
C     SALT CONCENTRATIONS, THE PORE WALL FLUXES OF REACTIVE SPECIES, AND THE
C     CURRENT DISTRIBUTIONS.  THESE PARAMETERS ARE WRITEN TO AN OUTPUT FILE
C     WHICH IS SPECIFIED AT THE TIME OF EXECUTION.  SO THE PROGRAM DOES NOT
C     HAVE TO USE OUTRAGEUOS AMOUNTS OF MEMORY, THE DATA ARE OUTPUT AFTER
C     EACH TIME STEP.  THUS, THE VARIABLES ARE ONLY FUNCTIONS OF POSITION
C     WITHIN THE PROGRAM.

C     AS NOTED BELOW, THE VARIABLE C REPRESENTS ALL THE MAIN VARIABLES FOR
C     WHICH BAND SOLVES.  THIS PROGRAM IS WRITEN IN TERMS OF "CHANGE
C     VARIABLES", THAT IS THE VARIABLES THAT 'BAND' SOLVES FOR ARE ONLY THE
C     CHANGES THAT NEED TO BE MADE TO THE VARIABLES IN ORDER TO BRING THE
C     EQUATIONS CLOSER TO CONVERGENCE AT A PARTICULAR TIME STEP.
C     IN THE ELECTRODES, ALL FOUR OF THE VARIABLES
C     WILL BE USED, BUT IN THE SEPARATOR PHASE ONLY THE CONCENTRATION-
C     DISTRIBUTION WILL BE NECESSARY TO SOLVE FOR.
C
C     SO THAT FUTURE EYES THAT LOOK UPON THIS PROGRAM WILL NOT BE
C     OVERWHELMED BY ARCANE NOTATION, I HAVE TRIED TO NAME THE VARIABLES
C     COMMON-SENSICALLY.  EX. I= CURRENT
C
C     WHEN READING THE DICTIONARY OF VARIABLES, WHEN I SAY THE "DERIVATIVE"
C     I USUALLY MEAN WITH RESPECT TO CONCENTRATION.  IF I MEAN W/ RESPECT TO
C     "X", THE DISTANCE THROUGH THE CELL, AS IS THE CASE WITH THE FOUR MAIN
C     VARIABLES- CON,I2,OPN, AND CS; OR IF I MEAN W/ RESPECT TO "I2" (WHICH
C     IS THE CASE ONLY FOR THE VOLUME AVE. VELOCITY),
C     THEN I WILL SAY SO EXPLICITLY. THE VARIABLE SYMBOLS ALSO REFLECT THIS
C     NOTATION AS CAN BE SEEN BELOW.

C     SEVERAL VARIABLES GIVEN BELOW ARE TERMED"OLD"VALUES WHICH MEAN THAT IT
C     WAS NECESSARY TO"CARRY OVER" SOME OF THE VALUES FROM THE PREVIOUS TIME
C     STEP.  THIS IS NECESSARY BECAUSE OF THE USE OF THE CRANK-NICHOLSON
C     METHOD THAT IS USED TO SOLVE THE TIME-DEPENDENT CONC. EQUATION.
C     SOME OF THE OLD VARIABLES NEEDED FOR THIS CALCULATION ARE CARRIED OVER
C     IN THE FORM OF ARRAYS FROM THE PREVIOUS TIME STEP, AND SOME ARE
RECALCULATED
C     AT EACH POINT OF THE ARRAY.

C     ---------- -- ---------
```

```
C      DICTIONARY OF VARIABLES
C      ---------- -- ---------

C    NAME      TYPE      STRUCTURE     USAGE
C    ----      ----      ---------     -----
C    C         REAL-DP   2-DIM     THIS VARIABLE IS THE VARIABLE WHICH
C                                  REPRESENTS THE CHANGE VARIABLES FOR WHICH
C                                  BAND SOLVES.
C                                  C(1,N) = KOH CONCENTRATION (MOL/cm^3)
C                                  C(2,N) = SOLUTION-PHASE CURRENT (A/cm^2)
C                                  C(3,N) = OVERPOTENTIAL
C                                  C(4,N) = SURFACE CONC. OF H IN SOLID PHASE
C    I          REAL-DP   SCALAR  THIS IS THE OVERALL CURRENT DENSITY
C                                  ACROSS THE BATTERY (A/cm^2)
C    DELNEG    REAL-DP   SCALAR  NEGATIVE ELECTRODE THICKNESS (cm)
C    DELSEP    REAL-DP   SCALAR  SEPARATOR THICKNESS (cm)
C    DELPOS    REAL-DP   SCALAR  POSITIVE ELECTRODE THICKNESS (cm)
C    PORNEG    REAL-DP   SCALAR  NEGATIVE ELECTRODE POROSITY
C    PORSEP    REAL-DP   SCALAR  SEPARATOR POROSITY
C    PORPOS    REAL-DP   SCALAR  POSITVE ELECTRODE POROSITY
C    POR       REAL-DP   SCALAR  A "DUMMY" POROSITY USED IN THE PROGRAM
C    RADNEG    REAL-DP   SCALAR  RADIUS OF THE NEGATIVE PARTICLES (cm)
C    RADPOS    REAL-DP   SCALAR  RADIUS OF THE POSITIVE PARTICLES (cm)
C
C    CNDNEG    REAL-DP    SCALAR  CONDUCTIVITY OF THE NEGATIVE ELECTRODE
C    CNDPOS    REAL-DP   SCALAR  CONDUCTIVITY OF THE POSITIVE ELECTRODE
C    MKOH      REAL-DP   SCALAR  MOLECULAR WEIGHT OF KOH (g/mol)
C    MH2O      REAL-DP   SCALAR  MOLECULAR WEIGHT OF H2O (g/mol)
C    TPOS      REAL-DP   SCALAR  TRANSFERENCE NUMBER OF K+
C    ATCN      REAL-DP   SCALAR  ANODIC TRANSFER COEFFICIENT - NEG. ELCTRD.
C    CTCN      REAL-DP   SCALAR  CATHODIC TRANSFER COEFFICIENT- NEG. ELCTRD.
C    ATCP      REAL-DP   SCALAR  ANODIC TRANSFER COEFFICIENT - POS. ELCTRD.
C    CTCP      REAL-DP   SCALAR  CATHODIC TRANSFER COEFFICIENT- POS. ELCTRD.
C    EXCDN     REAL-DP   SCALAR  EXCHANGE CURRENT DENSITY OF THE NEG. ELEC.
C    EXCDP     REAL-DP   SCALAR  EXCHANGE CURRENT DENSITY OF THE POS. ELEC.
C    DSNEG     REAL-DP   SCALAR  SS DIFF. COEF OF NEG. ELEC MATERIAL (cm^2/s)
C    DSPOS     REAL-DP   SCALAR  SS DIFF. COEF OF POS. ELEC MATERIAL (cm^2/s)
C    SSANEG    REAL-DP   SCALAR  SPECIFIC SURFACE AREA OF THE NEG. ELECTRODE
C    SSAPOS    REAL-DP   SCALAR  SPECIFIC SURFACE AREA OF THE POS. ELECTRODE
C    ACTNEG    REAL-DP   SCALAR  THE ACTIVE MATERIAL VOLUME FRACTION (NEG.)
C    ACTPOS    REAL-DP   SCALAR  THE ACTIVE MATERIAL VOLUME FRACTION (POS.)
C    CINIT     REAL-DP   SCALAR  INITIAL KOH CONCENTRATION (TIME=0)
C    POWER     REAL-DP   SCALAR  THE INSTANTANEOUS POWER OF THE CELL
C    PAVE      REAL-DP   SCALAR  THE AVERAGE POWER OF THE CELL
C    ENERGY    REAL-DP   SCALAR  THE TOTAL USABLE ENERGY RELEASED BY THE CELL
C    NUMBND    INTEGER   SCALAR  THE TOTAL NUMBER OF TIMES BAND IS CALLED
C    NUMPTS    REAL-DP   SCALAR  NUMBER OF MESH POINTS
C    H         REAL-DP   SCALAR  MESH SPACING (cm)
C    DELTIM    REAL-DP   SCALAR  TIME STEP SIZE (s)
C    TIME      REAL-DP   SCALAR  REAL TIME DURING THE PROGRAM (s)
C    TNORM     REAL-DP   SCALAR  NORMALIZED TIME DURING THE PROGRAM
C    CELPOT    REAL-DP   SCALAR  THE CELL POTENTIAL (V)
C    CELOLD    REAL-DP   SCALAR  THE CELL POT. AT THE PREVIOUS TIME STEP (V)
C    CUTOFF    REAL-DP    SCALAR  THE CELL CUTOFF POTENTIAL (V)
C    RECOV     REAL-DP   SCALAR  THE FRACTION OF CAPACITY RECOVERED
```

```
C    VMAX      REAL-DP   SCALAR   THE MAXIMUM VOLTAGE ON CHARGE (V)
C    FEL       REAL-DP   SCALAR   ELEC. POTENTIAL DEPENDENCE ON
C                                  HYDROGEN CONCEN. IN THE SOLID PHASE (V)
C    FEL1D     REAL-DP   SCALAR   1st DERIVATIVE OF FEL WRT CS
C    FEL2D     REAL-DP   SCALAR   2nd DERIVATIVE OF FEL WRT CS
C    DC        REAL-DP   1-DIM    SALT DIFFUSION COEF AT CURRENT
C                                  TIME STEP (cm^2/s)
C    DOLD      REAL-DP   1-DIM    SALT DIFFUSION COEF AT PREVIOUS
C                                  TIME STEP (cm^2/s)
C    D1D       REAL-DP   1-DIM    1st DERIVATIVE OF DC (cm^5/mol s)
C    DN        REAL-DP   1-DIM    SOLUTION DENSITY (g/cm^3)
C    DN1D      REAL-DP   1-DIM    1st DERIV. OF DN (g/mol)
C    DN2D      REAL-DP   1-DIM    2nd DERIV. OF DN (g cm^3/mol^2)
C    K         REAL-DP   1-DIM    SOLUTION CONDUCTIVITY (S/cm)
C    K1D       REAL-DP   1-DIM    1st DERIVATIVE OF K (S cm^2/mol)
C    AC        REAL-DP   1-DIM    MEAN MOLAR ACTIVITY COEF.
C    AC1D      REAL-DP   1-DIM    1st DERIVATIVE OF AC (cm^3/mol)
C    AC2D      REAL-DP   1-DIM    2nd DERIVATIVE OF AC (cm^6/mol^2)
C    WAC       REAL-DP   1-DIM    WATER ACTIVITY COEF.
C    WAC1D     REAL-DP   1-DIM    1st DERIVATIVE OF WA (cm^3/mol)
C    V         REAL-DP   1-DIM    VOLUME AVE. VELOCITY (cm/s)
C    VOLD      REAL-DP   1-DIM    VOL. AVE. VELOCITY AT OLD TIME STEP
C    V1D       REAL-DP   1-DIM    1st DERIVIATIVE OF V (cm^4/mol s)
C    V1I2      REAL-DP   1-DIM    1st DERIV. OF V WRT I2
C
C
C    CON       REAL-DP   1-DIM    KOH CONC. AT PRESENT TIME STEP (mol/cm^3)
C    CON1X     REAL-DP   SCALAR   1st DERIVATIVE OF CON WRT X (mol/cm^4)
C    CONOLD    REAL-DP   1-DIM    KOH CONC. AT PREVIOUS TIME STEP   "
C    I2        REAL-DP   1-DIM    SOLUTION PHASE CURRENT AT THE
C                                  CURRENT TIME STEP (A/cm^2)
C    I2OLD     REAL-DP   1-DIM    SOLUTION PHASE CURRENT AT THE
C                                  PREVIOUS TIME STEP (A/cm^2)
C    OPN       REAL-DP   1-DIM    OVER POTENTIAL OF THE NEG. OR POS.ELECT. (V)
C    OPN1X     REAL-DP   SCALAR   1st DERIVATIVE OF OPN WRT X (V/cm)
C    CS        REAL-DP   2-DIM    CONCENTRATION OF HYDROGEN IN THE SOLID
C                         PHASE OF NEG. ELEC. AT THE SURFACE (MOL/cm^3)
C                                  (CS IS ALSO A FUNCTION  OF TIME)
C    CS1X      REAL-DP   SCALAR   1st DERIV. OF CS AT THE SURFACE OF THE
C                                  PARTICLE WRT X.
C    CNGMAX    REAL-DP   SCALAR   MAXIMUM CONC. OF H IN NEG. ELECT.(mol/cm^3)
C    CPSMAX    REAL-DP   SCALAR   MAXIMUM CONC. OF H IN POS. ELECT.(mol/cm^3)
C    CNGMIN    REAL-DP   SCALAR   MINIMUM CONC. OF H IN NEG. ELECT.(mol/cm^3)
C    CPSMIN    REAL-DP   SCALAR   MINIMUM CONC. OF H IN POS. ELECT.(mol/cm^3)
C    AN & AP   REAL-DP   1-DIM    VARIABLES USED FOR CALCULATING THE SURFACE
C                         CONCENTRATION USING THE SUPERPOSITION PRINCIPAL
C                         IN THE NEGATIVE AND POSITIVE ELECTRODES.
C    SUM       REAL-DP   SCALAR   ANOTHER VARIABLE FOR CALC. THE SURFACE CONC.
C    FLIP      REAL-DP   SCALAR     "          "     "
C    F         REAL-DP   SCALAR   FARADAY'S CONSTANT (C/EQ)
C    T         REAL-DP   SCALAR   TEMPERATURE (K)
C    RTF       REAL-DP   SCALAR   RT/F = 0.02567 VOLTS
C    J         INTEGER   SCALAR   A DUMMY VARIABLE USED FOR EXPEDIENCY
C    DUM       REAL-DP   SCALAR   A DUMMY VARIABLE USED FOR EXPEDIENCY
C    NUM       REAL-DP   SCALAR   A DUMMY VARIABLE USED FOR EXPEDIENCY
```

```
C    U1        REAL-DP   SCALAR   A DUMMY VARIABLE USED FOR EXPEDIENCY

C    U2        REAL-DP   SCALAR   A DUMMY VARIABLE USED FOR EXPEDIENCY
C    U3        REAL-DP   SCALAR   A DUMMY VARIABLE USED FOR EXPEDIENCY
C    U4        REAL-DP   SCALAR   A DUMMY VARIABLE USED FOR EXPEDIENCY
C    U5        REAL-DP   SCALAR   A DUMMY VARIABLE USED FOR EXPEDIENCY
C    U6        REAL-DP   SCALAR   A DUMMY VARIABLE USED FOR EXPEDIENCY
C    DP        REAL-DP   1-DIM    A DUMMY VARIABLE USED IN FINDING CELPOT
C    ER        REAL-DP   SCALAR   THE VARIABLE FOR RETURNING THE ERROR
C                                  FUNCTION FROM THE SUBROUTINE ERFC

C    A         REAL-DP   2-DIM    A VARIABLE FOR BAND (SEE NEWMAN TEXT)
C    B         REAL-DP   2-DIM    A VARIABLE FOR BAND (SEE NEWMAN TEXT)
C    D         REAL-DP   2-DIM    A VARIABLE FOR BAND (SEE NEWMAN TEXT)
C    G         REAL-DP   1-DIM    A VARIABLE FOR BAND (SEE NEWMAN TEXT)
C    X         REAL-DP   2-DIM    A VARIABLE FOR BAND (SEE NEWMAN TEXT)
C    Y         REAL-DP   2-DIM    A VARIABLE FOR BAND (SEE NEWMAN TEXT)

C
C    ERR       REAL-DP   SCALAR   THE FRACTIONAL ERROR BETWEEN THE NEWEST
                                  BAND GUESSES AND THE OLD VALUES
C    LIMIT     REAL-DP   SCALAR   THE CONVERGENCE CRITERION
C    N1        INTEGER   SCALAR   THE MESH J AT THE NEG. ELEC./SEPARATOR
                                  INTERFACE
C    N2        INTEGER   SCALAR   THE MESH J AT THE SEPARATOR/POS. ELEC.
                                  INTERFACE
C    FEXP      REAL-DP   FUNCTION ELIMINATES UNDERFLOW ERRORS IN DEXP
C    ERFC      REAL-DP   FUNCTION RETURNS THE COMPLIMENTARY ERROR FUNCT.


      DOUBLE PRECISION I,DELNEG,DELPOS,DELSEP,PORNEG,PORSEP,PORPOS,
     1  RADNEG,RADPOS,  CNDNEG,CNDPOS,MKOH,MH2O,TPOS,ATCN,H,DELTIM,
     1  CELPOT,CUTOFF,FEL(200),FEL1D(200),CTCN,ATCP,CTCP,NUMPTS,
     1  CINIT

      DOUBLE PRECISION DN1D(200),DN2D(200),K(200),K1D(200),POR,
     1  FEL2D(200),PI,DC(200),DOLD(200),D1D(200),ACTNEG,ACTPOS,
     1  DN(200),FEXP,ERFC,TAUNEG,TAUPOS,ATC,CTC,CSMAX,CELOLD

      DOUBLE PRECISION AC(200),AC1D(200),AC2D(200),EXCDN,EXCDP,DUM,
     1  WAC(200),WAC1D(200),V(200),VOLD(200),V1D(200),TNORM,
     1  CON(200),CON1X,CONOLD(200),CNORM,POWER,PAVE,ENERGY,RECOV

      DOUBLE PRECISION OPN(200),OPN1X,CS(-1:500,200),
     1  I2(200),I2OLD(200),AP(-1:1000),U7,U8,ANINC,NUM,NUMBND,
     1      U0,U11,U22,U33,U44,U55,U66,U77,U88,SUM1(200),CAPAC,DISTIM

      DOUBLE PRECISION CNGMAX,CPSMAX,VMAX,F,T,RTF,V1I2(200),
     1  U1,U2,U3,U4,U5,U6,CS1X,ERR,LIMIT,AN(-1:1000),DTIM(0:1000),
     1  FLIP,TIME,DSNEG,DSPOS,CNGMIN,CPSMIN,SSANEG,SSAPOS,DP(200)

      DOUBLE PRECISION A(4,4),B(4,4),C(4,200),D(4,9),G(4),X(4,4),
     1      Y(4,4)

      INTEGER J,N1,N2,N,NJ
```

```
      COMMON A,B,C,D,G,X,Y,N,NJ

C *** READ IN ADJUSTABLE PARAMETERS FROM AN INPUT FILE NAMED "MHINPUT" ***
      OPEN(UNIT=10,FILE='MHINPUT',STATUS='OLD')
      READ(10,*) DISTIM,DELNEG,DELSEP,DELPOS,PORNEG,PORSEP,PORPOS
      READ(10,*) ACTNEG,ACTPOS,RADNEG,RADPOS,NUMPTS
        CLOSE(UNIT=10,STATUS='KEEP')


C *** FORMATS ***
 5    FORMAT(F8.6,1X,F10.6,1X,F10.8,1X,I3)
 6    FORMAT(I4,1X,F10.8,1X,F10.8,1X,F10.8,1X,F10.8,1X,E14.6)
 7    FORMAT(I4,1X,E14.8,1X,E14.8,1X,E14.8,1X,E14.8,1X)
 8    FORMAT(F7.5,2X,F7.5,2X,F6.5,2X,F6.5,2X,F6.4,2X,F6.4,2X,
     1         F6.4,2X,F6.4,2X,F6.4)

C *** DEFINE MODEL CONSTANTS ***
C *** NOTE: EXCHANGE CURRENT DENSITIES CONTAIN THE REFERENCE
C           CONCENTRATION TERMS ***

      PI = 3.141592658979D0
      F = 96487.0D0
      T = 298.0D0
      RTF = 0.02567D0
      ATCN = 0.25D0
      CTCN = 0.54D0
      ATCP = 0.13D0
      CTCP = 0.074D0
      CNGMAX=0.10251D0
      CPSMAX=0.03829D0
      CNGMIN=0.03D0*CNGMAX
      CPSMIN=0.005D0*CPSMAX
      EXCDN= 7.85D-04 /(0.012644D0**CTCN*0.046814D0**ATCN*
     1             (0.5D0*CNGMAX)**(CTCN+ATCN))
        EXCDP= 1.04D-04 /(0.012644D0**CTCP*0.046814D0**ATCP*
     1          (0.5D0*CPSMAX)**(CTCP+ATCP))

      DSNEG=2.0D-8
      DSPOS=1.0D-7
      CNDNEG=1.0D3
      CNDPOS=27.7D0
      MKOH=56.11D0
      MH2O=18.016D0
      TPOS=0.23D0
      CUTOFF=0.85D0
      VMAX=1.7D0
      LIMIT=1.0D-09
      CINIT=0.006912D0
      SSANEG=3.0D0*ACTNEG/RADNEG
      SSAPOS=3.0D0*ACTPOS/RADPOS
      CAPAC=ACTNEG*DELNEG*7.49D0*1320.5D0*0.94D0
      I=CAPAC/DISTIM
      DELTIM=DISTIM/400.0D0
```

```
      N = 4
      H=(DELNEG+DELSEP+DELPOS)/NUMPTS
      NJ = IDNINT(NUMPTS)
      N1 = IDNINT(DELNEG/H)
      N2 = IDNINT((DELNEG+DELSEP)/H)

C     *** PRINTOUT THE VARIABLES FROM THIS RUN ***
      PRINT*, 'MODEL PARAMETERS'
      PRINT*, '----- ----------'
      PRINT*, 'CURRENT = ',I,' A/cm^2'
      PRINT*, 'DISCHARGE TIME = ',DISTIM,' s'
      PRINT*, 'CAPACITY = ',CAPAC,' C/cm^2'
      PRINT*, 'NEG. ELECTRODE THICKNESS = ',DELNEG,' cm'
      PRINT*, 'SEPARATOR THICKNESS = ',DELSEP,' cm'
      PRINT*, 'POS. ELECTRODE THICKNESS = ',DELPOS,' cm'
      PRINT*, 'POROSITY OF NEG. ELECTRODE = ',PORNEG,' cm'
      PRINT*, 'POROSITY OF SEPERATOR = ',PORSEP,' cm'
      PRINT*, 'POROSITY OF POS. ELECTRODE = ',PORPOS,' cm'
      PRINT*, 'ACTIVE MATERIAL VOL. FRACTION (NEG.) = ',ACTNEG
      PRINT*, 'ACTIVE MATERIAL VOL. FRACTION (POS.) = ',ACTPOS
      PRINT*, 'SPECIFIC SURFACE AREA OF NEG. ELECTORDE = ',
     1SSANEG,' cm-1'
      PRINT*, 'SPECIFIC SURFACE AREA OF POS. ELECTORDE = ',
     1SSAPOS,' cm-1'
      PRINT*, 'RADIUS OF HYDRIDE PARTICLES = ',RADNEG,' cm'
      PRINT*, 'RADIUS OF NICKEL PARTICLES = ',RADPOS,' cm'
      PRINT*, 'NUMBER OF MESH POINTS = ',NUMPTS
      PRINT*, 'EX.CURR.DN.POS. (W/REF.CONS) = ',EXCDP,' A/cm^2'
      PRINT*, 'EX.CURR.DN.NEG. (W/REF.CONS) = ',EXCDN,' A/cm^2'
      PRINT*, 'TIME STEP SIZE = ',DELTIM,' s'
      PRINT*, ' '
      PRINT*, ' '


C     *** INITIALIZE VARIABLES FOR DISCHARGE ***
C     *** NOTE: I2 IS SET TO BE A LINEAR FUNCTION ACROSS THE ELECTRODE ***

      NUMBND = 0.0D0
      CELPOT = 0.0D0
      POWER = 0.0D0
      PAVE = 0.0D0
      ENERGY = 0.0D0

C     *** NEGATIVE ELECTRODE ***
      DO 50 J = 1,N1
         CON(J)=CINIT
         OPN(J)=0.01D0
         I2(J) = 0.0D0 + (J-1)*I/(N1-1)
         CS(0,J) = 0.97D0*CNGMAX
C        * NOTE: A LITTLE CAPACITY OF THE MH ELECTRODE IS USUALLY LEFT
C          UNUNUSED TO PROVIDE  A BUFFER IN CASE OF OVERCHARGE OR
C          OVERDISCHARGE *
 50   CONTINUE

C     *** SEPARATOR ***
```

```
      DO 60 J= N1+1,N2
         CON(J) = CINIT
         I2(J) = I
         CS(0,J)=0.0D0
         OPN(J)=0.0D0
 60   CONTINUE

C    *** POSITIVE ELECTRODE ***
      DO 70 J= N2,NJ
         CON(J) = CINIT
         OPN(J) = -0.01D0
         I2(J) = I*(NJ-J)/(NJ-N2)
         CS(0,J)=CPSMIN
 70   CONTINUE

C     *** THIS IS THE FORMAT FOR THE OUTPUT ***

      PRINT*, ' '
      PRINT*, ' TIME   VOLTAGE  CNGAVE  CPSAVE   SEP    OPN@N1  POTNIC
     1OPN@N2  ETA@N2'
      PRINT*, '------  -------  ------  ------  ------  ------  ------
     1------  ------'


C       *** THIS BLOCK OF CODE DETERMINES SOME PARAMETERS THAT WE NEED TO
C         SOLVE FOR THE DIFFUSION IN THE SOLID PHASE.  THESE "CONSTANTS"
C         ARE ONLY FUNCTIONS OF THE RADIUS OF THE PARTICLES AND THE SOLID
C         PHASE DIFF. COEFFICIENTS, SO THEY ONLY NEED TO BE CALCULATED
C         AT THE BEGINNING OF THE CONVERGENCE ROUTINE FOR EACH TIME STEP.
C         THEREFORE, THE SAME AN(T) VALUES CAN BE USED FOR EVERY POINT IN
C         THE NEGATIVE ELECTRODE AND AP(T) VALUES CAN BE USED FOR EVERY
C         POINT IN THE POSITIVE ELECTRODE.  ***

        FLIP=1.8D-02
      AN(0) = 0.0D0
      AP(0) = 0.0D0
      ANINC=DISTIM/1000.0D0
        DO 287 T=1,1000
        TIME=T*ANINC
C         * FOR NEGATIVE ELECTRODE *

        U2=(DSNEG*T*ANINC)**0.5D0
        TAUNEG=(U2/RADNEG)**2
        IF (TAUNEG.LT.FLIP) THEN
           U1=0.0D0
           DO 202 ZZ=1,7
              DUM=ZZ*RADNEG/U2
              U1=U1+FEXP(-(DUM**2.0D0))-DUM*DSQRT(PI)*ERFC(DUM)
 202       CONTINUE
           AN(T)=-TIME/RADNEG + 2.0D0*(TIME/(PI*DSNEG))**0.5D0*
     1               (1.0D0+2.0D0*U1)
        ELSE
             U1=0.0D0
             DO 272 ZZ=1,500
                U1=U1+(1.0D0 -FEXP(-(ZZ*PI*U2/RADNEG)**2.0D0))/ZZ**2.0D0
```

```
 272          CONTINUE
              AN(T)= 2.0D0*RADNEG*U1/PI**2.0D0/DSNEG
         ENDIF

C          * FOR POSITIVE ELECTRODE *

         U2=(DSPOS*T*ANINC)**0.5D0
         TAUPOS=(U2/RADPOS)**2.0D0
         IF (TAUPOS.LT.FLIP) THEN
            U1=0.0D0
            DO 203 ZZ=1,7
               DUM=ZZ*RADPOS/U2
             U1=U1+FEXP(-(DUM**2.0D0))-DUM*DSQRT(PI)*ERFC(DUM)
 203        CONTINUE
            AP(T)=-TIME/RADPOS + 2.0D0*(TIME/(PI*DSPOS))**0.5D0*
     1                (1.0D0+2.0D0*U1)
         ELSE
              U1=0.0D0
              DO 273 ZZ=1,500
                 U1=U1+(1.0D0 -FEXP(-(ZZ*PI*U2/RADPOS)**2.0D0))/ZZ**2.0D0
 273          CONTINUE
              AP(T)= 2.0D0*RADPOS*U1/PI**2.0D0/DSPOS
         ENDIF
 287     CONTINUE

C *** THE MAIN LOOP OF THE PROGRAM STARTS HERE. IT IS A DO-WHILE LOOP.
ON DISCHARGE,
C      THE LOOP STOPS WHEN THE CELL POTENTIAL DROPS BELOW THE CUTOFF
VOLTAGE.  ON CHARGE,
C      THE LOOP STOPS WHEN THE CELL POTENTIAL RISES ABOVE THE MAXIMUM
VOLTAGE ALLOWED. ***

       DTIM(0)=0.0D0
       TIME=0.0D0
       DO 100 T = 0,10000
         IF (TNORM.GE.0.985) THEN
            IF (Q.GE.4) DELTIM=DELTIM/2
            IF (Q.LE.2) DELTIM=DELTIM*2
         ELSEIF (TNORM.LE.0.02 .OR.TNORM.GE.0.95 .OR.CELPOT.LT.1.04) THEN
            IF (Q.GE.6) DELTIM=DELTIM/2
            IF (Q.LE.3 .AND. T.GT.1) DELTIM=DELTIM*2
         ELSE IF (TNORM.LE.0.085 .OR. TNORM.GE.0.88) THEN
            IF (Q.GE.7) DELTIM=DELTIM/2
            IF (Q.LE.4 .AND. T.GT.1) DELTIM=DELTIM*2
         ELSE
            IF (Q.GE.9) DELTIM=DELTIM/2
            IF (Q.LE.5) DELTIM=DELTIM*2
         ENDIF
         IF (T.NE.0) DTIM(T)=DTIM(T-1) +DELTIM
         TIME=DTIM(T)
         TNORM=TIME/DISTIM
       if (t.ge.499) stop

C        *** IF TIME=0 (i.e. THE FIRST GUESS) THEN SKIP OVER THE RESETTING
C            OF NEW GUESSES FOR CS AND THE DEFINITION OF AN(T) AND AP(T).
```

```
C           THESE WON'T BE NEEDED DURING THE FIRST TIME STEP WHERE WE
C           ONLY SOLVE FOR I2 AND OPN ACROSS THE ELECTRODE ***
        IF (T.EQ.0) GOTO 723

C       *** SET NEW GUESSES FOR CS ***
           DO 105 J = 1,NJ
              CS(T,J)=CS(T-1,J)
 105       CONTINUE
 723    CONTINUE

C       *** RESET THE CHANGE VARIABLES ***
        DO 115 Z=1,N
           DO 116 J=1,NJ
              C(Z,J) = 0.0D0
 116       CONTINUE
 115    CONTINUE


C       *** THIS IS THE CONVERGENCE LOOP.  THIS IS A DO WHILE LOOP.  THIS
C           LOOP CONTINUES UNTIL THE CHANGE VARIABLES GET SUFFICIENTLY
            CLOSE TO ZERO ***

          DO 150 Q = 1,1000
       if (q.eq.50) then
          print*, 'iteration #',q
          stop
       endif
          NUMBND=NUMBND+1.0D0


C         *** RESET THE X's  AND Y's THAT ARE SENT TO BAND ***

          DO 119 YY=1,N
             DO 120 ZZ=1,N
                X(YY,ZZ)=0.0D0
                Y(YY,ZZ)=0.0D0
 120         CONTINUE
 119       CONTINUE

C          *** DETERMINE KOH CONC.-DEPENDENT PROPERTIES, OPEN CIRCUIT
C            DEPENDENCIES, AND DERIVATIVES OF THE MAIN VARIABLES AT EVERY
C            POINT  OF THE MESH.  WE EVALUATE THESE AT EVERY POINT B/C
C            AT EACH POINT, WE HAVE TO KNOW THE VALUES ON EITHER SIDE OF
C            IT (i.e. AT J+1 AND J-1) ***

          DO 171 J=1,NJ

C            *** SET "OLD" TIME STEP VALUES BEFORE THE FIRST ITERATION ***
             IF (Q.EQ.1) THEN
                CONOLD(J)=CON(J)
                I2OLD(J)=I2(J)
                DOLD(J)=DC(J)
                VOLD(J)=V(J)
             ENDIF
```

```
            IF (J.GE.1.AND.J.LE.N1) THEN
              POR=PORNEG
            ELSE IF (J.GT.N1.AND.J.LT.N2) THEN
               POR=PORSEP
            ELSE
               POR=PORPOS
            ENDIF

            DN(J) = 1.001D0 + 47.57D0*CON(J) - 776.22D0*CON(J)**2
            DN1D(J) = 47.57D0 - 1552.44D0*CON(J)
            DN2D(J) = -1552.44D0
            DC(J) = (2.8509D-05 -2.9659D-04*CON(J)**0.5D0
     1                  +1.3768D-02*CON(J)-0.14199D0*CON(J)**1.5D0
     1                +0.42661D0*CON(J)**2.0D0)*POR**0.5D0
            D1D(J) = -7.4148D-05*CON(J)**-0.5D0 +1.3768D-02 -0.212985D0
     1                          *CON(J)**0.5D0 +0.85322D0*CON(J)
            D1D(J) = D1D(J)*POR**0.5D0
            AC(J) = 0.7002 +2.8992D01*CON(J) +1.9438D04*CON(J)**2.0D0
            AC1D(J) = 2.8992D01 + 3.8876D04*CON(J)
            AC2D(J) = 3.8876D04
            WAC(J) = 1.0002D0 + 2.125D0*CON(J) - 2.0168D03*CON(J)**2.0D0
     1               + 4.0378D04*CON(J)**3.0D0
            WAC1D(J)= 2.1251D0 -4033.6D0*CON(J) +1.21134D05*CON(J)**2.0D0
            K(J) = 2.325D-02 + 210.95D0*CON(J) -2.2077D04*CON(J)**2.0D0
     1                    +6.2907D05*CON(J)**3.0D0
            K(J) = K(J)*POR**1.5D0
            K1D(J) = 210.95D0 -4.4154D04*CON(J)
     1               +1.8872D06*CON(J)**2.0D0
            K1D(J) = K1D(J)*POR**1.5D0
            U1=DN(J)-CON(J)*DN1D(J)
C           V(J) = (MH2O - TPOS*MKOH + TPOS*DN1D(J))*I2(J)/(U1*F)
C           V1D(J) =(I2(J)*TPOS*U1*DN2D(J) +I2(J)*(MH2O -TPOS*MKOH
C     1             + TPOS*DN1D(J))*CON(J)*DN2D(J))/(U1**2.0D0*F)
C           V1I2(J) = (MH2O - TPOS*(MKOH-DN1D(J)))/(U1*F)

C     *** DETERMINE THE NEG. & POS. ELECTRODE OCP DEPENDENCES ON HYDROGEN
C         CONCENTRATION IN THE SOLID PHASE ***

            IF (J.GE.1.AND.J.LE.N1) THEN
               CNORM=CS(T,J)/CNGMAX
               U1=CNORM-1.01989D0
               U2=FEXP(-28.057D0*CNORM)
               FEL(J)=9.712D-04 +0.23724D0*U2 -2.7302D-04/(U1**2.0D0
     1                +0.010768D0)
               FEL1D(J) = -6.6562D0*U2 +5.4604D-04*U1
     1                     /(U1**2 + 0.010768D0)**2
               FEL2D(J) =(186.753*U2 -(1.6382D-03*U1**2.0D0-5.8798D-06)/
     1                   (U1**2.0D0 + 0.010768D0)**3.0D0)
               FEL1D(J) = FEL1D(J)/CNGMAX
               FEL2D(J) = FEL2D(J)/CNGMAX**2
            ELSE IF (J.GE.N2.AND.J.LE.NJ) THEN
               CNORM=CS(T,J)/CPSMAX
               IF (CNORM.LE.0.9455) THEN
                  FEL(J)= RTF*DLOG((1.0D0-CNORM)/CNORM)
                  FEL1D(J)=-RTF/CNORM/(1.0D0-CNORM)
```

```
                  FEL2D(J)=RTF*(1.0D0-2.0D0*CNORM)/(CNORM-CNORM**2)**2
               ELSE
                  U1=FEXP(-18.652D0*(1.0D0-CNORM))
                  U2=FEXP(-104.15D0*(1.0D0-CNORM))
                  FEL(J) = -0.052335 -0.054284D0*U1 -0.37142D0*U2
                  FEL1D(J) = -1.01251D0*U1 -38.6834D0*U2
                      FEL2D(J) = -18.8853D0*U1 -4028.876D0*U2
               ENDIF
             FEL1D(J) = FEL1D(J)/CPSMAX
             FEL2D(J) = FEL2D(J)/CPSMAX**2
            ENDIF

171      CONTINUE

C        *** PRINT OUT THE ARRAY OF MAIN VARIABLES IF NECESSARY  ***

         IF (t.gt.11000 .and. q.eq.1) THEN
           PRINT*, 'TIME = ',TIME
           PRINT*, 'NORMALIZED TIME = ',TNORM
           PRINT*, ' '
           PRINT*, '  J     CON         I2          OPN         CS
     1 JIN OH-'
           PRINT*, '---- ---------  ---------  ---------  --------- --
     1----------'
           DO 850 J=1,4
              PRINT6, J,CON(J),I2(J),OPN(J),CS(T,J),
     1                (I2(J+1)-I2(J))/H/SSANEG/F
850        CONTINUE
           DO 851 J=5,N1-4,4
              PRINT6, J,CON(J),I2(J),OPN(J),CS(T,J),
     1                (I2(J+1)-I2(J))/H/SSANEG/F
851        CONTINUE
           DO 852 J=N1-3,N1+3
              PRINT6, J,CON(J),I2(J),OPN(J),CS(T,J),
     1                (I2(J+1)-I2(J))/H/SSANEG/F
852        CONTINUE
           DO 853 J=N1+4,N2-4,4
              PRINT6, J,CON(J),I2(J),OPN(J),CS(T,J),
     1                (I2(J+1)-I2(J))/H/SSANEG/F
853        CONTINUE
           DO 854 J=N2-3,N2+3
              PRINT6, J,CON(J),I2(J),OPN(J),CS(T,J),
     1                (I2(J)-I2(J-1))/H/SSAPOS/F
854        CONTINUE
           DO 855 J=N2+4,NJ-4,4
              PRINT6, J,CON(J),I2(J),OPN(J),CS(T,J),
     1                (I2(J)-I2(J-1))/H/SSAPOS/F
855        CONTINUE
           DO 856 J=NJ-3,NJ
              PRINT6, J,CON(J),I2(J),OPN(J),CS(T,J),
     1                (I2(J)-I2(J-1))/H/SSAPOS/F
856        CONTINUE
         ENDIF

         ERR=0.0D0
```

```
          DO 200 J = 1,NJ
C            *** RESET THE A's, B's, D's, AND G's THAT ARE SENT TO BAND.
C                THIS IS DONE SO WE DON'T HAVE TO DEFINE A BUNCH OF ZERO
VALUES
C                INSIDE EACH IF-THEN BLOCK OF THE BAND LOOP ***
             DO 125 YY=1,N
                DO 126 ZZ=1,N
                   A(YY,ZZ)=0.0D0
                   B(YY,ZZ)=0.0D0
                   D(YY,ZZ)=0.0D0
 126            CONTINUE
                G(YY)=0.0D0
 125          CONTINUE

C           *** NOW IS TIME TO START GIVING VALUES TO THE A's,B's,D's, and
C               G's THAT BAND WILL USE TO CALCULATE THE PRIMARY CHANGE
C               VARIABLES.

C            *** WRITE IN THE FIRST EQUATION FOR ALL THE POINTS EXCEPT
C                J=1 AND J=NJ ***
             IF (J.EQ.1) THEN
                CON1X=(-1.5D0*CON(1)+2.0D0*CON(2)-0.5D0*CON(3))/H
                B(1,1)=-1.5D0/H
                D(1,1)=2.0D0/H
                X(1,1)=-0.5D0/H
                G(1)=-CON1X

             ELSE IF (J.GT.1 .AND. J.LT.NJ) THEN
                IF (J.GE.N2) THEN
                   POR=PORPOS
                ELSEIF (J.GE.N1) THEN
                   POR=PORSEP
                ELSE
                   POR=PORNEG
                ENDIF
                G(1)= -0.5D0*H*POR*(CON(J)-CONOLD(J))/DELTIM
     1 +0.5D0*(POR*(DC(J)+DC(J+1))*(CON(J+1)-CON(J))/2.0D0/H
     1 - 0.5D0*TPOS*(I2(J)+I2(J+1))/F)
     1 +0.5D0*(POR*(DOLD(J)+DOLD(J+1))*(CONOLD(J+1)-CONOLD(J))/2.0D0/H
     1 - 0.5D0*TPOS*(I2OLD(J)+I2OLD(J+1))/F)
                B(1,1)=0.5D0*POR*H/DELTIM +0.25D0*POR* (DC(J) + DC(J+1)
     1                    -(CON(J+1)-CON(J))*D1D(J))/H
                D(1,1)=-0.25D0*POR*(DC(J)+DC(J+1)+(CON(J+1)-CON(J))
     1                    *D1D(J+1))/H
                D(1,2)=0.25*TPOS/F

                IF (J.GT.N2) THEN
                   POR=PORPOS
                ELSEIF (J.GT.N1) THEN
                   POR=PORSEP
                ELSE
                   POR=PORNEG
                ENDIF
```

```
            G(1)= G(1) -0.5D0*H*POR*(CON(J)-CONOLD(J))/DELTIM
     1 +0.5D0*(-POR*(DC(J)+DC(J-1))*(CON(J)-CON(J-1))/2.0D0/H
     1 +0.5D0*TPOS*(I2(J)+I2(J-1))/F)
     1 +0.5D0*(-POR*(DOLD(J)+DOLD(J-1))*(CONOLD(J)-CONOLD(J-1))/2.0D0/H
     1 +0.5D0*TPOS*(I2OLD(J)+I2OLD(J-1))/F)
               A(1,1)=-0.25D0*POR*(DC(J) +DC(J-1) -(CON(J)-CON(J-1))
     1                    *D1D(J-1))/H
               B(1,1)=B(1,1) +0.5D0*POR*H/DELTIM + 0.25D0*POR*
     1                   (DC(J) +DC(J-1) +(CON(J)-CON(J-1))*D1D(J))/H
               A(1,2)=-0.25D0*TPOS/F
               B(1,2)=0.0D0
            ELSE
               CON1X=(1.5D0*CON(NJ)-2.0D0*CON(NJ-1)+0.5D0
     1                *CON(NJ-2))/H
               Y(1,1)=0.5D0/H
               A(1,1)=-2.0D0/H
               B(1,1)=1.5D0/H
               G(1)=-CON1X

            ENDIF
C           *** ENTER THE SECOND EQUATION ***

            IF (J.EQ.1 .OR. J.EQ.NJ) THEN
               B(2,2)=1.0D0
               G(2)=-I2(J)
            ELSE IF (J.GE.2 .AND. J.LE.N1) THEN
             CON1X=(CON(J)-CON(J-1))/H
             OPN1X=(OPN(J)-OPN(J-1))/H
             CS1X=(CS(T,J)-CS(T,J-1))/H
             U1=DN(J)-CON(J)*MKOH
             U2=DN1D(J)-MKOH
             U11=DN(J-1)-CON(J-1)*MKOH
             U22=DN1D(J-1)-MKOH
             U3= OPN1X*U2 + (I-I2(J))*U2/CNDNEG +CS1X*U2*FEL1D(J)
     1                -I2(J)*U2/K(J) + U1*I2(J)*K1D(J)/K(J)**2.0D0
             U3=U3 -RTF* CON1X * ( (TPOS*U1+MH2O*CON(J)) *((AC(J)
     1                *AC2D(J)-AC1D(J)**2.0D0)/(AC(J)**2.0D0)-1.0D0/CON(J)
     1               **2.0D0)+(AC1D(J)/AC(J)+1.0D0/CON(J))* (TPOS*U2+MH2O))
             U33= OPN1X*U22 + (I-I2(J-1))*U22/CNDNEG +CS1X*
     1                U22*FEL1D(J-1)-I2(J-1)*U22/K(J-1) + U11*I2(J-1)
     1                *K1D(J-1)/K(J-1)**2.0D0
             U33= U33 -RTF* CON1X * ((TPOS*U11+MH2O*CON(J-1))*
     1           (AC2D(J-1)/AC(J-1) -(AC1D(J-1)/AC(J-1))**2.0D0 -1.0D0
     1            /CON(J-1)**2.0D0)+(AC1D(J-1)/AC(J-1)+1.0D0/CON(J-1))
     1            * (TPOS*U22+MH2O))
             U4=-RTF*TPOS*(AC1D(J)*DN(J)/AC(J) +DN(J)/CON(J)) -RTF*(MH2O
     1          -TPOS*MKOH)*(AC1D(J)*CON(J)/AC(J) + 1.0D0)
             U44=-RTF*TPOS*(AC1D(J-1)*DN(J-1)/AC(J-1)+DN(J)/CON(J-1))-RTF
     1            *(MH2O-TPOS*MKOH)*(AC1D(J-1)*CON(J-1)/AC(J-1) + 1.0D0)
             U5= -U1/CNDNEG -U1/K(J)
             U55= -U11/CNDNEG -U11/K(J-1)
             U6= U1*CS1X*FEL2D(J)
             U66= U11*CS1X*FEL2D(J-1)
             U7= U1*FEL1D(J)
             U77= U11*FEL1D(J-1)
```

```
      A(2,1)=0.5D0*U33 - (U4+U44)/2.0D0/H
      B(2,1)=0.5D0*U3  + (U4+U44)/2.0D0/H
      A(2,2)=0.5D0*U55
      B(2,2)=0.5D0*U5
      A(2,3)=-(U1+U11)/2.0D0/H
      B(2,3)=(U1+U11)/2.0D0/H
      A(2,4)=0.5D0*U66 - (U7+U77)/2.0D0/H
      B(2,4)=0.5D0*U6 + (U7+U77)/2.0D0/H
      U8=-U1*OPN1X + (I2(J)-I)*U1/CNDNEG +U1*I2(J)/K(J) +
     1     RTF*(TPOS*U1+MH2O*CON(J))*(AC1D(J)/AC(J) +1.0D0/CON(J))
     1     *CON1X - U1*CS1X*FEL1D(J)
      U88=-U11*OPN1X +(I2(J-1)-I)*U11/CNDNEG +U11*I2(J-1)/
     1      K(J-1)+RTF*(TPOS*U11+MH2O*CON(J-1))*(AC1D(J-1)/AC(J-1)
     1      +1.0D0/CON(J-1))*CON1X - U11*CS1X*FEL1D(J-1)
      G(2)=(U8+U88)/2.0D0

     ELSE IF (J.GE.N2 .AND. J.LT.NJ) THEN
      CON1X=(CON(J+1)-CON(J))/H
      OPN1X=(OPN(J+1)-OPN(J))/H
      CS1X=(CS(T,J+1)-CS(T,J))/H
      U1=DN(J)-CON(J)*MKOH
      U2=DN1D(J)-MKOH
      U11=DN(J+1)-CON(J+1)*MKOH
      U22=DN1D(J+1)-MKOH
      U3= OPN1X*U2 + (I-I2(J))*U2/CNDPOS +CS1X*U2*FEL1D(J)
     1          -I2(J)*U2/K(J) + U1*I2(J)*K1D(J)/K(J)**2.0D0
      U3= U3 -RTF* CON1X * ((TPOS*U1+MH2O*CON(J)) *(AC2D(J)
     1     /AC(J) - (AC1D(J)/AC(J))**2.0D0-1.0D0/CON(J)**
     1     2.0D0)+(AC1D(J)/AC(J)+1.0D0/CON(J))* (TPOS*U2+MH2O))
      U33= OPN1X*U22 + (I-I2(J+1))*U22/CNDPOS +CS1X
     1      *U22*FEL1D(J+1)-I2(J+1)*U22/K(J+1) + U11*I2(J+1)*
     1      K1D(J+1)/K(J+1)**2.0D0
      U33= U33 -RTF* CON1X * ((TPOS*U11+MH2O*CON(J+1))*
     1     (AC2D(J+1)/AC(J+1) -(AC1D(J+1)/AC(J+1))**2.0D0 -1.0D0
     1     /CON(J+1)**2.0D0)+(AC1D(J+1)/AC(J+1)+1.0D0/CON(J+1))
     1          * (TPOS*U22+MH2O))
      U4=-RTF*TPOS*(AC1D(J)*DN(J)/AC(J) +DN(J)/CON(J))-RTF*(MH2O
     1      -TPOS*MKOH)*(AC1D(J)*CON(J)/AC(J) + 1.0D0)
      U44=-RTF*TPOS*(AC1D(J+1)*DN(J+1)/AC(J+1) +DN(J)/CON(J+1))
     1     -RTF*(MH2O-TPOS*MKOH)*(AC1D(J+1)*CON(J+1)/AC(J+1)+1.0D0)
      U5= -U1/CNDPOS -U1/K(J)
      U55= -U11/CNDPOS -U11/K(J+1)
      U6=+U1*CS1X*FEL2D(J)
      U66=+U11*CS1X*FEL2D(J+1)
      U7=+U1*FEL1D(J)
      U77=+U11*FEL1D(J+1)
      B(2,1)=0.5D0*U3 - (U4+U44)/2.0D0/H
      D(2,1)=0.5D0*U33 + (U4+U44)/2.0D0/H
      B(2,2)=0.5D0*U5
      D(2,2)=0.5D0*U55
      B(2,3)=-(U1+U11)/2.0D0/H
      D(2,3)=(U1+U11)/2.0D0/H
      B(2,4)=0.5D0*U6 - (U7+U77)/2.0D0/H
      D(2,4)=0.5D0*U66 + (U7+U77)/2.0D0/H
      U8=-U1*OPN1X + (I2(J)-I)*U1/CNDPOS +U1*I2(J)/K(J) +
```

```
     1          RTF*(TPOS*U1+MH2O*CON(J))*(AC1D(J)/AC(J) +1.0D0/CON(J))
     1          *CON1X - U1*CS1X*FEL1D(J)
           U88=-U11*OPN1X +(I2(J+1)-I)*U11/CNDPOS +U11*I2(J+1)/
     1          K(J+1)+RTF*(TPOS*U11+MH2O*CON(J+1))*(AC1D(J+1)/AC(J+1)
     1          +1.0D0/CON(J+1))*CON1X - U11*CS1X*FEL1D(J+1)
           G(2)=(U8+U88)/2.0D0
          ELSE
             B(2,3)=1.0D0
             G(2)=-OPN(J)
          ENDIF

C         *** ENTER THE THIRD EQUATION ***

          IF (J.GE.1.AND.J.LT.N1) THEN
           U0=SSANEG*EXCDN/MH2O**ATCN
           U1=DN(J)-CON(J)*MKOH
           U2=DN1D(J)-MKOH
           U3= (AC(J)*CON(J))**CTCN*(WAC(J)*U1)**ATCN
           U4= CS(T,J)**CTCN*(CNGMAX-CS(T,J))**ATCN
           U5= FEXP(ATCN*OPN(J)/RTF) - FEXP(-CTCN*OPN(J)/RTF)
           U6= (AC(J)*CON(J))**CTCN*ATCN*(WAC(J)*U1)**(ATCN-1.0D0)*
     1          (WAC(J)*U2+WAC1D(J)*U1)+(WAC(J)*U1)**ATCN*CTCN*
     1          (AC(J)*CON(J))**(CTCN-1.0D0)*(AC(J)+CON(J)*AC1D(J))
           U7= CTCN*(CNGMAX-CS(T,J))**ATCN*CS(T,J)**(CTCN-1.0D0)-
     1          ATCN*CS(T,J)**CTCN*(CNGMAX-CS(T,J))**(ATCN-1.0D0)
           U8= ATCN*FEXP(ATCN*OPN(J)/RTF)/RTF +
     1               CTCN*FEXP(-CTCN*OPN(J)/RTF)/RTF
           U11=DN(J+1)-CON(J+1)*MKOH
           U22=DN1D(J+1)-MKOH
           U33= (AC(J+1)*CON(J+1))**CTCN*(WAC(J+1)*U11)**ATCN
           U44= CS(T,J+1)**CTCN*(CNGMAX-CS(T,J+1))**ATCN
           U55= FEXP(ATCN*OPN(J+1)/RTF) - FEXP(-CTCN*OPN(J+1)/RTF)
           U66= (AC(J+1)*CON(J+1))**CTCN*ATCN*(WAC(J+1)*U11)**
     1          (ATCN-1.0D0)*(WAC(J+1)*U22+WAC1D(J+1)*U11)+(WAC(J+1)
     1          *U11)**ATCN*CTCN*(AC(J+1)*CON(J+1))**(CTCN-1.0D0)*
     1               (AC(J+1)+CON(J+1)*AC1D(J+1))
           U77=CTCN*(CNGMAX-CS(T,J+1))**ATCN*CS(T,J+1)**(CTCN-1.0D0)-
     1          ATCN*CS(T,J+1)**CTCN*(CNGMAX-CS(T,J+1))**(ATCN-1.0D0)
           U88= ATCN*FEXP(ATCN*OPN(J+1)/RTF)/RTF +
     1               CTCN*FEXP(-CTCN*OPN(J+1)/RTF)/RTF
           B(3,1)= -0.5D0*U0*U4*U5*U6
           D(3,1)= -0.5D0*U0*U44*U55*U66
           B(3,2)= -1.0D0/H
           D(3,2)= 1.0D0/H
           B(3,3)= -0.5D0*U0*U3*U4*U8
           D(3,3)= -0.5D0*U0*U33*U44*U88
           B(3,4)= -0.5D0*U0*U3*U5*U7
           D(3,4)= -0.5D0*U0*U33*U55*U77
           G(3)=0.5D0*U0*(U3*U4*U5 +U33*U44*U55) -(I2(J+1)-I2(J))/H

          ELSE IF (J.GE.N1 .AND. J.LE.N2) THEN
           B(3,2)=1.0D0
           G(3)=I-I2(J)

          ELSE
```

```
      U0=SSAPOS*EXCDP/MH2O**ATCP
      U1=DN(J)-CON(J)*MKOH
      U2=DN1D(J)-MKOH
      U3= (AC(J)*CON(J))**CTCP*(WAC(J)*U1)**ATCP
      U4= CS(T,J)**CTCP*(CPSMAX-CS(T,J))**ATCP
      U5= FEXP(ATCP*OPN(J)/RTF) - FEXP(-CTCP*OPN(J)/RTF)
      U6= (AC(J)*CON(J))**CTCP*ATCP*(WAC(J)*U1)**(ATCP-1.0D0)*
     1     (WAC(J)*U2+WAC1D(J)*U1)+(WAC(J)*U1)**ATCP*CTCP*
     1     (AC(J)*CON(J))**(CTCP-1.0D0)*(AC(J)+CON(J)*AC1D(J))
      U7= CTCP*(CPSMAX-CS(T,J))**ATCP*CS(T,J)**(CTCP-1.0D0)-
     1     ATCP*CS(T,J)**CTCP*(CPSMAX-CS(T,J))**(ATCP-1.0D0)
      U8= ATCP*FEXP(ATCP*OPN(J)/RTF)/RTF +
     1           CTCP*FEXP(-CTCP*OPN(J)/RTF)/RTF
      U11=DN(J-1)-CON(J-1)*MKOH
      U22=DN1D(J-1)-MKOH
      U33= (AC(J-1)*CON(J-1))**CTCP*(WAC(J-1)*U11)**ATCP
      U44= CS(T,J-1)**CTCP*(CPSMAX-CS(T,J-1))**ATCP
      U55= FEXP(ATCP*OPN(J-1)/RTF) - FEXP(-CTCP*OPN(J-1)/RTF)
      U66= (AC(J-1)*CON(J-1))**CTCP*ATCP*(WAC(J-1)*U11)**
     1     (ATCP-1.0D0)*(WAC(J-1)*U22+WAC1D(J-1)*U11)+(WAC(J-1)*
     1     U11)**ATCP*CTCP*(AC(J-1)*CON(J-1))**(CTCP-1.0D0)*
     1           (AC(J-1)+CON(J-1)*AC1D(J-1))
      U77=CTCP*(CPSMAX-CS(T,J-1))**ATCP*CS(T,J-1)**(CTCP-1.0D0)-
     1   ATCP*CS(T,J-1)**CTCP*(CPSMAX-CS(T,J-1))**(ATCP-1.0D0)
      U88= ATCP*FEXP(ATCP*OPN(J-1)/RTF)/RTF +
     1           CTCP*FEXP(-CTCP*OPN(J-1)/RTF)/RTF
      A(3,1)= -0.5D0*U0*U44*U55*U66
      B(3,1)= -0.5D0*U0*U4*U5*U6
      A(3,2)= -1.0D0/H
      B(3,2)= 1.0D0/H
      A(3,3)= -0.5D0*U0*U33*U44*U88
      B(3,3)= -0.5D0*U0*U3*U4*U8
      A(3,4)= -0.5D0*U0*U33*U55*U77
            B(3,4)= -0.5D0*U0*U3*U5*U7
      G(3)=0.5D0*U0*(U3*U4*U5 +U33*U44*U55) -(I2(J)-I2(J-1))/H

      ENDIF

C     *** WRITE IN THE FOURTH EQUATION FOR ALL POINTS ***

      IF (J.LE.N1 .OR. J.GE.N2) THEN
         IF (Q.EQ.1) THEN
         SUM1(J)=0.0D0
         IF (J.LE.N1) THEN
          DO 210 TT=1,T-1
C           * INTERPOLATE TO FIND THE CORRECT AN(T) VALUES *
            NUM=DINT((TIME-DTIM(TT-1))/ANINC)
            U33=TIME-DTIM(TT-1)-NUM*ANINC
            U44=AN(NUM) + U33*(AN(NUM+1)-AN(NUM))/ANINC
            NUM=DINT((TIME-DTIM(TT))/ANINC)
            U55=TIME-DTIM(TT)-NUM*ANINC
            U66=AN(NUM) + U55*(AN(NUM+1)-AN(NUM))/ANINC
            SUM1(J)=SUM1(J) +(CS(TT,J)-CS(TT-1,J))*(U44-U66)/
     1                        (DTIM(TT)-DTIM(TT-1))
 210       CONTINUE
```

```
                ELSE
                   DO 211 TT=1,T-1
C                    * INTERPOLATE TO FIND THE CORRECT AP(T) VALUES *
                     NUM=DINT((TIME-DTIM(TT-1))/ANINC)
                     U33=TIME-DTIM(TT-1)-NUM*ANINC
                     U44=AP(NUM) + U33*(AP(NUM+1)-AP(NUM))/ANINC
                     NUM=DINT((TIME-DTIM(TT))/ANINC)
                     U55=TIME-DTIM(TT)-NUM*ANINC
                     U66=AP(NUM) + U55*(AP(NUM+1)-AP(NUM))/ANINC
                     SUM1(J)=SUM1(J) +(CS(TT,J)-CS(TT-1,J))*(U44-U66)/
     1                                (DTIM(TT)-DTIM(TT-1))
 211               CONTINUE
                ENDIF
                ENDIF
                  IF (J.LE.N1) THEN
                   U0=EXCDN/DSNEG/F/MH2O**ATCN
                   NUM=DINT(DELTIM/ANINC)
                   U11=DELTIM-NUM*ANINC
                   U22=(AN(NUM) +U11*(AN(NUM+1)-AN(NUM))/ANINC)/DELTIM
                   ATC=ATCN
                   CTC=CTCN
                   CSMAX=CNGMAX
                ELSE
                   U0=EXCDP/DSPOS/F/MH2O**ATCP
                   NUM=DINT(DELTIM/ANINC)
                   U11=DELTIM-NUM*ANINC
                   U22=(AP(NUM) +U11*(AP(NUM+1)-AP(NUM))/ANINC)/DELTIM
                   ATC=ATCP
                   CTC=CTCP
                   CSMAX=CPSMAX
                ENDIF
                U1=DN(J)-CON(J)*MKOH
                U2=DN1D(J)-MKOH
                U3= (AC(J)*CON(J))**CTC*(WAC(J)*U1)**ATC
                U4= CS(T,J)**CTC*(CSMAX-CS(T,J))**ATC
                U5= FEXP(ATC*OPN(J)/RTF) - FEXP(-CTC*OPN(J)/RTF)
                U6= (AC(J)*CON(J))**CTC*ATC*(WAC(J)*U1)**(ATC-1.0D0)*
     1               (WAC(J)*U2+WAC1D(J)*U1)+(WAC(J)*U1)**ATC*CTC*
     1               (AC(J)*CON(J))**(CTC-1.0D0)*(AC(J)+CON(J)*AC1D(J))
                U7= CTC*(CSMAX-CS(T,J))**ATC*CS(T,J)**(CTC-1.0D0)-
     1               ATC*CS(T,J)**CTC*(CSMAX-CS(T,J))**(ATC-1.0D0)
                U8= ATC*FEXP(ATC*OPN(J)/RTF)/RTF +
     1                    CTC*FEXP(-CTC*OPN(J)/RTF)/RTF
                B(4,1) = U0*U4*U5*U6
                B(4,3) = U0*U3*U4*U8
                B(4,4) = U0*U3*U5*U7 + U22
                G(4)= -SUM1(J) + U22*(CS(T-1,J)-CS(T,J)) - U0*U3*U4*U5

               ELSE
                  B(4,4)=1.0D0
                  G(4)=-CS(T,J)
               ENDIF


C     *** IF THIS IS THE FIRST TIME STEP, WE RE-WRITE THE FIRST AND
```

```
C        FOURTH EQUATIONS SO THAT THE VALUES FOR THE SOLUTION AND
C        SOLID CONCENTRATIONS ARE CONSTANT.  THIS ALLOWS US TO
C        FIND THE POTENTIAL AND CURRENT DISTRIBUTIONS AT TIME =0 ***

            IF (T.EQ.0) THEN
               IF (J.EQ.1) X(1,1)=0.0D0
               IF (J.EQ.NJ) Y(1,1)=0.0D0
               DO 483 XX=1,N
                  DO 484 YY=1,4,3
                     A(YY,XX)=0.0D0
                     B(YY,XX)=0.0D0
                     D(YY,XX)=0.0D0
484                CONTINUE
483             CONTINUE
                B(1,1)=1.0D0
                G(1)=CINIT-CON(J)
                B(4,4)=1.0D0
                IF (J.GE.1.AND.J.LE.N1) THEN
                   G(4)=0.97D0*CNGMAX-CS(T,J)
                ELSE IF (J.GT.N1.AND.J.LT.N2) THEN
                   G(4)=-CS(T,J)
                ELSE
                   G(4)=CPSMIN-CS(T,J)
                ENDIF
               ENDIF
               ERR=ERR +DABS(G(1)) +DABS(G(2)) +DABS(G(3)) +DABS(G(4))
                     CALL BAND(J)
200         CONTINUE

C        *** CALCULATE THE NEW VALUES OF THE THREE MAIN VARIABLES--
C            CON, I2, AND OPN.  THE LOGICAL IF STATMENTS LIMIT THE AMOUNT
C            OF CHANGE THAT CAN OCCUR ON ANY ONE CONVERGENCE LOOP.  THIS
C            PREVENTS THE VALUES FROM "EXPLODING" DURING THE FIRST
C            COUPLE OF ITERATIONS IF THE GUESSES ARE NOT GOOD. ***

            DO 321 J = 1,NJ
               IF (C(1,J).GT.0.000692) C(1,J)=0.0006920D0
               IF (C(1,J).LT.-0.000692) C(1,J)=-0.0006920D0
               CON(J)=CON(J)+C(1,J)
               IF (CON(J).LE.0.0) CON(J)=0.000001D0

               IF (C(2,J).GT.0.1D0*I) C(2,J)=0.1D0*I
               IF (C(2,J).LT.-0.1D0*I) C(2,J)=-0.1D0*I
               IF (DABS(C(2,J)).LT.1.0D-13) C(2,J)=0.0D0
               I2(J)=I2(J)+C(2,J)
               IF (I2(J).GT.I) I2(J)=I
               IF (I2(J).LT.0.0) I2(J)=0.0D0

               IF (C(3,J).GT.0.05) C(3,J)=0.05D0
               IF (C(3,J).LT.-0.05) C(3,J)=-0.05D0
               OPN(J)=OPN(J)+C(3,J)
               IF (J.LE.N1.AND.OPN(J).LT.0) OPN(J)=0.0D0
               IF (J.GE.N2.AND.OPN(J).GT.0) OPN(J)=0.0D0

               IF (C(4,J).GT.0.0004) C(4,J)=0.0004D0
```

```
            IF (C(4,J).LT.-0.0004) C(4,J)=-0.0004D0
            CS(T,J)=CS(T,J)+C(4,J)
            IF (J.LE.N1.AND.CS(T,J).LT.0.0001) CS(T,J)=0.0001D0
            IF (J.LE.N1.AND.CS(T,J).GT.0.97*CNGMAX)
     1              CS(T,J)=0.969D0*CNGMAX
            IF (J.GE.N2.AND.CS(T,J).LT.0.00001) CS(T,J)=0.00001D0
            IF (J.GE.N2.AND.CS(T,J).GT.0.999*CPSMAX)
     1              CS(T,J)=0.999D0*CPSMAX

 321      CONTINUE


C              *** FIND THE ERROR AND CHECK FOR CONVERGENCE ***

          ERR=ERR/(NJ*N)
          IF (ERR.LT.LIMIT.AND.Q.GT.2) GOTO 500

 150    CONTINUE
          PRINT*, 'ERROR - PROGRAM DID NOT CONVERGE'
          PRINT*, 'TIME STEP = ',T
          STOP

 500    CONTINUE

        CELOLD=CELPOT
        CELPOT=1.327D0
        U11=0.0D0
        U22=0.0D0
        U33=0.0D0
C  *** FIND POTENTIAL DROP ACROSS THE ELECTRODE.  NOTE: HOW WE DO THIS IS
C  START WITH THE DIFFERENCE BETWEEN THE POS. AND NEGATIVE (HYPOTHETICAL)
C  REFERENCE ELECTRODES USED IN DEFINING PHI2. THIS VALUE IS 1.327 VOLTS.
C  THEN WE ADD UP THE POTENTIAL DROPS ACROSS THE ELECTRODE: SINCE THE 3rd
C  VARIABLE, ETA, IS DEFINED AT PHI1 MINUS PHI2 MINUS THE CONCENTRATION
C  DEPENDENCE OF THE OVERPOT'L, WE MUST ADD THIS TERM BACK IN TO REALLY
C  FIND THE POTENTIAL DROP ACROSS THE ELECTRODE/SEPERATOR INTERFACE. ***
C
C *** NOTE:WE USE SIMPSON'S RULE HERE TO INTEGRATE TO FIND THE CELL POT'L.
C  SINCE SIMPSON'S RULE REQUIRES AN ODD NUMBER OF POINTS, WE FIRST HAVE TO
C  CHECK TO SEE IF THERE ARE AN ODD OR EVEN NUMBER OF POINTS AND ADJUST THE
C  ROUTINE APPROPRIATELY ***
C
C       * NEGATIVE ELECTRODE *
        IF (DNINT(N1/2.0D0).NE.N1/2.0D0) THEN
          U11=U11-H*I2(1)/(3.0D0*CNDNEG)
            DO 400 J= 2, N1-3,2
              U11=U11- H*(4.0D0*I2(J)+2.0D0*I2(J+1))/CNDNEG/3.0D0
 400      CONTINUE
            U11=U11 -4.0*H*I2(N1-1)/(3.0D0*CNDNEG)
          U11=U11 -H*I2(N1)/(3.0D0*CNDNEG)
        ELSE
          U11=U11-H*I2(1)/(3.0D0*CNDNEG)
            DO 410 J= 2, N1-4,2
              U1=U1- H*(4.0D0*I2(J)+2.0D0*I2(J+1))/CNDNEG/3.0D0
 410      CONTINUE
```

```
          U11=U11 -4.0*H*I2(N1-2)/(3.0D0*CNDNEG)
          U11=U11 -H*I2(N1-1)/(3.0D0*CNDNEG)
          U11=U11 -0.5D0*(I2(N1)-I2(N1-1))*H/CNDNEG
        ENDIF
        CELPOT=CELPOT+U11

C       * OVERPOTENTIAL AT NEGATIVE ELECTRODE *
        CELPOT=CELPOT-OPN(N1)-FEL(N1)

C       * SEPARATOR *
        U1=N2-N1+1
        DO 501 J=N1,N2
           CON1X = 0.5D0*(CON(J+1)-CON(J-1))/H
           DP(J)=-I/K(J)-RTF*TPOS*(CON1X/CON(J)+AC1D(J)*CON1X/AC(J))
 501    CONTINUE
        IF (DNINT(U1/2.0D0).NE.U1/2.0D0) THEN
          U22 = U22 + H*DP(N1)/3.0D0
            DO 510 J= N1+1, N2-3,2
             U22 = U22+ H*(4.0D0*DP(J)+2.0D0*DP(J+1))/3.0D0
 510      CONTINUE
          U22 = U22 +4.0D0*H*DP(N2-1)/3.0D0
          U22 = U22 +H*DP(N2)/3.0D0
        ELSE
          U22 = U22 + H*DP(N1)/3.0D0
            DO 520 J= N1+1, N2-4,2
             U22 = U22+ H*(4.0D0*DP(J)+2.0D0*DP(J+1))/3.0D0
 520      CONTINUE
          U22 = U22 +4.0D0*H*DP(N2-2)/3.0D0
          U22= U22 + H*DP(N2-1)/3.0D0
          U22= U22 + 0.5*H*(DP(N2)+DP(N2-1))
        ENDIF
        CELPOT = CELPOT+U22

C       * OVERPOTENTIAL AT POSITIVE ELECTRODE *
        CELPOT=CELPOT+OPN(N2)+FEL(N2)

C       * POSITIVE ELECTRODE *
        U1=NJ-N2
        IF (DNINT(U1/2.0D0).NE.U1/2.0D0) THEN
          U33=U33-H*I2(N2)/(3.0D0*CNDPOS)
            DO 401 J= N2+1, NJ-2,2
              U33=U33- (4.0D0*I2(J)+2.0D0*I2(J+1))*H/3.0D0/CNDPOS
 401      CONTINUE
          U33=U33 -4.0D0*H*I2(NJ-1)/(3.0D0*CNDPOS)
          U33=U33 -H*I2(NJ)/(3.0D0*CNDPOS)
        ELSE
          U33=U33-H*I2(N2)/(3.0D0*CNDPOS)
            DO 411 J= N2+1, NJ-4,2
              U33=U33- (4.0D0*I2(J)+2.0D0*I2(J+1))*H/3.0D0/CNDPOS
 411      CONTINUE
          U33=U33 -4.0D0*H*I2(NJ-2)/(3.0D0*CNDPOS)
          U33=U33 -H*I2(NJ-1)/(3.0D0*CNDPOS)
          U33=U33 -0.5D0*(I2(NJ)-I2(NJ-1))*H/CNDPOS
        ENDIF
        CELPOT=CELPOT+U33
```

```
C       *** CALCULATE AVERAGE SPECIFIC POWER AND ENERGY ***
        IF (T.GE.1) THEN
           POWER = I*CELPOT
           ENERGY = ENERGY+POWER*DELTIM
           PAVE = ENERGY/TIME
        ENDIF

C       *** OUTPUT DATA FROM THIS TIME STEP ***

        if (mod(t,1).eq.0) then
           u2=0.0d0
           u3=0.0d0
           do 148 j=1,n1
              u3=u3+cs(t,j)/n1/cngmax
 148       continue
           do 149 j=n2,nj
              u2=u2+cs(t,j)/(nj-n2+1)/cpsmax
 149       continue
           PRINT8, TNORM,CELPOT,U3,U2,U22,-opn(n1)-fel(n1),
     1          0.400+u33+opn(n2)+fel(n2),opn(n2)+fel(n2),opn(n2)
        endif

        IF (CELPOT.LE.CUTOFF) THEN
           RECOV = (TIME-(CUTOFF-CELPOT)*DELTIM/(CELOLD-CELPOT))/DISTIM
           PRINT*, 'CUTOFF VOLTAGE WAS REACHED'
           PRINT*, 'TOTAL NUMBER OF TIME STEPS = ',T
           PRINT*, 'TOTAL NUMBER OF TIMES BAND WAS CALLED = ',NUMBND
           PRINT*, 'AVERAGE POWER = ',PAVE,' WATTS/CM^2'
           PRINT*, 'ENERGY RELEASED = ',ENERGY,' JOULES/CM^2'
           PRINT*, 'FRACTION OF CAPACITY RECOVERED = ',RECOV
           PRINT*, 'TOTAL RUN TIME = ', RECOV*DISTIM,' s'
           PRINT*, '  '
           STOP
        ENDIF

 100    CONTINUE

        STOP
        END

C             *** ERFC ***
C       *** THIS SUBROUTINE CALCULATES THE COMPLIMENTARY ERROR FUNCTION ***
C       FUNCTIONS ARE FRON ABROMOWITZ AND STEGUN EQUATIONS 7.1.23 AND 7.1.26

        FUNCTION ERFC(DUM)
              DOUBLE PRECISION ERFC,DUM,ERFC,A1,A2,A3,A4,A5,B1,B2,B3,B4,
     1        B5,B6,B7
        EXTERNAL FEXP

              A1=0.254829592D0
              A2=-0.284496736D0
              A3=1.421413741
              A4=-1.453152027D0
              A5=1.061405429D0
```

```
          IF (DUM .LT. 2.747192D0) THEN
            B1=1.0D0/(1.0D0+0.3275911D0*DUM)
            ERFC=(A1*B1+A2*B1*B1+A3*B1**3.0D0+A4*B1**4.0D0+A5*B1**5.0D0)*
     1             FEXP(-DUM*DUM)
          ELSE IF (DUM .GT. 25.0D0) THEN
            ERFC=0.0D0
          ELSE
            B2=0.0D0
            B3=DUM*DUM+0.5
            B4=-0.5D0/DUM/DUM
            B2=B4
            B5=B4
            B6=1
 23         B6=B6+1
            IF (B6 .GT. B3) GOTO 17
            B7=B5*(2.0D0*B6-1.0D0)*B4
            B2=B2+B7
            IF (B7 .LT. 1.0D-06) GOTO 17
            B5=B7
            GOTO 23
 17         ERFC=(FEXP(-DUM*DUM))*(1.0D0+B2)/DSQRT(3.1415926535D0)/DUM
          ENDIF
          RETURN
          END

C        *** FEXP ***
C       *NOTE: JUST PREVENTS UNDERFLOW ERRORS WHEN USING THE DEXP COMMAND*

          FUNCTION FEXP(DUM)
          DOUBLE PRECISION FEXP,DUM

          IF (DUM.LT.-100) THEN
             FEXP=0.0D0
          ELSE
             FEXP=DEXP(DUM)
          ENDIF
          RETURN
          END


C      *** BAND! ***

       subroutine band(j)
       implicit double precision(a-h,o-z)
       common a(4,4),b(4,4),c(4,200),d(4,9),g(4),x(4,4),
      1y(4,4),n,nj
       dimension e(4,5,200)
  101  format (15h determ=0 at j=,i4)
       if (j-2)  1,6,8
     1 npl= n + 1
       do 2 i=1,n
       d(i,2*n+1)= g(i)
       do 2 l=1,n
       lpn= l + n
```

```
 2 d(i,lpn)= x(i,l)
   call matinv(n,2*n+1,determ)
   if (determ)  4,3,4
 3 print 101, j
 4 do 5 k=1,n
   e(k,np1,1)= d(k,2*n+1)
   do 5 l=1,n
   e(k,l,1)= - d(k,l)
   lpn= l + n
 5 x(k,l)= - d(k,lpn)
   return
 6 do 7 i=1,n
   do 7 k=1,n
   do 7 l=1,n
 7 d(i,k)= d(i,k) + a(i,l)*x(l,k)
 8 if (j-nj)  11,9,9
 9 do 10 i=1,n
   do 10 l=1,n
   g(i)= g(i) - y(i,l)*e(l,np1,j-2)
   do 10 m=1,n
10 a(i,l)= a(i,l) + y(i,m)*e(m,l,j-2)
11 do 12 i=1,n
   d(i,np1)= - g(i)
   do 12 l=1,n
   d(i,np1)= d(i,np1) + a(i,l)*e(l,np1,j-1)
   do 12 k=1,n
12 b(i,k)= b(i,k) + a(i,l)*e(l,k,j-1)
   call matinv(n,np1,determ)
   if (determ)  14,13,14
13 print 101, j
14 do 15 k=1,n
   do 15 m=1,np1
15 e(k,m,j)= - d(k,m)
   if (j-nj)  20,16,16
16 do 17 k=1,n
17 c(k,j)= e(k,np1,j)
   do 18 jj=2,nj
   m= nj - jj + 1
   do 18 k=1,n
   c(k,m)= e(k,np1,m)
   do 18 l=1,n
18 c(k,m)= c(k,m) + e(k,l,m)*c(l,m+1)
   do 19 l=1,n
   do 19 k=1,n
19 c(k,1)= c(k,1) + x(k,l)*c(l,3)
20 return
   end

   subroutine matinv(n,m,determ)
   implicit double precision(a-h,o-z)
   common a(4,4),b(4,4),c(4,200),d(4,9)
   dimension id(4)
   determ=1.0
   do 1 i=1,n
1  id(i)=0
```

```
      do 18 nn=1,n
      bmax=1.1
      do 6 i=1,n
      if(id(i).ne.0) go to 6
      bnext=0.0
      btry=0.0
      do 5 j=1,n
      if(id(j).ne.0) go to 5
      if(dabs(b(i,j)).le.bnext) go to 5
      bnext=dabs(b(i,j))
      if(bnext.le.btry) go to 5
      bnext=btry
      btry=dabs(b(i,j))
      jc=j
    5 continue
      if(bnext.ge.bmax*btry) go to 6
      bmax=bnext/btry
      irow=i
      jcol=jc
    6 continue
      if(id(jc).eq.0) go to 8
      determ=0.0
      return
    8 id(jcol)=1
      if(jcol.eq.irow) go to 12
      do 10 j=1,n
      save=b(irow,j)
      b(irow,j)=b(jcol,j)
   10 b(jcol,j)=save
      do 11 k=1,m
      save=d(irow,k)
      d(irow,k)=d(jcol,k)
   11 d(jcol,k)=save
   12 f=1.0/b(jcol,jcol)
      do 13 j=1,n
   13 b(jcol,j)=b(jcol,j)*f
      do 14 k=1,m
   14 d(jcol,k)=d(jcol,k)*f
      do 18 i=1,n
      if(i.eq.jcol) go to 18
      f=b(i,jcol)
      do 16 j=1,n
   16 b(i,j)=b(i,j)-f*b(jcol,j)
      do 17 k=1,m
   17 d(i,k)=d(i,k)-f*d(jcol,k)
   18 continue
      return
      end
```

Appendix B: Computer Program for the Nickel Oxide/$LaNi_5$ Cell Incorporating the 2-D Model of the Nickel Oxide Electrode

```
C     BLAINE PAXTON
C     DR. NEWMAN'S GROUP
C     METAL HYDRIDE BATTERY MODEL - FULL 2-D VERSION
C     BEGAN: JANUARY 1995
C     WORKING: FEBRUARY 28, 1995


C     THIS IS A MODEL FOR THE GALVANOSTATIC DISCHARGE OF A METAL HYDRIDE
C     BATTERY.  SEVERAL DESIGN PARAMETERS ARE INPUT FROM A DATA FILE NAMED
C     "MHDATA".  THESE PARAMETERS ARE THEN USED TO CALCULATE THE TIME-
C     DEPENDENT OUTPUT PARAMETERS SUCH AS THE CELL VOLTAGE, THE SOL'N AND
C     SALT CONCENTR'NS, THE PORE WALL FLUXES OF REACTIVE SPECIES, AND THE
C     CURRENT DISTRIBUTIONS. THESE PARAMETERS ARE WRITEN TO AN OUTPUT FILE
C     WHICH IS SPECIFIED AT THE TIME OF EXECUTION.  SO THE PROGRAM DOESN'T
C     HAVE TO USE OUTRAGEUOS AMOUNTS OF MEMORY, THE DATA ARE OUTPUT AFTER
C     EACH TIME STEP.  THUS, THE VARIABLES ARE ONLY FUNCTIONS OF POSITION
C     WITHIN THE PROGRAM.

C     AS NOTED BELOW, THE VARIABLE C REPRESENTS ALL THE MAIN VARIBLES FOR
C     WHICH BAND SOLVES.  THIS PROGRAM IS WRITEN IN TERMS OF "CHANGE
C     VARIABLES", THAT IS THE VARIABLES THAT 'BAND' SOLVES FOR ARE ONLY THE
C     CHANGES THAT NEED TO BE MADE TO THE VARIABLES IN ORDER TO BRING THE
C     EQUATIONS CLOSER TO CONVERGENCE AT A PARTICULAR TIME STEP.
C     IN THE ELECTRODES, ALL FOUR OF THE VARIABLES
C     WILL BE USED, BUT IN THE SOLUTION PHASE ONLY THE CONCENTRATION-
C     DISTRIBUTION WILL BE NECESSARY TO SOLVE FOR.
C
C     SO THAT FUTURE EYES THAT LOOK UPON THIS PROGRAM WILL NOT BE
C     OVERWHELMED BY ARCANE NOTATION, I HAVE TRIED TO NAME THE VARIABLES
C     COMMON-SENSICALLY.  EX. I= CURRENT
C
C     WHEN READING THE DICITONARY OF VARIBLES BELOW, WHEN I SAY THE
C     "DERIVATIVE" I USUALLY MEAN WITH RESPECT TO CONCENTRATION. IF I MEAN
C     WITH RESPECT TO "X", THE DISTANCE THROUGH THE CELL, AS IS THE CASE
C     WITH THE FOUR MAIN VARIABLES- CON,I2,OPN, AND CS; OR IF I MEAN WITH
C     RESPECT TO "I2" (WHICH IS THE CASE ONLY FOR THE VOLUME AVE. VELOCITY),
C     THEN I WILL SAY THAT EXPLICITLY.  THE VARIABLE SYMBOLS ALSO REFLECT
C     THIS NOTATION AS CAN BE SEEN BELOW.

C   SEVERAL VARIABLES GIVEN BELOW ARE TERMED"OLD"VALUES WHICH MEANS THAT IT
C   WAS NECESSARY TO "CARRY OVER" SOME OF THE VALUES FROM THE PREVIOUS TIME
C     STEP.  THIS IS NECESSARY BECAUSE OF THE USE OF THE CRANK-NICHOLSON
C     METHOD THAT IS USED TO SOLVE THE TIME-DEPENDENT CONCENTRATION EQU'N.
C     SOME OF THE OLD VARIABLES NEEDED FOR THIS CALCUL'N ARE CARRIED OVER
C     IN THE FORM OF ARRAYS FROM THE PREVIOUS TIME STEP, AND SOME ARE
C     RECALCULATED AT EACH POINT OF THE ARRAY.

C     ---------- -- ---------
```

```
C      DICTIONARY OF VARIABLES
C      ---------- -- ---------

C     NAME    TYPE      STRUCTURE       USAGE
C     ----    ----      ---------       -----
C     C        REAL-DP  2-DIM     THIS VARIABLE IS THE VARIABLE WHICH
C                                      REPRESENTS THE CHANGE VARIABLES FOR
C                                      WHICH BAND SOLVES.
C                                      C(1,N) = KOH CONCENTRATION (MOL/cm^3)
C                                      C(2,N) = SOLUTION-PHASE CURRENT (A/cm^2)
C                                      C(3,N) = OVERPOTENTIAL
C                                    C(4,N) = SURFACE CONC. OF H IN SOLID PHASE
C     I        REAL-DP  SCALAR    THIS IS THE OVERALL CURRENT DENSITY
C                                      ACROSS THE BATTERY (A/cm^2)
C     DELNEG   REAL-DP  SCALAR    NEGATIVE ELECTRODE THICKNESS (cm)
C     DELSEP   REAL-DP  SCALAR    SEPARATOR THICKNESS (cm)
C     DELPOS   REAL-DP  SCALAR    POSITIVE ELECTRODE THICKNESS (cm)
C     PORNEG   REAL-DP  SCALAR    NEGATIVE ELECTRODE POROSITY
C     PORSEP   REAL-DP  SCALAR    SEPARATOR POROSITY
C     PORPOS   REAL-DP  SCALAR    POSITVE ELECTRODE POROSITY
C     POR      REAL-DP  SCALAR    A "DUMMY" POROSITY USED IN THE PROGRAM
C     RADNEG   REAL-DP  SCALAR    RADIUS OF THE NEGATIVE PARTICLES (cm)
C     RADPOS   REAL-DP  SCALAR    RADIUS OF THE POSITIVE PARTICLES (cm)
C
C     CNDNEG   REAL-DP  SCALAR    CONDUCTIVITY OF THE NEGATIVE ELECTRODE
C     CNDPOS   REAL-DP  SCALAR    CONDUCTIVITY OF THE POSITIVE ELECTRODE
C     MKOH     REAL-DP  SCALAR    MOLECULAR WEIGHT OF KOH (g/mol)
C     MH2O     REAL-DP  SCALAR    MOLECULAR WEIGHT OF H2O (g/mol)
C     TPOS     REAL-DP  SCALAR    TRANSFERENCE NUMBER OF K+
C     ATCN     REAL-DP  SCALAR    ANODIC TRANSFER COEFFICIENT - NEG. ELCTRD.
C     CTCN     REAL-DP  SCALAR    CATHODIC TRANSFER COEFFICIENT- NEG. ELCTRD.
C     ATCP     REAL-DP  SCALAR    ANODIC TRANSFER COEFFICIENT - POS. ELCTRD.
C     CTCP     REAL-DP  SCALAR    CATHODIC TRANSFER COEFFICIENT- POS. ELCTRD.
C     EXCDN    REAL-DP  SCALAR    EXCHANGE CURRENT DENSITY OF THE NEG. ELEC.
C     EXCDP    REAL-DP  SCALAR    EXCHANGE CURRENT DENSITY OF THE POS. ELEC.
C     DSNEG    REAL-DP  SCALAR    SS DIFFUSION COEF OF NEG. ELEC MAT'L (cm^2/s)
C     DSPOS    REAL-DP  SCALAR    SS DIFFUSION COEF OF POS. ELEC MAT'L (cm^2/s)
C     SSANEG   REAL-DP  SCALAR    SPECIFIC SURFACE AREA OF THE NEG. ELECTRODE
C     SSAPOS   REAL-DP  SCALAR    SPECIFIC SURFACE AREA OF THE POS. ELECTRODE
C     ACTNEG   REAL-DP  SCALAR    THE ACTIVE MATERIAL VOLUME FRACTION (NEG.)
C     ACTPOS   REAL-DP  SCALAR    THE ACTIVE MATERIAL VOLUME FRACTION (POS.)
C     CINIT    REAL-DP  SCALAR    INITIAL KOH CONCENTRATION (TIME=0)
C     POWER    REAL-DP  SCALAR    THE INSTANTANEOUS POWER OF THE CELL
C     PAVE     REAL-DP  SCALAR    THE AVERAGE POWER OF THE CELL
C     ENERGY   REAL-DP  SCALAR    THE TOTAL USABLE ENERGY RELEASED BY THE CELL
C     NUMBND   INTEGER  SCALAR    THE TOTAL NUMBER OF TIMES BAND IS CALLED
C     NUMPTS   REAL-DP  SCALAR    NUMBER OF MESH POINTS
C     H        REAL-DP  SCALAR    MESH SPACING (cm)
C     DELTIM   REAL-DP  SCALAR    TIME STEP SIZE (s)
C     TIME     REAL-DP  SCALAR    REAL TIME DURING THE PROGRAM (s)
C     CELPOT   REAL-DP  SCALAR    THE CELL POTENTIAL (V)
C     CELOLD   REAL-DP  SCALAR    THE CELL POT'L AT THE PREVIOUS TIME STEP (V)
C     RECOV    REAL-DP  SCALAR    THE FRACTION OF CAPACITY RECOVERED
C     CUTOFF   REAL-DP  SCALAR    THE CELL CUTOFF POTENTIAL (V)
C     VMAX     REAL-DP  SCALAR    THE MAXIMUM VOLTAGE ON CHARGE (V)
```

```
C    FEL       REAL-DP SCALAR   ELEC. POTENTIAL DEPENDENCE ON
C                                HYDROGEN CONCEN. IN THE SOLID PHASE (V)
C    FEL1D     REAL-DP SCALAR   1st DERIVATIVE OF FEL WRT CS
C    FEL2D     REAL-DP SCALAR   2nd DERIVATIVE OF FEL WRT CS
C    DC        REAL-DP 1-DIM    SALT DIFFUSION COEF AT CURRENT
C                                TIME STEP (cm^2/s)
C    DOLD      REAL-DP 1-DIM    SALT DIFFUSION COEF AT PREVIOUS
C                                TIME STEP (cm^2/s)
C    D1D       REAL-DP 1-DIM    1st DERIVATIVE OF DC (cm^5/mol s)
C    DN        REAL-DP 1-DIM    SOLUTION DENSITY (g/cm^3)
C    DN1D      REAL-DP 1-DIM    1st DERIV. OF DN (g/mol)
C    DN2D      REAL-DP 1-DIM    2nd DERIV. OF DN (g cm^3/mol^2)
C    K         REAL-DP 1-DIM    SOLUTION CONDUCTIVITY (S/cm)
C    K1D       REAL-DP 1-DIM    1st DERIVATIVE OF K (S cm^2/mol)
C    AC        REAL-DP 1-DIM    MEAN MOLAR ACTIVITY COEF.
C    AC1D      REAL-DP 1-DIM    1st DERIVATIVE OF AC (cm^3/mol)
C    AC2D      REAL-DP 1-DIM    2nd DERIVATIVE OF AC (cm^6/mol^2)
C    WAC       REAL-DP 1-DIM    WATER ACTIVITY COEF.
C    WAC1D     REAL-DP 1-DIM    1st DERIVATIVE OF WA (cm^3/mol)
C    V         REAL-DP 1-DIM    VOLUME AVE. VELOCITY (cm/s)
C    VOLD      REAL-DP 1-DIM    VOL. AVE. VELOCITY AT OLD TIME STEP
C    V1D       REAL-DP 1-DIM    1st DERIVIATIVE OF V (cm^4/mol s)
C    V1I2      REAL-DP 1-DIM    1st DERIV. OF V WRT I2
C
C
C    CON       REAL-DP  1-DIM   KOH CONC. AT PRESENT TIME STEP (mol/cm^3)
C    CON1X     REAL-DP  SCALAR  1st DERIVATIVE OF CON WRT X (mol/cm^4)
C    CONOLD    REAL-DP  1-DIM   KOH CONC. AT PREVIOUS TIME STEP   "
C    I2        REAL-DP  1-DIM   SOLUTION PHASE CURRENT AT THE
C                                CURRENT TIME STEP (A/cm^2)
C    I2OLD     REAL-DP  1-DIM   SOLUTION PHASE CURRENT AT THE
C                                PREVIOUS TIME STEP (A/cm^2)
C    OPN       REAL-DP  1-DIM   OVER POT'L OF THE NEG. OR POS. ELECTRODE (V)
C    OPN1X     REAL-DP  SCALAR  1st DERIVATIVE OF OPN WRT X (V/cm)
C    CS        REAL-DP  2-DIM   CONCENTRATION OF HYDROGEN IN THE SOLID
C                                PHASE OF NEG. ELEC. AT THE SURFACE (MOL/cm^3)
C                                (CS IS ALSO A FUNCTION  OF TIME)
C    CS1X      REAL-DP  SCALAR  1st DERIV. OF CS AT THE SURFACE OF THE
C                                PARTICLE WRT X.
C    CNGMAX    REAL-DP  SCALAR  MAXIMUM CONC. OF H IN NEG. ELECT. (mol/cm^3)
C    CPSMAX    REAL-DP  SCALAR  MAXIMUM CONC. OF H IN POS. ELECT. (mol/cm^3)
C    CNGMIN    REAL-DP  SCALAR  MINIMUM CONC. OF H IN NEG. ELECT. (mol/cm^3)
C    CPSMIN    REAL-DP  SCALAR  MINIMUM CONC. OF H IN POS. ELECT. (mol/cm^3)
C    F         REAL-DP  SCALAR  FARADAY'S CONSTANT (C/EQ)
C    T         REAL-DP  SCALAR  TEMPERATURE (K)
C    RTF       REAL-DP  SCALAR  RT/F = 0.02567 VOLTS
C    J         INTEGER  SCALAR  A DUMMY VARIABLE USED FOR EXPEDIENCY
C    DUM       REAL-DP  SCALAR  A DUMMY VARIABLE USED FOR EXPEDIENCY
C    U1        REAL-DP  SCALAR  A DUMMY VARIABLE USED FOR EXPEDIENCY

C    U2        REAL-DP  SCALAR  A DUMMY VARIABLE USED FOR EXPEDIENCY
C    U3        REAL-DP  SCALAR  A DUMMY VARIABLE USED FOR EXPEDIENCY
C    U4        REAL-DP  SCALAR  A DUMMY VARIABLE USED FOR EXPEDIENCY
C    U5        REAL-DP  SCALAR  A DUMMY VARIABLE USED FOR EXPEDIENCY
C    U6        REAL-DP  SCALAR  A DUMMY VARIABLE USED FOR EXPEDIENCY
```

```
C    DP       REAL-DP  1-DIM    A DUMMY VARIABLE USED IN FINDING CELPOT
C    ER       REAL-DP  SCALAR   THE VARIABLE FOR RETURNING THE ERROR
C                               FUNCTION FROM THE SUBROUTINE ERFC

C    A        REAL-DP  2-DIM    A VARIABLE FOR BAND (SEE NEWMAN TEXT)
C    B        REAL-DP  2-DIM    A VARIABLE FOR BAND (SEE NEWMAN TEXT)
C    D        REAL-DP  2-DIM    A VARIABLE FOR BAND (SEE NEWMAN TEXT)
C    G        REAL-DP  1-DIM    A VARIABLE FOR BAND (SEE NEWMAN TEXT)
C    X        REAL-DP  2-DIM    A VARIABLE FOR BAND (SEE NEWMAN TEXT)
C    Y        REAL-DP  2-DIM    A VARIABLE FOR BAND (SEE NEWMAN TEXT)

C
C    ERR      REAL-DP  SCALAR   THE FRACTIONAL ERROR BETWEEN THE NEWEST
                                BAND GUESSES AND THE OLD VALUES
C    LIMIT    REAL-DP  SCALAR   THE CONVERGENCE CRITERION
C    N1       INTEGER  SCALAR   THE MESH J AT THE NEG. ELEC./SEPARATOR
                                INTERFACE
C    N2       INTEGER  SCALAR   THE MESH J AT THE SEPARATOR/POS. ELEC.
                                INTERFACE
C    FEXP     REAL-DP  FUNCTION ELIMINATES UNDERFLOW ERRORS IN DEXP
C    ERFC     REAL-DP  FUNCTION RETURNS THE COMPLIMENTARY ERROR FUNCT.

C     ---------- -- --------- --- -------- ---------
C     DICTIONARY OF VARIABLES FOR PARTICLE DIFFUSION
C     ---------- -- --------- --- -------- ---------

C     NAME  TYPE     STRUCTURE    USAGE
C     ----  ----     ---------    -----
C     CC    REAL-DP  2-DIM    THIS VARIABLE IS THE VARIABLE WHICH
C                               REPRESENTS THE CHANGE VARIABLES FOR WHICH
C                               BAND2 SOLVES.
C     AA    REAL-DP  2-DIM    A VARIABLE FOR BAND2 (SEE NEWMAN TEXT)
C     BB    REAL-DP  2-DIM    A VARIABLE FOR BAND2 (SEE NEWMAN TEXT)
C     DD    REAL-DP  2-DIM    A VARIABLE FOR BAND2 (SEE NEWMAN TEXT)
C     GG    REAL-DP  1-DIM    A VARIABLE FOR BAND2 (SEE NEWMAN TEXT)
C     XX    REAL-DP  2-DIM    A VARIABLE FOR BAND2 (SEE NEWMAN TEXT)
C     YY    REAL-DP  2-DIM    A VARIABLE FOR BAND2 (SEE NEWMAN TEXT)
C     HH    REAL-DP  SCALAR   MESH SPACING INSIDE PARTICLE (cm)
C     DS    REAL-DP  1-DIM    HYDROGEN DIFFUSION COEF IN SOLID AT CURRENT
C                               TIME STEP (cm^2/s)
C     DSOLD REAL-DP  1-DIM    HYDROGEN DIFFUSION COEF IN SOLID AT PREVIOUS
C                               TIME STEP (cm^2/s)
C     DS1D  REAL-DP  1-DIM    1st DERIVATIVE OF DS (cm^5/mol s)
C     ERR2  REAL-DP  SCALAR   THE ERROR PARAMETER WHICH IS AN AVERAGE OF
C                               THE GG VALUES SENT TO BAND
C     DIST  REAL-DP  SCALAR   THE DISTANCE FROM THE CENTER OF THE PARTICLE
C     DM    REAL-DP  SCALAR   DISTANCE MINUS 1/2 MESH SPACE
C     DP    REAL-DP  SCALAR   DISTANCE PLUS 1/2 MESH SPACE


      DOUBLE PRECISION I,DELNEG,DELPOS,DELSEP,PORNEG,PORSEP,PORPOS,
     1  RADNEG,RADPOS,CNDNEG,CNDPOS,MKOH,MH2O,TPOS,ATCN,H,DELTIM,
     1  CELPOT,CUTOFF,FEL(200),FEL1D(200),CTCN,ATCP,CTCP,NUMPTS

        DOUBLE PRECISION DN1D(200),DN2D(200),K(200),K1D(200),POR,
```

```
     1  FEL2D(200),PI,DC(200),DOLD(200),D1D(200),CINIT,ACTNEG,ACTPOS,
     1  DN(200),FEXP,ERFC,TAUNEG,POWER,PAVE,ENERGY,SUM1(200)

        DOUBLE PRECISION AC(200),AC1D(200),AC2D(200),EXCDN,EXCDP,
     1  WAC(200),WAC1D(200),V(200),VOLD(200),V1D(200),
     1  CON(200),CON1X,CONOLD(200),CNORM,FLIP,DUM,RECOV,CELOLD

        DOUBLE PRECISION OPN(200),OPN1X,CS(-1:4000,200),
     1  I2(200),I2OLD(200),U7,U8,U0,U11,U22,U33,
     1      U44,U55,U66,U77,U88,CAPAC,DISTIM,ANINC,DTIM(0:1000)

        DOUBLE PRECISION CNGMAX,CPSMAX,VMAX,F,T,RTF,V1I2(200),
     1  U1,U2,U3,U4,U5,U6,CS1X,ERR,LIMIT,AN(-1:1000),
     1  TIME,DSNEG,CNGMIN,CPSMIN,SSANEG,SSAPOS,DDP(200)

        DOUBLE PRECISION DS(200,150),DSOLD(200,150),DS1D(150),
     1  ERR2,DIST,DM,DP,HH,CSS(200,150),CSSOLD(200,150),LIMIT2

        DOUBLE PRECISION A(4,4),B(4,4),C(4,200),D(4,9),G(4),X(4,4),
     1      Y(4,4)

        DOUBLE PRECISION AA(1,1),BB(1,1),CC(1,150),DD(1,3),GG(1),
     1  XX(1,1),YY(1,1)

        INTEGER J,JJ,N1,N2,N,NJ,NN,NNJ

       COMMON /A/ A,B,C,D,G,X,Y,N,NJ
       COMMON /B/ AA,BB,CC,DD,GG,XX,YY,NN,NNJ

C *** READ IN ADJUSTABLE PARAMETERS FROM AN INPUT FILE NAMED "MHINPUT" ***
       OPEN(UNIT=10,FILE='MHINPUT',STATUS='OLD')
       READ(10,*) DISTIM,DELNEG,DELSEP,DELPOS,PORNEG,PORSEP,PORPOS
       READ(10,*) ACTNEG,ACTPOS,RADNEG,RADPOS,NUMPTS
         CLOSE(UNIT=10,STATUS='KEEP')


C *** FORMATS ***
 5     FORMAT(F8.6,1X,F10.6,1X,F10.8,1X,I3)
 6     FORMAT(I4,1X,F10.8,1X,F10.8,1X,F10.8,1X,F10.8,1X,E14.6)
 7     FORMAT(I4,1X,E14.8,1X,E14.8,1X,E14.8,1X,E14.8,1X)
 8     FORMAT(F7.5,2X,F7.5,2X,F6.5,2X,F6.5,2X,F6.4,2X,F6.4,2X,
     1         F6.4,2X,F6.4,2X,F6.4)

C *** DEFINE MODEL CONSTANTS ***
C  *** NOTE: EXCHANGE CURRENT DENSITIES CONTAIN THE REFERENCE
C            CONCENTRATION TERMS ***

       PI = 3.141592658979D0
       F = 96487.0D0
       T = 298.0D0
       RTF = 0.02567D0
       ATCN = 0.25D0
       CTCN = 0.54D0
       ATCP = 0.13D0
       CTCP = 0.074D0
```

```
      CNGMAX=0.10251D0
      CPSMAX=0.03829D0
      CNGMIN=0.03D0*CNGMAX
      CPSMIN=0.005D0*CPSMAX
      EXCDN= 7.85D-04 /(0.012644D0**CTCN*0.046814D0**ATCN*
     1              (0.5D0*CNGMAX)**(CTCN+ATCN))
      EXCDP= 1.04D-04 /(0.012644D0**CTCP*0.046814D0**ATCP*
     1          (0.5D0*CPSMAX)**(CTCP+ATCP))

      DSNEG=2.0D-8
      CNDNEG=1.0D3
      CNDPOS=27.69D0
      MKOH=56.11D0
      MH2O=18.016D0
      TPOS=0.23D0
      CUTOFF=0.85D0
      VMAX=1.7D0
      LIMIT=1.0D-09
      LIMIT2=1.0D-17
      AN(0) = 0.0D0
      CINIT=0.006912D0
      SSANEG=3.0D0*ACTNEG/RADNEG
      SSAPOS=3.0D0*ACTPOS/RADPOS
      CAPAC=ACTNEG*DELNEG*7.49D0*1320.5D0*0.94D0
      I=CAPAC/DISTIM
      DELTIM=DISTIM/400.0D0

      NNJ=150
      HH=RADPOS/(NNJ-1)

      N = 4
      NN = 1
      H=(DELNEG+DELSEP+DELPOS)/NUMPTS
      NJ = IDNINT(NUMPTS)
      N1 = IDNINT(DELNEG/H)
      N2 = IDNINT((DELNEG+DELSEP)/H)

C     *** PRINTOUT THE VARIABLES FROM THIS RUN ***
      PRINT*, 'MODEL PARAMETERS'
      PRINT*, '----- ----------'
      PRINT*, 'CURRENT = ',I,' A/cm^2'
      PRINT*, 'DISCHARGE TIME = ',DISTIM,' s'
      PRINT*, 'CAPACITY = ',CAPAC,' C/cm^2'
      PRINT*, 'NEG. ELECTRODE THICKNESS = ',DELNEG,' cm'
      PRINT*, 'SEPARATOR THICKNESS = ',DELSEP,' cm'
      PRINT*, 'POS. ELECTRODE THICKNESS = ',DELPOS,' cm'
      PRINT*, 'POROSITY OF NEG. ELECTRODE = ',PORNEG,' cm'
      PRINT*, 'POROSITY OF SEPERATOR = ',PORSEP,' cm'
      PRINT*, 'POROSITY OF POS. ELECTRODE = ',PORPOS,' cm'
      PRINT*, 'ACTIVE MATERIAL VOL. FRACTION (NEG.) = ',ACTNEG
      PRINT*, 'ACTIVE MATERIAL VOL. FRACTION (POS.) = ',ACTPOS
      PRINT*, 'SPECIFIC SURFACE AREA OF NEG. ELECTORDE = ',
     1SSANEG,' cm-1'
      PRINT*, 'SPECIFIC SURFACE AREA OF POS. ELECTORDE = ',
     1SSAPOS,' cm-1'
```

```
      PRINT*, 'RADIUS OF HYDRIDE PARTICLES = ',RADNEG,' cm'
      PRINT*, 'RADIUS OF NICKEL PARTICLES = ',RADPOS,' cm'
      PRINT*, 'NUMBER OF MESH POINTS = ',NUMPTS
      PRINT*, 'EX.CURR.DN.POS. (W/REF.CONS) = ',EXCDP,' A/cm^2'
      PRINT*, 'EX.CURR.DN.NEG. (W/REF.CONS) = ',EXCDN,' A/cm^2'
      PRINT*, 'INITIAL TIME STEP SIZE = ',DELTIM,' s'
      PRINT*, ' '
      PRINT*, ' '


C     *** INITIALIZE VARIABLES FOR DISCHARGE ***
C     *** NOTE: I2 IS SET TO BE A LINEAR FUNCTION ACROSS THE ELECTRODE ***

      NUMBND = 0.0D0
      CELPOT = 0.0D0
      POWER = 0.0D0
      PAVE = 0.0D0
      ENERGY = 0.0D0

C     *** NEGATIVE ELECTRODE ***
      DO 50 J = 1,N1
         CON(J)=CINIT
         OPN(J)=0.01D0
         I2(J) = 0.0D0 + (J-1)*I/(N1-1)
         CS(0,J) = 0.97D0*CNGMAX
C     * NOTE: A LITTLE CAPACITY OF THE MH ELECTRODE IS USUALLY LEFT
C     UNUNUSED TO PROVIDE  A BUFFER IN CASE OF OVERCHARGE OR OVERDISCHARGE*
 50   CONTINUE


C     *** SEPARATOR ***
      DO 60 J= N1+1,N2
         CON(J) = CINIT
         I2(J) = I
         CS(0,J)=0.0D0
         OPN(J)=0.0D0
 60   CONTINUE

C     *** POSITIVE ELECTRODE ***
      DO 70 J= N2,NJ
         CON(J) = CINIT
         OPN(J) = -0.01D0
         I2(J) = I*(NJ-J)/(NJ-N2)
         CS(0,J)=CPSMIN
         DO 62 JJ=1,150
            CSS(J,JJ) = CPSMIN
            DS(J,JJ) = 3.5d-09
 62      CONTINUE
 70   CONTINUE


C     *** THIS IS THE FORMAT FOR THE OUTPUT ***

      PRINT*, ' '
      PRINT*, ' TIME   VOLTAGE  CNGAVE  CPSAVE   SEP    OPN@N1  POTNIC
```

```
     1OPN@N2  ETA@N2'
      PRINT*, '------  -------  ------  ------  ------  ------  ------
     1------  ------'

C  *** THIS BLOCK OF CODE DETERMINES SOME PARAMETERS THAT WE NEED TO
C   SOLVE FOR THE DIFFUSION IN THE SOLID PHASE.  THESE "CONSTANTS"
C   ARE ONLY FUNCTIONS OF THE RADIUS OF THE PARTICLES AND THE SOLID
C   PHASE DIFFUSION COEFFICIENTS, SO THEY ONLY NEED TO BE CALCULATED
C   AT THE BEGINNING OF THE PROGRAM.  AN ARRAY OF AN(T) AND AP(T) VALUES
C   IS GENERATED AND THE EXACT VALUES NEEDED DURING THE COURSE OF THE
C   RUNNING OF THE PROGRAM ARE INTERPOLATED FROM THESE VALUES. ***

      FLIP=1.8D-02
      AN(0) = 0.0D0
      ANINC=DISTIM/1000.0D0
      DO 287 T=1,1000
        TIME=T*ANINC
C         * FOR NEGATIVE ELECTRODE *
        U2=(DSNEG*T*ANINC)**0.5D0
        TAUNEG=(U2/RADNEG)**2
        IF (TAUNEG.LT.FLIP) THEN
           U1=0.0D0
           DO 202 ZZ=1,7
              DUM=ZZ*RADNEG/U2
            U1=U1+FEXP(-(DUM**2.0D0))-DUM*DSQRT(PI)*ERFC(DUM)
 202       CONTINUE
           AN(T)=-TIME/RADNEG + 2.0D0*(TIME/(PI*DSNEG))**0.5D0*
     1               (1.0D0+2.0D0*U1)
        ELSE
             U1=0.0D0
             DO 272 ZZ=1,500
                U1=U1+(1.0D0 -FEXP(-(ZZ*PI*U2/RADNEG)**2.0D0))/ZZ**2.0D0
 272       CONTINUE
           AN(T)= 2.0D0*RADNEG*U1/PI**2.0D0/DSNEG
        ENDIF
 287  CONTINUE


C *** THE MAIN LOOP OF THE PROGRAM STARTS HERE.  IT IS A DO-WHILE LOOP.
ON DISCHARGE,
C     THE LOOP STOPS WHEN THE CELL POTENTIAL DROPS BELOW THE CUTOFF
VOLTAGE.  ON CHARGE,
C     THE LOOP STOPS WHEN THE CELL POTENTIAL RISES ABOVE THE MAXIMUM
VOLTAGE ALLOWED. ***

      DTIM(0)=0.0D0
      TIME=0.0D0
      DO 100 T = 0,10000
        IF (TNORM.GE.0.95 .OR. CELPOT.LE.0.98) THEN
           IF (Q.GE.6) DELTIM=DELTIM/2
           IF (Q.LE.3 .AND. T.GT.1) DELTIM=DELTIM*2
        ELSE IF (TNORM.LE.0.02.OR.TNORM.GE.0.935.OR.CELPOT.LT.1.04) THEN
           IF (Q.GE.7) DELTIM=DELTIM/2
           IF (Q.LE.4 .AND. T.GT.1) DELTIM=DELTIM*2
        ELSE IF (TNORM.LE.0.085 .OR. TNORM.GE.0.88) THEN
```

```
            IF (Q.GE.8) DELTIM=DELTIM/2
            IF (Q.LE.5) DELTIM=DELTIM*2
         ELSE
            IF (Q.GE.10) DELTIM=DELTIM/2
            IF (Q.LE.6) DELTIM=DELTIM*2
         ENDIF
         IF (T.NE.0) DTIM(T)=DTIM(T-1) +DELTIM
         IF (DELTIM.LT.DISTIM/10000) THEN
            PRINT*, 'TIME STEP SIZE FELL BELOW MINUMUM VALUE'
            PRINT*, 'NORMALIZED TIME STEP SIZE = ', DELTIM/DISTIM
            DELTIM = DELTIM*2
            PRINT*, 'TIME STEP SIZE WAS MULTIPLIED BY A FACTOR OF 2'
         ENDIF
         TIME=DTIM(T)
         TNORM=TIME/DISTIM
       if (t.ge.2000) stop
C        *** SET NEW GUESSES FOR CS ***
           IF (T.NE.0) THEN
           DO 105 J = 1,NJ
              CS(T,J)=CS(T-1,J)
 105       CONTINUE
         ENDIF

C        *** RESET THE CHANGE VARIABLES ***
         DO 115 Z=1,N
            DO 116 J=1,NJ
               C(Z,J) = 0.0D0
 116        CONTINUE
 115     CONTINUE


C   *** THIS IS THE CONVERGENCE LOOP.  THIS IS A DO WHILE LOOP.  THIS LOOP
C   CONTINUES UNTIL THE CHANGE VARIABLES GET SUFFICIENTLY CLOSE TO ZERO ***

         DO 150 Q = 1,100
         IF (Q.EQ.40) THEN
            PRINT*, 'PROGRAM DID NOT REACH CUTOFF.  NO CONVERGENCE!'
            PRINT*, 'ITERATION # ',Q
            PRINT*, 'TOTAL NUMBER OF TIME STEPS = ',T
            PRINT*, 'TOTAL NUMBER OF TIMES BAND WAS CALLED = ',NUMBND
            PRINT*, 'AVERAGE POWER = ',PAVE,' WATTS/CM^2'
            PRINT*, 'ENERGY RELEASED = ',ENERGY,' JOULES/CM^2'
            PRINT*, '  '
            STOP
         ENDIF
         NUMBND=NUMBND+1.0D0

C          *** RESET THE X's  AND Y's THAT ARE SENT TO BAND ***

           DO 119 Y2=1,N
              DO 120 Z2=1,N
                 X(Y2,Z2)=0.0D0
                 Y(Y2,Z2)=0.0D0
 120           CONTINUE
 119        CONTINUE
```

```
C          *** DETERMINE KOH CONC.-DEPENDENT PROPERTIES, OPEN CIRCUIT
C            DEPENDENCIES, AND DERIVATIVES OF THE MAIN VARIABLES AT EVERY
C            POINT  OF THE MESH.  WE EVALUATE THESE AT EVERY POINT BECAUSE
C            AT EACH POINT, WE HAVE TO KNOW THE VALUES ON EITHER SIDE OF
C            IT (i.e. AT J+1 AND J-1) ***

           DO 171 J=1,NJ

C             *** SET "OLD" TIME STEP VALUES BEFORE THE FIRST ITERATION **
              IF (Q.EQ.1) THEN
                 CONOLD(J)=CON(J)
                 I2OLD(J)=I2(J)
                 DOLD(J)=DC(J)
                 VOLD(J)=V(J)
              ENDIF

              IF (J.GE.1.AND.J.LE.N1) THEN
                POR=PORNEG
              ELSE IF (J.GT.N1.AND.J.LT.N2) THEN
                 POR=PORSEP
              ELSE
                 POR=PORPOS
              ENDIF

              DN(J) = 1.001D0 + 47.57D0*CON(J) - 776.22D0*CON(J)**2
              DN1D(J) = 47.57D0 - 1552.44D0*CON(J)
              DN2D(J) = -1552.44D0
              DC(J) = (2.8509D-05 -2.9659D-04*CON(J)**0.5D0
     1                    +1.3768D-02*CON(J)-0.14199D0*CON(J)**1.5D0
     1                  +0.42661D0*CON(J)**2.0D0)*POR**0.5D0
              D1D(J) = -7.4148D-05*CON(J)**-0.5D0 +1.3768D-02 -0.212985D0
     1                           *CON(J)**0.5D0 +0.85322D0*CON(J)
              D1D(J) = D1D(J)*POR**0.5D0
              AC(J) = 0.7002 +2.8992D01*CON(J) +1.9438D04*CON(J)**2.0D0
              AC1D(J) = 2.8992D01 + 3.8876D04*CON(J)
              AC2D(J) = 3.8876D04
              WAC(J) = 1.0002D0 + 2.125D0*CON(J) - 2.0168D03*CON(J)**2.0D0
     1                  + 4.0378D04*CON(J)**3.0D0
              WAC1D(J)= 2.1251D0 -4033.6D0*CON(J) +1.21134D05*CON(J)**2.0D0
              K(J) = 2.325D-02 + 210.95D0*CON(J) -2.2077D04*CON(J)**2.0D0
     1              +6.2907D05*CON(J)**3.0D0
              K(J) = K(J)*POR**1.5D0
              K1D(J) = 210.95D0 -4.4154D04*CON(J)
     1                  +1.8872D06*CON(J)**2.0D0
              K1D(J) = K1D(J)*POR**1.5D0
              U1=DN(J)-CON(J)*DN1D(J)

C          *** DETERMINE THE NEG. & POS. ELECTRODE OCP DEPENDENCES ON HYDROGEN
C              CONCENTRATION IN THE SOLID PHASE ***

              IF (J.GE.1.AND.J.LE.N1) THEN
                 CNORM=CS(T,J)/CNGMAX
                 U1=CNORM-1.01989D0
                 U2=FEXP(-28.057D0*CNORM)
```

```
              FEL(J)=9.712D-04 +0.23724D0*U2 -2.7302D-04/(U1**2.0D0
     1                 +0.010768D0)
              FEL1D(J) = -6.6562D0*U2 +5.4604D-04*U1
     1                    /(U1**2 + 0.010768D0)**2
             FEL2D(J) = (186.753*U2 -(1.6382D-03*U1**2.0D0 -5.8798D-06)/
     1                  (U1**2.0D0 + 0.010768D0)**3.0D0)
             FEL1D(j) = FEL1D(j)/CNGMAX
             FEL2D(j) = FEL2D(j)/CNGMAX**2
            ELSE IF (J.GE.N2.AND.J.LE.NJ) THEN
               CNORM=CS(T,J)/CPSMAX
               IF (CNORM.LE.0.9455) THEN
                  FEL(J)= RTF*DLOG((1.0D0-CNORM)/CNORM)
                  FEL1D(J)=-RTF/CNORM/(1.0D0-CNORM)
                  FEL2D(J)=RTF*(1.0D0-2.0D0*CNORM)/(CNORM-CNORM**2)**2
             ELSE
                  U1=FEXP(-18.652D0*(1.0D0-CNORM))
                U2=FEXP(-104.15D0*(1.0D0-CNORM))
                  FEL(J) = -0.052335 -0.054284D0*U1 -0.37142D0*U2
                  FEL1D(J) = -1.01251D0*U1 -38.6834D0*U2
                      FEL2D(J) = -18.8853D0*U1 -4028.876D0*U2
                   ENDIF
             FEL1D(j) = FEL1D(j)/CPSMAX
             FEL2D(j) = FEL2D(j)/CPSMAX**2
            ENDIF

 171      CONTINUE

C         *** PRINT OUT THE ARRAY OF MAIN VARIABLES IF NECESSARY  ***

          IF (t.eq.4000 .and. q.eq.4) THEN
            PRINT*, '  J      CON          I2          OPN         CS
     1 JIN OH-'
            PRINT*, '---- ---------  ---------  ---------  --------- --
     1----------'
            DO 850 J=1,4
               PRINT6, J,CON(J),I2(J),OPN(J),CS(T,J),
     1                 (I2(J+1)-I2(J))/H/SSANEG/F
 850        CONTINUE
            DO 851 J=5,N1-4,4
               PRINT6, J,CON(J),I2(J),OPN(J),CS(T,J),
     1                 (I2(J+1)-I2(J))/H/SSANEG/F
 851        CONTINUE
            DO 852 J=N1-3,N1+3
               PRINT6, J,CON(J),I2(J),OPN(J),CS(T,J),
     1                 (I2(J+1)-I2(J))/H/SSANEG/F
 852        CONTINUE
            DO 853 J=N1+4,N2-4,4
               PRINT6, J,CON(J),I2(J),OPN(J),CS(T,J),
     1                 (I2(J+1)-I2(J))/H/SSANEG/F
 853        CONTINUE
            DO 854 J=N2-3,N2+3
               PRINT6, J,CON(J),I2(J),OPN(J),CS(T,J),
     1                 (I2(J)-I2(J-1))/H/SSAPOS/F
 854        CONTINUE
            DO 855 J=N2+4,NJ-4,4
```

```
               PRINT6, J,CON(J),I2(J),OPN(J),CS(T,J),
     1                    (I2(J)-I2(J-1))/H/SSAPOS/F
 855         CONTINUE
             DO 856 J=NJ-3,NJ
               PRINT6, J,CON(J),I2(J),OPN(J),CS(T,J),
     1                    (I2(J)-I2(J-1))/H/SSAPOS/F
 856         CONTINUE
           ENDIF

           ERR=0.0D0


           DO 200 J = 1,NJ

C      *** RESET THE A's, B's, D's, AND G's THAT ARE SENT TO BAND.
C          THIS IS DONE SO WE DON'T HAVE TO DEFINE A BUNCH OF ZERO VALUES
C          INSIDE EACH IF-THEN BLOCK OF THE BAND LOOP ***
              DO 125 Y2=1,N
                 DO 126 Z2=1,N
                    A(Y2,Z2)=0.0D0
                    B(Y2,Z2)=0.0D0
                    D(Y2,Z2)=0.0D0
 126             CONTINUE
                 G(Y2)=0.0D0
 125          CONTINUE

C     *** NOW IS TIME TO START GIVING VALUES TO THE A's,B's,D's, and
C         G's THAT BAND WILL USE TO CALCULATE THE PRIMARY CHANGE
C         VARIABLES.

C              *** WRITE IN THE FIRST EQUATION FOR ALL THE POINTS ***
               IF (J.EQ.1) THEN
                  CON1X=(-1.5D0*CON(1)+2.0D0*CON(2)-0.5D0*CON(3))/H
                  B(1,1)=-1.5D0/H
                  D(1,1)=2.0D0/H
                  X(1,1)=-0.5D0/H
                  G(1)=-CON1X

               ELSE IF (J.GT.1 .AND. J.LT.NJ) THEN
                  IF (J.GE.N2) THEN
                     POR=PORPOS
                  ELSEIF (J.GE.N1) THEN
                     POR=PORSEP
                  ELSE
                     POR=PORNEG
                  ENDIF
                  G(1)= -0.5D0*H*POR*(CON(J)-CONOLD(J))/DELTIM
     1 +0.5D0*(POR*(DC(J)+DC(J+1))*(CON(J+1)-CON(J))/2.0D0/H
     1 - 0.5D0*TPOS*(I2(J)+I2(J+1))/F)
     1 +0.5D0*(POR*(DOLD(J)+DOLD(J+1))*(CONOLD(J+1)-CONOLD(J))/2.0D0/H
     1 - 0.5D0*TPOS*(I2OLD(J)+I2OLD(J+1))/F)
                  B(1,1)=0.5D0*POR*H/DELTIM +0.25D0*POR* (DC(J) + DC(J+1)
     1                    -(CON(J+1)-CON(J))*D1D(J))/H
                  D(1,1)=-0.25D0*POR*(DC(J)+DC(J+1)+(CON(J+1)-CON(J))
     1                    *D1D(J+1))/H
```

```
            D(1,2)=0.25*TPOS/F

            IF (J.GT.N2) THEN
               POR=PORPOS
            ELSEIF (J.GT.N1) THEN
               POR=PORSEP
            ELSE
               POR=PORNEG
            ENDIF
            G(1)= G(1) -0.5D0*H*POR*(CON(J)-CONOLD(J))/DELTIM
     1 +0.5D0*(-POR*(DC(J)+DC(J-1))*(CON(J)-CON(J-1))/2.0D0/H
     1 +0.5D0*TPOS*(I2(J)+I2(J-1))/F)
     1 +0.5D0*(-POR*(DOLD(J)+DOLD(J-1))*(CONOLD(J)-CONOLD(J-1))/2.0D0/H
     1 +0.5D0*TPOS*(I2OLD(J)+I2OLD(J-1))/F)
            A(1,1)=-0.25D0*POR*(DC(J) +DC(J-1) -(CON(J)-CON(J-1))
     1                  *D1D(J-1))/H
            B(1,1)=B(1,1) +0.5D0*POR*H/DELTIM + 0.25D0*POR*
     1                  (DC(J) +DC(J-1) +(CON(J)-CON(J-1))*D1D(J))/H
            A(1,2)=-0.25D0*TPOS/F
            B(1,2)=0.0D0
         ELSE
            CON1X=(1.5D0*CON(NJ)-2.0D0*CON(NJ-1)+0.5D0
     1             *CON(NJ-2))/H
            Y(1,1)=0.5D0/H
            A(1,1)=-2.0D0/H
            B(1,1)=1.5D0/H
            G(1)=-CON1X

         ENDIF

C        *** ENTER THE SECOND EQUATION ***

         IF (J.EQ.1 .OR. J.EQ.NJ) THEN
            B(2,2)=1.0D0
            G(2)=-I2(J)
         ELSE IF (J.GE.2 .AND. J.LE.N1) THEN
          CON1X=(CON(J)-CON(J-1))/H
          OPN1X=(OPN(J)-OPN(J-1))/H
          CS1X=(CS(T,J)-CS(T,J-1))/H
          U1=DN(J)-CON(J)*MKOH
          U2=DN1D(J)-MKOH
          U11=DN(J-1)-CON(J-1)*MKOH
          U22=DN1D(J-1)-MKOH
          U3= OPN1X*U2 + (I-I2(J))*U2/CNDNEG +CS1X*U2*FEL1D(J)
     1                -I2(J)*U2/K(J) + U1*I2(J)*K1D(J)/K(J)**2.0D0
          U3=U3 -RTF* CON1X * ( (TPOS*U1+MH2O*CON(J)) *((AC(J)
     1        *AC2D(J)-AC1D(J)**2.0D0)/(AC(J)**2.0D0)-1.0D0/CON(J)
     1        **2.0D0)+(AC1D(J)/AC(J)+1.0D0/CON(J))* (TPOS*U2+MH2O))
          U33= OPN1X*U22 + (I-I2(J-1))*U22/CNDNEG +CS1X*
     1                U22*FEL1D(J-1)-I2(J-1)*U22/K(J-1) + U11*I2(J-1)
     1                *K1D(J-1)/K(J-1)**2.0D0
          U33= U33 -RTF* CON1X * ((TPOS*U11+MH2O*CON(J-1))*
     1        (AC2D(J-1)/AC(J-1) -(AC1D(J-1)/AC(J-1))**2.0D0 -1.0D0
     1        /CON(J-1)**2.0D0)+(AC1D(J-1)/AC(J-1)+1.0D0/CON(J-1))
     1              * (TPOS*U22+MH2O))
```

```
      U4=-RTF*TPOS*(AC1D(J)*DN(J)/AC(J) +DN(J)/CON(J)) -RTF*(MH2O
     1          -TPOS*MKOH)*(AC1D(J)*CON(J)/AC(J) + 1.0D0)
      U44=-RTF*TPOS*(AC1D(J-1)*DN(J-1)/AC(J-1)+DN(J)/CON(J-1))-RTF
     1     *(MH2O-TPOS*MKOH)*(AC1D(J-1)*CON(J-1)/AC(J-1) + 1.0D0)
      U5= -U1/CNDNEG -U1/K(J)
      U55= -U11/CNDNEG -U11/K(J-1)
      U6= U1*CS1X*FEL2D(J)
      U66= U11*CS1X*FEL2D(J-1)
      U7= U1*FEL1D(J)
      U77= U11*FEL1D(J-1)
      A(2,1)=0.5D0*U33 - (U4+U44)/2.0D0/H
      B(2,1)=0.5D0*U3  + (U4+U44)/2.0D0/H
      A(2,2)=0.5D0*U55
      B(2,2)=0.5D0*U5
      A(2,3)=-(U1+U11)/2.0D0/H
      B(2,3)=(U1+U11)/2.0D0/H
      A(2,4)=0.5D0*U66 - (U7+U77)/2.0D0/H
      B(2,4)=0.5D0*U6 + (U7+U77)/2.0D0/H
      U8=-U1*OPN1X + (I2(J)-I)*U1/CNDNEG +U1*I2(J)/K(J) +
     1     RTF*(TPOS*U1+MH2O*CON(J))*(AC1D(J)/AC(J) +1.0D0/CON(J))
     1     *CON1X - U1*CS1X*FEL1D(J)
      U88=-U11*OPN1X +(I2(J-1)-I)*U11/CNDNEG +U11*I2(J-1)/
     1      K(J-1)+RTF*(TPOS*U11+MH2O*CON(J-1))*(AC1D(J-1)/AC(J-1)
     1      +1.0D0/CON(J-1))*CON1X - U11*CS1X*FEL1D(J-1)
      G(2)=(U8+U88)/2.0D0

     ELSE IF (J.GE.N2 .AND. J.LT.NJ) THEN
      CON1X=(CON(J+1)-CON(J))/H
      OPN1X=(OPN(J+1)-OPN(J))/H
      CS1X=(CS(T,J+1)-CS(T,J))/H
      U1=DN(J)-CON(J)*MKOH
      U2=DN1D(J)-MKOH
      U11=DN(J+1)-CON(J+1)*MKOH
      U22=DN1D(J+1)-MKOH
      U3= OPN1X*U2 + (I-I2(J))*U2/CNDPOS +CS1X*U2*FEL1D(J)
     1          -I2(J)*U2/K(J) + U1*I2(J)*K1D(J)/K(J)**2.0D0
        U3= U3 -RTF* CON1X * ((TPOS*U1+MH2O*CON(J)) *(AC2D(J)
     1      /AC(J) - (AC1D(J)/AC(J))**2.0D0-1.0D0/CON(J)**
     1      2.0D0)+(AC1D(J)/AC(J)+1.0D0/CON(J))* (TPOS*U2+MH2O))
      U33= OPN1X*U22 + (I-I2(J+1))*U22/CNDPOS +CS1X
     1          *U22*FEL1D(J+1)-I2(J+1)*U22/K(J+1) + U11*I2(J+1)*
     1          K1D(J+1)/K(J+1)**2.0D0
      U33= U33 -RTF* CON1X * ((TPOS*U11+MH2O*CON(J+1))*
     1     (AC2D(J+1)/AC(J+1) -(AC1D(J+1)/AC(J+1))**2.0D0 -1.0D0
     1     /CON(J+1)**2.0D0)+(AC1D(J+1)/AC(J+1)+1.0D0/CON(J+1))
     1          * (TPOS*U22+MH2O))
      U4=-RTF*TPOS*(AC1D(J)*DN(J)/AC(J) +DN(J)/CON(J))-RTF*(MH2O
     1          -TPOS*MKOH)*(AC1D(J)*CON(J)/AC(J) + 1.0D0)
      U44=-RTF*TPOS*(AC1D(J+1)*DN(J+1)/AC(J+1) +DN(J)/CON(J+1))
     1     -RTF*(MH2O-TPOS*MKOH)*(AC1D(J+1)*CON(J+1)/AC(J+1)+1.0D0)
      U5= -U1/CNDPOS -U1/K(J)
      U55= -U11/CNDPOS -U11/K(J+1)
      U6=+U1*CS1X*FEL2D(J)
      U66=+U11*CS1X*FEL2D(J+1)
      U7=+U1*FEL1D(J)
```

```
      U77=+U11*FEL1D(J+1)
      B(2,1)=0.5D0*U3 - (U4+U44)/2.0D0/H
      D(2,1)=0.5D0*U33 + (U4+U44)/2.0D0/H
      B(2,2)=0.5D0*U5
      D(2,2)=0.5D0*U55
      B(2,3)=-(U1+U11)/2.0D0/H
      D(2,3)=(U1+U11)/2.0D0/H
      B(2,4)=0.5D0*U6 - (U7+U77)/2.0D0/H
      D(2,4)=0.5D0*U66 + (U7+U77)/2.0D0/H
      U8=-U1*OPN1X + (I2(J)-I)*U1/CNDPOS +U1*I2(J)/K(J) +
     1     RTF*(TPOS*U1+MH2O*CON(J))*(AC1D(J)/AC(J) +1.0D0/CON(J))
     1     *CON1X - U1*CS1X*FEL1D(J)
      U88=-U11*OPN1X +(I2(J+1)-I)*U11/CNDPOS +U11*I2(J+1)/
     1     K(J+1)+RTF*(TPOS*U11+MH2O*CON(J+1))*(AC1D(J+1)/AC(J+1)
     1     +1.0D0/CON(J+1))*CON1X - U11*CS1X*FEL1D(J+1)
      G(2)=(U8+U88)/2.0D0
     ELSE
      B(2,3)=1.0D0
      G(2)=-OPN(J)
     ENDIF

C    *** ENTER THE THIRD EQUATION ***

     IF (J.GE.1.AND.J.LT.N1) THEN
      U0=SSANEG*EXCDN/MH2O**ATCN
      U1=DN(J)-CON(J)*MKOH
      U2=DN1D(J)-MKOH
      U3= (AC(J)*CON(J))**CTCN*(WAC(J)*U1)**ATCN
      U4= CS(T,J)**CTCN*(CNGMAX-CS(T,J))**ATCN
      U5= FEXP(ATCN*OPN(J)/RTF) - FEXP(-CTCN*OPN(J)/RTF)
      U6= (AC(J)*CON(J))**CTCN*ATCN*(WAC(J)*U1)**(ATCN-1.0D0)*
     1     (WAC(J)*U2+WAC1D(J)*U1)+(WAC(J)*U1)**ATCN*CTCN*
     1     (AC(J)*CON(J))**(CTCN-1.0D0)*(AC(J)+CON(J)*AC1D(J))
      U7= CTCN*(CNGMAX-CS(T,J))**ATCN*CS(T,J)**(CTCN-1.0D0)-
     1     ATCN*CS(T,J)**CTCN*(CNGMAX-CS(T,J))**(ATCN-1.0D0)
      U8= ATCN*FEXP(ATCN*OPN(J)/RTF)/RTF +
     1          CTCN*FEXP(-CTCN*OPN(J)/RTF)/RTF
      U11=DN(J+1)-CON(J+1)*MKOH
      U22=DN1D(J+1)-MKOH
      U33= (AC(J+1)*CON(J+1))**CTCN*(WAC(J+1)*U11)**ATCN
      U44= CS(T,J+1)**CTCN*(CNGMAX-CS(T,J+1))**ATCN
      U55= FEXP(ATCN*OPN(J+1)/RTF) - FEXP(-CTCN*OPN(J+1)/RTF)
      U66= (AC(J+1)*CON(J+1))**CTCN*ATCN*(WAC(J+1)*U11)**
     1     (ATCN-1.0D0)*(WAC(J+1)*U22+WAC1D(J+1)*U11)+(WAC(J+1)
     1     *U11)**ATCN*CTCN*(AC(J+1)*CON(J+1))**(CTCN-1.0D0)*
     1          (AC(J+1)+CON(J+1)*AC1D(J+1))
      U77=CTCN*(CNGMAX-CS(T,J+1))**ATCN*CS(T,J+1)**(CTCN-1.0D0)-
     1     ATCN*CS(T,J+1)**CTCN*(CNGMAX-CS(T,J+1))**(ATCN-1.0D0)
      U88= ATCN*FEXP(ATCN*OPN(J+1)/RTF)/RTF +
     1          CTCN*FEXP(-CTCN*OPN(J+1)/RTF)/RTF
      B(3,1)= -0.5D0*U0*U4*U5*U6
      D(3,1)= -0.5D0*U0*U44*U55*U66
      B(3,2)= -1.0D0/H
      D(3,2)= 1.0D0/H
      B(3,3)= -0.5D0*U0*U3*U4*U8
```

```
      D(3,3)= -0.5D0*U0*U33*U44*U88
      B(3,4)= -0.5D0*U0*U3*U5*U7
      D(3,4)= -0.5D0*U0*U33*U55*U77
      G(3)=0.5D0*U0*(U3*U4*U5 +U33*U44*U55) -(I2(J+1)-I2(J))/H

     ELSE IF (J.GE.N1 .AND. J.LE.N2) THEN
      B(3,2)=1.0D0
      G(3)=I-I2(J)

     ELSE
      U0=SSAPOS*EXCDP/MH2O**ATCP
      U1=DN(J)-CON(J)*MKOH
      U2=DN1D(J)-MKOH
      U3= (AC(J)*CON(J))**CTCP*(WAC(J)*U1)**ATCP
      U4= CS(T,J)**CTCP*(CPSMAX-CS(T,J))**ATCP
      U5= FEXP(ATCP*OPN(J)/RTF) - FEXP(-CTCP*OPN(J)/RTF)
      U6= (AC(J)*CON(J))**CTCP*ATCP*(WAC(J)*U1)**(ATCP-1.0D0)*
     1     (WAC(J)*U2+WAC1D(J)*U1)+(WAC(J)*U1)**ATCP*CTCP*
     1     (AC(J)*CON(J))**(CTCP-1.0D0)*(AC(J)+CON(J)*AC1D(J))
      U7= CTCP*(CPSMAX-CS(T,J))**ATCP*CS(T,J)**(CTCP-1.0D0)-
     1     ATCP*CS(T,J)**CTCP*(CPSMAX-CS(T,J))**(ATCP-1.0D0)
      U8= ATCP*FEXP(ATCP*OPN(J)/RTF)/RTF +
     1           CTCP*FEXP(-CTCP*OPN(J)/RTF)/RTF
      U11=DN(J-1)-CON(J-1)*MKOH
      U22=DN1D(J-1)-MKOH
      U33= (AC(J-1)*CON(J-1))**CTCP*(WAC(J-1)*U11)**ATCP
      U44= CS(T,J-1)**CTCP*(CPSMAX-CS(T,J-1))**ATCP
      U55= FEXP(ATCP*OPN(J-1)/RTF) - FEXP(-CTCP*OPN(J-1)/RTF)
      U66= (AC(J-1)*CON(J-1))**CTCP*ATCP*(WAC(J-1)*U11)**
     1     (ATCP-1.0D0)*(WAC(J-1)*U22+WAC1D(J-1)*U11)+(WAC(J-1)*
     1     U11)**ATCP*CTCP*(AC(J-1)*CON(J-1))**(CTCP-1.0D0)*
     1           (AC(J-1)+CON(J-1)*AC1D(J-1))
      U77=CTCP*(CPSMAX-CS(T,J-1))**ATCP*CS(T,J-1)**(CTCP-1.0D0)-
     1    ATCP*CS(T,J-1)**CTCP*(CPSMAX-CS(T,J-1))**(ATCP-1.0D0)
      U88= ATCP*FEXP(ATCP*OPN(J-1)/RTF)/RTF +
     1           CTCP*FEXP(-CTCP*OPN(J-1)/RTF)/RTF
      A(3,1)= -0.5D0*U0*U44*U55*U66
      B(3,1)= -0.5D0*U0*U4*U5*U6
      A(3,2)= -1.0D0/H
      B(3,2)= 1.0D0/H
      A(3,3)= -0.5D0*U0*U33*U44*U88
      B(3,3)= -0.5D0*U0*U3*U4*U8
      A(3,4)= -0.5D0*U0*U33*U55*U77
            B(3,4)= -0.5D0*U0*U3*U5*U7
      G(3)=0.5D0*U0*(U3*U4*U5 +U33*U44*U55) -(I2(J)-I2(J-1))/H

     ENDIF

C    *** WRITE IN THE FOURTH EQUATION FOR ALL POINTS ***

     IF (J.GT.N1 .AND.J.LT.N2) THEN
       B(4,4)=1.0D0
       G(4)= - CS(T,J)
     ELSE IF (J.LE.N1) THEN
        IF (Q.EQ.1) THEN
```

```
                SUM1(J)=0.0D0
               DO 210 TT=1,T-1
C                * INTERPOLATE TO FIND THE CORRECT AN(T) VALUES *
                 NUM=DINT((TIME-DTIM(TT-1))/ANINC)
                 U33=TIME-DTIM(TT-1)-NUM*ANINC
                 U44=AN(NUM) + U33*(AN(NUM+1)-AN(NUM))/ANINC
                 NUM=DINT((TIME-DTIM(TT))/ANINC)
                 U55=TIME-DTIM(TT)-NUM*ANINC
                 U66=AN(NUM) + U55*(AN(NUM+1)-AN(NUM))/ANINC
                 SUM1(J)=SUM1(J) +(CS(TT,J)-CS(TT-1,J))*(U44-U66)/
     1                          (DTIM(TT)-DTIM(TT-1))
 210            CONTINUE
               ENDIF
               U0=EXCDN/DSNEG/F/MH2O**ATCN
               NUM=DINT(DELTIM/ANINC)
               U11=DELTIM-NUM*ANINC
               U22=(AN(NUM) +U11*(AN(NUM+1)-AN(NUM))/ANINC)/DELTIM
             U1=DN(J)-CON(J)*MKOH
             U2=DN1D(J)-MKOH
             U3= (AC(J)*CON(J))**CTCN*(WAC(J)*U1)**ATCN
             U4= CS(T,J)**CTCN*(CNGMAX-CS(T,J))**ATCN
             U5= FEXP(ATCN*OPN(J)/RTF) - FEXP(-CTCN*OPN(J)/RTF)
             U6= (AC(J)*CON(J))**CTCN*ATCN*(WAC(J)*U1)**(ATCN-1.0D0)*
     1           (WAC(J)*U2+WAC1D(J)*U1)+(WAC(J)*U1)**ATCN*CTCN*
     1           (AC(J)*CON(J))**(CTCN-1.0D0)*(AC(J)+CON(J)*AC1D(J))
             U7= CTCN*(CNGMAX-CS(T,J))**ATCN*CS(T,J)**(CTCN-1.0D0)-
     1           ATCN*CS(T,J)**CTCN*(CNGMAX-CS(T,J))**(ATCN-1.0D0)
             U8= ATCN*FEXP(ATCN*OPN(J)/RTF)/RTF +
     1                CTCN*FEXP(-CTCN*OPN(J)/RTF)/RTF
             B(4,1) = U0*U4*U5*U6
             B(4,3) = U0*U3*U4*U8
             B(4,4) = U0*U3*U5*U7 + U22
             G(4)= -SUM1(J) + U22*(CS(T-1,J)-CS(T,J)) - U0*U3*U4*U5
            ELSE
            IF (T.NE.0) THEN
C    ------------------------------------------------------------------
C    THIS IS WHERE THE 2-D PART OF THE MODEL COMES IN.  FIRST WE USE THE
C    B.V. EQUATION TO SPECIFY THE PORFLUX INTO THE PARTICLE.  THEN WE
C    ITERATE TO FIND THE CONCENTRATION PROFILE IN THE PARTICLE.  AFTER
C    WE FIND THE CONCENTRATION PROFILE, ALL WE HAVE TO ENTER IS THE CHANGE
C    IN THE SURFACE CONCENTRATION THAT WE FIND FROM THIS CALCULATION.
C    ------------------------------------------------------------------
            U0=SSAPOS*EXCDP/MH2O**ATCP
            U1=DN(J)-CON(J)*MKOH
            U2=DN1D(J)-MKOH
            U3= (AC(J)*CON(J))**CTCP*(WAC(J)*U1)**ATCP
            U4= CS(T,J)**CTCP*(CPSMAX-CS(T,J))**ATCP
            U5= FEXP(ATCP*OPN(J)/RTF) - FEXP(-CTCP*OPN(J)/RTF)
            PORFLX=EXCDP*U3*U4*U5/F/MH2O**ATCP

C             SOLVE FOR CONCENTRATION PROFILE FOR ALL VALUES OF X
C             ---------------------------------------------------

C             * RESET CHANGE VARIABLE **
              DO 376 JJ=1,NNJ
```

```
                CC(1,JJ) = 0.0D0
 376            CONTINUE

C               --> CONVERGENCE LOOP STARTS HERE <--
                DO 112 QQ=1,10
C               * SOLVE FOR DS AS A FUNCTION OF CONCENTRATION *
                DO 114 JJ=1,NNJ
                  IF (Q.EQ.1 .AND. QQ.EQ.1) THEN
                    CSSOLD(J,JJ)=CSS(J,JJ)
                    DSOLD(J,JJ)=DS(J,JJ)
                  ENDIF -
                  U1=1.0D0-0.956614D0*(CSS(J,JJ)/CPSMAX)
                  DS(J,JJ)=3.4D-08*U1**2.0D0
                  DS1D(JJ)=-6.505D-08*U1
 114            CONTINUE
                ERR2=0.0D0
                DO 888 JJ=1,NNJ
C                 --> ASSIGN VALUES TO "BAND2" <--
                  DIST=HH*(JJ-1)
                  DP=DIST+HH/2.0D0
                  DM=DIST-HH/2.0D0
                  IF (JJ.EQ.1) THEN
                    BB(1,1)=HH**3.0D0/DELTIM/6.0D0 + 0.25D0*HH*(DS(J,JJ)+
     1                       DS(J,JJ+1)-(CSS(J,JJ+1)-CSS(J,JJ))*DS1D(JJ))
                    DD(1,1)=-0.25D0*HH*(DS(J,JJ) +DS(J,JJ+1)
     1                     +(CSS(J,JJ+1)-CSS(J,JJ))*DS1D(JJ+1))
                    GG(1)=-HH**3.0D0*(CSS(J,JJ)-CSSOLD(J,JJ))/6.0D0
     1                    /DELTIM+0.25D0*HH*(DS(J,JJ+1)+DS(J,JJ))
     1                    *(CSS(J,JJ+1)-CSS(J,JJ))+0.25D0*HH*(DSOLD(J,JJ+1)
     1                    +DSOLD(J,JJ))*(CSSOLD(J,JJ+1)-CSSOLD(J,JJ))
                  ELSE IF (JJ.EQ.NNJ) THEN
                    AA(1,1)=0.25*DM**2.0D0*(-DS(J,JJ)-DS(J,JJ-1)+
     1                     (CSS(J,JJ)-CSS(J,JJ-1))*DS1D(JJ-1))/HH
                    BB(1,1)=0.5D0*DM**2.0D0*HH/DELTIM +0.25D0*DM**2.0D0*
     1                     (DS(J,JJ)+DS(J,JJ-1)+(CSS(J,JJ)-CSS(J,JJ-1))*
     1                     DS1D(JJ))/HH
                    GG(1)=-0.5D0*DM**2.0D0*HH*(CSS(J,JJ)-CSSOLD(J,JJ))/
     1                    DELTIM-0.25D0*DM**2.0D0*(DS(J,JJ)+DS(J,JJ-1))*
     1                    (CSS(J,JJ)-CSS(J,JJ-1))/HH -0.25D0*DM**2.0D0*
     1                    (DSOLD(J,JJ)+DSOLD(J,JJ-1))*(CSSOLD(J,JJ)
     1                    -CSSOLD(J,JJ-1))/HH - PORFLX*DIST**2.0D0
                  ELSE
                    AA(1,1)=0.25D0*DM**2.0D0*(-DS(J,JJ) -DS(J,JJ-1)
     1                     +(CSS(J,JJ)-CSS(J,JJ-1))*DS1D(JJ-1))/HH
                    BB(1,1)=HH*DIST**2.0D0/DELTIM + 0.25D0*DM**2.0D0*
     1                     (DS(J,JJ)+DS(J,JJ-1)+(CSS(J,JJ)-CSS(J,JJ-1))*
     1                  DS1D(JJ))/HH +0.25D0*DP**2.0D0*(DS(J,JJ)+DS(J,JJ+1)
     1                   -(CSS(J,JJ+1)-CSS(J,JJ))*DS1D(JJ))/HH
                    DD(1,1)=-0.25D0*DP**2.0D0*(DS(J,JJ) +DS(J,JJ+1)
     1                     +(CSS(J,JJ+1)-CSS(J,JJ))*DS1D(JJ+1))/HH
                    GG(1)=-HH*DIST**2.0D0*(CSS(J,JJ)-CSSOLD(J,JJ))/DELTIM
     1                  +0.25D0*(-DM**2.0D0*(DS(J,JJ)+DS(J,JJ-1))*(CSS(J,JJ)
     1                     -CSS(J,JJ-1))+DP**2.0D0*(DS(J,JJ+1)+DS(J,JJ))*
     1                    (CSS(J,JJ+1)-CSS(J,JJ)))/HH
     1                 +0.25D0*(-DM**2.0D0*(DSOLD(J,JJ)+DSOLD(J,JJ-1))*
```

```
     1                    (CSSOLD(J,JJ)-CSSOLD(J,JJ-1))+DP**2.0D0*
     1                    (DSOLD(J,JJ+1)+DSOLD(J,JJ))*(CSSOLD(J,JJ+1)
     1                  -CSSOLD(J,JJ)))/HH
                ENDIF
                ERR2=ERR2+DABS(GG(1))
                CALL BAND2(JJ)
 888          CONTINUE

                DO 322 JJ=1,NNJ
                  CSS(J,JJ)=CSS(J,JJ)+CC(1,JJ)
 322          CONTINUE

C               --> CHECK TO SEE IF CONCENTRATIONS CONVERGED <--
                ERR2=ERR2/NNJ
                IF (ERR2.LT.LIMIT2) GOTO 345

 112          CONTINUE
              PRINT*, 'SOLID PHASE DIFFUSION DID NOT CONVERGE!'
              PRINT*, 'TIME STEP = ',T
              PRINT*, 'J = ',J
              STOP

 345          continue
            B(4,4)=1.0D0
              G(4)=CSS(J,NNJ)-CS(T,J)
            ENDIF
            ENDIF

C     *** IF THIS IS THE FIRST TIME STEP, WE RE-WRITE THE FIRST AND
C         FOURTH EQUATIONS SO THAT THE VALUES FOR THE SOLUTION AND
C         SOLID CONCENTRATIONS ARE CONSTANT.  THIS ALLOWS US TO
C         FIND THE POTENTIAL AND CURRENT DISTRIBUTIONS AT TIME =0 ***

            IF (T.EQ.0) THEN
               IF (J.EQ.1) X(1,1)=0.0D0
               IF (J.EQ.NJ) Y(1,1)=0.0D0
               DO 483 X2=1,N
                  DO 484 Y2=1,4,3
                     A(Y2,X2)=0.0D0
                     B(Y2,X2)=0.0D0
                     D(Y2,X2)=0.0D0
 484              CONTINUE
 483           CONTINUE
               B(1,1)=1.0D0
               G(1)=CINIT-CON(J)
               B(4,4)=1.0D0
               IF (J.GE.1.AND.J.LE.N1) THEN
                  G(4)=0.97D0*CNGMAX-CS(T,J)
               ELSE IF (J.GT.N1.AND.J.LT.N2) THEN
                  G(4)=-CS(T,J)
               ELSE
                  G(4)=CPSMIN-CS(T,J)
               ENDIF
            ENDIF
            ERR=ERR +DABS(G(1)) +DABS(G(2)) +DABS(G(3)) +DABS(G(4))
```

```
                  CALL BAND(J)
 200      CONTINUE

C         *** CALCULATE THE NEW VALUES OF THE THREE MAIN VARIABLES--
C           CON, I2, AND OPN.  THE LOGICAL IF STATMENTS LIMIT THE AMOUNT
C           OF CHANGE THAT CAN OCCUR ON ANY ONE CONVERGENCE LOOP.  THIS
C           PREVENTS THE VALUES FROM "EXPLODING" DURING THE FIRST
C           COUPLE OF ITERATIONS IF THE GUESSES ARE NOT GOOD. ***

          DO 321 J = 1,NJ
             IF (C(1,J).GT.0.000692) C(1,J)=0.0006920D0
             IF (C(1,J).LT.-0.000692) C(1,J)=-0.0006920D0
             CON(J)=CON(J)+C(1,J)
             IF (CON(J).LE.0.0) CON(J)=0.000001D0

             IF (C(2,J).GT.0.1D0*I) C(2,J)=0.1D0*I
             IF (C(2,J).LT.-0.1D0*I) C(2,J)=-0.1D0*I
             IF (DABS(C(2,J)).LT.1.0D-13) C(2,J)=0.0D0
             I2(J)=I2(J)+C(2,J)
             IF (I2(J).GT.I) I2(J)=I
             IF (I2(J).LT.0.0) I2(J)=0.0D0

             IF (C(3,J).GT.0.05) C(3,J)=0.05D0
             IF (C(3,J).LT.-0.05) C(3,J)=-0.05D0
             OPN(J)=OPN(J)+C(3,J)
             IF (J.LE.N1.AND.OPN(J).LT.0) OPN(J)=0.0D0
             IF (J.GE.N2.AND.OPN(J).GT.0) OPN(J)=0.0D0

             IF (C(4,J).GT.0.0004) C(4,J)=0.0004D0
             IF (C(4,J).LT.-0.0004) C(4,J)=-0.0004D0
             CS(T,J)=CS(T,J)+C(4,J)
             IF (J.LE.N1.AND.CS(T,J).LT.0.0001) CS(T,J)=0.0001D0
             IF (J.LE.N1.AND.CS(T,J).GT.0.97*CNGMAX)
     1              CS(T,J)=0.9699D0*CNGMAX
             IF (J.GE.N2.AND.CS(T,J).LT.0.00001) CS(T,J)=0.00001D0
             IF (J.GE.N2.AND.CS(T,J).GT.0.995*CPSMAX)
     1              CS(T,J)=0.995D0*CPSMAX

 321      CONTINUE


C      *** FIND THE ERROR AND CHECK FOR CONVERGENCE ***

          ERR=ERR/(NJ*N)
c       print*, 'q = ',q,' ; error = ',err
          IF (ERR.LT.LIMIT.AND.Q.GT.2) GOTO 500

 150    CONTINUE
          PRINT*, 'ERROR - PROGRAM DID NOT CONVERGE'
          PRINT*, 'TIME STEP = ',T
          STOP

 500    CONTINUE

        CELOLD = CELPOT
```

```
      CELPOT=1.327D0
      U11=0.0D0
      U22=0.0D0
      U33=0.0D0
C     *** FIND POTENTIAL DROP ACROSS THE ELECTRODE.  NOTE: HOW WE DO THIS IS
C     START WITH THE DIFFERENCE BETWEEN THE POS. AND NEGATIVE (HYPOTHETICAL)
C     REFERENCE ELECTRODES USED IN DEFINING PHI2.  THIS VALUE IS 1.327 VOLTS.
C     THEN WE ADD UP THE POTENTIAL DROPS ACROSS THE ELECTRODE. SINCE THE 3rd
C     VARIABLE, ETA, IS DEFINED AT PHI1 MINUS PHI2 MINUS THE CONCENTRATION
C     DEPENDENCE OF THE OVERPOT'L, WE MUST ADD THIS TERM BACK IN TO REALLY
C     FIND THE POTENTIAL DROP ACROSS THE ELECTRODE/SEPERATOR INTERFACE. ***
C
C     *** NOTE: WE USE SIMPSON'S RULE HERE TO INTEGRATE TO FIND THE CELL POT.
C     SINCE SIMPSON'S RULE REQUIRES AN ODD NUMBER OF POINTS, WE FIRST HAVE TO
C     CHECK TO SEE IF THERE ARE AN ODD OR EVEN NUMBER OF POINTS AND ADJUST
C     THE ROUTINE APPROPRIATELY ***
C
C       * NEGATIVE ELECTRODE *
      IF (DNINT(N1/2.0D0).NE.N1/2.0D0) THEN
        U11=U11-H*I2(1)/(3.0D0*CNDNEG)
          DO 400 J= 2, N1-3,2
            U11=U11- H*(4.0D0*I2(J)+2.0D0*I2(J+1))/CNDNEG/3.0D0
 400    CONTINUE
          U11=U11 -4.0*H*I2(N1-1)/(3.0D0*CNDNEG)
        U11=U11 -H*I2(N1)/(3.0D0*CNDNEG)
      ELSE
        U11=U11-H*I2(1)/(3.0D0*CNDNEG)
          DO 410 J= 2, N1-4,2
            U1=U1- H*(4.0D0*I2(J)+2.0D0*I2(J+1))/CNDNEG/3.0D0
 410    CONTINUE
        U11=U11 -4.0*H*I2(N1-2)/(3.0D0*CNDNEG)
        U11=U11 -H*I2(N1-1)/(3.0D0*CNDNEG)
        U11=U11 -0.5D0*(I2(N1)-I2(N1-1))*H/CNDNEG
      ENDIF
      CELPOT=CELPOT+U11

C       * OVERPOTENTIAL AT NEGATIVE ELECTRODE *
      CELPOT=CELPOT-OPN(N1)-FEL(N1)

C       * SEPARATOR *
      U1=N2-N1+1
      DO 501 J=N1,N2
         CON1X = 0.5D0*(CON(J+1)-CON(J-1))/H
         DDP(J)=-I/K(J)-RTF*TPOS*(CON1X/CON(J)+AC1D(J)*CON1X/AC(J))
 501  CONTINUE
      IF (DNINT(U1/2.0D0).NE.U1/2.0D0) THEN
        U22 = U22 + H*DDP(N1)/3.0D0
          DO 510 J= N1+1, N2-3,2
            U22 = U22+ H*(4.0D0*DDP(J)+2.0D0*DDP(J+1))/3.0D0
 510    CONTINUE
        U22 = U22 +4.0D0*H*DDP(N2-1)/3.0D0
        U22 = U22 +H*DDP(N2)/3.0D0
      ELSE
        U22 = U22 + H*DDP(N1)/3.0D0
          DO 520 J= N1+1, N2-4,2
```

```
            U22 = U22+ H*(4.0D0*DDP(J)+2.0D0*DDP(J+1))/3.0D0
 520      CONTINUE
          U22 = U22 +4.0D0*H*DDP(N2-2)/3.0D0
          U22= U22 + H*DDP(N2-1)/3.0D0
          U22= U22 + 0.5*H*(DDP(N2)+DDP(N2-1))
        ENDIF
        CELPOT = CELPOT+U22

C       * OVERPOTENTIAL AT POSITIVE ELECTRODE *
        CELPOT=CELPOT+OPN(N2)+FEL(N2)

C       * POSITIVE ELECTRODE *
        U1=NJ-N2
        IF (DNINT(U1/2.0D0).NE.U1/2.0D0) THEN
          U33=U33-H*I2(N2)/(3.0D0*CNDPOS)
            DO 401 J= N2+1, NJ-2,2
              U33=U33- (4.0D0*I2(J)+2.0D0*I2(J+1))*H/3.0D0/CNDPOS
 401      CONTINUE
          U33=U33 -4.0D0*H*I2(NJ-1)/(3.0D0*CNDPOS)
          U33=U33 -H*I2(NJ)/(3.0D0*CNDPOS)
        ELSE
          U33=U33-H*I2(N2)/(3.0D0*CNDPOS)
            DO 411 J= N2+1, NJ-4,2
              U33=U33- (4.0D0*I2(J)+2.0D0*I2(J+1))*H/3.0D0/CNDPOS
 411      CONTINUE
          U33=U33 -4.0D0*H*I2(NJ-2)/(3.0D0*CNDPOS)
          U33=U33 -H*I2(NJ-1)/(3.0D0*CNDPOS)
          U33=U33 -0.5D0*(I2(NJ)-I2(NJ-1))*H/CNDPOS
        ENDIF
        CELPOT=CELPOT+U33

C       *** CALCULATE AVERAGE SPECIFIC POWER AND ENERGY ***
        IF (T.GE.1) THEN
           POWER = I*CELPOT
           ENERGY = ENERGY+POWER*DELTIM
           PAVE = ENERGY/TIME
        ENDIF

C       *** OUTPUT DATA FROM THIS TIME STEP ***

        if (mod(t,1).eq.0 .or. celpot.le.0.9) then
           u2=0.0d0
           u3=0.0d0
           do 148 j=1,n1
              u3=u3+cs(t,j)/n1/cngmax
 148       continue
           do 149 j=n2,nj
              u2=u2+cs(t,j)/(nj-n2+1)/cpsmax
 149       continue
         PRINT8, TIME/DISTIM,CELPOT,U3,U2,U22,-opn(n1)-fel(n1),
     1           0.40D0-U33+OPN(N2)+FEL(N2),opn(n2)+fel(n2),opn(n2)
        endif

        IF (CELPOT.LE.CUTOFF) THEN
           PRINT*, ' '
```

```
            PRINT*, ' '
            PRINT*, 'MESH POINT     CONCENTRATION (NORML)'
            PRINT*, '----------     ---------------------'
            DO 672 JJ=1,NNJ
               PRINT*,'   ',JJ,'    ',CSS(144,JJ)/CPSMAX
672         CONTINUE
            PRINT*, ' '
            PRINT*, 'CUTOFF VOLTAGE WAS REACHED'
            PRINT*, 'TOTAL NUMBER OF TIME STEPS = ',T
            PRINT*, 'TOTAL NUMBER OF TIMES BAND WAS CALLED = ',NUMBND
            PRINT*, 'AVERAGE POWER = ',PAVE,' WATTS/CM^2'
            PRINT*, 'ENERGY RELEASED = ',ENERGY,' JOULES/CM^2'
            RECOV = (TIME-(CUTOFF-CELPOT)*DELTIM/(CELOLD-CELPOT))/DISTIM
            PRINT*, 'FRACTION OF CAPACITY RECOVERED = ',RECOV
            PRINT*, 'TOTAL RUN TIME = ', RECOV*DISTIM,' s'
            PRINT*, '  '
            STOP
          ENDIF

100   CONTINUE

      STOP
      END

C           *** ERFC ***
C    * CALCULATES THE COMPLIMENTARY ERROR FUNCTION *
C      *** THIS SUBROUTINE CALCULATES THE COMPLIMENTARY ERROR FUNCTION ***
C      FUNCTIONS ARE FRON ABROMOWITZ AND STEGUN EQUATIONS 7.1.23 AND 7.1.26

        FUNCTION ERFC(DUM)
             DOUBLE PRECISION ERFC,DUM,ERFC,A1,A2,A3,A4,A5,B1,B2,B3,B4,
     1       B5,B6,B7
        EXTERNAL FEXP

             A1=0.254829592D0
             A2=-0.284496736D0
             A3=1.421413741
             A4=-1.453152027D0
             A5=1.061405429D0

          IF (DUM .LT. 2.747192D0) THEN
            B1=1.0D0/(1.0D0+0.3275911D0*DUM)
            ERFC=(A1*B1+A2*B1*B1+A3*B1**3.0D0+A4*B1**4.0D0+A5*B1**5.0D0)*
     1             FEXP(-DUM*DUM)
          ELSE IF (DUM .GT. 25.0D0) THEN
            ERFC=0.0D0
          ELSE
            B2=0.0D0
            B3=DUM*DUM+0.5
            B4=-0.5D0/DUM/DUM
            B2=B4
            B5=B4
            B6=1
23          B6=B6+1
            IF (B6 .GT. B3) GOTO 17
```

```
            B7=B5*(2.0D0*B6-1.0D0)*B4
            B2=B2+B7
            IF (B7 .LT. 1.0D-06) GOTO 17
            B5=B7
            GOTO 23
 17         ERFC=(FEXP(-DUM*DUM))*(1.0D0+B2)/DSQRT(3.1415926535D0)/DUM
          ENDIF
          RETURN
          END

C         *** FEXP ***
C       * NOTE: JUST PREVENTS UNDERFLOW ERRORS WHEN USING THE DEXP COMMAND *

          FUNCTION FEXP(DUM)
          DOUBLE PRECISION FEXP,DUM

          IF (DUM.LT.-100) THEN
             FEXP=0.0D0
          ELSE
             FEXP=DEXP(DUM)
          ENDIF
          RETURN
          END



C       *** BAND! ***

        subroutine band(j)
        implicit double precision(a-h,o-z)
        common /a/ a(4,4),b(4,4),c(4,200),d(4,9),g(4),x(4,4),
       1y(4,4),n,nj
        dimension e(4,5,200)
  101   format (15h determ=0 at j=,i4)
        if (j-2)  1,6,8
    1   np1= n + 1
        do 2 i=1,n
        d(i,2*n+1)= g(i)
        do 2 l=1,n
        lpn= l + n
    2   d(i,lpn)= x(i,l)
        call matinv(n,2*n+1,determ)
        if (determ)  4,3,4
    3   print 101, j
    4   do 5 k=1,n
        e(k,np1,1)= d(k,2*n+1)
        do 5 l=1,n
        e(k,l,1)= - d(k,l)
        lpn= l + n
    5   x(k,l)= - d(k,lpn)
        return
    6   do 7 i=1,n
        do 7 k=1,n
```

```
      do 7 l=1,n
    7 d(i,k)= d(i,k) + a(i,l)*x(l,k)
    8 if (j-nj)  11,9,9
    9 do 10 i=1,n
      do 10 l=1,n
      g(i)= g(i) - y(i,l)*e(l,np1,j-2)
      do 10 m=1,n
   10 a(i,l)= a(i,l) + y(i,m)*e(m,l,j-2)
   11 do 12 i=1,n
      d(i,np1)= - g(i)
      do 12 l=1,n
      d(i,np1)= d(i,np1) + a(i,l)*e(l,np1,j-1)
      do 12 k=1,n
   12 b(i,k)= b(i,k) + a(i,l)*e(l,k,j-1)
      call matinv(n,np1,determ)
      if (determ)  14,13,14
   13 print 101, j
   14 do 15 k=1,n
      do 15 m=1,np1
   15 e(k,m,j)= - d(k,m)
      if (j-nj)  20,16,16
   16 do 17 k=1,n
   17 c(k,j)= e(k,np1,j)
      do 18 jj=2,nj
      m= nj - jj + 1
      do 18 k=1,n
      c(k,m)= e(k,np1,m)
      do 18 l=1,n
   18 c(k,m)= c(k,m) + e(k,l,m)*c(l,m+1)
      do 19 l=1,n
      do 19 k=1,n
   19 c(k,1)= c(k,1) + x(k,l)*c(l,3)
   20 return
      end

      subroutine matinv(n,m,determ)
      implicit double precision(a-h,o-z)
      common /a/ a(4,4),b(4,4),c(4,200),d(4,9),g(4),x(4,4),
     1y(4,4),nx,nj
      dimension id(4)
      determ=1.0
      do 1 i=1,n
    1 id(i)=0
      do 18 nn=1,n
      bmax=1.1
      do 6 i=1,n
      if(id(i).ne.0) go to 6
      bnext=0.0
      btry=0.0
      do 5 j=1,n
      if(id(j).ne.0) go to 5
      if(dabs(b(i,j)).le.bnext) go to 5
      bnext=dabs(b(i,j))
      if(bnext.le.btry) go to 5
      bnext=btry
```

```
      btry=dabs(b(i,j))
      jc=j
    5 continue
      if(bnext.ge.bmax*btry) go to 6
      bmax=bnext/btry
      irow=i
      jcol=jc
    6 continue
      if(id(jc).eq.0) go to 8
      determ=0.0
      return
    8 id(jcol)=1
      if(jcol.eq.irow) go to 12
      do 10 j=1,n
      save=b(irow,j)
      b(irow,j)=b(jcol,j)
   10 b(jcol,j)=save
      do 11 k=1,m
      save=d(irow,k)
      d(irow,k)=d(jcol,k)
   11 d(jcol,k)=save
   12 f=1.0/b(jcol,jcol)
      do 13 j=1,n
   13 b(jcol,j)=b(jcol,j)*f
      do 14 k=1,m
   14 d(jcol,k)=d(jcol,k)*f
      do 18 i=1,n
      if(i.eq.jcol) go to 18
      f=b(i,jcol)
      do 16 j=1,n
   16 b(i,j)=b(i,j)-f*b(jcol,j)
      do 17 k=1,m
   17 d(i,k)=d(i,k)-f*d(jcol,k)
   18 continue
      return
      end


C     *** BAND2! ***
      subroutine band2(j)
      implicit double precision(a-h,o-z)
      common /b/ aa(1,1),bb(1,1),cc(1,150),dd(1,3),gg(1),xx(1,1),
     1yy(1,1),nn,nnj
      dimension e(1,2,150)
  101 format (15h determ=0 at j=,i4)
      if (j-2)  1,6,8
    1 np1= nn + 1
      do 2 i=1,nn
      dd(i,2*nn+1)= gg(i)
      do 2 l=1,nn
      lpn= l + nn
    2 dd(i,lpn)= xx(i,l)
      call matinv2(nn,2*nn+1,determ)
      if (determ)  4,3,4
    3 print 101, j
```

```
  4 do 5 k=1,nn
    e(k,np1,1)= dd(k,2*nn+1)
    do 5 l=1,nn
    e(k,l,1)= - dd(k,l)
    lpn= l + nn
  5 xx(k,l)= - dd(k,lpn)
    return
  6 do 7 i=1,nn
    do 7 k=1,nn
    do 7 l=1,nn
  7 dd(i,k)= dd(i,k) + aa(i,l)*xx(l,k)
  8 if (j-nnj)  11,9,9
  9 do 10 i=1,nn
    do 10 l=1,nn
    gg(i)= gg(i) - yy(i,l)*e(l,np1,j-2)
    do 10 m=1,nn
 10 aa(i,l)= aa(i,l) + yy(i,m)*e(m,l,j-2)
 11 do 12 i=1,nn
    dd(i,np1)= - gg(i)
    do 12 l=1,nn
    dd(i,np1)= dd(i,np1) + aa(i,l)*e(l,np1,j-1)
    do 12 k=1,nn
 12 bb(i,k)= bb(i,k) + aa(i,l)*e(l,k,j-1)
    call matinv2(nn,np1,determ)
    if (determ)  14,13,14
 13 print 101, j
 14 do 15 k=1,nn
    do 15 m=1,np1
 15 e(k,m,j)= - dd(k,m)
    if (j-nnj)  20,16,16
 16 do 17 k=1,nn
 17 cc(k,j)= e(k,np1,j)
    do 18 jj=2,nnj
    m= nnj - jj + 1
    do 18 k=1,nn
    cc(k,m)= e(k,np1,m)
    do 18 l=1,nn
 18 cc(k,m)= cc(k,m) + e(k,l,m)*cc(l,m+1)
    do 19 l=1,nn
    do 19 k=1,nn
 19 cc(k,1)= cc(k,1) + xx(k,l)*cc(l,3)
 20 return
    end

    subroutine matinv2(nn,m,determ)
    implicit double precision(a-h,o-z)
    common /b/ aa(1,1),bb(1,1),cc(1,150),dd(1,3),gg(1),xx(1,1),
   1yy(1,1),nx,nnj
    dimension id(1)
    determ=1.0
    do 1 i=1,nn
 1  id(i)=0
    do 18 nm=1,nn
    bmax=1.1
    do 6 i=1,nn
```

```
      if(id(i).ne.0) go to 6
      bnext=0.0
      btry=0.0
      do 5 j=1,nn
      if(id(j).ne.0) go to 5
      if(dabs(bb(i,j)).le.bnext) go to 5
      bnext=dabs(bb(i,j))
      if(bnext.le.btry) go to 5
      bnext=btry
      btry=dabs(bb(i,j))
      jc=j
    5 continue
      if(bnext.ge.bmax*btry) go to 6
      bmax=bnext/btry
      irow=i
      jcol=jc
    6 continue
      if(id(jc).eq.0) go to 8
      determ=0.0
      return
    8 id(jcol)=1
      if(jcol.eq.irow) go to 12
      do 10 j=1,nn
      save=bb(irow,j)
      bb(irow,j)=bb(jcol,j)
   10 bb(jcol,j)=save
      do 11 k=1,m
      save=dd(irow,k)
      dd(irow,k)=dd(jcol,k)
   11 dd(jcol,k)=save
   12 f=1.0/bb(jcol,jcol)
      do 13 j=1,nn
   13 bb(jcol,j)=bb(jcol,j)*f
      do 14 k=1,m
   14 dd(jcol,k)=dd(jcol,k)*f
      do 18 i=1,nn
      if(i.eq.jcol) go to 18
      f=bb(i,jcol)
      do 16 j=1,nn
   16 bb(i,j)=bb(i,j)-f*bb(jcol,j)
      do 17 k=1,m
   17 dd(i,k)=dd(i,k)-f*dd(jcol,k)
   18 continue
      return
      end
```

Appendix C: Input File for Either the 1-D or 2-D Program

```
3600.0, 0.035D0, 0.025D0, 0.08428D0, 0.3965D0, 0.05D0, 0.387D0
0.04906D0, 0.0507D0, 1.5D-04, 2.5D-04, 200.0D0
```

LAWRENCE BERKELEY LABORATORY
UNIVERSITY OF CALIFORNIA
TECHNICAL AND ELECTRONIC
INFORMATION DEPARTMENT
BERKELEY, CALIFORNIA 94720